Universidad de Valladolid

ESCUELA DE INGENIERÍAS INDUSTRIALES

DEPARTAMENTO DE INGENIERÍA QUÍMICA Y
TECNOLOGÍA DEL MEDIO AMBIENTE

TESIS DOCTORAL:

CONVERSION OF CELLULOSIC BIOMASS TOWARDS ADDED VALUE PRODUCTS OVER BIFUNCTIONAL CATALYSTS

Presentada por Alberto Romero Camacho
para optar al grado de
doctor con mención internacional por la
Universidad de Valladolid

Dirigida por:
Dra. Gloria Esther Alonso Sánchez
Dr. Antonio Nieto Márquez Ballesteros

Memoria para optar al grado de Doctor, con **Mención Doctor Internacional,**

presentada por el Ingeniero Químico:

Alberto Romero Camacho

Siendo el tutor en la **Universidad de Valladolid:**

Dra. Gloria Esther Alonso Sánchez

En la **Universidad Politécnica de Madrid:**

Dr. Antonio Nieto-Márquez Ballesteros

Y en el **Institut de recherches sur la catalyse et l'environnement de Lyon** (Francia):

Dra. Nadine Essayem

Valladolid, Julio de 2017

UNIVERSIDAD DE VALLADOLID

ESCUELA DE INGENIERÍAS INDUSTRIALES

Secretaría

La presente tesis doctoral queda registrada en el folio Nº_____

del correspondiente Libro de Registro con el Nº_____

Valladolid, a _____ de _____ de 2017

Fdo. El encargado del Registro

Gloria Esther Alonso Sánchez

Profesora Titular de Universidad

Departamento de Ingeniería Química y Tecnología del Medio Ambiente

Universidad de Valladolid (UVa)

y

Antonio Nieto Márquez Ballesteros

Profesora Titular de Universidad (interino)

Escuela Técnica Superior de Ingeniería Y Diseño Industrial (ETSIDI)

Universidad Politécnica de Madrid (UPM)

CERTIFICAN QUE:

ALBERTO ROMERO CAMACHO ha realizado bajo su dirección el trabajo ***"CONVERSION OF CELLULOSIC BIOMASS TOWARDS ADDED VALUE PRODUCTS OVER BIFUNCTIONAL CATALYSTS***", en el Departamento de Ingeniería Química y Tecnología del Medio Ambiente de la Escuela de Ingenierías Industriales de la Universidad de Valladolid. Considerando que dicho trabajo reúne los requisitos para ser presentado como Tesis Doctoral expresan su conformidad con dicha presentación.

Valladolid a _____ de_____ de 2017.

Fdo. Gloria Esther Alonso Sánchez Fdo. Antonio Nieto-Márquez Ballesteros

Reunido el tribunal que ha juzgado la tesis doctoral "***CONVERSION OF CELLULOSIC BIOMASS TOWARDS ADDED VALUE PRODUCTS OVER BIFUNCTIONAL CATALYSTS***" presentada por Alberto Romero Camacho y en cumplimiento con lo establecido por el Real Decreto 861/2010 (BOE 28.01.2011) ha acordado conceder por _____ la calificación de_____.

Valladolid, a de de 2017

PRESIDENTE SECRETARIO

1er Vocal 2do Vocal 3er Vocal

ABSTRACT:

CONVERSION OF CELLULOSIC BIOMASS TOWARDS ADDED VALUE PRODUCTS OVER BIFUNCTIONAL CATALYSTS.

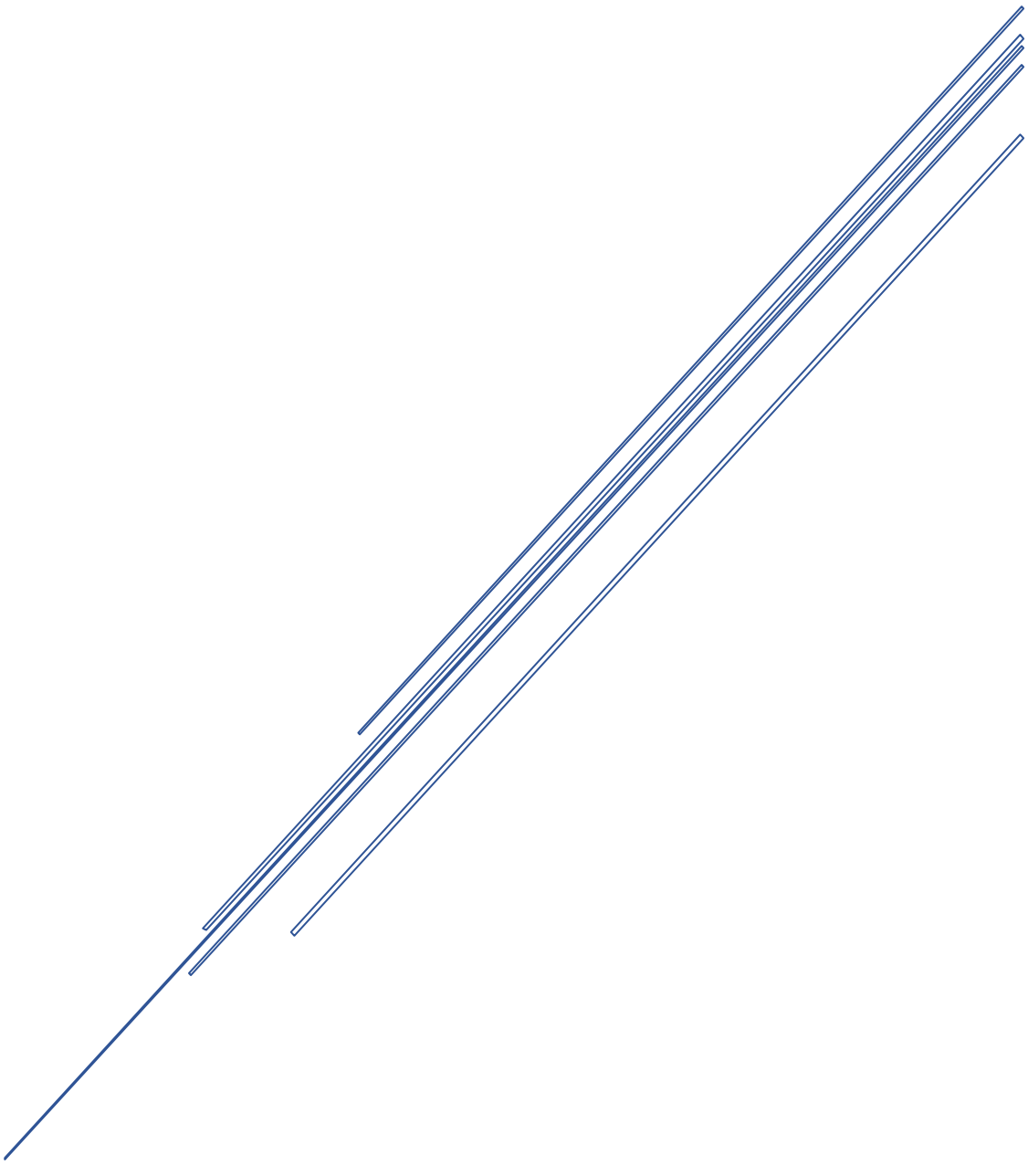

In view of the current problems such as global warming, high oil prices, more severe environmental laws and other geopolitical consequences surrounding the use of fossil feedstocks, the efficient conversion of cellulosic biomass towards chemicals, energy and fuels, has achieved a good piece of attention. In this sense, the use of heterogeneous catalysts could allow to develop environmentally clean processes working under relatively mild conditions, for the selective production of high added value products from cellulosic biomass.

In the present thesis, Ru and Ni deposited on mesoporous silica materials (MSM) were evaluated in order to produce sugar alcohols, ethylene glycol and straight-chain alkanes. Differing from other catalytic supports such as activated carbon, which have been highly used as support material for biomass conversion, not many works have reported the use of MSM for this purpose. The thermal and mechanical stability and the interesting pore structure of catalysts based on MSM, make them promising candidates for their application in conversion of biomass, being an interesting alternative to overcome diffusional problems in this kind of applications. This PhD thesis has been structured in five chapters. In each of them, a literature review was done in order to know the main achievements and challenges previously reported about the selected topic. In addition, the partial objectives and the obtained results were presented and discussed. The main content of each chapter is described below.

In **Chapter 1**, the synthesis and characterization of a bifunctional solid catalyst using MCM-48 as the support and ruthenium as the metal phase, is presented. Hydrolytic and hydrogenation capacities were the desired features of this catalyst to perform the synthesis of sorbitol from cellulose. MCM-48 demonstrated a good catalytic response for the hydrolysis of cellulose into D-Glucose attributable to surface acidity, with a yield of 14,1% of glucose in 30 min at 230ºC, much more higher than that reported in the literature. Catalytic activity of Ru/MCM-48 (4 wt. % Ru) prepared by wet impregnation method, was compared to that obtained by commercial Ru/C and a Ru deposited on a commercial TiO_2 in D-Glucose hydrogenation towards sorbitol. Ru/MCM-48 showed a high activity in the hydrogenation of D-Glucose, being 100 % selective to sorbitol working at 80 – 120 ºC and 5 MPa H_2. Activation energy for Ru/MCM-48 was around 45 $KJ \cdot mol^{-1}$. Moreover, Ru/MCM-48 demonstrated a good stability after three reaction cycles, both in terms of specific catalytic activity and ruthenium crystallite size.

According to the previous results, Ru/MCM-48 stands as a promising candidate for the conversion of cellulose into hexitols (sorbitol and mannitol). Thus, in **Chapter 2**, one – pot hydrolytic hydrogenation of cellulose was studied using Ru/MCM-48 (4 wt. % Ru). Alternatively, Supercritical water (SCW) hydrolysis in ultrafast reactors was performed at 400 ºC – 25 MPa and extremely low reaction times ~ 0.20 s to partially depolymerize cellulose with high selectivity to sugars (70 % $w \cdot w^{-1}$) avoiding degradation reactions. From this SCW hydrolysis step, although the 100% of cellulose was converted, a high yield of the hydrolysed products were detected as oligosaccharides. The hydrogenation of the liquid product from SCW hydrolysis of cellulose over Ru/MCM-48 allowed to complete the hydrolysis of oligosaccharides to monomeric sugars and maximize the yield to hexitols by changing experimental parameters such as temperature and reaction time. A greater yield to hexitols was obtained by the subsequent hydrogenation of the liquid product from cellulose hydrolysis in SCW (49 %) than using the one – pot catalytic hydrogenation from untreated cellulose (21 %). Ru/MCM-48 showed better behaviour than standard Ru/C during the hydrogenation processes, under comparable experimental conditions in all the cases. Thus, Ru/MCM-48 was also tested in the hydrogenation of the product from sugar beet pulp (SBP) hydrolysis in SCW. SBP was used in order to evaluate the behaviour of a real biomass in the proposed two-steps process. A yield to hexitols of 15 % was achieved by hydrogenation of SBP hydrolysates, ethylene glycol was the main compound in the liquid product with a yield of 21 % and glycerol was also obtained as by-product. These results have shown the potential of coupling the SCW hydrolysis with the hydrogenation using Ru/MCM-48 as catalyst for the production of biomass derived alcohols.

The high price of noble metals such as Ru, could represent an important drawback for the development of these catalytic systems. Thus, the development of novel bimetallic nickel-based catalytic systems with comparable high activity to noble metal catalysts still remains a technological challenge. In **Chapter 3**, the preparation of three different bimetallic Ru:Ni catalysts supported on a mesoporous silica MCM-48 by consecutive wet impregnations is proposed. These catalysts were compared with the corresponding monometallic Ni/MCM-48. All the catalytic materials were characterized by means of X-Ray Diffraction (XRD), Transmission Electron Microscopy (TEM), adsorption / desorption of N_2, Temperature Programmed Reduction (H_2-TPR),

desorption at programmed temperature of ammonia (NH_3– TPD) and Atomic Absorption (AA) and tested in the liquid phase hydrogenation of D-Glucose into sorbitol in the temperature range 120 – 140 ºC under 2.5 MPa of H_2 pressure. The catalyst so prepared presented a total metal loading of ca. 3 % ($w \cdot w^{-1}$), where Ru:Ni ratios spanned the range of 0.15 – 1.39 ($w \cdot w^{-1}$). Ru:Ni/MCM-48 catalysts with Ru:Ni ratios higher than 0.45 enhanced the specific activity of the monometallic Ni/MCM-48 in the hydrogenation of D-Glucose to sorbitol, increasing the reaction rate and showing complete selectivity to sorbitol. Activation energy values of 36 $KJ \cdot mol^{-1}$ and 70 $KJ \cdot mol^{-1}$ were obtained for Ni/MCM-48 and Ru:Ni/MCM-48 (0.45). In addition, Ru:Ni/MCM-48 (0.45) demonstrated a good stability after three reaction cycles, standing as a good option for the effective hydrogenation of carbohydrate sugars into sugar alcohols.

The experimental work corresponding to the first three chapters were carried out at the University of Valladolid, within the High Pressure Processes Group. However, next two chapters were developed in the Institut de recherches sur la catalyse et l'environement de Lyon (Lyon, France) within a three-month stay, where different mesoporous catalyst were prepared and tested for biomass conversion purposes. In **Chapter 4**, bifunctional Ru/Al-MCM-48 was prepared by wet impregnation method and characterized by means of adsorption-desorption of N_2, small angle X-Ray scattering (SAXS), H_2-TPR, XRD, TEM, NH_3-TPD and AA. The so prepared Ru/Al-MCM-48 (3.5 wt. % Ru) was tested in the catalytic hydrogenolysis of cellobiose towards hexitols. The introduction of Aluminum into MCM-48 structure increased the number of acid sites compared to MCM-48 and these features played an important role for hydrolysis steps involved in the global reaction mechanism. Moreover, hydrogenation steps took place on metallic ruthenium sites. A kinetic study of the hydrogenolysis of cellobiose to hexitols over Ru/Al-MCM-48 was developed, where different parameters such as pressure of hydrogen, temperature and reaction time were evaluated. Cellobitol was the main intermediate of the conversion of cellobiose to hexitols over Ru/Al-MCM48. Temperatures in the range of 140 – 180 ºC and pressures between 30 and 50 MPa H_2 were studied and it was noticed a positive influence of both parameters in order to maximize the production of hexitols. A maximum yield of 91 % of hexitols was achieved by catalytic hydrogenolysis of cellobiose over Ru/Al-MCM48 at 180 ºC, 5 MPa H_2 and 7 min, where sorbitol was the main compound in the final product with a yield of 82 %. A kinetic model covering different reaction temperatures

was also developed, which predicted well the concentration of the different compounds involved in the proposed reaction pathway. Specific reaction rates and activation energy values were also obtained for the different steps of the catalytic process. In addition, mass transfer effects were evaluated in detailed.

Besides conversion of biomass into sugar alcohols, further transformation into liquid alkanes has currently attracted a great deal of attention in order to reduce the dependence of fossil fuels. In **Chapter 5**, conversion of D-Glucose into short-chain alkanes (mainly n-butane, n-pentane, n-hexane) in a one-pot biphasic catalytic system is reported. Catalytic tests were performed at 190 ºC under 5 MPa of H_2 in a biphasic n-decane – water reaction medium, where different catalytic materials were used for the production of straight-chain alkanes. Catalytic behaviour of supported Ru/Al-MCM-48 and acidified Ru/MCM-48 with tungstophosphoric acid (TPA) was compared with that obtained by a standard Ru/C. Mesoporous catalytic materials were characterized by means of adsorption / desorption of N_2, XRD, TEM, H_2-TPR, NH_3 – TPD and AA. A higher yield to alkanes around 57 % was obtained over Ru/Al-MCM-48, while a yield to alkanes of 29 % was achieved by commercial Ru/C. Moreover, the addition of Al-MCM-48 combined with Ru/C resulted in an important improvement in the production of alkanes compared to that achieved by Ru/C. The influence of TPA as homogeneous catalyst was also studied with Ru/Al-MCM-48 and commercial Ru/C. The highest yield of alkanes around 81.9 % (n-butane 7.1 %, n-pentane 29.3 % and n-hexane 45.4 %) was obtained over Ru/C + Al-MCM-48 system.

INTRODUCTION:

CONVERSION OF CELLULOSIC BIOMASS INTO CHEMICALS OVER METAL CATALYSTS

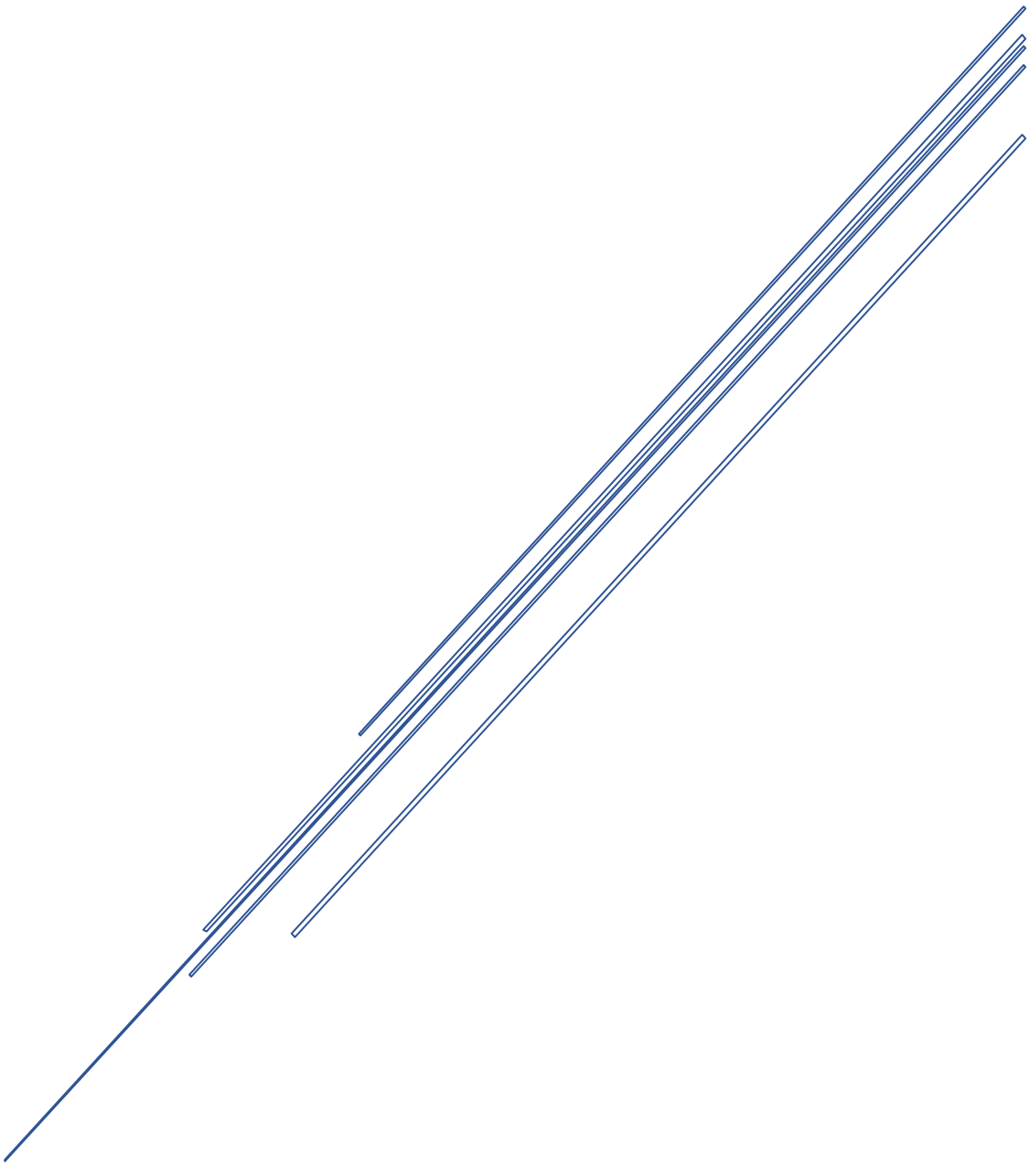

2.1. THESIS FRAMEWORK

The present work is included into CATHYCEL project financed by the Spanish Government of Science and Innovation (MICINN, CTQ2011-27347) entitled "Synthesis of catalysts in supercritical carbon dioxide for the selective conversion of cellulose into commodities" and leaded by Dr. Gloria Esther Alonso Sánchez from University of Valladolid (UVa). Dr. Antonio Nieto-Márquez from Technical University of Madrid (UPM) who is the co-director of this PhD thesis, was included in the team work of this project. Cathycel project had a total duration of 43 months, starting on January of 2012. The total funding received for this national project was 145.200 €.

The current challenge in conversion of cellulosic biomass towards fine chemicals is focused on the development of green and economically competitive processes. In general terms, the global process of conversion of cellulose into chemicals consists on at least two different steps: hydrolysis of cellulose and further reaction pathways to use the glucose as platform molecule. Hydrogenation is one possibility of valorization since biomass is a strongly oxygenated raw material. Heterogeneous catalysis represents a key point to develop such kind of processes. Therefore, the development of novel, cheaper and more selective heterogeneous catalysts seems to be a very important task.

Different transition metals such as Ni, Ru, Fe or Co have been introduced into many supports. In these terms, Ru-based catalysts, which are cheaper than other noble metals such as Pd and Pt, has shown reasonable high activity and selectivity in hydrogenation reactions [1]. In addition, Ru-based catalysts have performed a good catalytic behaviour in order to convert cellulose into sorbitol under hydrogen atmosphere [2]. Tungsten and nickel based catalyst also shown high yields to ethylene glycol production using cellulose as raw material [3, 4].

The general aim of this project and its novelty lies in synthesizing supported Ru, W and Ni catalysts over mesoporous silica for the selective hydrolysis of cellulose to glucose and the production of sugar alcohols, together with the use of supercritical carbon dioxide media for their preparation in comparison with incipient wetness impregnation as conventional method.. These facts contribute to the development of the research for the conversion of biomass in two different aspects: i) Design of novel, effective, selective and reusable catalysts for hydrolysis of cellulose to glucose and the

production of sugar alcohols. ii) Develop a "green" technology for the preparation of supported metal catalyst based on supercritical carbon dioxide.

The project supports the following specific objectives:

1. Study of the effect of the different experimental parameters in the deposition of metals (Ru, W, Ni) over different supports (TiO_2, activated carbon, mesoporous silica) using sc-CO_2. Temperature, and pressure of CO_2, as well as concentration and the type of metal precursor are studied. In addition, the experimental conditions and methodology in order to reduce metal particles and operational time are also considered.
2. Characterization of the prepared catalytic materials. Different properties of the materials are analysed, such as morphology, cristallinity, textural properties, dispersion of the active metal on the support, oxidation state, etc.
3. Catalytic activity tests of the synthesized materials. Catalytic activity of the synthesized materials are evaluated in the hydrolysis of cellulose in hot compressed water (HCW), as well as in the hydrogenation of cellulose and its related model compounds, such as cellobiose, glucose and fructose. Catalytic activity of the materials prepared in sc-CO_2 is compared to that obtained by catalyst synthesizes by conventional methods in the laboratory.
4. Proposal of reaction pathways for the studied catalytic processes.

In this thesis, the aspects related with objectives 2, 3 and 4 of CATHYCEL project have been developed. Therefore, in the present research work catalytic conversion of cellulose and its related model compounds into sugar alcohols over mesoporous metal catalysts prepared by wet impregnation method, have been carried out.

2.2. CONVERSION OF CELLULOSIC BIOMASS INTO CHEMICALS OVER METAL CATALYSTS

Cellulosic biomass has been extensively used for many years in order to produce different kind of products, such as paper, vessels, buildings, ropes and cloth, since it is a fiber-rich material which provides hardness and high-tension strength. Nowadays, due to the depletion of fossil energy resources and pressing environmental issues, cellulosic biomass appears as one of the most promising alternatives to produce chemicals, energy and fuels [5]. This fact is involved in the actual *"biorefinery concept"*, which presents similar goals to the classical petroleum refineries but using bioderived feedstocks [6].

Differing from fossil fuels such as petroleum or coal, cellulose comprises a high content of oxygen in its structure (c.a. 50 wt. %) besides hydrogen and carbon elements, which is a great advantage in order to synthesize oxygen-containing chemicals like sugar alcohols [7]. The present introduction shows some alternatives for the conversion of cellulose and their related model compounds into sugar alcohols over different metal catalysts.

2.2.1. HYDROGENATION OF D-GLUCOSE

As it was listed by the U.S Department of Energy [8], sorbitol is one of the top 12 bioderived building blocks, that can be easily converted into fuels and chemicals [9, 10]. More than 800.000 ton·y^{-1} of sorbitol are produced by catalytic hydrogenation of the carbonyl group of D-Glucose (Scheme 1) [11]. Sorbitol is a large-scale industrial product, which is used for a wide range of applications, such as additive in many industrial products, mainly in paper, cosmetic and food industry. In addition, it is also employed as building block for synthesizing fine chemicals such as vitamin C.

Sorbitol is produced by the hydrogenation of D-Glucose solutions obtained by hydrolysis of starch-containing crops (D-Glucose concentration up to 65 wt. %) in discontinuous batch slurry reactors at hydrogen pressures between 5 – 15 MPa and temperatures in the range of 100 and 180 ºC. During the hydrogenation process some by-products can be obtained as a result of different side reactions: 1) D-Glucose can isomerize into fructose and mannose by Lobry de Bruyn–Alberda van Ekenstein rearrangements [12], which are further hydrogenated into mannitol and sorbitol [13, 14]. 2) The obtained sorbitol from the hydrogenation of D-Glucose, can be also isomerized into mannitol [15]. Although different active metals, such as Ru, Ni, Rd and Pd, can be used for the conversion of D-Glucose into sorbitol, Raney nickel catalysts (sponge or skeletal nickel) are the most used at industrial scale for this purpose. In order to improve the specific catalytic activity of monometallic nickel catalysts, the addition of promoting metals was studied [16]. Gallezot et al. tested Mo-, Cr- and Fe- promoted Raney-type nickel catalysts for the hydrogenation of D-Glucose, showing an enhancement of the reaction rate around 7-fold compared to the unpromoted catalytic material [17]. The authors found that electropositive metal promoters act as Lewis acid sites, which polarize carbonyl group of D-Glucose (C=O) improving the reaction rate of the hydrogenation process. However, Fe-promoted Raney-type nickel catalysts deactivated very fast due to leaching of the promoting agent, while Cr- and Mo-

promoted materials were more robust against deactivation. In essence, nickel-based catalysts prone to deactivate by leaching and sintering, resulting in a decrease in the catalytic activity. Moreover, leached nickel is an important disadvantage when the desired product is used for food, medical or cosmetic applications, since its removal from the final solution resulting in additional costs to the overall production process [9].

D-Glucose hydrogenation was also developed in continuous processes, such as in trickle-bed reactors [18, 19]. Differing from the discontinuous process, supported nickel catalysts were employed for this purpose. Déchamp et al. carried out the hydrogenation of D-Glucose solution (40 wt. %) towards sorbitol over Kieselguhr-supported nickel catalyst (48.4 wt. % Ni) at 8 MPa and 130 ºC, where the catalytic material demonstrated a poor activity around 5 $mmol \cdot h^{-1} \cdot g_{Ni}^{-1}$ [18]. The specific reaction rate decreased even more when time on stream was increasing, owing to the progressive leaching of Ni and SiO_2 in the aqueous reaction media. Kusserow et al. reported the preparation of Ni/SiO_2 by aqueous impregnation using nickel ethylenediamine as metal precursor, demonstrating high resistance to leach after 5 h on stream [19]. However, Ni/SiO_2 showed lower activity and selectivity to sorbitol in comparison with other similar commercial catalysts.

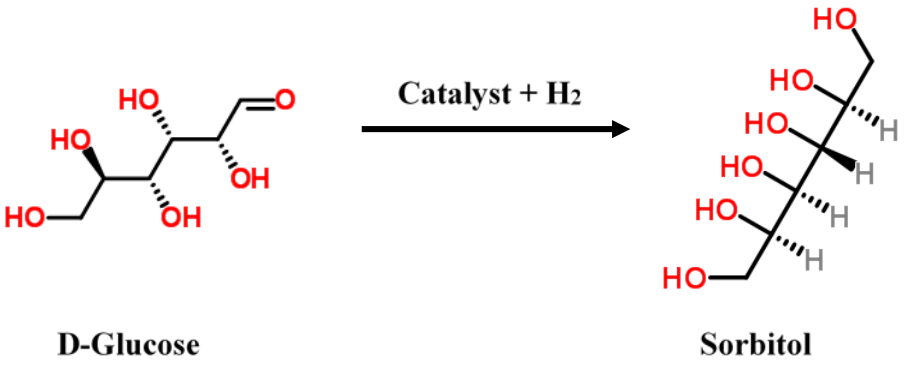

Scheme 1. D-Glucose hydrogenation into sorbitol

According to the aforementioned explanations, leaching and sintering of the active metal in the case of nickel catalysts are significant drawbacks to take into account for its utilisation in the hydrogenation of D-Glucose. Consequently, the challenge consisted on testing catalytic materials based on different active metals, such as Ru-, Pt-, Pd- and Pt-based catalyst [20-23]. The following sequence of decreasing activity for D-Glucose hydrogenation over different metal supported catalysts has been observed in the

literature: Ru > Ni > Rh > Pd [24]. Therefore, the best catalytic performance was found for ruthenium-supported catalysts.

Ruthenium has been dispersed over different kind of supports showing 50-fold higher catalytic activity than nickel, under comparable experimental conditions. Ruthenium over activated carbon (Ru/C) offer an interesting alternative to nickel catalyst, since they have demonstrated that Ru is not dissolved, being stable to leaching in the reaction media, under the reaction conditions for D-Glucose hydrogenation [9, 11]. Hoffer et al. reported the use of Ru/C for this purpose, concluding that the activity of ruthenium was proportional to its specific surface area and independent of the preparation procedure [25].

It is well known that support materials are also subjected to deactivation phenomena. Therefore, while activated carbon and TiO_2 have shown good stability against leaching, other support materials such as Al_2O_3 and SiO_2 deactivated due to changes in their physical properties [26, 27]. Ru/TiO_2 with a metal loading around 1 wt. % was reported by Mishra et al., showing high selectivity to sorbitol production around 93 %, at 120 ºC, 5.5 MPa H_2 and 120 min [28]. The authors observed an interesting increase of the selectivity to sorbitol up to 97 %, after the modification of TiO_2 by impregnation nickel chloride and the following calcination ($Ru/NiO\text{-}TiO_2$, 1 wt % Ru). Modified $NiO\text{-}TiO_2$ avoided isomerization of D-Glucose to D-Fructose, enhancing the selectivity to sorbitol in comparison with the unmodified TiO_2. Ru/Al_2O_3 was also tested for the hydrogenation of D-Glucose in a trickle-bed reactor for a long time on stream [27], showing deactivation of the catalyst due to the disruption of the structure of Al_2O_3 and to the poisoning by gluconic acid obtained from Cannizarro reaction, sulphur and iron. Maris et al. described the use of Ru/SiO_2 catalyst, reporting the growth of Ru nanoparticles after extended exposure to glucose in a H_2-saturated aqueous solution (approximately 6 h of reaction time) [26]. Consequently, the growth of Ru particles resulted in a significant reduction of the reaction rate. Ru has also been deposited over other silica materials, such as MCM-41. Zhang et al. tested 3.80 % Ru/MCM-41, achieving a yield to sorbitol around 83 %, which decreased after four recycling cycles to 68 % [29]. The authors attributed this fact to the accumulation of some reaction product to the surface of the catalyst, which resulted in a clear decrease of the catalytic activity. The use of supported Ru-based catalysts has been also extensively used for the hydrogenation of disaccharides, such as cellobiose.

2.2.2. Hydrogenolysis of cellobiose

For the hydrolytic hydrogenation of cellobiose, two competing reaction mechanisms have been observed (Scheme 2).

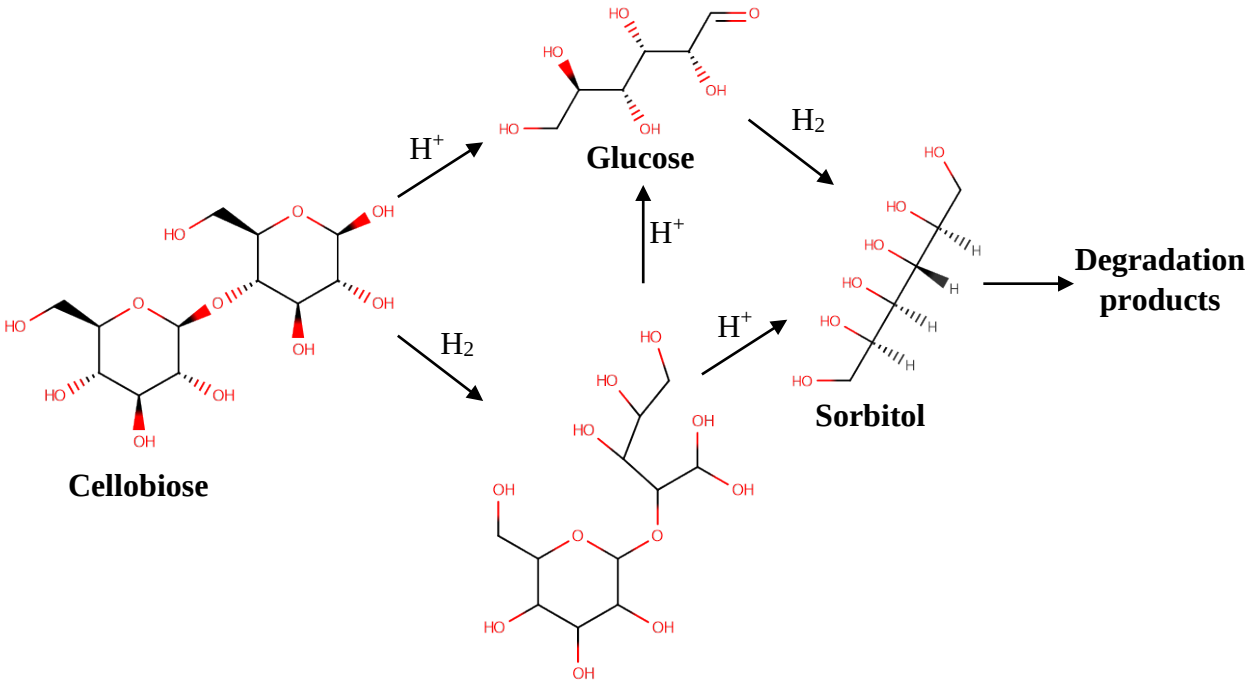

Scheme 2. Proposed reaction pathway for the catalyticconversion of cellobiose into sorbitol by Neghadar et al. [30].

Cellobiose can be converted to sorbitol following the cleavage of the glycosidic (C–O–C) bonds, via hydrolysis of cellobiose into glucose and the consecutive hydrogenation of glucose to sorbitol. However, different authors have reported other alternative reaction route for the conversion of cellobiose to sorbitol. Under acid experimental conditions and using supported metal catalyst, cellobiose either undergoes hydrolysis to glucose or as an alternative pathway proceeds through the hydrogenation of the C–O bond on one of the glucose rings leading to cellobitol (3-β-D-glucopyranosyl-D-glucitol). Then, cellobitol can be hydrolysed to sorbitol and glucose [7].

Some efforts related to the catalytic conversion of cellobiose towards sorbitol have been reported in the literature. Deng et al. studied conversion of cellobiose into sorbitol over Ru/CNT using different concentrations of HNO_3, where different key factor of the

catalyst for this purpose were evaluated [31]. The authors stated that Ru nanoparticles higher than 8.7 nm, which exhibited higher acidity values, resulted in higher yield to sorbitol. A maximum yield to sorbitol around 87 % was achieved over Ru/CNT at 185 ºC, 5 MPa H_2 and 3h. It was elucidated that the main pathway for the conversion of cellobiose into sorbitol was the production of cellobitol and its subsequent hydrogenation to sorbitol, although glucose pathway was also detected. Zhang et al. studied the direct conversion of cellobiose into sorbitol over Ru/C catalyst (3.6 wt. % Ru) and 0.05 wt. % H_3PO_4 solution [32]. The authors stated that a sorbitol yield around 87 % was attained at 185 ºC for 1 h under 3MPa H_2. The obtained sorbitol yield over fresh catalyst decreased from 87 % to 41 % after three recycling cycles, due to the deactivation of the catalyst. Deactivation was associated to a significantly adsorption of organic molecules, which produced a decrease of the specific surface area, resulting in the reduction of the activity of Ru/C. Li et al. investigated the conversion of cellobiose into sorbitol using $ZnCl_2$ salt and Ru/C, achieving a maximum yield to sorbitol of 95 % at 125 ºC, 4 MPa H_2 and 375 min [33]. The presented results by those authors demonstrated a competition between glucose and cellobitol pathways, concluding that the second one was the main pathway. The authors stated that the contribution of both pathways is attributed to different experimental variables of the reaction, such as temperature, metal loading of the catalysts and presence of mineral acids. Neghadar et al. developed a kinetic study of the catalytic conversion of cellobiose into sorbitol using a combination of heteropolyacids and Ru/C (5 wt. % Ru) [30]. A maximum selectivity to sorbitol around 75 % was obtained at 170 ºC, 5 MPa H_2 and 1.25 h. The authors proposed a kinetic model for the global process and reaction rates and activation energy values were obtained using non-linear regression analysis. Neghadar et al. also observed that cellobitol pathway was the most important, especially at lower reaction temperatures. Regardless of the reaction pathway, hydrolysis was the rate determining step of the overall reaction process. Ru/Zr-SBA-15, combining acid and active metal sites in its mesoporous structure, was proposed by Niu et al.[34] for the production of hexitols. A yield of sorbitol around 72 % was produced over Ru/Zr-SBA-15 (1.81 wt. % Ru) at 140 ºC, 5 MPa and 1 h. Kinetic study demonstrated that the hydrolysis of cellobitol to sorbitol and glucose, which took place on the acid sites of the catalyst was the rate-determining step of the global process, while Ru-catalyzed hydrogenation steps were much faster. Comparing the catalytic behaviour of Ru/Zr-SBA-15 after three reaction cycles under similar experimental conditions, it was observed that yield to

sorbitol was 8-fold lower than using the fresh catalyst. The catalyst was active for the hydrogenation of cellobiose to cellobitol, but it deactivated for the subsequent hydrolysis of cellobitol to sorbitol. Recently, Almeida et al. studied the catalytic behaviour of bifunctional RuNPs/A15 (3 wt. % Ru) [35]. Experimental results pointed that 80 % of yield to sorbitol was obtained at 150 ºC 4 MPa and 5 h, which is higher than the yield of sorbitol achieved using the physical mixture of Ru/C (5 wt. %) and Amberlyst 15.

2.2.3. Conversion of cellulose into hexitols

Conversion of cellulose into hexitols consist of two different steps: 1) *Hydrolysis of cellulose into glucose,* where acidity of the reaction medium plays an important role in order to improve the rate of this step and *2) hydrogenation of glucose,* which is performed over active metals such Ru, Rh, Pd, Ni. Cellulose is a highly complex and stable polysaccharide, consisting on *β*-1,4-glycosidic linkages and organized in microcrystalline domains. These facts hinder its hydrolysis towards D-Glucose, except by enzymes under mild conditions, while D-Glucose is easily degraded under harsh reaction conditions (subcritical water at 180 – 260 ºC) [36] due to the presence of a hemiacetal group in its chemical structure [37]. Thus, this trade-off is a key factor for the catalytic conversion of cellulose. In addition, collisions between cellulose and solid acid catalysts have represented an important challenge for the hydrolytic conversion of cellulose.

Regarding the difficulty to convert cellulose to platform molecules, physical and chemical treatments combined with catalytic reactions have been proposed [38, 39]. Pre-treatments such as ball-milling have been extensively used to overcome the low reactivity of cellulose, by decreasing its particle size and crystallinity, resulting in an important improvement of the accessibility of the substrate to the active sites of the catalysts during hydrolysis step. In this sense, crystallinity is the key factor regarding cellulose reactivity in hot compressed water, while particle size only plays a secondary role [40].

In general terms, the major part of the studies are focused on the production of sugar alcohols by one-pot hydrolysis-hydrogenation processes over bifunctional supported metal catalysts or the combination of metal catalysts and homogeneous catalysts (liquid acids) [41]. This one-pot process is an interesting alternative that is able to avoid the

aforementioned challenges related to D-Glucose degradation under the selected reaction conditions. Thus, cellulose is firstly hydrolysed to glucose, which is subsequently hydrogenated into thermally more stable products (sugar alcohols) than D-Glucose, avoiding its degradation before hydrogenation step.

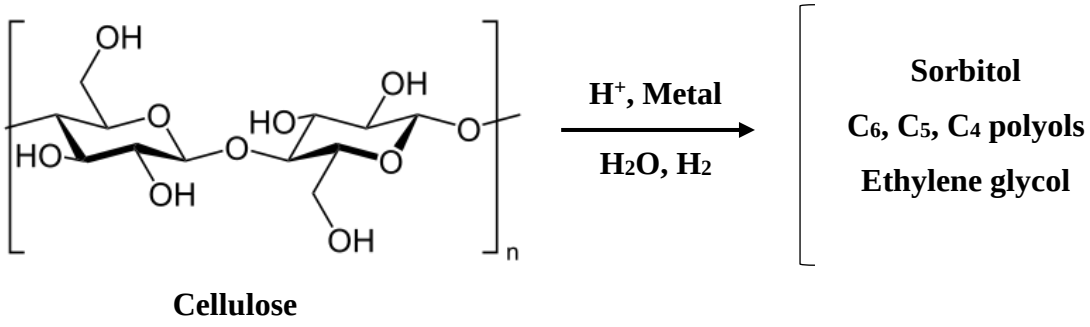

Cellulose

Scheme 3. One-pot hydrolysis/hydrogenation of cellulose over supported metal catalysts.

Fukuoka et al. demonstrated for the first time in 2006 that supported metal catalysts can convert cellulose towards sugar alcohols over Pt/γ-Al_2O_3 (2.5 wt. %) by an environmentally friendly method such as one-pot process [37]. In that research work, the authors achieved a yield of sorbitol around 25 % and a yield of mannitol of 6 % was also obtained converting microcrystalline cellulose at 190 ºC, 5 MPa H_2 and 24 h. Kobayashi et al. tested Pt/BP2000 (BP2000: carbon black, Cabot) increasing the yield to hexitols up to 43 % using microcrystalline cellulose (80 % crystallinity) at similar experimental conditions than that used for Pt/γ-Al_2O_3 [42]. In addition, the same authors study the influence of ball-milling of cellulose in the final yield to hexitols. The use of 2 days ball-milled cellulose using Pt/BP2000 (2 wt. %) resulted in an important increase of the yield to hexitols from 43 to 58 %, since the lower crystallinity of cellulose after 2 days of ball-milling (22 %) allows enhancing cellulose conversion. Other noble metals such as Ru, Rh, Pd and Ir were also deposited over BP2000 in the same research work, but Ru/BP2000 demonstrated being also effective for the conversion of cellulose into hexitols, while Rh, Pd and Ir gave lower amounts of hexitols.

Most of the subsequent research on this field has been developed over ruthenium supported catalysts. Luo et al. tested Ru/C (4 wt. %) for the conversion of microcrystalline cellulose at 245 ºC, 6 MPa and 30 min, obtaining a yield to hexitols around 39 %. Both the high activity of ruthenium and the severe experimental condition selected in that work, promoted hydrogenolysis of the so obtained sorbitol to other

byproducts (11 % sorbitan, 5 % xylitol, 6 % erythritol, 6 % glycerol, 7 % propylenglycol, 6 % ethylene glycol). Bifunctional sulfonic acid-functionalized Ru/SiO_2-SO_3H (3 wt. % Ru), combining Brønsted acidic sites and metal sites, was also employed for the conversion of 30 h ball-milled cellulose and a high yield of hexitols of 68 % was produced, at 150 ºC, 4 MPa H_2 and 10 h [43]. Xi et al. used a mesoporous niobium phosphate supported ruthenium bifunctional catalyst $Ru/NbOPO_4$ (5 wt. % Ru) for the conversion of ball-milled cellulose at 170 ºC, 4 MPa H_2 and 24 h [44]. $Ru/NbOPO_4$ demonstrated an excellent catalytic performance (69 % yield to sorbitol) associated to the synergic effect between mesoporous niobium phosphate for hydrolysis of cellulose step and ruthenium nanoparticles for hydrogenation step. In addition, $Ru/NbOPO_4$ was very stable to recycling after several runs. A supported ruthenium on ordered mesoporous carbon Ru/CMK-3 (2 wt. % Ru) reported by Kobayashi et al., produced hexitols with a yield of 45 % from ball-milled cellulose at 190 ºC and 18 h, using 2-propanol as source of hydrogen [45].

Although ruthenium based catalysts have shown promising results, their high price limits their use at industrial scale for the hydrolytic hydrogenation of cellulose. Thus, nickel based catalysts have been tested for the catalytic conversion of cellulose into hexitols. Liang et al. studied the catalytic hydrogenation of cellulose over Ni/ZSM-5 (40 wt. % Ni) at 240 ºC, 4MPa and 4 h, achieving a yield to hexitols of 49 %. This result was comparable to that obtained by Ding et al. [46], where a yield of hexitols of 53 % was obtained from the conversion of microcrystalline cellulose at 225 ºC, 6 MPa H_2 and 1.5 h over Ni_2P/AC (16 wt. %). In that case, the excess of phosphide presented in the catalyst was able to promote hydrolysis of cellulose, while nickel catalysed the hydrogenation step. Recently, Kobayashi et al. reported the catalytic performance of carbon-supported Ni catalyst Ni(50)/KB (50 wt. %) gave 64% yield of hexitols (sorbitol 57% and mannitol 6.8%) with 71% selectivity based on the conversion of cellulose (90%) [47]. Thus, Ni(50)/KB was very active for the catalytic production of hexitols from cellulose, being fairly durable. In that work it was observed that Ni loading was a key factor in this process, since higher nickel loadings enhanced both hexitols yields and durability of the catalyst.

Under typical experimental conditions (hot compressed water at around 230 ºC) for the conversion of cellulose towards hexitols, nickel easily deactivated and it has demonstrated lower activity compared to other active metals. In order to overcome these

drawbacks, different bimetallic catalysts have been proposed in the literature, combining noble metals such as Rh, Pt, Pd, Ir and Ru with Ni [48]. Shrotri et al. shown that the addition of small amounts of Pt to Ni catalysts resulted in a significantly enhance of the specific catalytic activity [49]. Those authors improved the yield to hexitols over bimetallic Pt-Ni/Al_2O_3 (32.4 %) up to 6.5-folds in comparison with monometallic Ni/Al_2O_3 (5 %), at 200 ºC, 5 MPa H_2 and 6 h. In addition, Pt-Ni deposited over mesoporous β-zeolite was also tested in that research work, obtaining even higher yield to hexitols (36.6 %) than that achieved over Pt-Ni/Al_2O_3. Bimetallic combination of Pt-Ni promoted the protonation of water and H_2, which spills over to nickel sites creating in situ acid sites to enhance hydrolysis of cellulose step. Pang et al. reported the conversion of microcrystalline cellulose at 245 ºC, 6 MPa and 0.5 h, over bimetallic Rh-Ni dispersed on mesoporous three-dimensional carbon (Rh-Ni/MC, 1 wt. % Rh and 5 wt. %) [50]. Rh-Ni/MC gave a maximum yield to hexitols of 59.8 %.

Up to our knowledge, the highest yields to hexitols have been obtained from the conversion of ball-milled cellulose using combinations of soluble acids and metal catalysts. Geboers et al. successfully tested $Cs_{3.5}SiW$ + Ru/C for the production of hexitols from ball-milled cellulose [51]. Caesium salts were highly selective avoiding hydrogenolysis side reactions, allowing the achievement of an important yield to hexitols of 90 % under mild reaction conditions (190 ºC, 5 MPa H_2 and 24 h). The combination of heteropolyacid $H_4SiW_{12}O_{40}$ and Ru/C, also resulted in a high yield to hexitols around 92 %, at 190 ºC 5 MPa H_2 and 0.33 h, using ball-milled cellulose [52]. In addition, a significantly yield to hexitols was achieved from the conversion of ball-milled cellulose over Ru-loaded zeolites and trace amounts of mineral acid. Ru/H-USY (0.2 wt. % Ru) combined with a low concentration of HCl (35 ppm, pH=3), at 190 ºC, 5 MPa H_2 and 24 h, shows excellent yield to hexitols up to 93 % [53]. HCl converted cellulose to oligosaccharides, which were subsequently depolymerized into D-Glucose over the acid sites of H-USY. Then, ruthenium active sites hydrogenated D-Glucose adsorbed in the pore channels of the zeolite into hexitols, reducing the diffusion path of D-Glucose [48].

References

1. Sapunov, V.N., et al., *d-Glucose Hydrogenation over Ru Nanoparticles Embedded in Mesoporous Hypercrosslinked Polystyrene.* The Journal of Physical Chemistry A, 2013. **117**(20): p. 4073-4083.

2. Deng, W., et al., *Conversion of Cellulose into Sorbitol over Carbon Nanotube-Supported Ruthenium Catalyst.* Catalysis Letters, 2009. **133**(1): p. 167.

3. Ji, N., et al., *Direct Catalytic Conversion of Cellulose into Ethylene Glycol Using Nickel-Promoted Tungsten Carbide Catalysts.* Angewandte Chemie, 2008. **120**(44): p. 8638-8641.

4. Zhao, G., et al., *Catalytic Conversion of Cellulose to Ethylene Glycol over Tungsten Phosphide Catalysts.* Chinese Journal of Catalysis, 2010. **31**(8): p. 928-932.

5. Dabbawala, A.A., D.K. Mishra, and J.-S. Hwang, *Selective hydrogenation of D-glucose using amine functionalized nanoporous polymer supported Ru nanoparticles based catalyst.* Catalysis Today, 2016. **265**: p. 163-173.

6. Shuttleworth, P.S., et al., *Applications of nanoparticles in biomass conversion to chemicals and fuels.* Green Chemistry, 2014. **16**(2): p. 573-584.

7. Zheng, M., et al., *Mechanism and Kinetic Analysis of the Hydrogenolysis of Cellulose to Polyols*, in *Reaction Pathways and Mechanisms in Thermocatalytic Biomass Conversion I: Cellulose Structure, Depolymerization and Conversion by Heterogeneous Catalysts*, M. Schlaf and Z.C. Zhang, Editors. 2016, Springer Singapore: Singapore. p. 227-260.

8. Wang, S., et al., *Ru–B amorphous alloy deposited on mesoporous silica nanospheres: An efficient catalyst for d-glucose hydrogenation to d-sorbitol.* Catalysis Today, 2015. **258, Part 2**: p. 327-336.

9. Corma, A., S. Iborra, and A. Velty, *Chemical Routes for the Transformation of Biomass into Chemicals.* Chemical Reviews, 2007. **107**(6): p. 2411-2502.

10. Murillo Leo, I., et al., *Selective conversion of sorbitol to glycols and stability of nickel–ruthenium supported on calcium hydroxide catalysts.* Applied Catalysis B: Environmental, 2016. **185**: p. 141-149.

11. Besson, M., P. Gallezot, and C. Pinel, *Conversion of Biomass into Chemicals over Metal Catalysts.* Chemical Reviews, 2014. **114**(3): p. 1827-1870.

12. Schimpf, S., C. Louis, and P. Claus, *Ni/SiO2 catalysts prepared with ethylenediamine nickel precursors: Influence of the pretreatment on the catalytic properties in glucose hydrogenation.* Applied Catalysis A: General, 2007. **318**: p. 45-53.

13. Heinen, A.W., J.A. Peters, and H. van Bekkum, *Hydrogenation of fructose on Ru/C catalysts.* Carbohydrate Research, 2000. **328**(4): p. 449-457.

14. Mishra, D.K. and J.-S. Hwang, *Selective hydrogenation of d-mannose to d-mannitol using NiO-modified TiO2 (NiO-TiO2) supported ruthenium catalyst.* Applied Catalysis A: General, 2013. **453**: p. 13-19.

15. De, S. and R. Luque, *Nanomaterials for the Production of Biofuels*, in *Nanomaterials for Sustainable Energy*, Q. Li, Editor. 2016, Springer International Publishing: Cham. p. 559-582.

16. Chen, B., et al., *New developments in hydrogenation catalysis particularly in synthesis of fine and intermediate chemicals.* Applied Catalysis A: General, 2005. **280**(1): p. 17-46.

17. Gallezot, P., et al., *Glucose hydrogenation on promoted raney-nickel catalysts.* Journal of Catalysis, 1994. **146**(1): p. 93-102.

18. Déchamp, N., et al., *Kinetics of glucose hydrogenation in a trickle-bed reactor.* Catalysis Today, 1995. **24**(1): p. 29-34.

19. Kusserow, B., S. Schimpf, and P. Claus, *Hydrogenation of Glucose to Sorbitol over Nickel and Ruthenium Catalysts.* Advanced Synthesis & Catalysis, 2003. **345**(1-2): p. 289-299.

20. Mishra, D.K., et al., *Selective hydrogenation of d-glucose to d-sorbitol over HY zeolite supported ruthenium nanoparticles catalysts.* Catalysis Today, 2014. **232**: p. 99-107.

21. Lazaridis, P.A., et al., *d-Glucose hydrogenation/hydrogenolysis reactions on noble metal (Ru, Pt)/activated carbon supported catalysts.* Catalysis Today, 2015. **257, Part 2**: p. 281-290.

22. Sanz-Moral, L.M., et al., *Tuned Pd/SiO2 aerogel catalyst prepared by different synthesis techniques.* Journal of the Taiwan Institute of Chemical Engineers, 2016. **65**: p. 515-521.

23. Zhang, X., et al., *Platinum-Catalyzed Aqueous-Phase Hydrogenation of d-Glucose to d-Sorbitol.* ACS Catalysis, 2016: p. 7409-7417.

24. Wisnlak, J. and R. Simon, *Hydrogenation of Glucose, Fructose, and Their Mixtures.* Industrial & Engineering Chemistry Product Research and Development, 1979. **18**(1): p. 50-57.

25. Hoffer, B.W., et al., *Carbon supported Ru catalysts as promising alternative for Raney-type Ni in the selective hydrogenation of d-glucose.* Catalysis Today, 2003. **79–80**: p. 35-41.

26. Maris, E.P., et al., *Metal Particle Growth during Glucose Hydrogenation over Ru/SiO2 Evaluated by X-ray Absorption Spectroscopy and Electron Microscopy.* The Journal of Physical Chemistry B, 2006. **110**(15): p. 7869-7876.

27. Arena, B.J., *Deactivation of ruthenium catalysts in continuous glucose hydrogenation.* Applied Catalysis A: General, 1992. **87**(2): p. 219-229.

28. Mishra, D.K., et al., *Liquid phase hydrogenation of d-glucose to d-sorbitol over the catalyst (Ru/NiO–TiO2) of ruthenium on a NiO-modified TiO2 support.* Catalysis Today, 2012. **185**(1): p. 104-108.

29. Zhang, J., et al., *Efficient conversion of d-glucose into d-sorbitol over MCM-41 supported Ru catalyst prepared by a formaldehyde reduction process.* Carbohydrate Research, 2011. **346**(11): p. 1327-1332.

30. Negahdar, L., et al., *Kinetic investigation of the catalytic conversion of cellobiose to sorbitol.* Applied Catalysis B: Environmental, 2014. **147**: p. 677-683.

31. Deng, W., et al., *Conversion of cellobiose into sorbitol in neutral water medium over carbon nanotube-supported ruthenium catalysts.* Journal of Catalysis, 2010. **271**(1): p. 22-32.

32. Zhang, J., et al., *Direct conversion of cellobiose into sorbitol and catalyst deactivation mechanism.* Catalysis Communications, 2012. **29**: p. 180-184.

33. Li, J., et al., *Simultaneous hydrolysis and hydrogenation of cellobiose to sorbitol in molten salt hydrate media.* Catalysis Science & Technology, 2013. **3**(6): p. 1565-1572.

34. Niu, Y., et al., *Ru supported on zirconia-modified SBA-15 for selective conversion of cellobiose to hexitols.* Microporous and Mesoporous Materials, 2014. **198**: p. 215-222.

35. Almeida, J.M.A.R., et al., *Screening of mono- and bi-functional catalysts for the one-pot conversion of cellobiose into sorbitol.* Catalysis Today.

36. Sasaki, M., et al., *Reaction kinetics and mechanism for hydrothermal degradation and electrolysis of glucose for producing carboxylic acids.* Research on Chemical Intermediates, 2011. **37**(2): p. 457-466.

37. Fukuoka, A. and P.L. Dhepe, *Catalytic Conversion of Cellulose into Sugar Alcohols.* Angewandte Chemie International Edition, 2006. **45**(31): p. 5161-5163.

38. Rinaldi, R. and F. Schüth, *Acid Hydrolysis of Cellulose as the Entry Point into Biorefinery Schemes.* ChemSusChem, 2009. **2**(12): p. 1096-1107.

39. Yabushita, M., H. Kobayashi, and A. Fukuoka, *Catalytic transformation of cellulose into platform chemicals.* Applied Catalysis B: Environmental, 2014. **145**: p. 1-9.

40. Yu, Y. and H. Wu, *Effect of ball milling on the hydrolysis of microcrystalline cellulose in hot-compressed water.* AIChE Journal, 2011. **57**(3): p. 793-800.

41. Kobayashi, H., et al., *Conversion of cellulose into renewable chemicals by supported metal catalysis.* Applied Catalysis A: General, 2011. **409–410**: p. 13-20.

42. Kobayashi, H., et al., *Synthesis of sugar alcohols by hydrolytic hydrogenation of cellulose over supported metal catalysts.* Green Chemistry, 2011. **13**(2): p. 326-333.

43. Zhu, W., et al., *Efficient hydrogenolysis of cellulose into sorbitol catalyzed by a bifunctional catalyst.* Green Chemistry, 2014. **16**(3): p. 1534-1542.

44. Xi, J., et al., *Direct conversion of cellulose into sorbitol with high yield by a novel mesoporous niobium phosphate supported Ruthenium bifunctional catalyst.* Applied Catalysis A: General, 2013. **459**: p. 52-58.

45. Kobayashi, H., et al., *Transfer hydrogenation of cellulose to sugar alcohols over supported ruthenium catalysts.* Chemical Communications, 2011. **47**(8): p. 2366-2368.

46. Ding, L.-N., et al., *Selective Transformation of Cellulose into Sorbitol by Using a Bifunctional Nickel Phosphide Catalyst.* ChemSusChem, 2010. **3**(7): p. 818-821.

47. Kobayashi, H., et al., *Control of selectivity, activity and durability of simple supported nickel catalysts for hydrolytic hydrogenation of cellulose.* Green chemistry, 2014. **16**(2): p. 637-644.

48. Li, Y., et al., *Advances in hexitol and ethylene glycol production by one-pot hydrolytic hydrogenation and hydrogenolysis of cellulose.* Biomass and Bioenergy, 2015. **74**: p. 148-161.

49. Shrotri, A., et al., *Conversion of cellulose to polyols over promoted nickel catalysts.* Catalysis Science & Technology, 2012. **2**(9): p. 1852-1858.

50. Pang, J., et al., *Catalytic conversion of cellulose to hexitols with mesoporous carbon supported Ni-based bimetallic catalysts.* Green Chemistry, 2012. **14**(3): p. 614-617.

51. Geboers, J., et al., *Hydrolytic hydrogenation of cellulose with hydrotreated caesium salts of heteropoly acids and Ru/C.* Green Chemistry, 2011. **13**(8): p. 2167-2174.

52. Geboers, J., et al., *Efficient catalytic conversion of concentrated cellulose feeds to hexitols with heteropoly acids and Ru on carbon.* Chemical Communications, 2010. **46**(20): p. 3577-3579.

53. Geboers, J., et al., *Efficient hydrolytic hydrogenation of cellulose in the presence of Ru-loaded zeolites and trace amounts of mineral acid.* Chemical Communications, 2011. **47**(19): p. 5590-5592.

AIMS

CONVERSION OF CELLULOSIC BIOMASS TOWARDS ADDED VALUE PRODUCTS OVER BIFUNCTIONAL CATALYSTS.

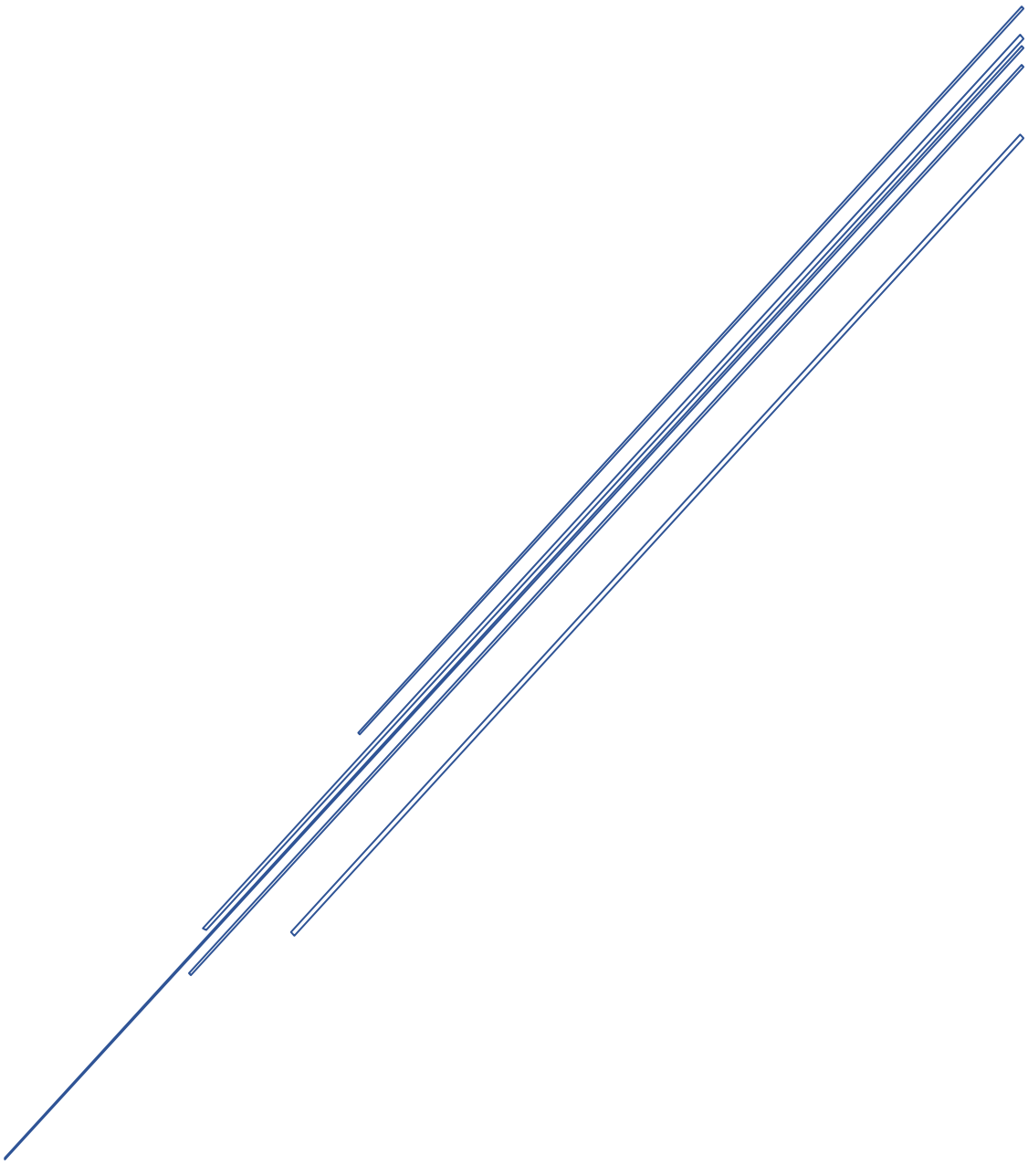

The general aim of this work is to study the catalytic behaviour of mesoporous noble metal-based catalysts for the effective conversion of cellulose and its related model compounds into chemicals. Mesoporous silica materials were chosen as catalytic supports due to their appropriate porous structure to solve diffusional problems of large molecules in catalytic applications and their stability under hydrothermal conditions. According to their remarkable activity for hydrogenation processes, Ru and Ni were selected as active metals.

With this general aim, the present thesis comprises the following partial goals:

- Synthesis of mesoporous silica materials as catalytic supports.
  Different mesoporous silica supports were synthesized by conventional sol-gel method. In this sense, the synthesis of MCM-48 and Al-MCM-48 was performed. In addition, acidified MCM-48 with a heteropolyacid (MCM-48/TPA) was also prepared.

- Synthesis of monometallic Ru- and Ni-based catalysts.
  Both ruthenium and nickel were deposited over MCM-48 by classical wet impregnation method. Ruthenium was also deposited over Al-MCM-48 and MCM-48/TPA using the same preparation method.

- Synthesis of bimetallic Ru:Ni-based catalysts.
  Ruthenium and nickel were deposited together over MCM-48 by consecutive impregnation steps.

- Characterization of the so obtained supports and metal catalysts.
  The prepared catalytic materials were characterized in order to study their features, such as textural properties, morphology, metal dispersion over the support, metal-support interactions, metal state, acidity and metal loading.

- Design and construction of an experimental setup in order to study the conversion of biomass in a hydrothermal medium under hydrogen atmosphere.

- Catalytic activity tests of the synthesised catalyst.

- Hydrolysis of cellulose over different catalytic materials. Study of the influence of acidity of MCM-48, TiO_2 and commercial Ru/C in this reaction step.
- Hydrogenation of D-Glucose to hexitols over Ru/MCM-48, commercial Ru/C and Ru deposited over commercial TiO_2, Ni/MCM-48 and Ru:Ni/MCM-48. Calculation of specific reaction rates and activation energy values. Recycling of the prepared catalysts.
- Hydrolysis/hydrogenation of cellobiose over Ru/Al-MCM-48. Study of the effect of temperature and pressure of H_2 to maximize final yield to hexitols. Development of a kinetic model and the reaction mechanism covering the studied experimental conditions.
- One-pot hydrogenation of cellulose to hexitols. Catalytic behaviour of Ru/MCM-48 against commercial Ru/C. Development of a kinetic model and detailed study of mass transfer limitations.
- Ultrafast Supercritical Water (SCW) Hydrolysis of cellulose + hydrogenation of the so obtained products (two-steps process). Use of SCW hydrolysis as cellulose pre-treatment to enhance production of hexitols. Comparison between one-pot and two-step process.
- Checking the two-steps process (SCW hydrolysis + catalytic hydrogenation) for the synthesis of alcohols from a real lignocellulosic biomass (Sugar Beet Pulp).
- Conversion of D-Glucose into straight-chain alkanes over Ru/Al-MCM-48, Ru/MCM-48/TPA and commercial Ru/C. Study of the influence of TPA combined with the catalyst in the reaction. Influence of Al-MCM-48 enhancing activity of commercial Ru/C.

CHAPTER 1

CONVERSION OF BIOMASS INTO SORBITOL: CELLULOSE HYDROLYSIS ON MCM-48 AND D-GLUCOSE HYDROGENATION ON RU/MCM-48

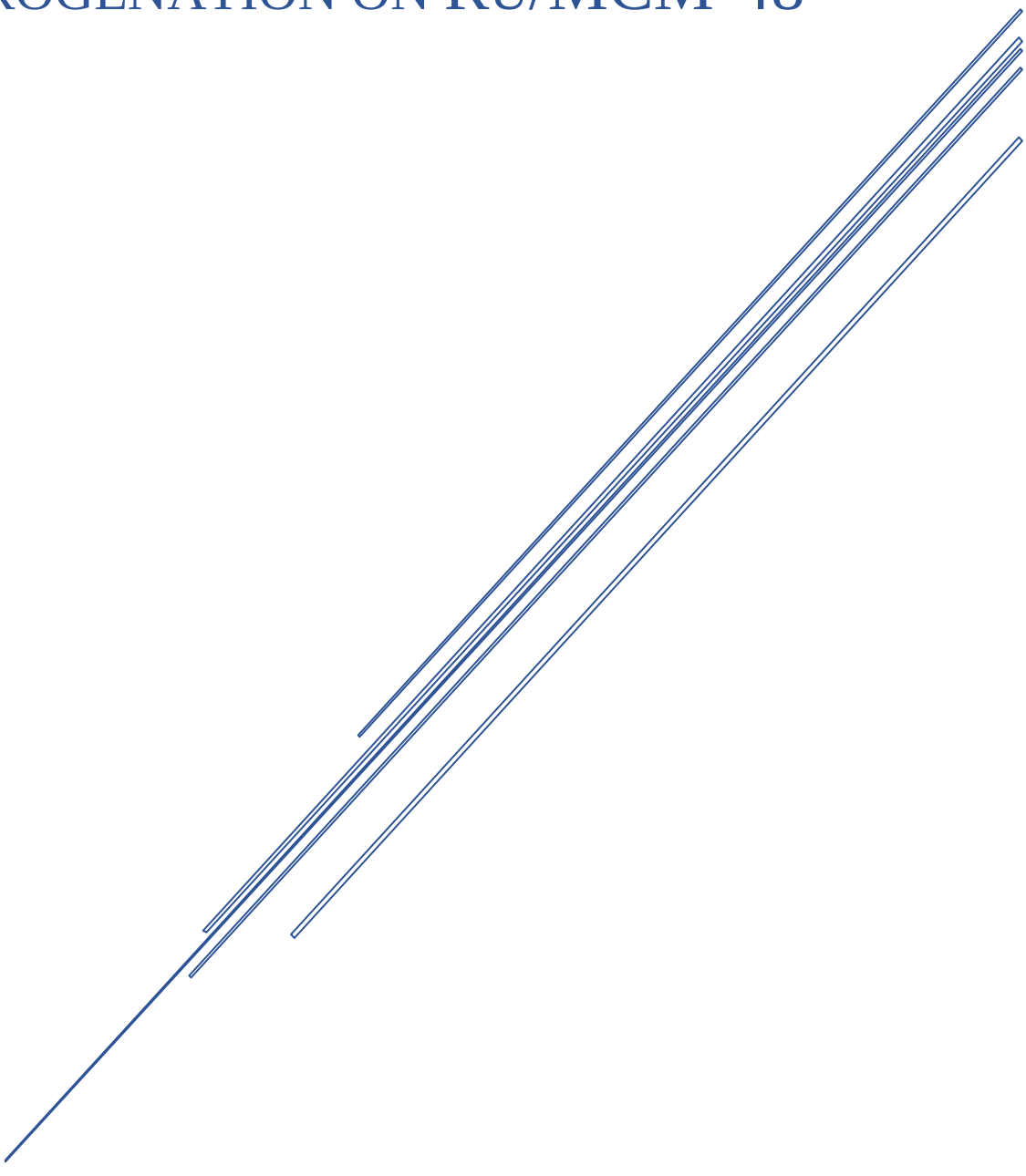

CONVERSION OF BIOMASS INTO SORBITOL: CELLULOSE HYDROLYSIS ON MCM-48 AND D-GLUCOSE HYDROGENATION ON RU/MCM-48

Abstract

Mesoporous silica was prepared by the sol-gel method and characterized by means of Small Angle X-Ray Scattering, Scanning Electron Microscopy, Light Scattering, adsorption/desorption of N_2 and acid-base titration. This material was tested in cellulose hydrolysis, showing a good catalytic response, attributable to surface acidity, which promoted D-glucose production. MCM-48 supported ruthenium nanoparticles were prepared by the wet impregnation method and characterized using X-Ray Diffraction, Transmission Electron Microscopy, adsorption/desorption of N_2, acid-base titrations, Temperature Programmed Reduction and Atomic Absorption, and tested in the hydrogenation of D-Glucose into sorbitol. Its behavior was compared with Ru deposited on commercial TiO_2 and with commercial Ru/C, revealing both high activity and selectivity to D-Sorbitol, standing as a promising candidate for future scale-up and one-pot conversion of biomass.

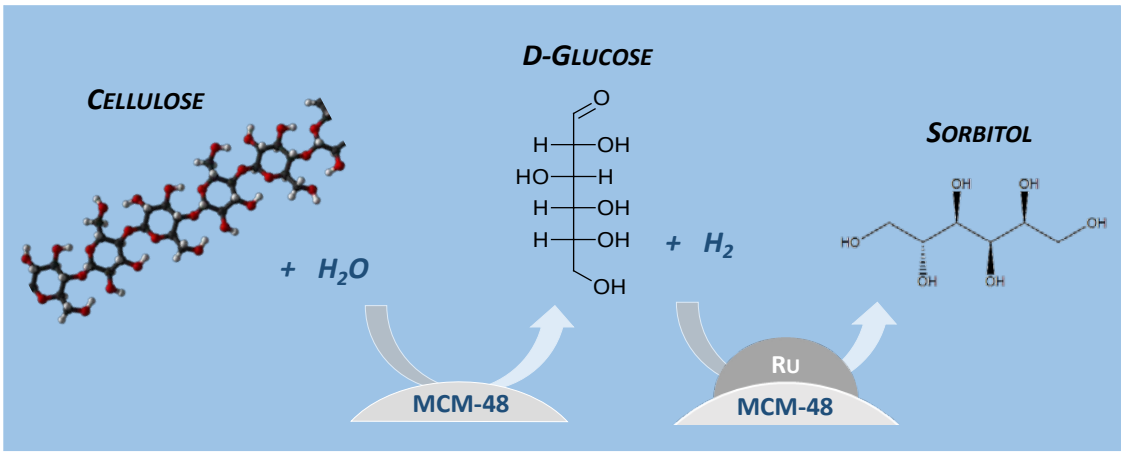

Keywords

Ru/MCM-48, biomass hydrogenation, hydrolysis of cellulose, sorbitol, glucose.

1. INTRODUCTION

Currently, due to the depletion of fossil fuels and the problems arising from global warming, the use of renewable resources as feedstock for chemicals, fuels and energy has achieved a good piece of attention [1, 2]. In this sense, polyols from the hydrogenation of biomass are versatile compounds with a wide range of uses. Biomass comprises various plant components, such as cellulose, hemicelluloses and lignin. Average composition of lignocellulosic materials is 34-50% cellulose, 19-34% hemicelluloses and 11-30% lignin [3]. Cellulose is the most common source of biomass and is nowadays considered as a promising substitute to fossil fuels for the sustainable production of fuels and chemicals. Due to its complex structure, with β-1,4-glycosidic bonds of D-Glucose, it is neither soluble in water, nor digestible by human beings and consequently not suitable for nutritional purposes [4]. There are several alternatives for its valorization. Hydrolytic hydrogenation of cellulose into D-Sorbitol appears as a very attractive alternative in this field because D-Sorbitol is the sugar alcohol with the most widespread uses in food industry, personal care products, cosmetics, medical and industrial applications [5].

It is possible to obtain small amounts of D-Sorbitol from different kind of fruits working at small scale [6], however, D-Glucose hydrogenation is the most common reaction route to its production at industrial scale. In general terms, the conversion of cellulose into sugar alcohols with supported metal catalysts is a two-step reaction. First, biomass is hydrolyzed over acid sites of the support to obtain a high yield to D-Glucose and this product is subsequently hydrogenated into sugar alcohols by metals under H_2 pressure [7]. Catalytic hydrogenation of D-Glucose into D-Sorbitol has been well studied in the literature. D-Sorbitol production has been performed on nickel based catalysts (Raney Nickel) [8] due to their low cost and high activity, however, they have shown low stability in the reaction medium [9]. Alternatively, several catalysts including ruthenium have been reported to be active for this reaction, and in many cases they have shown higher activities than Raney nickel. As a noble metal, ruthenium is more expensive than nickel; therefore ruthenium has been deposited over different kind of solid supports in order to reduce the final cost of the catalyst. Ruthenium has been dispersed on activated carbon (AC) [10], silica [11], titanium dioxide (TiO_2) or NiO-modified TiO_2 [12, 13], alumina (Al_2O_3) [14], zeolites [15] and ordered mesoporous silica, such as MCM-41 [16], where structure and textural properties of the support play

an important role in these reactions. Regarding mesoporous silica, MCM-41 has a hexagonal array of unidirectional pores, while MCM-48 has an ordered cubic structure based on a narrow tridimensional pore network [17]. Thus, interwoven and branched pore structure from MCM-48 seems to be an interesting alternative to solve diffusional problems of large molecules in catalytic applications [18].

The aim of this work is the preparation of a solid bifunctional catalyst using MCM-48 as the support and ruthenium as the metal phase. MCM-48 provides a high surface area acid structure with good diffusional properties for the hydrolytic step, while ruthenium acts as the active phase for the hydrogenation of D-Glucose. With this aim, Ru has been deposited on a MCM-48 prepared in the laboratory and compared with a Ru deposited on a commercial TiO_2 and with a standard commercial Ru/C. Thus, the individual steps of cellulose transformation into D-Sorbitol are studied, in order to gain further understanding of the role of support acidity and ruthenium activity in cellulose hydrolysis and D-Glucose hydrogenation, respectively. Linking the best results from hydrolysis and hydrogenation steps, it will be possible to choose the most appropriate catalytic system for further one-pot hydrolytic hydrogenation.

2. EXPERIMENTAL

2.1. SUPPORT AND CATALYSTS PREPARATION

Synthesis of mesoporous silica MCM-48 has been carried out using a conventional hydrothermal pathway similar to the procedure described by Schumacher et al [17, 18]. Firstly, n-Hexadecyltrimethylammonium bromide template ($CH_3(CH_2)_{15}N(Br)(CH_3)_3 \geq$ 98%, Sigma – Aldrich) was dissolved in the mixed solution of 42 cm^3 of distilled water, 13 cm^3 of aqueous ammonia (20% as NH_3, Panreac), and 18 cm^3 of absolute ethanol (partially denaturated QP, Panreac) by stirring for 15 min; then 4 cm^3 of TEOS (≥ 99% GC, Sigma – Aldrich), were added dropwise. The solution was further stirred for 18 h; the white precipitate was then collected by filtration and washed with distilled water. After that, the precipitate was dried at 60 ºC overnight. Dried samples were calcined with a heating rate of 2 $ºC \cdot min^{-1}$ from 80 ºC to 550 ºC and maintained at 550 ºC overnight. Two ruthenium catalysts, with a metal loading close to 5%, were synthesized by the wetness impregnation (WI) technique using the so prepared MCM-48 and TiO_2 supplied by Sigma Aldrich (Hombikat catalyst grade) as supports. For this preparation,

ruthenium (III) chloride anhydrous ($RuCl_3$.anhydrous, Strem Chemicals Inc.) and the corresponding support were sonicated in water previously to their mixture during ten minutes. Then, ruthenium trichloride solution and a dispersion containing MCM-48 or TiO_2 were mixed and heated with a rate of 1 ºC·min^{-1} from room temperature to 105 ºC using a Stuart model SD162 heating plate. The impregnation finished when the solvent was completely evaporated. Then, catalysts were dried overnight at 105 ºC. Finally, the samples were reduced under H_2 atmosphere at 150 ºC. A commercial Ru/C catalyst (Ruthenium, 5% on activated carbon, reduced, 50 % water wet paste (Escat™ 4401)) has been used for comparison purposes. This catalyst was supplied in its reduced form.

2.2. SUPPORT AND CATALYST CHARACTERIZATION

Small Angle X-Ray Scattering (SAXS) and X-Ray Diffraction (XRD) were performed in a Bruker Discover D8 diffractometer using the Cu Kα radiation (λ = 0.15406 nm). The diffraction intensities were measured, for XRD, over an angular range of $30° < 2\theta < 90°$ with a step size of 0.03° and a count time of 2 s per step. In case of SAXS, $2° < 2\theta < 6º$ was selected as angular range with a step size of 0.02° and a count time of 1 s per step. Surface area/porosity measurements of the supports and the different catalysts were conducted using a Quantasorb Sorption System (Quantachrome Instruments) with N_2 (at -196 ºC) as sorbate. Prior to analysis, the samples were outgassed overnight at 350 ºC for silica and titanium materials, while carbonaceous samples were outgassed at 180 ºC. Total specific surface areas were determined by the multipoint BET method at $P/P_0 \leq 0.3$, total specific pore volumes were evaluated from N_2 uptake at $P/P_0 \geq 0.97$. Temperature Programmed Reduction (TPR) profiles were recorded using the commercial Micromeritics TPD/TPR 2900 unit. The samples were loaded into a U-shaped quartz cell (100 mm × 3.76 mm i.d.), ramped (10 ºC·min^{-1}) from room temperature to 800 ºC under a flow of H_2/N_2 (5% v/v; 50 cm^3·min^{-1}, Air Liquide) and kept at the final temperature until the signal returned to the baseline. Hydrogen consumption was monitored by a thermal conductivity detector (TCD) with data acquisition/manipulation using the ChemiSoft TPX V1.03™ software. Transmission electron microscopy (TEM) analyses used a JEOL 2100 unit with an accelerating voltage of 200 kV. Samples were prepared by ultrasonic dispersion in acetone with a drop of the resultant suspension evaporated onto a holey carbon-supported grid. A counting of ruthenium nanoparticles were carried out from TEM images of the different catalysts. At least 240 ruthenium nanoparticles were counted in

each case and the mean Ru particle sizes were obtained from the following expression (Eq. 1) [19] .

$$\bar{d}_s = \frac{\sum_i n_i \cdot d_i^3}{\sum_i n_i \cdot d_i^2} \quad (1)$$

where $\bar{d}_s$ is surface-area weighted diameter and n_i is the number of ruthenium particles with a diameter d_i. Since chemical reactions occurs on catalyst surface, surface-area weighted diameter is selected as the most meaningful parameter to obtain mean Ru particles sizes for catalysis purposes. Scanning electron microscopy (SEM) analyses were obtained using a JEOL JSM 820 unit with a voltage of 10 kV. Acid–base titrations were performed by immersing 25 mg of solid in 100 cm^3 NaCl 0.1 M, acidified with 1 cm^3 HCl 0.1 M with constant stirring. A 0.1 M NaOH solution was used as the titrant, added dropwise and the pH was monitored using a Crison pH-meter. The starting NaCl (+HCl) solution served as a blank. Light scattering (LS) was used for determining grain size distribution of MCM-48. Metal loading was determined by atomic absorption (AA) using a VARIAN SPECTRA 220FS analyzer. Digestion of the samples was performed with HCl, H_2O_2 and HF using microwave at 250 ºC.

2.3. CELLULOSE HYDROLYSIS EXPERIMENTS

Catalytic depolymerization of cellulose has been studied in an experimental set-up where the main elements are: i) a stainless-steel high pressure reactor with an internal volume of 25 cm^3 (Berghof BR-25), agitated with a magnetic stirring bar and fitted up with a PID for temperature control, ii) nitrogen and hydrogen feeding lines, iii) valves to purge and vent the lines and the reactor. Microcrystalline cellulose (42 % C basis) used in the experiments was purchased from VWR. Nitrogen and hydrogen are supplied by Carburos Metálicos (Spain). In a typical hydrolysis experiment the reactor is loaded using cellulose (0.16 g), distilled water (20 cm^3) and the solid catalyst (0.05 g). After that, the reactor is successively purged and vented with N_2 at room temperature for 10 min. Then, the reactor is heated under nitrogen atmosphere (2 MPa) to the desired temperature (230 ºC) and kept constant during the desired reaction time (0 – 30 min). It was considered t = 0 when the reaction mixture achieved 230 ºC. Distilled water is degassed before the addition into the reactor. A pressure of 2 MPa is set to keep the mixture in the liquid phase during the reaction time. The stirring speed is set at 1400 rpm. When the final reaction time is achieved the reactor and its content is quenched

using an ice bath to rapidly stop the reaction. After that, the product mixture is centrifuged and the supernatant solution is then filtered prior to analysis by High Performance Liquid Chromatography (HPLC). The column used for the HPLC was Shodex SH-1011 at 50 °C, using sulphuric acid (0.01 N) as the mobile phase with a rate of 0.8 $cm^3 \cdot min^{-1}$. A Waters IR detector 2414 was used to identify the sugars and their derivatives. D-Glucose yield (%) was obtained as a result of dividing moles of carbon from D-Glucose in the reaction product by moles of carbon present in the starting cellulose (Eq. 2).

$$Y_{D-Glucose}(\%) = \frac{mole\ C\ in\ D\text{-}Glucose}{mole\ C\ in\ \ Celulose_0} \cdot 100 \quad (2)$$

2.4.D-GLUCOSE HYDROGENATION TESTS

Catalytic hydrogenation of D-Glucose was performed in the experimental setup described above. Hydrogenation tests were carried out in the temperature range 80–120 ºC at 2.5 MPa H_2 pressure using a stirring rate of 1400 rpm. Prior to reaction catalysts were activated *in situ* by reducing under H_2 atmosphere at 150ºC during 30 minutes. D-Glucose/Ru ratio (w/w) was kept in 42 in all the experiments. After flushing the reactor with N_2 for 10 minutes, H_2 is fed and reactor is heated up to the desired reaction temperature. Once the set point is reached a solution of 7.35 $g \cdot dm^{-3}$ D-Glucose is pumped. At the end of the experiments, recovery of the catalyst was made by filtering the product solution using a vacuum pump. Hydrogenation products were analyzed by HPLC. The HPLC column used was SUGAR SC-1011 from Shodex at 80 °C and a flow of 0.8 $cm^3 \cdot min^{-1}$ using water Milli-Q as the mobile phase. A Waters IR detector 2414 was used to identify sugars, polyols and their derivatives. D-Glucose conversions, D-Sorbitol and D-Manitol yields and selectivities were calculated using equations 3, 4 and 5.

$$X_{D-Glucose}(\%) = \frac{mole\ (D\text{-}Glucose_0) - mole\ (D\text{-}Glucose_f)}{mole\ (D\text{-}Glucose_0)} \cdot 100 \quad (3)$$

$$S_{Sorbitol}(\%) = \frac{mole\ (Sorbitol)}{mole\ (D\text{-}Glucose_0) - mole\ (D\text{-}Glucose_f)} \cdot 100 \quad (4)$$

$$Y_{Sorbitol}(\%) = \frac{mole\ (Sorbitol)}{mole\ (D\text{-}Glucose_0)} \cdot 100 = \frac{X \cdot S}{100} \quad (5)$$

In order to test catalyst reusability, after its recovery from reaction media, the solid catalyst was washed several times with deionized water and dried at 105 ºC overnight. Then, the catalyst was reactivated under TPR conditions and tested again in D-Glucose hydrogenation.

3. RESULTS AND DISCUSSION

3.1. CHARACTERIZATION OF SUPPORTS

The prepared MCM-48 consists on a conglomeration of pseudo-spherical particles in the micron range, as shown in Figure 1A. Light Scattering results for MCM-48 showed a monodisperse particle size distribution, where d (0.1), d (0.5) and d (0.9) parameters mean that ten, fifty or ninety percent of the particles had that size or lower, respectively (Figure 1B).

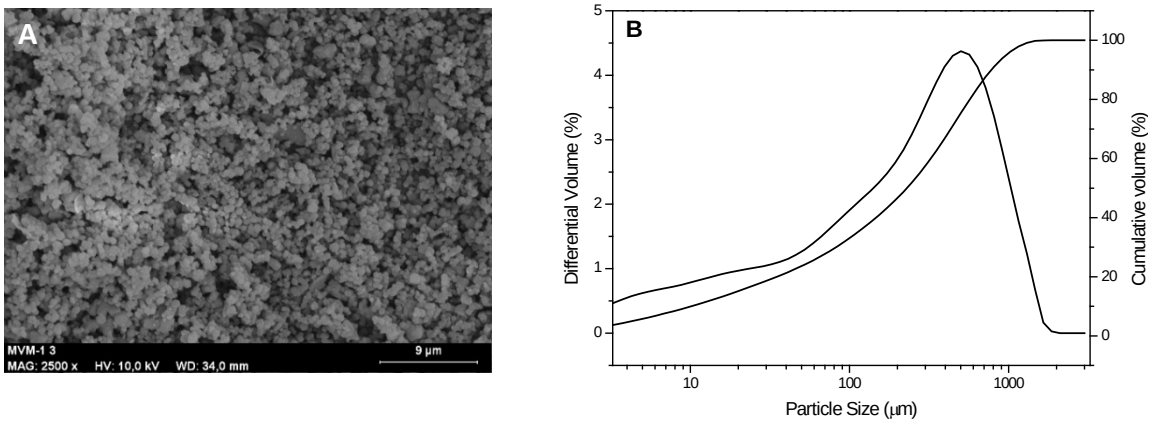

Figure 1. (A) Scanning electron micrograph and **(B)** differential and cumulative particle size distribution (d(0.1)=10.1 µm, d(0.5)=229.4 µm and d(0.9)=777.5 µm) of MCM-48.

MCM-48 structure was characterized by means of Small Angle X-Ray Scattering (SAXS). Figure 2A shows SAXS pattern of MCM-48. Calcined MCM-48 exhibits three main diffraction peaks at $2\theta = 2.55^0$, 2.94^0 and 4.92^0, that can be assigned to (211), (220) and (332) planes. This indicates a high quality of the cubic phase belonging to a Ia3d symmetry [18, 20].

A typical N_2 adsorption/desorption isotherm at -196 ºC of the calcined MCM-48 material is shown in Figure 2B. According to the IUPAC classification [21], the isotherm can be classified as a type IV, where a sharp increase in the volume of nitrogen adsorbed was observed at P/P_0 in the range of 0.1 – 0.35 and 0.9 – 0.99. This kind of

isotherm is typical of mesoporous silica materials. No hysteresis was observed between adsorption and desorption branches, therefore MCM-48 shows a reversible type IV isotherm, comparable to those reported by [22]. MCM-48 usually presents type H1 hysteresis loops, however, it has been reported that in the limit of small mesopores (2-4 nm) or with increasing temperature, the capillary condensation occurs without hysteresis, and the separation of parallel H1 branches increase with increasing pore size. Figure 2C depicts a unimodal mesoporous pore size distribution for MCM-48 with maximum centered at 3.6 nm, consistent with the absence of hysteresis [23].

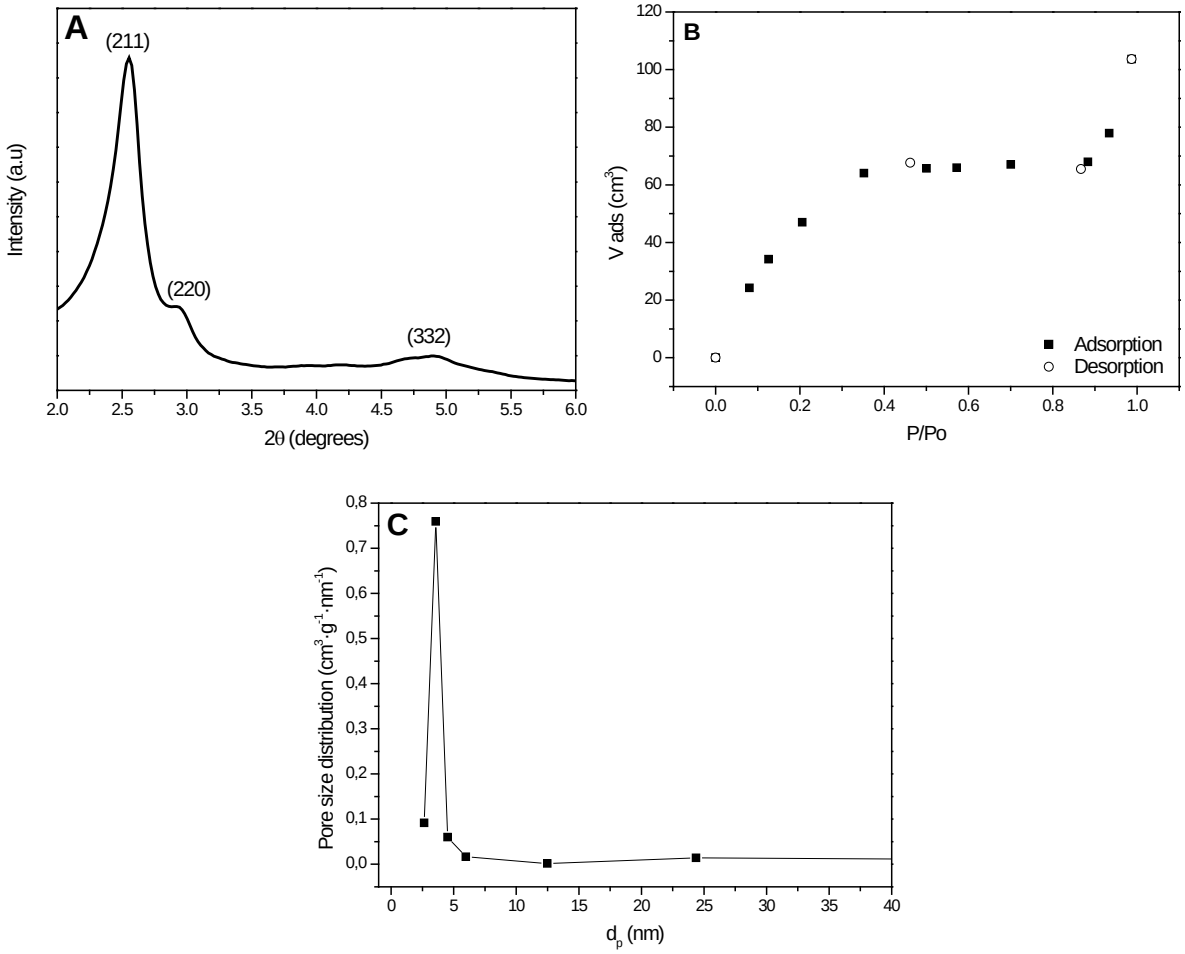

Figure 2. (A) SAXS pattern of MCM-48 support, **(B)** N_2 adsorption/desorption isotherms of MCM-48 and **(C)** pore size distribution**.**

Textural properties and acidity measurements for MCM-48 and TiO_2 are presented in Table 1. BET surface area and pore volume for MCM-48 were 1594 $m^2 \cdot g^{-1}$ and 0.9 $cm^3 \cdot g^{-1}$, respectively. Similar BET surface area and pore volume values were obtained by Wu et al. for MCM-48 prepared by hydrothermal method [24]. The TiO_2 used as support showed, as expected, lower porosity than MCM-48. Acid-base titrations

demonstrated that MCM-48 was more acidic than TiO_2, which will be important in the cellulose hydrolysis step, where acidity improves biomass conversion into sugars. MCM-48 acidity is due to terminal silanol groups (Si-OH) which show weak acidic sites [25]. Surface properties of TiO_2 change depending on the preparation method. However, in general, TiO_2 (anatase) is classified into a weak acidic metal oxide, where the acid sites are Lewis in nature [26].

Table 1. Textural properties and acid-base characterization of MCM-48 and TiO_2.

Sample	S_{BET} ($m^2 \cdot g^{-1}$)	Vp ($cm^3 \cdot g^{-1}$)	NaOH consumption ($cm^3 \cdot g^{-1}$)
MCM-48	1594	0.90	5.74
TiO_2	53	0.10	2.22

3.2. CHARACTERIZATION OF RU-BASED CATALYSTS

Figure 3 shows the H_2-TPR profiles of the Ru/MCM-48 and Ru/TiO_2 catalysts. TPR curves presented similar single reduction peaks at ca. 125 ºC and 145 ºC for Ru/MCM-48 and Ru/TiO_2, respectively. These peaks correspond to the reduction of Ru^{3+} to Ru^0 [27]. Reduction temperature was higher for Ru/TiO_2, suggesting a stronger interaction of Ru nanoparticles with TiO_2 support. Consequently, 150 ºC was selected as common reduction temperature for both catalysts, which ensures the activation of ruthenium.

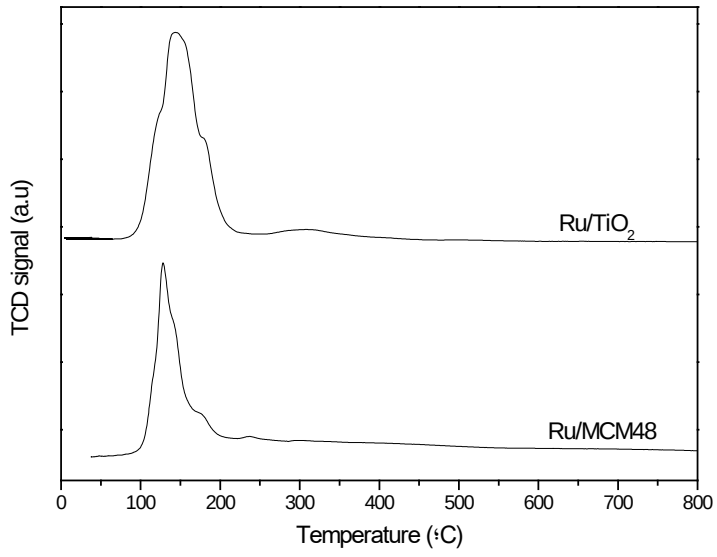

Figure 3. H_2-TPR profiles.

XRD patterns for Ru-based catalysts are shown in Figure 4 (A). A characteristic metallic diffraction peak was observed at $2\theta = 43.8^{o}$ (JCPDS No. 06–0663) in Ru/MCM-48 and Ru/C samples, indicating the presence of Hexagonal Close Packing (HCP) Ru^0 nanoparticles. In the case of Ru/TiO_2, and given the high intensity of anatase diffraction peaks, the corresponding to Ru^0 nanoparticles is better observed in Figure 4B, in the range $2\theta = 42 - 47^{o}$. Low intensity diffraction peaks were observed in all cases, characteristic of Ru^0 nanoparticles well-distributed on the support.

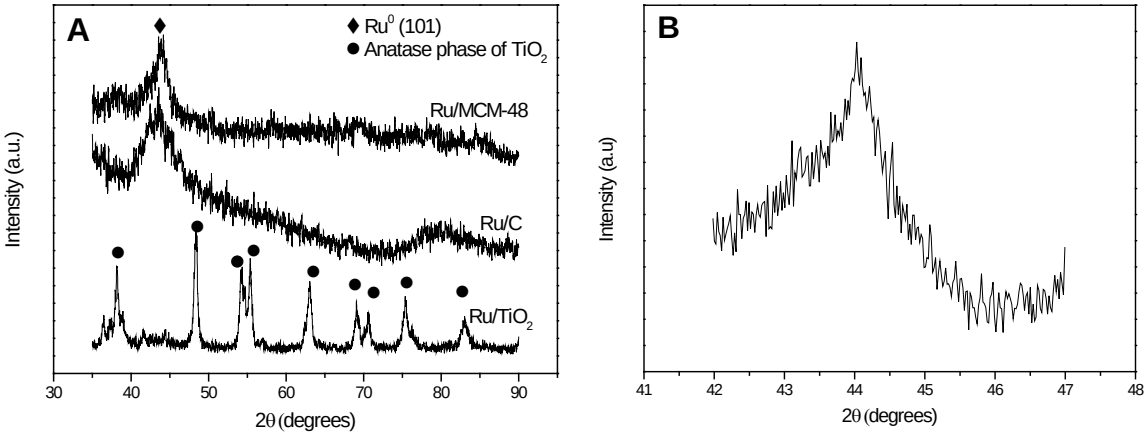

Figure 4. (A) XRD patterns of reduced catalysts and **(B)** expanded region for Ru/TiO_2.

Figure 5 shows TEM micrographs of Ru/MCM-48, Ru/TiO_2 and Ru/C catalysts. Figure 5A shows that Ru nanoparticles are homogenously distributed on the spherical MCM-48 support. However, TiO_2 particles are irregular in shape and size and Ru nanoparticles are agglomerated and not homogenously distributed on this support, as it is shown in Figure 5B. Finally, commercial Ru/C (Figure 5C) exhibits a good dispersion of Ru nanoparticles on activated carbon.

A counting of ruthenium nanoparticles from TEM images was performed. Histograms in Figure 6 show ruthenium particle size distributions for the three catalysts. In addition, Table 2 shows statistics from ruthenium particle size histograms, where mean Ru particle sizes were calculated from equation 1.

The three catalysts showed surface-area weighted diameters in a very narrow interval, and the following trend of increasing mean can be established: Ru/MCM-48 < Ru/TiO_2 < Ru/C. Additionally, Ru/MCM-48 exhibits the narrowest particle size distribution, with Ru-nanoparticles in the range 1.18-3.84 nm, showing the smallest standard deviation value. Ru/C catalyst presents the broadest particle size distribution,

with Ru nanoparticles in the range 0.46-7.13 nm, while Ru nanoparticles are between 0.85 and 6.26 nm in Ru/TiO_2.

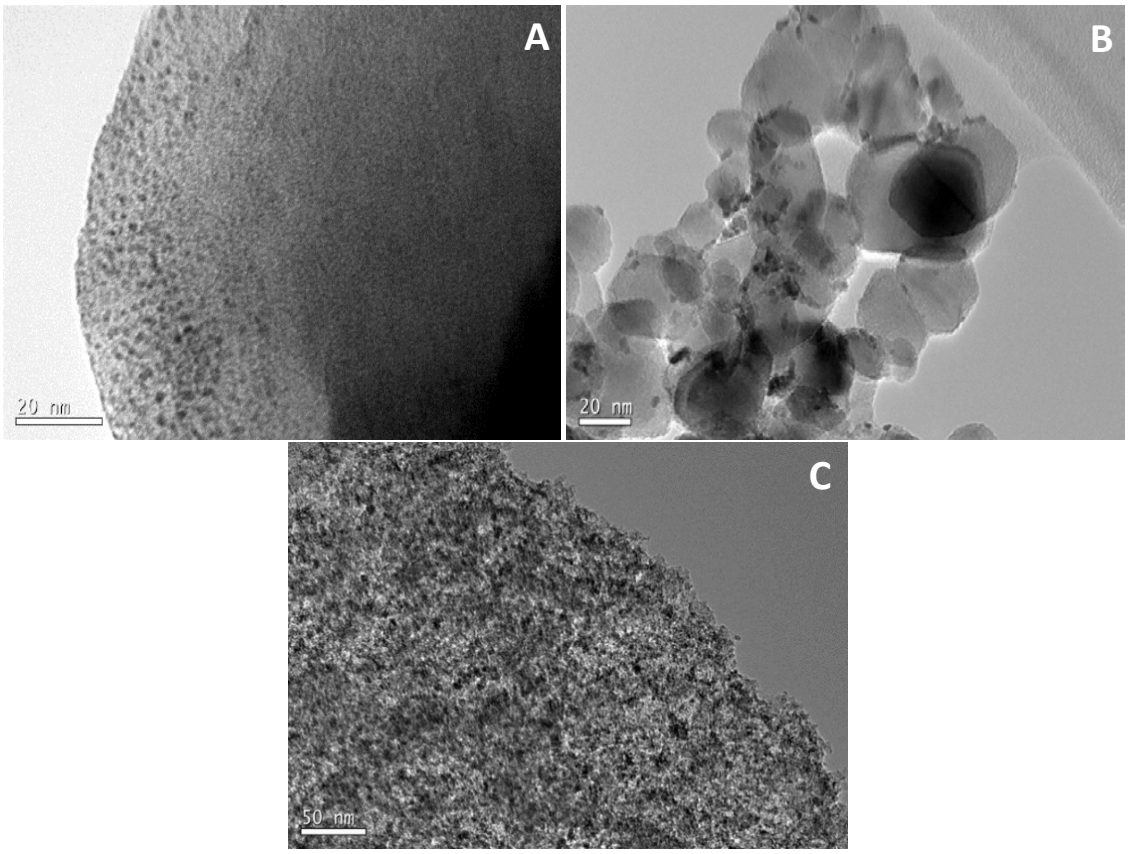

Figure 5. Transmission electron microscopy micrographs of **(A)** Ru/MCM-48, **(B)** Ru/TiO_2 and **(C)** Ru/C.

Table 2. Statistical summary of ruthenium particle size distributions.

Catalyst	Minimum (nm)	Maximum (nm)	$\bar{d}_s$ [a] (nm)	σ_m [b]
Ru/MCM-48	1.18	3.84	2.50	0.49
Ru/TiO_2	0.85	6.26	2.96	0.81
Ru/C	0.46	7.13	3.40	1.22

[a] Based on TEM measurements and Equation 1

[b] Standard deviation values from mean diameter. $\sigma = \sqrt{\frac{1}{n-1} \cdot \sum_{i=1}^{n} (d_i - \bar{d})^2}$

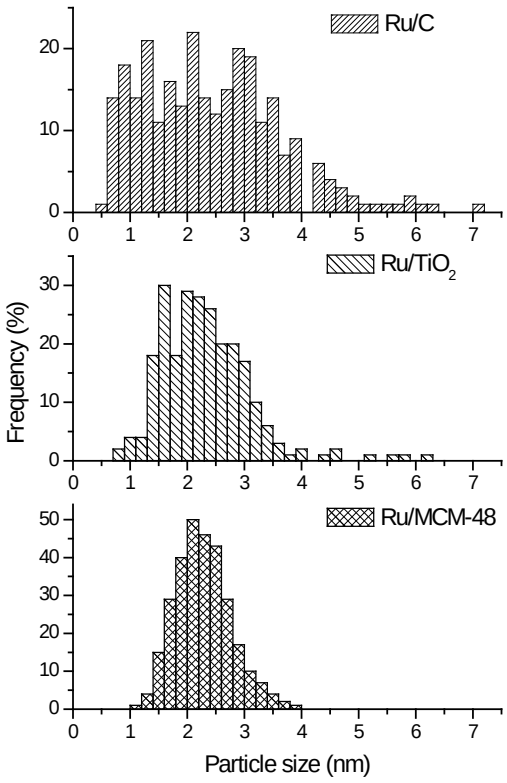

Figure 6. Ru particle size distributions in the catalysts.

BET surface area of MCM-48 decreased from 1594 to 1456 $m^2 \cdot g^{-1}$ upon Ru introduction, and pore volume shifted from 0.90 to 0.47 $cm^3 \cdot g^{-1}$, indicating an important blockage of the porous network. In the case of TiO_2, which presented a much lower surface area/porosity, the former slightly decreased from 53 to 43 $m^2 \cdot g^{-1}$, while pore volume remained almost the same (Table 3).

Table 3. Textural, metal loading and acid-base characterization of ruthenium catalysts.

Catalyst	Ru (%)	S_{BET} ($m^2 \cdot g^{-1}$)	Vp ($cm^3 \cdot g^{-1}$)	NaOH consumption ($cm^3 \cdot g^{-1}$)
Ru/MCM-48	4.04	1453	0.47	5.74
Ru/TiO_2	3.98	43	0.11	1.66
Ru/C	5.00	759	0.50	1.88

In addition, acidity value of Ru/MCM-48 was not modify after ruthenium deposition over MCM-48. However, a slight decrease of NaOH consumption was observed for Ru/TiO_2, since deposition of Ru nanoparticles over titania resulted in a partial blockage of surface groups which are responsible for the acidity features of the catalyst.

3.3. HYDROLYSIS OF CELLULOSE

Cellulose hydrolysis was studied on the supports, which are responsible of the acidity of the catalysts. In the case of Ru/C, no equivalent bare support could be obtained, so the supported catalyst was used instead. Cellulose hydrolysis conditions are described in section 2.3 and hydrolysis results are presented in Table 4.

Table 4. Cellulose hydrolysis tests. [a] Reaction time (t (min)).[b] Glucose Yield (%).

	t (min)[a]	D-Glucose (ppm)	$Y_{D\text{-}Glucose}$ (%)[b]
No catalyst	0	184	2.2
	5	277	3.3
	15	328	3.9
	30	474	5.6
MCM-48	0	819	9.8
	5	971	11.6
	15	1159	13.8
	30	1182	14.1
TiO_2	0	89	1.1
	5	198	2.4
	15	175	2.1
	30	270	3.2
Ru/C	0	19	0.2
	5	25	0.3
	15	9	0.1
	30	5	0.2

First, a blank test (no catalyst) was carried out. A D-Glucose production of 474 ppm was obtained after 30 min of reaction (5.6 % D-Glucose yield). It can be observed that MCM-48 improved D-Glucose production considerably to 1182 ppm. This D-Glucose concentration is related to a D-Glucose yield of 14.1 %. This result outperforms the obtained by Onda et al. on activated carbon [28] and SiO_2 [29], who reported yields of 6.4 % and 7 %, respectively. In the case of TiO_2, lower yields to D-Glucose than those obtained without catalyst were achieved, indicating that this support was not selective to the desired product, where 5-hydroxymethylfurfural (HMF) was the principal

compound (10.2 % HMF yield) after 30 min. This behavior is comparable with the results reported by Chareonlimkun et al., where the main product of cellulose hydrolysis over TiO_2 was HMF [30]. Ru/C exhibited a poor yield to D-Glucose during hydrolysis, lower than the corresponding to MCM-48, TiO_2 and in the absence of catalyst, and a maximum yield to D-glucose of 0.3 % was obtained after 5 min, detecting by-products such as fructose, glyceraldehydes, glycolaldehyde, lactic and formic acid at extended reaction times. Results presented above demonstrate that MCM-48 is a good catalyst to promote the hydrolysis of cellulose, whose acidity from silanol groups improves D-Glucose production.

3.4. HYDROGENATION OF D-GLUCOSE

Kinetic tests were carried out at temperatures between 80–120 ºC, 2.5 MPa H_2, 1400 rpm, using Ru/MCM-48, Ru/TiO_2 and Ru/C as catalysts. In preliminary tests, several screening experiments were performed in order to determine the most convenient temperature range. At temperatures above 120 ºC total conversion of D-Glucose was obtained in few minutes and a decrease in sorbitol yield was observed as a result of thermal degradation of D-Glucose and sorbitol isomerization into mannitol during this process. Therefore, 80-120 ºC was selected as optimal reaction temperature range. Preliminary experiments also confirmed that the process was not limited by mass transfer when stirring rate was 1400 rpm and catalyst particles were smaller than 70 µm, neither limited by H_2 diffusion when pressure was adjusted to 2.5 MPa.

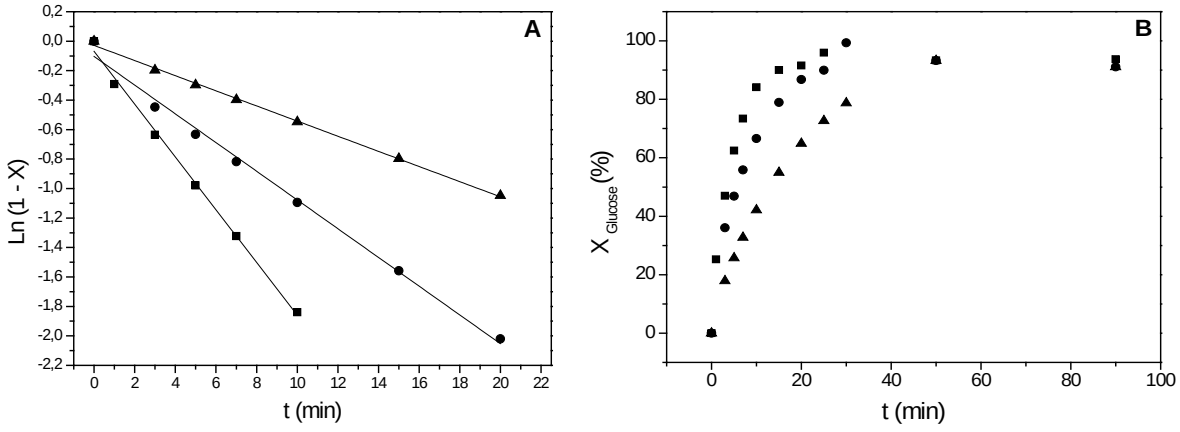

Figure 7. (A) Pseudo-first order fitting and **(B)** evolution of D-Glucose hydrogenation as a function of time-on-stream at 100 ºC and 2.5 MPa H_2. ▲Ru/MCM-48, ■ Ru/C and ● Ru/TiO_2.

Given the excess of H_2 employed, a pseudo-first order dependence respect to D-Glucose was observed in this reaction, in good agreement with the previously reported by other authors [13, 31]. For instance, Figure 7A shows pseudo-first order fittings at 100 ºC and 2.5 MPa H_2 using Ru/MCM-48, Ru/TiO_2 and Ru/C, with correlation coefficients $R^2 \geq 0.989$.

Figure 7B shows the effect of reaction time on D-Glucose conversion at 100 ºC using Ru/MCM-48, Ru/TiO_2 and Ru/C. Conversion increased fast to approach practically total conversion after ca. 40 min. A sorbitol selectivity of 100 % was achieved in all cases. Kinetic constants are given in Table 5. Ru/C shows the highest reaction rate at each temperature. Ru/TiO_2 had a similar kinetic constant to Ru/MCM-48 at 80 ºC and approaches that of Ru/C at 120 ºC. This behavior is illustrated in Figure 8A.

Activation energy values and pre-exponential factors (Table 6) have been calculated from Arrhenius plots in Figure 8A. It should be noted that activation energies obtained can be associated to kinetic control [32]. According to these results, it was not possible to make a relationship between reaction rate and activation energy because pre-exponential factor was not constant for all the catalysts. The activation energy for Ru/MCM-48 was the smallest, since this catalyst did not show significant changes in kinetic constants by changing reaction temperature. However, Ru/TiO_2 showed the highest activation energy value, being more sensitive to changes in temperature. A clear trend of increasing pre-exponential factor with increasing activation energy is observed. This behavior is attributed to a compensation phenomenon, behavior that is sometimes observed when the same reaction is conducted over different catalysts, under different reaction pressures, or with a set of related reactions over a fixed catalyst. In these cases, a correlation between activation energy and the pre-exponential factor is observed (Eq. 6).

$$Ln\,(A) = b \cdot Ea + C \qquad (6)$$

It can be understood as an increase in pre-exponential factor to compensate the decrease in reaction rate caused by an increase of the activation energy [33]. In a strict sense, this phenomenon implies the existence of a unique temperature which is called isokinetic temperature and that can be calculated as follows:

$$T_{iso} = {}^{1}/_{(b \cdot R)} \qquad (7)$$

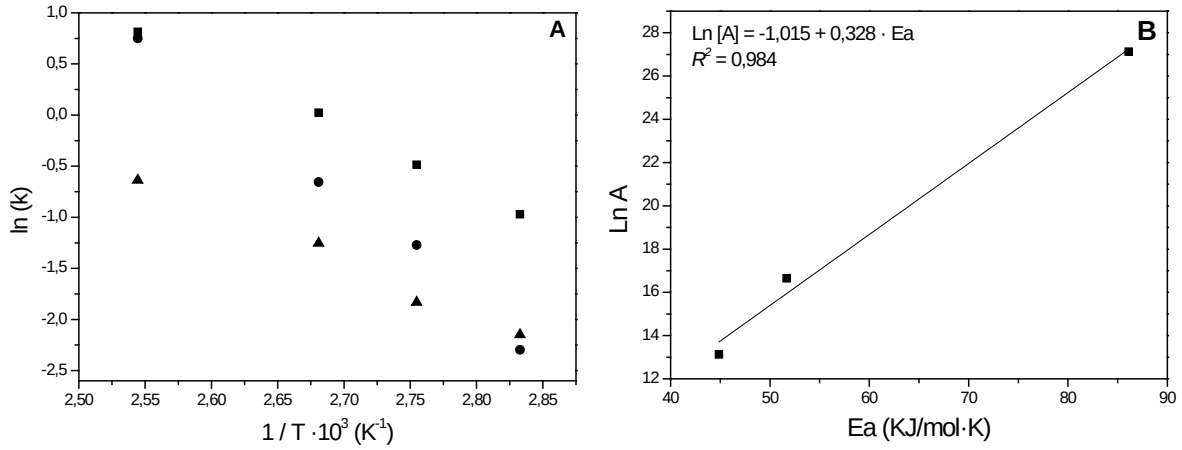

Figure 8. (A) Arrhenius plots of D-Glucose Hydrogenation, ▲Ru/MCM-48, ■ Ru/C and ● Ru/TiO_2 and **(B)** compensation plot**.**

Temperature at which the reaction rate is the same for the different catalytic systems. Graphically, T_{iso} can be obtained as the intersection of the Arrhenius plots corresponding to different systems. Thus, if we apply it to Arrhenius parameters obtained in this work, a good fit to the compensation plot can be observed (Figure 8B), having a calculated T_{iso} = 93 ºC, according to Eq. 7. However, the intersection of Arrhenius plots in our study was not common for the three catalysts, but they rather behaved as individual pairs at 80 ºC for Ru/TiO_2 and Ru/MCM-48 and at 120 ºC for Ru/TiO_2 and Ru/C. It has been distinguished in the literature between isokinetic phenomenon, where a single T_{iso} exists, and compensation phenomenon, when such an exclusive isokinetic temperature cannot be observed, but Arrhenius parameters vary sympathetically [34], as it is the case of the present data.

Table 6. Activation energy and pre-exponential factor from Arrhenius plots.

Catalyst	**Ea** **(KJ·mol^{-1})**	**A** **(dm^3·g^{-1}·min^{-1})**	**R^2**
Ru/MCM-48	44.87	$5.00 \cdot 10^5$	0.989
Ru/C	51.68	$1.70 \cdot 10^7$	0.999
Ru/TiO_2	86.11	$6.05 \cdot 10^{11}$	0.995

Ru/MCM-48 was recovered after each experiment in order to study the recycling and reusability of this catalyst in D-Glucose hydrogenation at 120 ºC after three cycles. Results confirmed that catalytic activity of Ru/MCM-48 remained constant and sorbitol yield was 90 % in all cases. Based on the Scherrer equation, Ru crystallite sizes were derived from XRD analyses, showing values of 2.70 and 2.74 nm, before and after the reaction, respectively, confirming the stability of the active phase.

Table 7. Comparison of different catalysts on the hydrogenation of D-Glucose.

Catalyst	Ru (%)	t (min)	T (ºC)	P (MPa)	Conversion (%)	Yield (%)	Reference
Ru/MCM-48	4.04	25	120	2.5	89.56	89.56	
Ru/TiO_2	3.98	20	120	2.5	91.39	91.39	This work
Ru/C	5	10	120	2.5	94.75	94.75	
Ru/MCM-41	3.98	120	120	3.0	100	83.13	[16]
Ru/TiO_2	1	120	120	5.5	92.5	86.67	[5]
Ru/C	5	120	120	3.0	70	41.79	[16]

Activity results obtained in this work are compared with those obtained previously by other authors (Table 7). While the intrinsic reaction rate constant is the most meaningful parameter to compare different catalytic systems, it is more common to obtain in the literature conversion and yield data. In these terms, the catalysts presented in this work outperformed comparable systems reported in the literature, even demonstrating to be more selective to sorbitol than the others working at lower hydrogen pressures and smaller reaction times. Additionally, Ru/MCM-48 showed better stability after three cycles of reaction than its counterpart in the literature Ru/MCM-41. Yield to sorbitol remained constant after three cycles of reaction over Ru/MCM-48, while it decreased from 83 % to 68 % in the case of Ru/MCM-41[16]. The best stability of Ru/MCM-48 can be attributed to the differences in pore structure between MCM-48 and MCM-41, since MCM-48 has a cubic pore system while MCM-41 presents a hexagonal array of unidirectional pores, what can conduct to further diffusional limitations or pore blockage. Ru/MCM-48, which is the novel system here

presented, stands as a good candidate for a future scale-up and possible one-pot applications since MCM-48 has revealed as the best catalytic material for hydrolysis of cellulose and ruthenium deposited over MCM-48 showed a good metallic dispersion and demonstrated high activity in D-Glucose hydrogenation.

4. CONCLUSIONS

The results presented above support the following conclusions:

i) MCM-48 presented a good catalytic activity in the hydrolysis of cellulose, attributable to its surface acidity.

ii) Ru/MCM-48 was the catalysts with the narrowest ruthenium particle size distribution, presenting a comparable catalytic response to Ru/TiO_2 and Ru/C.

iii) Catalytic hydrogenation of D-Glucose over ruthenium catalysts was 100 % selective to sorbitol working in the temperature range between 80-120 ºC and a pseudo-first order dependency was observed with respect to D-Glucose.

iv) A good stability after three reaction cycles was observed for Ru/MCM-48, both in terms of catalytic response and Ru crystallite size.

v) In accordance to the results here presented, MCM-48 stands as a good material to support ruthenium nanoparticles in order to catalyze one-pot cellulose hydrogenolysis.

Acknowledgements

The authors acknowledge the Spanish Ministry, MINECO, for the financial support of this project (CTQ2011-27347). A. Romero thanks to the program of predoctoral scholarships from Junta of Castilla y León for his grant (E-47-2015-0062773).

References

1. Fukuoka, A. and P.L. Dhepe, *Catalytic Conversion of Cellulose into Sugar Alcohols.* Angewandte Chemie, 2006. **118**(31): p. 5285-5287.

2. Van de Vyver, S., et al., *Recent Advances in the Catalytic Conversion of Cellulose.* ChemCatChem, 2011. **3**(1): p. 82-94.

3. Rogalinski, T., T. Ingram, and G. Brunner, *Hydrolysis of lignocellulosic biomass in water under elevated temperatures and pressures.* The Journal of Supercritical Fluids, 2008. **47**(1): p. 54-63.

4. Xi, J., et al., *Direct conversion of cellulose into sorbitol with high yield by a novel mesoporous niobium phosphate supported Ruthenium bifunctional catalyst.* Applied Catalysis A: General, 2013. **459**: p. 52-58.

5. Mishra, D.K., et al., *Liquid phase hydrogenation of d-glucose to d-sorbitol over the catalyst (Ru/NiO–TiO_2) of ruthenium on a NiO-modified TiO_2 support.* Catalysis Today, 2012. **185**(1): p. 104-108.

6. Grembecka, M., *Sugar alcohols—their role in the modern world of sweeteners: a review.* European Food Research and Technology, 2015: p. 1-14.

7. Huang, Y.-B. and Y. Fu, *Hydrolysis of cellulose to glucose by solid acid catalysts.* Green Chemistry, 2013. **15**(5): p. 1095-1111.

8. Gallezot, P., et al., *Glucose hydrogenation on promoted raney-nickel catalysts.* Journal of Catalysis, 1994. **146**(1): p. 93-102.

9. Arena, B.J., *Deactivation of ruthenium catalysts in continuous glucose hydrogenation.* Applied Catalysis A: General, 1992. **87**(2): p. 219-229.

10. Hoffer, B.W., et al., *Carbon supported Ru catalysts as promising alternative for Raney-type Ni in the selective hydrogenation of d-glucose.* Catalysis Today, 2003. **79-80**: p. 35-41.

11. Maris, E.P., et al., *Metal Particle Growth during Glucose Hydrogenation over Ru/SiO_2 Evaluated by X-ray Absorption Spectroscopy and Electron Microscopy.* The Journal of Physical Chemistry B, 2006. **110**(15): p. 7869-7876.

12. Perkas, N., et al., *Sonochemically Prepared high Dispersed Ru/TiO_2 Mesoporous Catalyst for Partial Oxidation of Methane to Syngas.* Catalysis Letters, 2005. **103**(1-2): p. 9-14.

13. Mishra, D.K., et al., *Selective hydrogenation of d-glucose to d-sorbitol over HY zeolite supported ruthenium nanoparticles catalysts.* Catalysis Today, 2014. **232**(0): p. 99-107.

14. Eisenbeis, C., et al., *Monolith loop reactor for hydrogenation of glucose.* Catalysis Today, 2009. **147, Supplement**(0): p. S342-S346.

15. Guo, X., et al., *Selective hydrogenation of D-glucose to D-sorbitol over Ru/ZSM-5 catalysts.* Chinese Journal of Catalysis, 2014. **35**(5): p. 733-740.

16. Zhang, J., et al., *Efficient conversion of d-glucose into d-sorbitol over MCM-41 supported Ru catalyst prepared by a formaldehyde reduction process.* Carbohydrate Research, 2011. **346**(11): p. 1327-1332.

17. Schumacher, K., et al., *Characterization of MCM-48 Materials.* Langmuir, 2000. **16**(10): p. 4648-4654.

18. Schumacher, K., M. Grün, and K.K. Unger, *Novel synthesis of spherical MCM-48.* Microporous and Mesoporous Materials, 1999. **27**(2–3): p. 201-206.

19. Amorim, C. and M.A. Keane, *Palladium supported on structured and nonstructured carbon: A consideration of Pd particle size and the nature of reactive hydrogen.* Journal of Colloid and Interface Science, 2008. **322**(1): p. 196-208.

20. Schmidt, R., et al., *High-resolution electron microscopy and X-ray diffraction studies of MCM-48.* Microporous Materials, 1995. **5**(1–2): p. 1-7.

21. Brunauer, S., et al., *On a Theory of the van der Waals Adsorption of Gases.* Journal of the American Chemical Society, 1940. **62**(7): p. 1723-1732.

22. Morey, M., et al., *Pseudotetrahedral $O_{3/2}VO$ Centers Immobilized on the Walls of a Mesoporous, Cubic MCM-48 Support: Preparation, Characterization, and Reactivity toward Water As Investigated by 51V NMR and UV−Vis Spectroscopies.* Chemistry of Materials, 1996. **8**(2): p. 486-492.

23. Ravikovitch, P.I., et al., *Evaluation of Pore Structure Parameters of MCM-41 Catalyst Supports and Catalysts by Means of Nitrogen and Argon Adsorption.* The Journal of Physical Chemistry B, 1997. **101**(19): p. 3671-3679.

24. Wu, H.-Y., et al., *Preparation, characterization and catalytic properties of MCM-48 supported tungstophosphoric acid mesoporous materials for green synthesis of benzoic acid.* Journal of Solid State Chemistry, 2014. **211**(0): p. 51-57.

25. Xue, P., et al., *A novel support of MCM-48 molecular sieve for immobilization of penicillin G acylase.* Journal of Molecular Catalysis B: Enzymatic, 2004. **30**(2): p. 75-81.

26. Papp, J., et al., *Surface Acidity and Photocatalytic Activity of TiO2, WO3/TiO2, and MoO_3/TiO_2 Photocatalysts.* Chemistry of Materials, 1994. **6**(4): p. 496-500.

27. Liang, C., et al., *Hydrogen Spillover Effect in the Reduction of Barium Nitrate of Ru-Ba$(NO_3)_2$/AC Catalysts for Ammonia Synthesis*, in *Studies in Surface Science and Catalysis*, A. Guerrero-Ruiz and I. Rodríguez-Ramos, Editors. 2001, Elsevier. p. 283-290.

28. Onda, A., T. Ochi, and K. Yanagisawa, *Hydrolysis of Cellulose Selectively into Glucose Over Sulfonated Activated-Carbon Catalyst Under Hydrothermal Conditions.* Topics in Catalysis, 2009. **52**(6-7): p. 801-807.

29. Onda, A., T. Ochi, and K. Yanagisawa, *Selective hydrolysis of cellulose into glucose over solid acid catalysts.* Green Chemistry, 2008. **10**(10): p. 1033.

30. Chareonlimkun, A., et al., *Catalytic conversion of sugarcane bagasse, rice husk and corncob in the presence of TiO_2, ZrO_2 and mixed-oxide TiO_2–ZrO_2 under hot compressed water (HCW) condition.* Bioresource Technology, 2010. **101**(11): p. 4179-4186.

31. Wisnlak, J. and R. Simon, *Hydrogenation of Glucose, Fructose, and Their Mixtures.* Industrial & Engineering Chemistry Product Research and Development, 1979. **18**(1): p. 50-57.

32. Crezee, E., *Three-phase hydrogenation of D-glucose over a carbon supported ruthenium catalyst—mass transfer and kinetics.* Applied Catalysis A: General, 2003. **251**(1): p. 1-17.

33. Bond, G.C., *Kinetics of alkane reactions on metal catalysts: activation energies and the compensation effect.* Catalysis Today, 1999. **49**(1–3): p. 41-48.

34. Corma, A., et al., *On the Compensation Effect in Acid-Base Catalyzed Reactions on Zeolites.* Journal of Catalysis, 1993. **142**(1): p. 97-109.

CHAPTER 2

SUPERCRITICAL WATER HYDROLYSIS OF CELLULOSIC BIOMASS AS EFFECTIVE PRETREATMENT TO CATALYTIC PRODUCTION OF HEXITOLS AND ETHYLENE GLYCOL OVER RU/MCM-48

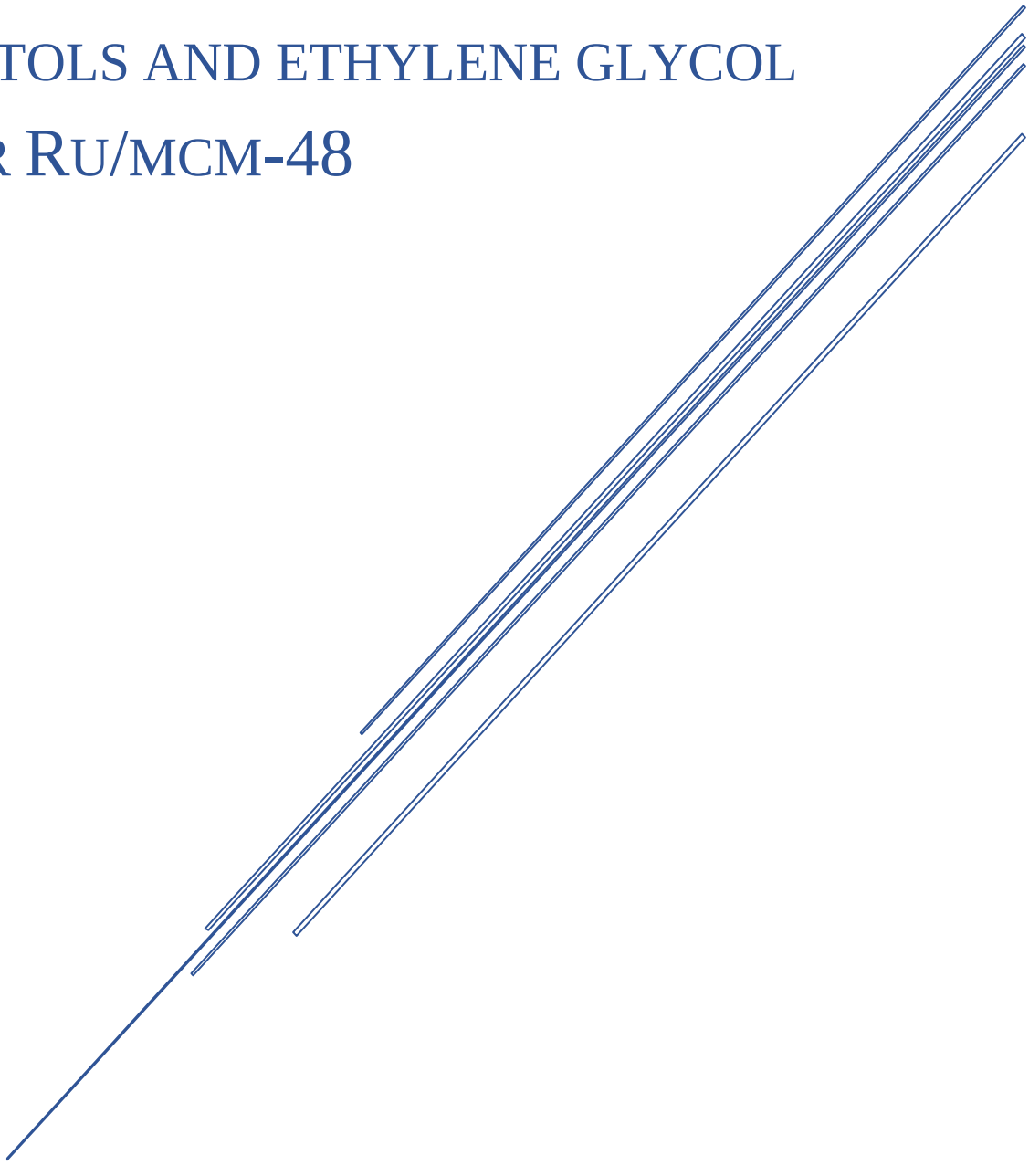

SUPERCRITICAL WATER HYDROLYSIS OF CELLULOSIC BIOMASS AS EFFECTIVE PRETREATMENT TO CATALYTIC PRODUCTION OF HEXITOLS AND ETHYLENE GLYCOL OVER Ru/MCM-48

Abstract

A novel combination, based on supercritical water hydrolysis of cellulose and the subsequent hydrogenation of the so-obtained hydrolysates on mesoporous Ru/MCM-48, was proposed as a potential alternative to classical one-pot hydrolytic hydrogenation process. Supercritical water (SCW) was used as reaction medium for cellulose hydrolysis, since in this reaction medium it is possible to depolymerize cellulose with high selectivity to sugars (70 % $w \cdot w^{-1}$) avoiding degradation reactions. The SCW hydrolysis was carried out at 400 ºC – 25 MPa with extremely low reaction times (0.20 s). The hydrogenation of the liquid product from cellulose hydrolysis in SCW allowed maximizing yield to hexitols by changing temperature and reaction time. The results demonstrated the achievement of higher yields to hexitols by the subsequent hydrogenation of the liquid product from cellulose hydrolysis in SCW (49 %) than using the one – pot catalytic hydrogenation of cellulose. Ru/MCM-48 showed better behavior than commercial Ru/C during the hydrogenation process in all the cases. Thus, Ru/MCM-48 was also employed in the hydrogenation of the product from sugar beet pulp (SBP) hydrolysis in SCW. SBP was used in order to evaluate the behavior of a real biomass in this process. A yield to hexitols of 15 % was achieved from SBP, ethylene glycol was the main compound in the liquid product and glycerol was obtained as byproduct too.

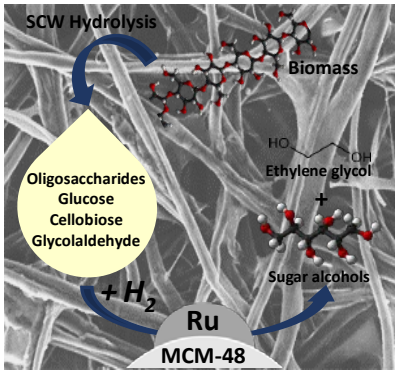

Keywords

Cellulose, ethylene glycol, hexitols, Ru/MCM-48, sugar beet pulp, supercritical water.

1. INTRODUCTION

Nowadays, catalytic conversion of cellulosic biomass has achieved a great attention as a sustainable reaction route to obtain chemicals, fuels and energy from renewable raw materials, inhibiting global warming as a result of the decrease in CO_2 emissions [1]. In this sense, cellulose is the most abundant component in lignocellulosic biomass [2] and therefore appears as one of the most promising feedstock in selective hydrolytic processes to produce fuels and chemicals. Cellulose is a linear polymer that consists on glucose units linked by β-1,4-glycosidic bonds with inter- and intra- hydrogen bonds [3]. This characteristic makes cellulose insoluble in water and non-edible by humans and thus it is not suitable for nutritional purposes [4].

In essence, hydrolytic conversion of cellulosic biomass into hexitols is a process that consists on two different steps. Firstly, cellulose must be *depolymerized* into glucose, being this step a challenge. Generally, harsh conditions of temperature and acidity are required to obtain high yields of glucose. However, at these conditions, glucose is rapidly decomposed because the conversion rate of sugars is faster than cellulose hydrolysis and therefore a low yield of glucose is obtained [5]. Once the sugars are available as monomers, they are *hydrogenated* into mannitol and sorbitol, which are thermally more stable than glucose. Thus, a selective and high-yielding glucose production during hydrolysis step seems to be necessary for the efficient conversion of cellulose into hexitols.

Different alternatives for cellulose hydrolysis are proposed in the literature such as the use of supercritical water (SCW) [6], enzymes [7] and mineral acids [8]. Enzymatic hydrolysis and processes based on mineral acids showed some disadvantages such as separation of the products from the catalysts, long reaction times, high production of byproducts and strict controls of enzymes [7, 8]. In order to circumvent such drawbacks, the use of SCW as reaction medium appears as an environmentally friendly method and a very promising alternative for biomass processing [9]. SCW has achieved a good piece of attention because its use as a reaction media promotes the reduction of derived products during hydrolysis step [5, 10]. This is possible since the process allows an effective control on reaction time, working in the range of milliseconds. Therefore, the hydrolysis can be stopped before the starting of glucose degradation reactions [6]. In addition, this kind of processes are able to convert 100 % of cellulose in reaction times as low as 0.02 s [6]. This fact represents a reduction in the reaction time of between 10^5 and 10^7 times in comparison to the acid and enzymatic hydrolysis. A process with high selectivity that

requires extremely low reaction times is the key for the development of the decentralized and sustainable production of chemicals from renewable plant biomass [6]. On the other hand, the hydrogenation of sugar products is carried out using supported metal catalyst under H_2 pressure [11]. The efficiency of the catalyst is one of the keys at this point. In this sense, Ru-based catalysts have been reported to be more active than nickel, cobalt or platinum in glucose hydrogenation into sorbitol [12-14].

Sugar beet pulp (SBP) is a valuable and cheap (100 US$ per metric ton) by-product from the manufacturing of sugar from beet pulp, produced in large amounts [15]. Approximately, its composition has been reported to be 85 % carbohydrates (cellulose, hemicellulose, pectin, an others), 10-15 % protein and 1-2 % lignin ($w \cdot w^{-1}$, dry basis) [16]. Therefore, SBP appears as an interesting feedstock to produce valuable chemicals and fuels.

The aim of this work is to study the catalytic performance of bifunctional Ru/MCM-48 in hydrolytic hydrogenation of cellulose comparing the one-pot methodology with a two-steps process based on SCW hydrolysis and the subsequently hydrogenation of the product so obtained. Catalytic behavior of Ru/MCM-48 is compared with a commercial Ru/C. The interwoven and branched pore structure of MCM-48 enhances diffusional limitations of large molecules [17] and its acidity plays an important role during hydrolysis step, while ruthenium, as active phase, promotes sugars hydrogenation into hexitols. As previously described, degradation of glucose during hydrolysis step drives to the obtaining of low hexitols yield during the hydrogenation process. Therefore, in this study SCW serves as reaction medium for cellulose hydrolysis, since it demonstrated to be an excellent solvent and reaction medium to improve the cellulose hydrolysis selectivity into glucose by controlling the reaction time. In this sense, it is possible to achieve higher hexitols yield using SCW hydrolysis as depolymerization step before the hydrogenation process rather than carrying out a one-pot reaction from untreated cellulose. In order to check this process in a real kind of biomass, SBP pretreated under SCW was also hydrogenated.

2. MATERIALS AND METHODS

2.1. CATALYST PREPARATION

The synthesis of MCM-48 ordered mesoporous silica was performed according to the conventional hydrothermal procedure described in refs. [18, 19]. N-

hexadecyltrimethylammonium bromide ($CH_3(CH_2)_{15}N(Br)(CH_3)_3$ ≥ 98 %, Sigma – Aldrich), which was used as template, was dissolved into 42 mL deionized water in order to dissolve it. Then, 13 mL of aqueous ammonia (20 % as NH_3, Panreac) and 18 mL of absolute ethanol (partially denaturated QP, Panreac) were added into the solution for 15 minutes. 4 mL of tetraethyl ortosilicate was added dropwise and stirred for 18 hours. The gel was filtered obtaining white precipitates; thereafter they were washed with distilled water, dried at 60 ºC overnight and calcined at 550 ºC.

Ruthenium was deposited on MCM-48 by the wetness impregnation (WI) method with an aqueous solution of ruthenium chloride ($RuCl_3$.anhydrous, Strem Chemical) according to the desired metal loading. The impregnation process was carried out at 105 ºC using a heating plate until solvent was completely evaporated. The catalyst was dried at 105 ºC and reduced at 150ºC under TPR-H_2 conditions. Commercial Ru/C catalysts supplied by Strem Chemical has been used in this work for comparison purposes. More detailed information about these procedures can be found in a previous work ref. [20].

2.2. CATALYST CHARACTERIZATION

The specific surface area of MCM-48, Ru/C and Ru/MCM-48 were conducted by the nitrogen adsorption/desorption method (Quantasorb Sorption system, Quantachrome instruments). Prior to the measurement, the support and the catalysts were outgassed at 350 ºC for MCM-48 and Ru/MCM-48, while Ru/C catalyst was outgassed at 180 ºC. The multipoint BET method was used to determine total specific surface area ($P/P_0 \leq 0.3$) and pore volumes were calculated from N_2 uptake at $P/P_0 \geq 0.97$. X-Ray powder diffraction (Bruker Discover D8) was conducted with Cu Kα radiation (λ = 0.15406 nm) and angular range of 30° < 2θ < 90° for XRD analysis of catalysts with a scanning rate of 1.8 degrees·min^{-1}. The metal loading of the ruthenium catalysts was determined by atomic absorption (AA) spectrophotometry, using a SPECTRA 220FS analyzer. Approximately, 0.05 g of the sample, 3 mL of HCl, 3 mL H_2O_2 and 3 mL HF were treated by microwave digestion at 250 ºC. Transmission electron microscopy (TEM) analyses were performed for ruthenium catalysts using a JEOL 2100 unit with an accelerating voltage of 200 kV. The catalysts were dispersed in acetone and a drop of the resultant suspension was evaporated onto a mesh carbon-supported grid. Ru particle size distribution of the catalyst was obtained by a counting of Ru particles from TEM images. Mean Ru crystallite sizes were expressed according to the surface – area weighted diameter (Eq 1.), where at least 240

ruthenium nanoparticles were counted in each case. In equation 1, $\bar{d}_s$ is surface-area weighted diameter and n_i is the number of ruthenium particles with a diameter d_i. Fourier transform infrared spectras of the materials were obtained by a FT-IR TENSOR analyzer from BRUKER. Acid – base titrations were carried out by immersing 25 mg of sample in 100 mL NaCl 0.1 M, acidified with 1 mL HCl 0.1 M using continuous stirring. A 0.1 M NaOH solution was used as the titrant and the pH was monitored by a Crison pH-meter. The initial NaCl + (HCl) solution served as a blank.

$$\bar{d}_s = \frac{\sum_i^n n_i \cdot d_i^3}{\sum_i^n n_i \cdot d_i^2} \quad (1)$$

2.3. CRYSTALLINITY OF CELLULOSE

The crystalline structure of Avicel microcrystalline cellulose (PH-101, Sigma-Aldrich) was analyzed by using Cu-Kα radiation (λ = 0.15406 nm) and angular range of 5° < 2θ < 70° by using XRD (Bruker Discover D8). The percentage of crystallinity was calculated according to Equation 2 where *CrI* is the percentage of crystallinity (%); I_{002} is the maximum intensity of the 002 peak at 2θ = 22.7° and I_{am} is the intensity at 2θ = 18.7°.

$$CrI = \frac{I_{002} - I_{am}}{I_{002}} \quad (2)$$

2.4. BIOMASS HYDROLYSIS IN SUPERCRITICAL WATER

The hydrolysis of cellulose and sugar beet pulp was carried out in a continuous experimental setup designed to operate at 400 ºC and 25 MPa. A plan of the facility is shown in Figure 1.

This facility was designed and built as detailed elsewhere [6], where the process showed to be an efficient method to depolymerize cellulose as well as lignocellulosic biomass like wheat bran [10]. The capabilities of the setup lie in the precise control of the reaction time, which allows working at high temperature (400 ºC) at extremely low reaction times (0.2 s). The combination of high reaction temperature and low reaction times make it possible to work with fast kinetics but also preventing from degradation products. A biomass suspension (cellulose or lignocellulosic biomass, 7% $w \cdot w^{-1}$) was continuously pumped up to the operation pressure (normally, 25 MPa) at room temperature to the inlet of the reactor. Up to the reactor inlet, the biomass remained with the same composition than in the raw material. The reaction started when the biomass stream was

instantaneously heated by mixing it with a supercritical water stream [6]. Therefore, the heating of the biomass (which is the beginning of the reactions) was achieved almost instantaneously. The mixing ratio of biomass to supercritical water streams was chosen to obtain a biomass concentration at the reactor inlet of approximately 1.5% $w \cdot w^{-1}$. After the desired temperature is reached at the reactor inlet, the contact time of biomass at reaction conditions is critical for the selectivity of the process. The hydrolysis of biomass in supercritical water is fast, so the reaction time should be lower than 0.3 s avoiding high amounts of degradation products. The reaction time of the experiments was modified by changing the flows and reactor volumes (length of tubular reactors). In order to make the reactor as thermally stable as possible it was insulated with Rockwool. The products from the reactor effluent (hydrolysates) were rapidly cooled down (end of reactions) by sudden expansion in a high temperature valve (Autoclave VRMM4812). The pressure drop was from 25 MPa to 0.1 MPa, obtaining in this way, an instantaneous cooling from the reaction temperature to 100 ± 10 ºC. Finally, the product stream was cooled down to room temperature prior to taking the sample in a dual tube coil heat exchanger. Product mixtures were centrifuged and the filtered solution was analyzed by High Performance Liquid Chromatography (HPLC). Shodex SH-1011 column was used for the separation of the compounds at 50 ºC, using H_2SO_4 (0.01 N, 0.8 $mL \cdot min^{-1}$) as mobile phase. Sugar and related products were detected by a Waters IR detector 2414. Shimadzu TOC-VCSH analyzer was used to measure total organic carbon (TOC, $mg \cdot l^{-1}$ C) content in hydrolysis products. Soluble oligosaccharides were determined by acid hydrolysis to glucose and HPLC determination [21] following the procedure reported by Sluiter et al. from National Renewable Energy Laboratory (NREL) [22]. More detailed descriptions of the pilot plant and the operation procedure are given in a previous work [6].

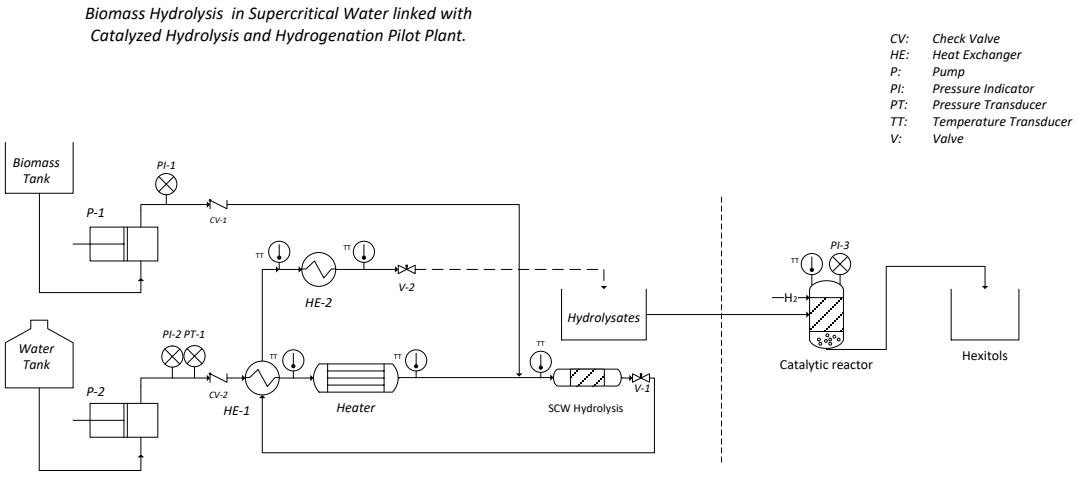

Figure 1. Biomass hydrolysis in Supercritical Water linked with hydrolytic hydrogenation pilot plant.

The main achievements of the experimental setup are: (a) the reactor can be considered isothermal due to the instantaneous heating and cooling; (b), products are not diluted in the cooling process; (c) the reaction time can be varied from 0.004 s to 40 s using Ni-alloy tubular reactors with different lengths and (d) most of the employed heat in the process can be integrated in order to produce energy in cogeneration cycles [23].

2.5. HYDROGENATION OF BIOMASS

On the right part of sketch in Figure 1, it can be observed the experimental set-up where catalytic hydrogenation of the products from SCW hydrolysis and one-pot catalytic hydrogenation of cellulose were performed. The hydrogenation experimental plant consists on the following elements: hydrogen-feeding, valves to vent the lines and the reaction block. The last element contains a commercial stainless-steel high-pressure reactor (Berghoff BR-25, 25 mL) PID controlled. Hydrogen (purity 99.99 %) was supplied by Carburos Metálicos (Spain). Hydrogenation reactions were carried out in the range of 120 ºC – 240 ºC at 5 MPa of H_2. Firstly, the reactor was preheated at 150 ºC with a continuous flow of hydrogen and under these conditions; catalysts were reduced during 30 min before the reaction. The amount of catalyst was selected according to a C / Ru ($mol \cdot mol^{-1}$) ratio = 142. Carbon was related to total organic carbon presented in the starting biomass. Thereafter, the reactor was heated up to the desired reaction temperature and 10 mL of the hydrolyzed biomass or cellulose suspension (2 % $w \cdot w^{-1}$) was pumped into the reactor. The reaction products were filtered in order to recover the catalyst from the liquid phase, which was analyzed by HPLC. A SUGAR SC-1011 column from Shodex at 80 ºC and a flow of 0.8 $mL \cdot min^{-1}$ was selected using water Milli-Q as the mobile phase. Yield to products based on carbon basis was calculated according to equation 3, where [P] is the concentration of the products analyzed by HPLC ($mg \cdot l^{-1}$), x_c is de mass fraction of carbon in each product and TOC ($mg \cdot l^{-1}$) is the total organic carbon from the starting raw material which was hydrogenated. For hydrolytic hydrogenation of cellulose experiments, cellulose was recovered, washed and dried in order to calculate conversion of cellulose ($X_{Cellulose,}$ %), which was evaluated from the weight change of cellulose, as given in equation 4. m_{C0} is the amount of cellulose introduced in the reactor in each test and m_C is the amount of cellulose recovered after the reaction.

$$Y\ (C\ \%) = \frac{[P] \cdot x_C}{TOC} \cdot 100 \quad (3)$$

$$X\ (\%) = \frac{m_{C0} - m_C}{m_{C0}} \cdot 100 \quad (4)$$

3. RESULTS AND DISCUSSION

3.1. CATALYST CHARACTERIZATION

Specific surface area, total pore volume, NaOH consumption from acid-base titration and Ru metal loadings of the catalytic materials are presented in Table 1. MCM-48 was successfully prepared by the sol gel method displaying a high specific surface area of 1594 $m^2 \cdot g^{-1}$ and pore volume of 0.9 $cm^3 \cdot g^{-1}$. Similar textural properties for other mesoporous silica MCM-48 prepared by hydrothermal methods have been reported in the literature [24, 25]. A decrease in the specific surface area and pore volume of Ru/MCM-48 are noticed after the deposition of the active metal from 1594 to 1453 $m^2 \cdot g^{-1}$ and from 0.90 to 0.47, respectively. This effect is due to a partial blocking of the porous network of the support. Ru/C supplied by Strem Chemical showed smaller specific surface area and similar pore volume than Ru/MCM-48. The ruthenium metal content for Ru/MCM-48 and Ru/C catalysts was determined to be 4 % and 5 % by atomic absorption spectrophotometry, respectively. Acid – Base properties of the catalytic materials were determined in terms of NaOH consumption. According to NaOH titration results, Ru/MCM-48 demonstrated higher acidity than commercial Ru/C. These acidic features of MCM-48 are due to weak acidity from terminal silanol groups (Si-OH) [26]. Non-appreciable changes in NaOH consumption were observed after ruthenium deposition on MCM-48. FT-IR measurements (Figure 2) confirmed the presence of Si-OH groups in MCM-48 and Ru/MCM-48 samples. FT-IR spectrum of MCM-48 and Ru/MCM-48 showed Si-OH stretching vibrations at 961 cm^{-1}. In general terms, Figure 2 A and B depicted similar FT-IR spectrum, but the main difference was found in the bands at 3393 cm^{-1} and 1625 cm^{-1} related to adsorbed water. 3393 cm^{-1} band is assigned to the O–H vibration of water molecules, and the peak around 1625 cm^{-1} corresponds to the deformation vibration of O–H binds in water molecules [27]. These bands are more intense for Ru/MCM-48 in comparison to calcined MCM-48, since Ru/MCM-48 was prepared by a wet impregnation method using water as solvent. Low acidic surface properties from Ru/C are attributed to the presence of oxygenated surface groups, such as carboxylic or lactones as other authors have reported in the literature [28].

H_2-TPR profile was determined for Ru/MCM-48. It was not necessary for Ru/C since this commercial catalyst was supplied in its active form. TPR curve for Ru/MCM-48 (Figure 3 (A)) depicted a single peak at 125 ºC corresponding to the reduction of Ru^{3+} to Ru^0 [29]. XRD patterns for Ru/MCM-48 and Ru/C are shown in Figure 3 (B). It was observed a diffraction peak at $2\theta = 43.8^{o}$ (JCPDS No. 06–0663) attributed to Hexagonal

Close Packing (HCP) Ru^0 nanoparticles in both cases. These results confirmed the proper reduction of Ru/MCM-48 under H_2-TPR conditions and metallic state of Ru nanoparticles in the case of the commercial catalyst. TEM images and ruthenium particle size distribution of Ru/C and Ru/MCM-48 are presented in Figure 4.

Table 1. Metal loading, textural and acid - base properties of the catalytic materials

Catalyst	Ru (%)	S_{BET} ($m^2 \cdot g^{-1}$)	Vp ($cm^3 \cdot g^{-1}$)	NaOH consumption ($cm^3 \cdot g^{-1}$)	$\bar{d}_s$ [a] (nm)
MCM-48	0	1594	0.90	5.8	-
Ru/MCM-48	4	1453	0.47	5.7	2.5
Ru/C	5	759	0.50	1.9	3.4

[a] Based on TEM measurements and Equation 1

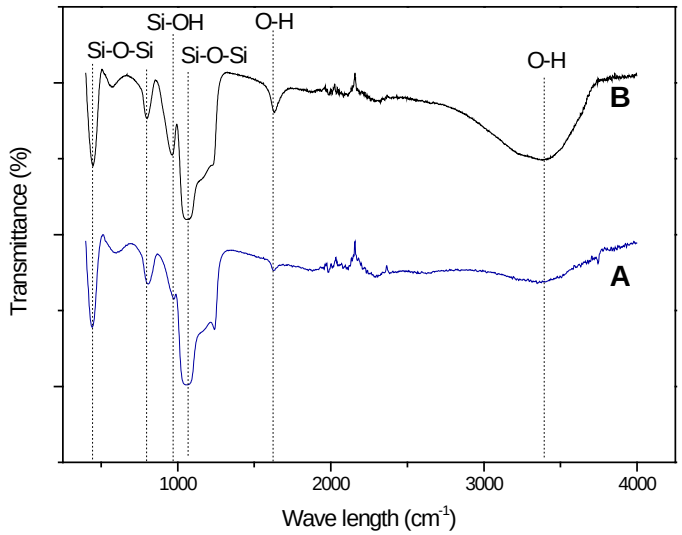

Figure 2. Fourier Transform Infrared (FT-IR) spectra of MCM-48 (A) and Ru/MCM-48 (B).

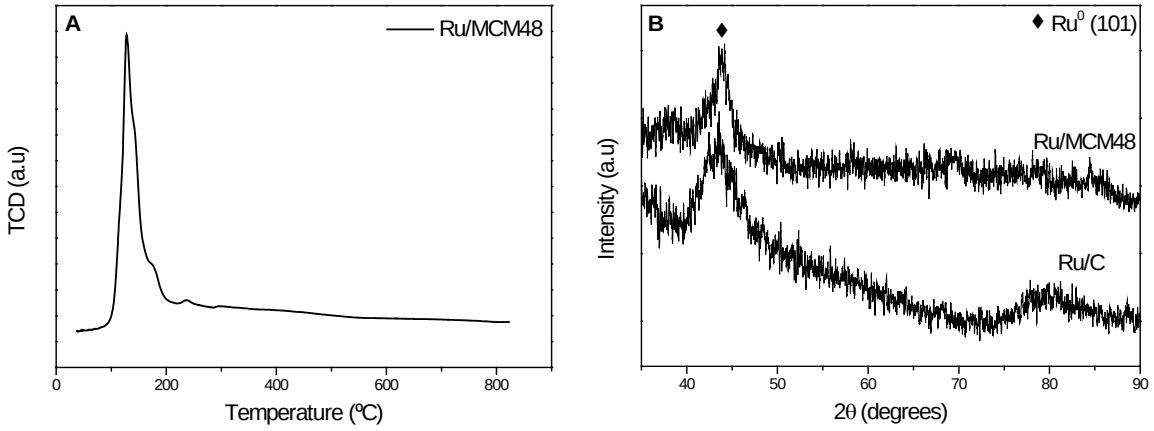

Figure 3. (A) H_2-TPR profile for Ru/MCM-48 and **(B)** XRD patterns of Ru/MCM-48 and Ru/C.

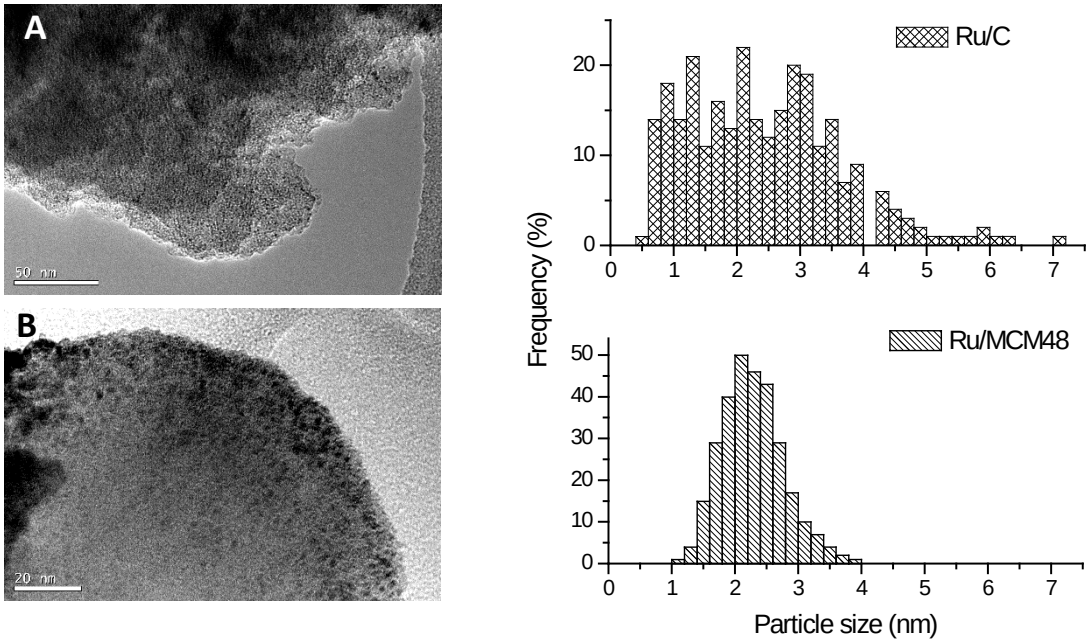

Figure 4. TEM micrographs and derived Ru particle size distribution of **(A)** Ru/C and **(B)** Ru/MCM-48.

The obtained distribution of ruthenium nanoparticles over carbon and MCM-48 was homogenous. Ru/MCM-48 showed the narrowest Ru particles size distribution in the range of 1-4 nm, having a surface-area weighted mean diameter of 2.5. In case of Ru/C, the particle distribution was in the range of 0.5-7 nm with a surface-area weighted mean diameter of 3.4 (Table 1).

3.2. CELLULOSE VALORIZATION INTO HEXITOLS

Different approaches have been done in the study of cellulose valorization into hexitols, but recently, one-pot hydrolytic hydrogenation of cellulose has achieved a good piece of attention [30, 31]. Results from hydrolytic hydrogenation of cellulose for 10 – 30 min over Ru/MCM-48 carried out in this research are summarized in Table 2. Commercial Ru/C was used for comparative purposes.

Table 2. One-pot catalytic hydrogenation of cellulose over Ru/MCM-48 and Ru/C at 240 ºC and 5 MPa H_2.

	t (min)	Conversion (%)	Yield (C %)				
			Glucose	Fructose	Mannitol	Sorbitol	Hexitols [a]
Ru/MCM-48	10	24.9	0.73	1.74	4.8	15.9	20.7
Ru/MCM-48	30	31.4	1.51	2.59	6.0	7.4	13.4
Ru/C	10	9.6	0.04	0.22	3.7	2.3	6.0
Ru/C	30	14.4	0.03	0.04	2.1	0.2	2.3

[a] Sum of yields to mannitol and sorbitol.

The maximum conversion of cellulose was 31.4 % using Ru/MCM-48 and 30 min of reaction time. The conversion was 14.4 % when the reaction was performed using Ru/C with the same reaction time. Regarding selectivity, the experiment using Ru/MCM-48 yielded 20.7 % to hexitols after 10 min and demonstrated to be more selective to sorbitol. For the Ru/C run, the yield to hexitols achieved 6.0 %, being more selective to mannitol. These experiments were carried out under subcritical water conditions, where the concentration of ions is higher than those obtained at supercritical water [32]. Thus, those experimental conditions promote the isomerization of glucose into fructose. In this sense, a considerable amount of mannitol was detected using both Ru/MCM-48 and Ru/C. This was a result of the subsequent hydrogenation of fructose produced by the hydrolysis of cellulose under subcritical water conditions [33]. Despite Ru/MCM-48 achieved higher yields to hexitols than commercial Ru/C, in general terms, low yields to hexitols were obtained in both cases. During the one-pot hydrolytic hydrogenation of cellulose, hydrolysis of cellulose and hydrogenation of sugars take place simultaneously. Thus, a low efficiency in the first step could affect final yield to sorbitol and mannitol. In this case, Ru/MCM-48 showed higher acidity values from NaOH consumption in comparison to Ru/C, but the weak acidity presented by Ru/MCM-48 was not enough to promote hydrolysis step efficiently. This task is even more difficult due to low reactivity of cellulose related to its high grade of crystallinity. In the case of the Avicel microcrystalline cellulose used in the present work, the crystallinity index was 76 %, which was estimated from XRD pattern of cellulose and Equation 2. To overcome these problems, it is necessary to work at higher temperatures [13], but these conditions could degrade or decompose sugar alcohols [34]. The influence of reaction time on the obtained yields is shown in Table 2. In the case of Ru/MCM-48, the sorbitol yield decreased from 15.9 to 7.4 %, suggesting the hydrogenolysis of sorbitol into isosorbide, iditol or sorbitan. On the other hand, a slight increase in mannitol yield was detected due to epimerization of sorbitol at longer reaction times [35]. A decrease of sorbitol and mannitol yield was observed for Ru/C working under the experimental conditions during 30 min. These results compare well with those reported by Luo et al. [36] under similar reaction environment (245 ºC, 6 MPa H_2, 20 $g \cdot l^{-1}$ cellulose and 5 min) where around 22 % of hexitols yield was obtained using Ru/C prepared by wet impregnation method. In addition, Negoi et al. stated that around 22 % of sorbitol yield was achieved from hydrolytic hydrogenation of cellulose over 3% Ru/BEA at 180 ºC, 1.6 MPa H_2, 20 $g \cdot l^{-1}$ cellulose and 24 h (Entry 2, Table 3). Ru/MCM-48 demonstrated similar selectivity to sorbitol (64 %) than Ru/BEA (62 %). 3 %

Ir/BEA catalyst was also tested, showing 22 % of yield to sorbitol (Entry 4, Table 3). In the case of Ir/BEA, selectivity to sorbitol was higher than that obtained for Ru/MCM-48. However, the final yield to hexitols was similar. Literature shows that the achievement of higher yields to hexitols is possible by hydrolytic hydrogenation of cellulose. However, important differences were observed in comparison to this work. A high yield to hexitols (around 86 %) was reached by Ennaert et al. (Entry 3, Table 3) over 0.2 % Ru/USY16 at 190 ºC, 5 MPa H_2 and 24 h. However, the addition of 50 mL of 0.96 mM aqueous HCl solution at the beginning of the catalytic test promoted hydrolysis of insoluble cellulose into soluble cello-oligomers. Thus, more cello-oligomers could be hydrolyzed into glucose in the zeolitic acid sites, allowing to obtain a high yield to hexitols by subsequently hydrogenation of glucose. Nickel-based catalyst Ni/ZSM-5 (40 % $w \cdot w^{-1}$ of nickel loading) was also employed for this task by Liang et al. (Entry 6, Table 3). In that work, 49 % of yield to hexitols was obtained. Finally, Negoi et al. greatly improved yield to hexitols up to 73 % by adding pure nanoscopic hydroxylated SnF_4 to 3 % Ir/BEA (Entry 5, Table 3).

Table 3. Conversion of cellulose into sugar alcohols.

Entry	Catalyst	Pretreatment of cellulose	t (h)	T (ºC)	P (MPa)	$Y_{HEXITOLS}$ (%)	Ref.
1	4 %, Ru/MCM-48	None	0.17	240	5	22	This work
2	3 %, Ru/BEA	None	24	180	1.6	22	[37]
3	0.2 % Ru/USY16	None	24	190	5	86	[38]
4	3 %, Ir/BEA	None	24	180	1.6	22	[37]
5	3 %, Ir/BEA-SnF_4	None	24	180	1.6	73	[37]
6	40 %, Ni/ZSM-5	None	4	230	4	49	[39]
7	2.5 %, Pt/γ-Al_2O_3	None	24	190	5	31	[1]
8	4 %, Ru/C	None	0.08	245	6	22	[36]
9	4 %, Ru/C	None	0.5	245	6	40	[36]
10	2 %, Ru/C	Ball-milled	18	190	0.8	38	[40]
11	3 %, Ni/CNF	None	24	210	6	35	[41]
12	4 %, Ru/MCM-48	SCW Hydrolysis	0.1	200	5	49	This work

To overcome the low reactivity of microcrystalline cellulose, most studies employed mechanical pretreatments such as milling to decrease the degree of crystallinity of the cellulosic material and improving its depolymerization [42, 43]. In this work, another method much more feasible was employed; the use of SCW as reaction medium to break and hydrolyze the crystalline cellulose. Cellulose and supercritical water streams were mixed at the inlet of a continuous reactor and cellulose was subjected to hydrolysis reactions for 0.2 s, at 400 ºC and 25 MPa. The product of this process was an aqueous

phase mainly composed of sugars. Table 4 shows the main composition of the liquid product after SCW pretreatment of cellulose. The product had 5940 $mg \cdot l^{-1}$ of total organic carbon, being 14.6 % cellobiose, 8.6 % glucose, 1.3 % glyceraldehyde and. 10.2 % glycolaldehyde. Additionally, a high amount of oligosaccharides of glucose (50 % of TOC) was detected from HPLC and quantified by acid hydrolysis, as explained in the experimental section.

Table 4. Composition of the hydrolyzed product ($mg \cdot l^{-1}$) and carbon basis yield (%) from SCW.

Cellobiose ($mg \cdot l^{-1}$ / C %)	**Glucose** ($mg \cdot l^{-1}$ / C %)	**Glyceraldehyde** ($mg \cdot l^{-1}$ / C %)	**Glycolaldehyde** ($mg \cdot l^{-1}$ / C %)	**Oligosaccharides** ($mg \cdot l^{-1}$ C / C %)	**TOC** ($mg \cdot l^{-1}$ C)
2055 / 14.6	1274 / 8.6	197 / 1.3	1521 / 10.2	2970 / 50	5940

Ru/MCM-48 and Ru/C were evaluated in the hydrogenation of the sugar product from the hydrolysis of cellulose in SCW. Additionally, a blank (no catalyst) test and a test with the bare MCM-48 were conducted (Figure 5A).

A blank experiment was carried out under hydrogen atmosphere, and it was observed that cellobiose and oligosaccharides could be hydrolyzed into glucose at a temperature of 180 º C. The yield to glucose increased from 8.6 %, which was detected in the hydrolysate from SCW, to 47.7 % in the liquid product. In addition, 4.2 % of fructose was obtained. Similar behavior was detected using MCM-48 as catalytic material; though yield to glucose increased to 55.7 %. Using MCM-48, 8% more of glucose was achieved in comparison to the blank test, which can be attributed to its weak acidity related to terminal silanol groups. The influence of the support during hydrolysis of cellulose was studied in a previous work [20]. As in the one-pot hydrogenolysis of cellulose, the use of Ru/MCM-48 showed better behavior than the use of Ru/C during the hydrogenation of the liquid product from SCW hydrolysis. The experiments employing Ru/MCM-48 achieved a yield to hexitols of 25.4 % while the use of the commercial Ru/C conducted to a yield of 10.7 %. The product obtained using Ru/MCM-48 was mainly composed of mannitol and sorbitol. However, in the reaction product using Ru/C, 9.6 % of cellobiose and 5.6 % of glucose were not converted into hexitols. Nevertheless, hexitols yield was still low because under these experimental conditions the hydrogenolysis of sorbitol is carried out simultaneously. This effect was checked by conducting experiments at the same experimental conditions but using sorbitol (2.5 $g \cdot l^{-1}$ of sorbitol) as starting material in the hydrogenation reaction.

For these experiments, Ru/MCM-48 was selected as catalysts and 10, 50 and 90 min were chosen as reaction times. Results presented in Figure 5 B, demonstrated 98.5 % of conversion of sorbitol when the reaction time was 90 min. Around 7 % of mannitol was obtained because of sorbitol isomerization. On the other hand, the products from the hydrogenolysis of sorbitol such as 1-4 sorbitan or isosorbide, could not be detected by HPLC analysis.

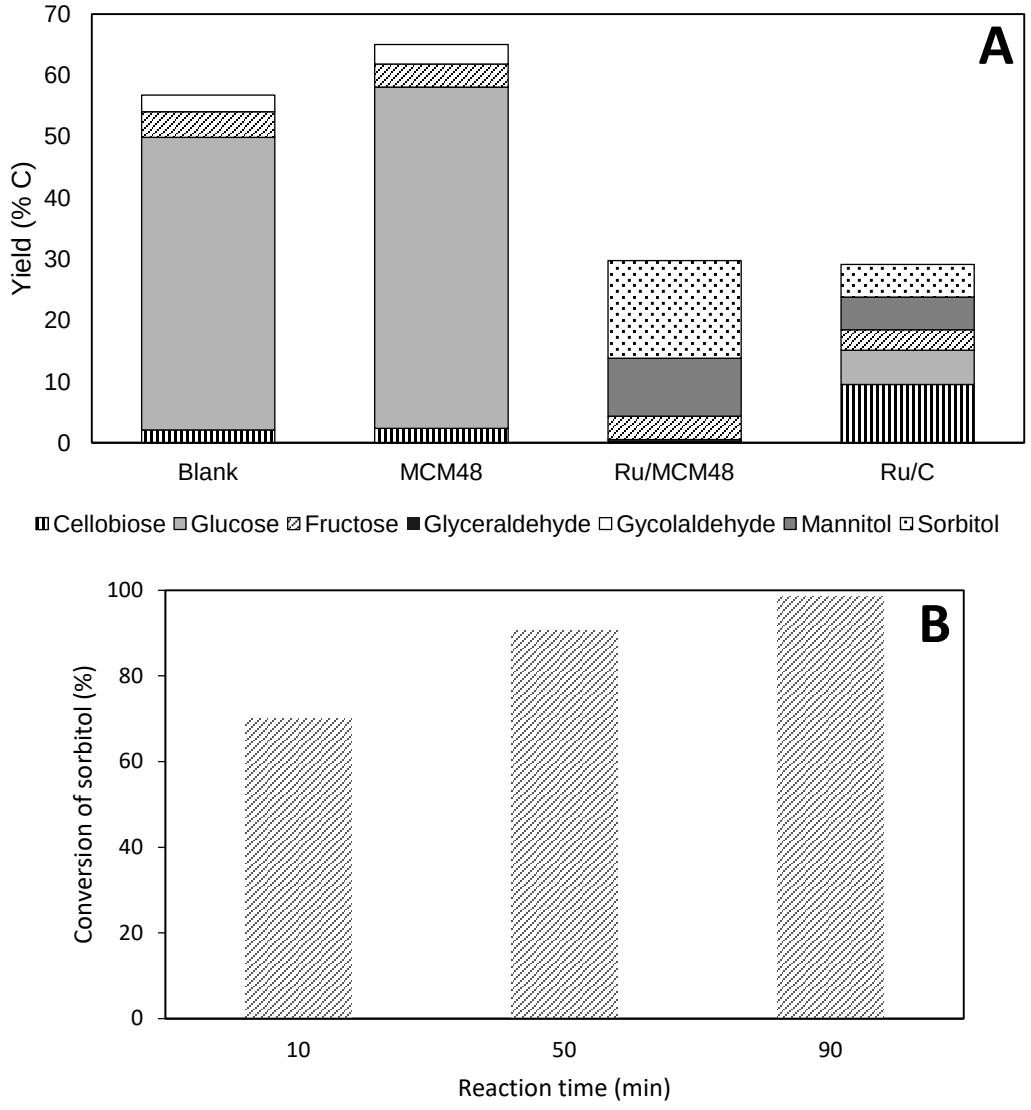

Figure 5. (A) Hydrogenation of liquid product from SCW hydrolysis using MCM-48, Ru/MCM-48 and Ru/C at 180 ºC, 5 MPa H_2 for 90 min and **(B)** Conversion of sorbitol at 180 ºC, 5 MPa and t = 10 - 90 min over Ru/MCM-48.

Concerning the evolution of sorbitol degradation with reaction time at 180 ºC and 5 MPa, it is possible to achieve a high understanding of the overall process of cellulose conversion into sugar alcohols. This reaction process consists on three different steps: 1)

cellulose hydrolysis to produce sugars, 2) hydrogenation of sugars to obtain hexitols and 3) hydrogenolysis of sorbitol and mannitol. A low yield of hexitols was achieved by one-pot hydrogenolysis of cellulose over Ru/MCM-48 because the first step is very slow, the sugars so obtained were rapidly hydrogenated into hexitols and they were converted into other products. In accordance with the results obtained in this work, it seems to be easier to convert sorbitol into other products than the conversion of cellulose into sugars and thus, hydrolysis is the limiting step of the one-pot process. However, when cellulose is firstly hydrolyzed using supercritical water and its product is subsequently hydrogenated, the limiting step is skipped. The product obtained from SCW hydrolysis of cellulose was composed of glucose oligosaccharides and cellobiose that are easier to hydrolyze into glucose in comparison to cellulose under similar experimental conditions. In this sense, it is possible to reduce reaction times in comparison with the one-pot process, avoiding to some extent the hydrogenolysis of hexitols and obtaining higher yields of mannitol and sorbitol.

$$R_0 = t \cdot \exp\left[\frac{T_r - 100}{14.75}\right] \quad (5)$$

According to the abovementioned results, the influence of temperature and reaction time was studied in order to optimize the yield to hexitols using the product obtained from SCW hydrolysis of cellulose. The obtained results are shown in Table 5 and Figure 6. Reaction times at each temperature were calculated in order to obtain severity factors, which were in the range 2.5 – 4.6 in all cases (Eq. 5). In equation 5, R_0 is the severity factor, T_r is the temperature (ºC) and t is the reaction time (min). The maximum yield to hexitols was 29 % at 120 ºC and using Ru/MCM-48 (Entry 3 and 4, Table 5). A clear decrease in mannitol yield (from 4.9 to 1.9 %) and an increase in yield to sorbitol from 12.7 to 27.1 % were observed at long reaction times. At 140 ºC, the maximum yield to hexitols (32.4 %) was achieved at 175 min of reaction time (Entry 6). When reaction time increased, the concentration of hexitols in the liquid product decreased. At 165 ºC, 190 ºC and 200 ºC, maximum yields to hexitols of 37.5, 44.5 and 48.5 % were obtained, respectively. At these experimental conditions, a similar behavior in mannitol production with time was observed. The yield to mannitol increased by rising reaction time in all cases due to the isomerization of sorbitol into mannitol. Consequently, the maximum yield of mannitol was detected when yield to sorbitol decreased (Entries 11, 15 and 18). According to these results, it can be concluded that high temperatures allowed achieving greater yields to hexitols. Due to the high amount of oligosaccharides, which were detected in the

product from SCW pretreatment, it is not possible to obtain a high amount of hexitols working at low temperatures. At these experimental conditions, less oligosaccharides and cellobiose were hydrolyzed into glucose, thus less glucose was available to be hydrogenated into hexitols. In addition, as temperature rose from 120 to 165 ºC, an increase in the yield to mannitol was observed in Figure 6, while sorbitol yield remained constant in the range 25 – 27 %. Nevertheless, a meaningful improvement in the yield to sorbitol was detected at temperatures higher than 165 ºC. At these experimental conditions, there was a higher amount of available sugars, which could be hydrogenated into sorbitol. In Table 5 (entries 5 and 12), it is shown the behavior of Ru/C during the catalytic hydrogenation of the product from SCW hydrolysis at 120 ºC and 165 ºC. At 120 ºC Ru/C achieved a yield to hexitols of 14.2 % after 90 min of reaction time and at the same experimental conditions the run using Ru/MCM-48 obtained a 17.6 % of hexitols. Both results at 120 ºC and 90 min were similar since at low temperatures, the generated hexitols were mainly obtained by hydrogenation of the available glucose and fructose in the product from SCW hydrolysis of cellulose. At 165 ºC, the differences between the behavior of Ru/C and Ru/MCM-48 are higher than at 120 ºC. A yield to hexitols of 12.1 % was achieved using Ru/C while 37.5 % was obtained with Ru/MCM-48. This behavior at 165 ºC is due to the highest acidity of Ru/MCM-48 in comparison with Ru/C. This fact allowed the conversion of a higher amount of oligosaccharides and cellobiose into glucose over Ru/MCM-48 and therefore the obtaining of higher yield to sorbitol and mannitol.

Upon the study of the proposed hydrolysis-hydrogenation process, many advantages of linking these two processes can be deduced. The first and directly observed advantage of the combination of SCW hydrolysis and hydrogenation is that the final yield of hexitols from cellulose increased in more than two times (20.7 % to 48.5 %). Other important contribution to the field of polyols production from cellulose is the intensification of the overall process. The best results obtained in this work were observed with a cellulose hydrolysis in SCW of 0.2 s and a sugars hydrogenation of 6 min. This implies a reduction in the reaction time required between 5-240 times when compared to other one-pot reactors found in the literature (Table 3). The reaction time reduction is an important challenge in the design of renewable and sustainable processes to convert biomass into useful products. The bio-industry concept should lay in the decentralized production of chemicals and fuels, with small scales (just enough production) and close to its source (countryside). To reach this way of production, it is highly required to develop reaction processes with high yield

and selectivity (in this case the achieved hexitols yield was 9 - 27 % higher than some of available yields for one-pot processes reported in the literature [1, 36, 40, 41]) and with small reaction time required (between 5-240 times less for the process developed in this work). These efficient and compact reactors would be an excellent option for the development of the decentralized just enough production of chemicals and fuels from biomass.

Table 5. Sorbitol, Mannitol and hexitols yield obtained at different experimental conditions by catalytic hydrogenation of the product from SCW hydrolysis.

Entry	Catalyst	Temperature (ºC)	Pressure (MPa)	t (min)	Mannitol Yield (%)	Sorbitol Yield (%)	Hexitols Yield (%)
1	Ru/MCM-48	120	5	90	4.9	12.7	17.6
2	Ru/MCM-48			720	3.1	17.1	20.2
3	Ru/MCM-48			1352	2.9	26.2	29.0
4	Ru/MCM-48			1440	1.9	27.1	29.0
5	Ru/C			90	4.1	10.1	14.2
6	Ru/MCM-48	140	5	175	7.8	24.6	32.4
7	Ru/MCM-48			349	3.9	20.4	24.3
8	Ru/MCM-48			2699	3.8	19.8	23.6
9	Ru/MCM-48	165	5	10	3.3	3.1	6.4
10	Ru/MCM-48			45	4.4	30.5	34.9
11	Ru/MCM-48			90	11.1	26.4	37.5
12	Ru/C			90	6.4	5.7	12.1
13	Ru/MCM-48	190	5	5	4.5	29.0	33.5
14	Ru/MCM-48			10	6.2	38.4	44.6
15	Ru/MCM-48			23	7.9	33.4	41.3
16	Ru/MCM-48	200	5	3	5.1	34.4	39.5
17	Ru/MCM-48			6	6.7	41.8	48.5
18	Ru/MCM-48			12	7.5	35.4	42.9

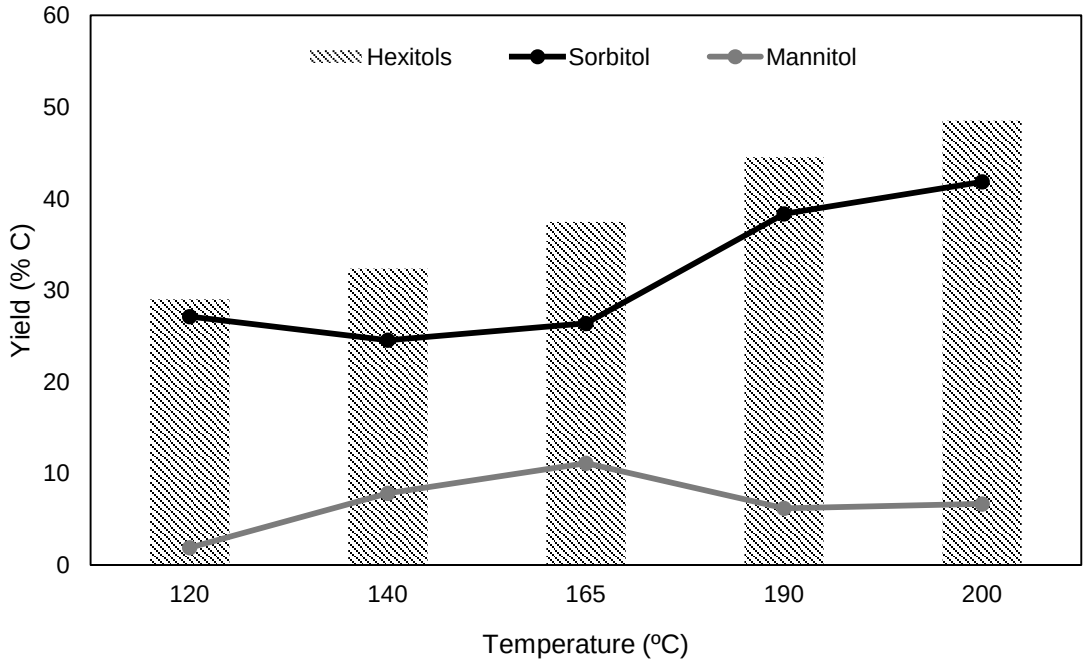

Figure 6. Maximum production of hexitols at each temperature.

3.3. SUGAR BEET PULP VALORIZATION

According to the results achieved in the previous section, experiments with a real biomass were carried out. Thus, SBP was depolymerized in SCW and the product so obtained was hydrogenated in order to obtain valuable chemicals. The composition of the solid sugar beet pulp was analyzed and its composition is shown in Table 6, presented as the dry basis percentages of extractives, lignin, hemicellulose, cellulose, proteins, pectins and ashes. Pectins and lignin were the major compounds in sugar beet pulp, whose composition were 25.52% $w \cdot w^{-1}$ and 19.55% $w \cdot w^{-1}$, respectively.

Table 6. Chemical composition of Sugar beet pulp (dry basis).

Material	Extractives	Lignin *	Hemicellulose	Cellulose	Protein	Pectin	Ash	Total
$g \cdot 100\ g^{-1}$ SBP	2.24	19.55	17.17	13.61	7.32	25.52	0.52	85.93

*Lignin content was calculated as a result of the sum of the soluble and insoluble lignin

Table 7. Composition of the hydrolyzed product ($mg \cdot l^{-1}$) and carbon basis yield (%) from SCW with SBP.

Cellobiose ($mg \cdot l^{-1}$ / C %)	Glucose ($mg \cdot l^{-1}$ / C %)	Fructose ($mg \cdot l^{-1}$ / C %)	Glyceraldehyde ($mg \cdot l^{-1}$ / C %)	Glycolaldehyde ($mg \cdot l^{-1}$ / C %)	TOC ($mg \cdot l^{-1}$ C)
822 / 7.1	1423 / 11.7	963 / 7.9	580 / 4.8	2575 / 21.2	4854

Sugar beet pulp was hydrolyzed with supercritical water for 0.24 s at 400 ºC and 25 MPa. The composition of the hydrolyzed product from SCW pretreatment is shown in Table 7. The product presented a total organic carbon value of 4854 $mg \cdot l^{-1}$, which was composed of 7.1 % cellobiose, to 11.7 % glucose, to 7.9 % fructose, to 4.8 glyceraldehyde and to 21.2 % glycolaldehyde. Oligosaccharides were also detected in the liquid product (≈16 % of TOC) by HPLC when sugar beet pulp was pretreated with supercritical water. When sugar beet pulp was used as raw material, the liquid product was richer in glycolaldehyde due to degradation of the sugars and pectins present in the raw material (retro-aldol condensation reaction) [5]. The low yield of sugars can be attributed to the small percentage of cellulose and hemicelluloses in the raw sugar beet pulp. A similar behavior related to glycolaldehyde production from real biomass has been observed in the literature. Cantero et al. observed a 20 % $w \cdot w^{-1}$ yield to glycolaldehyde after hydrolysis of wheat bran in supercritical water at 0.19 s, 400 ºC and 25 MPa, though in that case C5 and C6 recovered represented the highest yield in the liquid product [10]. Based on previous results with cellulose, 200 ºC was selected for hydrogenation reactions over Ru/MCM-48 (Figure 7).

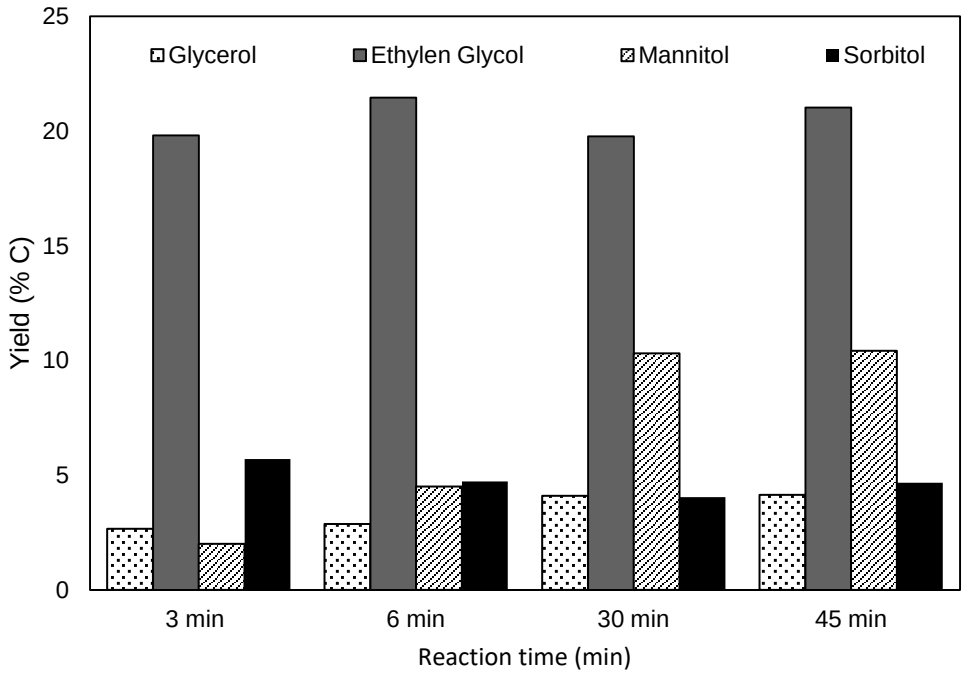

Figure 7. Product distribution of Ru/MCM-48 in the hydrogenation of SBP hydrolysates at 200 ºC and 5 MPa.

Yield to hexitols increased with reaction time, achieving a maximum yield of 15.1 %. Mannitol was the main compound in hexitols fraction in the hydrogenation product, whose

yield increased from 2 % to 10.4 % for reaction times of 3 and 45 min, respectively. However, sorbitol yield kept in the range of 4 – 5.7 %. In contrast, higher yield to sorbitol than to mannitol was achieved in the hydrogenation of pure cellulose hydrolysates. The presence of 7.9 % of fructose in SBP hydrolysates was one of the main differences when comparing to those obtained from cellulose, where fructose was detected in very low amounts. As a result, mannitol was obtained over sorbitol from hydrogenation of hydrolysates of SBP due to the presence of higher amounts of fructose, which is an important source of mannitol. In addition, sorbitol was isomerized into mannitol at longer reaction times. Thus, the hydrogenation of the hydrolyzed product from SBP reached a poor yield of hexitols. However, it was found that the main product of the hydrogenation was ethylene glycol with a maximum yield of 21.5 % after 6 min. In addition, glycerol was detected in the liquid fraction, and its yield increased with time from around 2.7 – 4.1 %. In this sense, ethylene glycol was the main compound, followed by mannitol, sorbitol and glycerol after 45 min. This difference in product distribution in comparison to its counterpart obtained from cellulose pretreated in SCW is in line with the composition of the raw materials. Cellulose represented a 13.6 % of the raw SBP (Table 6), so glucose was not the main compound after its pretreatment in supercritical water. The glycolaldehyde formed in the hydrolyzed product was instantly hydrogenated over Ru/MCM-48 into ethylene glycol [44]. Also, ethylene glycol could be obtained by hydrogenolysis of generated sorbitol during the hydrogenation process [45]. As stated in this work, other authors reported in the literature the high value of pretreatment technology combined with the design of novel metal catalysts. Both of them are two of the main factors for the conversion of raw lignocellulosic biomass into polyols. Yamaguchi et al. carried out the conversion of wood chips to hexitols and pentitols over 4 % Pt/C using ball milling as pretreatment of the raw material at 190 ºC, 5 MPa H_2 for16 h [46]. The major compounds presented in the final product were hexitols with a yield around 49 %, due to the high composition of cellulose (41 %) presented in wood chip. Galactitol, arabitol and xylitol were also detected with an overall yield of 14 %. Corn stalk (pretreated with ammonia) was selected by Pang et al. in order to produce ethylene glycol and 1,2- propylene glycol over 4% Ni-W2C/AC [47]. Sum of yields to ethylene glycol and 1,2- propylene glycol was around 23 % working at 245 ºC, 6 MPa H_2 for 2 h. This yield is much lower than the total yield of polyols (40 %) achieved in the present work with SBP pretreated with supercritical water. Comparing only ethylene glycol production, it is at least two times greater than those reported by Pang et al. The same authors could not detect the presence of polyols in

the final product when 2 % Ru/C was employed as catalyst. Finally, a greater yield of polyols (ethylene glycol and glycerol) around 73 % by hydrogenation of corn stalk, pretreated with steam explosion and alkali, over Ni-W2C/CSAC was reported by Sun et al. [48]. Comparable yield to ethylene glycol from corn stalk (20 %) with that described in this manuscript from SBP (21 %) was obtained.

4. CONCLUSIONS

A novel valorization scheme for plant biomass is presented and tested in this work. This scheme combines both, the ability of SCW hydrolysis to depolymerize cellulose selectively and the hydrogenation process using the synthesized catalyst Ru/MCM-48. It was found that SCW hydrolysis is an excellent hydrolysis stage for using cellulosic material to produce polyols. In comparison to the one-pot hydrolytic hydrogenation of cellulose, the yield increased almost 2.3 times. The use of Ru/MCM-48 is highly beneficial because it allowed the hydrolysis of the obtained oligosaccharides from SCW treatment to glucose selectively increasing the glucose production from 8.6% to 55.7%. Also, this catalyst showed to be very selective to convert glucose into hexitols, obtaining a yield to hexitols of 48.5%, which represents a sugars to hexitols conversion yield of 87.5%. Finally, it can be concluded that glycolaldehyde can be produced with high yields from SCW hydrolysis of biomass and it can be selectively converted into ethylene glycol. The same yield of glycolaldehyde obtained from SCW hydrolysis (21%) was then obtained as ethylene glycol after the hydrogenation process.

The partial goals achieved in this work can be listed as follows:

i) A yield to hexitols of 20.7 % was achieved in one–pot hydrogenation of cellulose over Ru/MCM-48 at 240 ºC, 5 Mpa and 10 min. At the same experimental conditions, commercial Ru/C showed a poor yield to hexitols around 6 %.

ii) SCW pretreatment of cellulose allowed obtaining a hydrolyzed product richer in sugars than in degradation products.

iii) MCM-48 surface acidity promoted hydrolysis of oligosaccharides and cellobiose selectively into glucose.

iv) A maximum yield of hexitols around 48.5 % was obtained at 200 ºC, 5 MPa and 6 min of reaction time. Commercial Ru/C showed worse catalytic behavior

than Ru/MCM-48 in the production of hexitols under similar experimental conditions.

v) Greater yield of hexitols was obtained using SCW as previous step before the hydrogenation process rather than carrying out a one-pot reaction from untreated cellulose.

vi) Ethylene glycol was the main product and 15 % of hexitols were obtained from the hydrogenation of SBP hydrolysates.

Acknowledgements

The authors acknowledge the Spanish Government financial support, through the MINECO project CTQ2011-27347. A. Romero thanks predoctoral scholarships program from Castilla y León Governement for his grant E-47-2015-0062773.

References

1. Fukuoka, A. and P.L. Dhepe, *Catalytic Conversion of Cellulose into Sugar Alcohols.* Angewandte Chemie, 2006. **118**(31): p. 5285-5287.
2. Palkovits, R., et al., *Heteropoly acids as efficient acid catalysts in the one-step conversion of cellulose to sugar alcohols.* Chemical Communications, 2011. **47**(1): p. 576.
3. Kobayashi, H., et al., *Control of selectivity, activity and durability of simple supported nickel catalysts for hydrolytic hydrogenation of cellulose.* Green Chemistry, 2014. **16**(2): p. 637.
4. Zhang, Y.-H.P. and L.R. Lynd, *Toward an aggregated understanding of enzymatic hydrolysis of cellulose: Noncomplexed cellulase systems.* Biotechnology and Bioengineering, 2004. **88**(7): p. 797-824.
5. Sasaki, M., et al., *Cellulose hydrolysis in subcritical and supercritical water.* The Journal of Supercritical Fluids, 1998. **13**(1–3): p. 261-268.
6. Cantero, D.A., M. Dolores Bermejo, and M. José Cocero, *High glucose selectivity in pressurized water hydrolysis of cellulose using ultra-fast reactors.* Bioresource Technology, 2013. **135**(0): p. 697-703.
7. Teeri, T.T., *Crystalline cellulose degradation: new insight into the function of cellobiohydrolases.* Trends in Biotechnology, 1997. **15**(5): p. 160-167.
8. Huang, Y.-B. and Y. Fu, *Hydrolysis of cellulose to glucose by solid acid catalysts.* Green Chemistry, 2013. **15**(5): p. 1095-1111.
9. Brunner, G., *Near critical and supercritical water. Part I. Hydrolytic and hydrothermal processes.* The Journal of Supercritical Fluids, 2009. **47**(3): p. 373-381.
10. Cantero, D.A., et al., *Simultaneous and selective recovery of cellulose and hemicellulose fractions from wheat bran by supercritical water hydrolysis.* Green Chemistry, 2015. **17**(1): p. 610-618.
11. Geyer, R., et al., *New Catalysts for the Hydrogenation of Glucose to Sorbitol.* Chemie Ingenieur Technik, 2012. **84**(4): p. 513-516.
12. Guo, H., et al., *Liquid phase glucose hydrogenation to d-glucitol over an ultrafine Ru-B amorphous alloy catalyst.* Journal of Molecular Catalysis A: Chemical, 2003. **200**(1-2): p. 213-221.

13. Gallezot, P., *Metal Catalysts for the Conversion of Biomass to Chemicals*, in *New and Future Developments in Catalysis*, Elsevier, Editor. 2013. p. 1-27.
14. Kusserow, B., S. Schimpf, and P. Claus, *Hydrogenation of Glucose to Sorbitol over Nickel and Ruthenium Catalysts.* Advanced Synthesis & Catalysis, 2003. **345**(1-2): p. 289-299.
15. Vučurović, V.M., R.N. Razmovski, and M.N. Tekić, *Methylene blue (cationic dye) adsorption onto sugar beet pulp: Equilibrium isotherm and kinetic studies.* Journal of the Taiwan Institute of Chemical Engineers, 2012. **43**(1): p. 108-111.
16. Zheng, Y., et al., *Integrating sugar beet pulp storage, hydrolysis and fermentation for fuel ethanol production.* Applied Energy, 2012. **93**(0): p. 168-175.
17. Kusema, B.T., et al., *Hydrolytic hydrogenation of hemicellulose over metal modified mesoporous catalyst.* Catalysis Today, 2012. **196**(1): p. 26-33.
18. Schumacher, K., et al., *Characterization of MCM-48 Materials.* Langmuir, 2000. **16**(10): p. 4648-4654.
19. Schumacher, K., M. Grün, and K.K. Unger, *Novel synthesis of spherical MCM-48.* Microporous and Mesoporous Materials, 1999. **27**(2–3): p. 201-206.
20. Romero, A., et al., *Conversion of biomass into sorbitol: Cellulose hydrolysis on MCM-48 and d-Glucose hydrogenation on Ru/MCM-48.* Microporous and Mesoporous Materials, 2016. **224**: p. 1-8.
21. Martínez, C., et al., *Hydrolysis of cellulose in supercritical water: reagent concentration as a selectivity factor.* Cellulose, 2015. **22**(4): p. 2231-2243.
22. Sluiter, J.B., et al., *Compositional Analysis of Lignocellulosic Feedstocks. 1. Review and Description of Methods.* Journal of Agricultural and Food Chemistry, 2010. **58**(16): p. 9043-9053.
23. Cantero, D.A., et al., *Energetic approach of biomass hydrolysis in supercritical water.* Bioresource Technology, 2015. **179**: p. 136-143.
24. Widenmeyer, M. and R. Anwander, *Pore Size Control of Highly Ordered Mesoporous Silica MCM-48.* Chemistry of Materials, 2002. **14**(4): p. 1827-1831.
25. Meng, J., et al., *Assembling of Al-MCM-48 supported H3PW12O40 mesoporous materials and their catalytic performances in the green synthesis of benzoic acid.* Materials Research Bulletin, 2014. **60**: p. 20-27.
26. Xue, P., et al., *A novel support of MCM-48 molecular sieve for immobilization of penicillin G acylase.* Journal of Molecular Catalysis B: Enzymatic, 2004. **30**(2): p. 75-81.

27. Meng, Y., *Synthesis and Adsorption Property of SiO2@Co(OH)2 Core-Shell Nanoparticles.* Nanomaterials, 2015. **5**(2): p. 554-564.
28. Boehm, H.P., *Surface oxides on carbon and their analysis: a critical assessment.* Carbon, 2002. **40**(2): p. 145-149.
29. Eliche-Quesada, D., et al., *Ru, Os and Ru–Os supported on mesoporous silica doped with zirconium as mild thio-tolerant catalysts in the hydrogenation and hydrogenolysis/hydrocracking of tetralin.* Applied Catalysis A: General, 2005. **279**(1-2): p. 209-221.
30. Li, Y., et al., *Advances in hexitol and ethylene glycol production by one-pot hydrolytic hydrogenation and hydrogenolysis of cellulose.* Biomass and Bioenergy, 2015. **74**(0): p. 148-161.
31. Rose, M. and R. Palkovits, *Isosorbide as a Renewable Platform chemical for Versatile Applications—Quo Vadis?* ChemSusChem, 2012. **5**(1): p. 167-176.
32. Cantero, D.A., M.D. Bermejo, and M.J. Cocero, *Governing Chemistry of Cellulose Hydrolysis in Supercritical Water.* ChemSusChem, 2015. **8**(6): p. 1026-1033.
33. Heinen, A.W., J.A. Peters, and H. Van Bekkum, *Hydrogenation of fructose on Ru/C catalysts.* Carbohydrate Research, 2000. **328**(4): p. 449-457.
34. Zhu, W., et al., *Efficient hydrogenolysis of cellulose into sorbitol catalyzed by a bifunctional catalyst.* Green Chemistry, 2014. **16**(3): p. 1534-1542.
35. Gallezot, P., et al., *Glucose Hydrogenation on Ruthenium Catalysts in a Trickle-Bed Reactor.* Journal of Catalysis, 1998. **180**(1): p. 51-55.
36. Luo, C., S. Wang, and H. Liu, *Cellulose Conversion into Polyols Catalyzed by Reversibly Formed Acids and Supported Ruthenium Clusters in Hot Water.* Angewandte Chemie International Edition, 2007. **46**(40): p. 7636-7639.
37. Negoi, A., et al., *The hydrolytic hydrogenation of cellulose to sorbitol over M (Ru, Ir, Pd, Rh)-BEA-zeolite catalysts.* Catalysis Today, 2014. **223**: p. 122-128.
38. Ennaert, T., et al., *Conceptual Frame Rationalizing the Self-Stabilization of H-USY Zeolites in Hot Liquid Water.* ACS Catalysis, 2015. **5**(2): p. 754-768.
39. Liang, G., et al., *Selective conversion of microcrystalline cellulose into hexitols on nickel particles encapsulated within ZSM-5 zeolite.* Green Chemistry, 2012. **14**(8): p. 2146-2149.
40. Kobayashi, H., et al., *Transfer hydrogenation of cellulose to sugar alcohols over supported ruthenium catalysts.* Chemical Communications, 2011. **47**(8): p. 2366-2368.

41. Van de Vyver, S., et al., *Selective Bifunctional Catalytic Conversion of Cellulose over Reshaped Ni Particles at the Tip of Carbon Nanofibers.* ChemSusChem, 2010. **3**(6): p. 698-701.
42. Kobayashi, H., et al., *Synthesis of sugar alcohols by hydrolytic hydrogenation of cellulose over supported metal catalysts.* Green Chem., 2011. **13**(2): p. 326-333.
43. Yabushita, M., H. Kobayashi, and A. Fukuoka, *Catalytic transformation of cellulose into platform chemicals.* Applied Catalysis B: Environmental, 2014. **145**: p. 1-9.
44. Zhang, J., et al., *Kinetic study of retro-aldol condensation of glucose to glycolaldehyde with ammonium metatungstate as the catalyst.* AIChE Journal, 2014. **60**(11): p. 3804-3813.
45. Besson, M., P. Gallezot, and C. Pinel, *Conversion of Biomass into Chemicals over Metal Catalysts.* Chemical Reviews, 2014. **114**(3): p. 1827-1870.
46. Yamaguchi, A., et al., *Direct production of sugar alcohols from wood chips using supported platinum catalysts in water.* Catalysis Communications, 2014. **54**: p. 22-26.
47. Pang, J., et al., *Catalytic Hydrogenation of Corn Stalk to Ethylene Glycol and 1,2-Propylene Glycol.* Industrial & Engineering Chemistry Research, 2011. **50**(11): p. 6601-6608.
48. Sun, Y.G., et al., *Evaluating and optimizing pretreatment technique for catalytic hydrogenolysis conversion of corn stalk into polyol.* Bioresource Technology, 2014. **158**: p. 307-312.

CHAPTER 3

BIMETALLIC RU:NI/MCM-48 CATALYSTS FOR THE EFFECTIVE HYDROGENATION OF D-GLUCOSE INTO SORBITOL

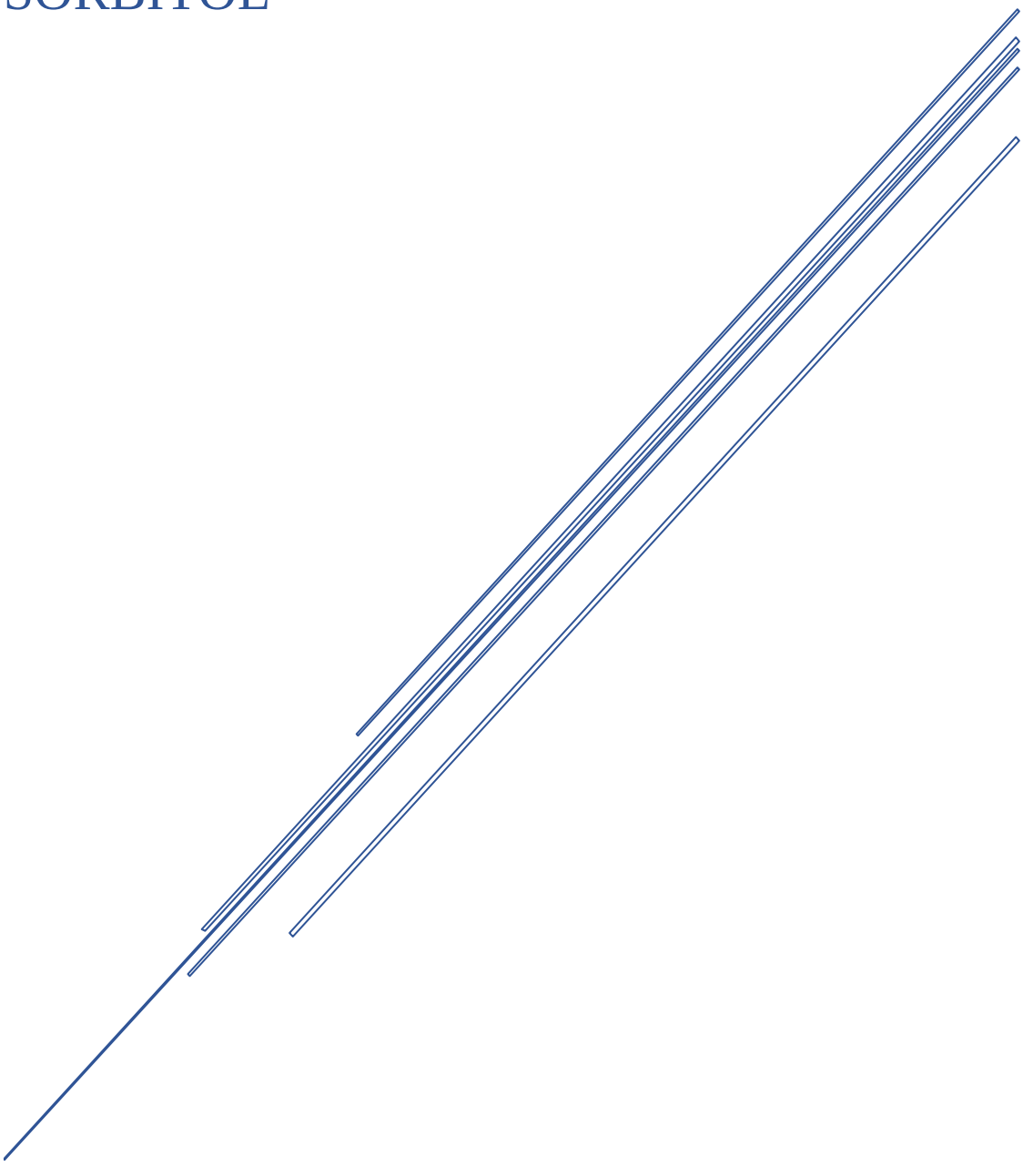

BIMETALLIC Ru:Ni/MCM-48 CATALYSTS FOR THE EFFECTIVE HYDROGENATION OF D-GLUCOSE INTO SORBITOL

Abstract

Three different bimetallic Ru:Ni catalysts supported on a mesoporous silica MCM-48 were prepared by consecutive wet impregnations, with a total metal loading of ca. 3 % ($w \cdot w^{-1}$). Ru:Ni ratios spanned the range of 0.15 – 1.39 ($w \cdot w^{-1}$) and were compared with the corresponding monometallic Ni/MCM-48. The catalysts so prepared were characterized by X-Ray Diffraction, Transmission Electron Microscopy, adsorption/desorption of N_2, Temperature Programmed Reduction, NH_3-TPD and Atomic Absorption, and tested in the liquid phase hydrogenation of D-Glucose into sorbitol in the temperature range 120 – 140 ºC under 2.5 MPa of H_2 pressure. Bimetallic catalysts with Ru:Ni ratios higher than 0.45 enhanced the catalytic behavior of the monometallic Ni/MCM-48 in the reaction, increasing the reaction rate and showing complete selectivity to sorbitol by minimizing the production of mannitol. Ru:Ni/MCM-48 (0.45) was recovered from the reaction media and tested for three reaction cycles, showing good stability under the selected experimental conditions.

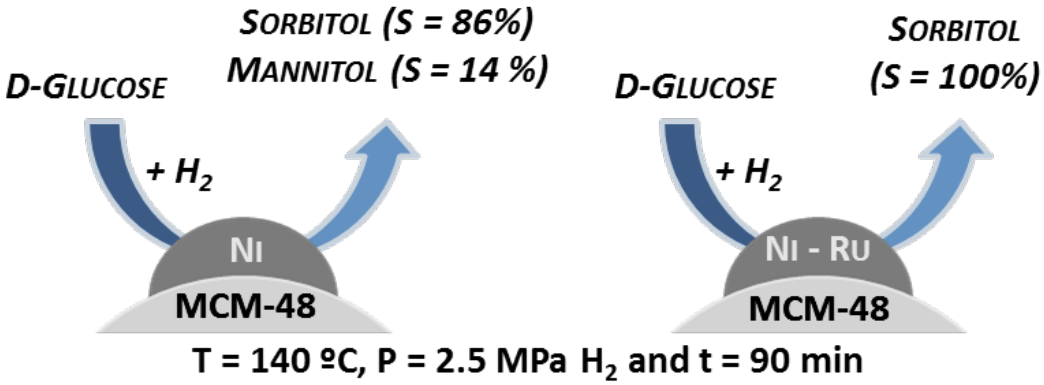

Keywords

Hydrogenation of sugars, sorbitol, ruthenium-nickel bimetallic catalysts, MCM-48, D-Glucose

1. INTRODUCTION

Nowadays, environmental issues such as the poor management of fossil fuels, the depletion of crude-oil reserves and the global warming have promoted a major effort in the valorization of biomass in order to produce fuels, energy and fine chemicals [1]. Lignocellulosic biomass is one of the most promising renewable sources of carbon and it is the only one that can be converted into solid, liquid or gas fuels by thermochemical or biological processes [2]. Essentially, lignocellulosic materials comprise three main fractions, whose average composition is 34 – 50 % cellulose, 19 – 34 % hemicellulose and 11 – 30 % lignin [3, 4] and it is a relatively low-priced source of biomass with a high availability all over the world. In this sense, hydrolytic hydrogenation of cellulose into sugar alcohols has attracted a lot of research interest [5-8].

Catalytic hydrogenolysis of cellulose consists of two consecutive steps where firstly cellulose is hydrolyzed into D-Glucose, which is subsequently hydrogenated into sugar alcohols like sorbitol and mannitol. Sorbitol is a versatile compound which has been used for many different applications, like building block for the synthesis of fine chemicals such as ascorbic acid (intermediate in the synthesis of Vitamin C) [9, 10], as additive in food, cosmetics and paper industries [2], and its annual production is about 700.000 tones/year [11]. Sorbitol is also used as feedstock for hydrolysis–hydrogenation processes in order to produce isosorbide and valuable polyols such as triols, tetrols, glycerol, ethylene glycol and 1,2-propanediol [12]. Most of the sorbitol processing at industrial scale is performed by catalytic hydrogenation of D-Glucose, which is a cheap raw material produced from starch and sucrose [13, 14], using Raney–nickel catalysts [15]. Both noble metals (Ru, Rh, Pd and Pt) and non-noble metals (Fe, Ni, Cu or Co) have been used as active phases in hydrogenation reactions. Nickel–based catalysts have achieved a good piece of attention according to their low cost and moderate to good catalytic activity [16]. Nevertheless, nickel–based catalysts are susceptible to show deactivation after its recycling [2, 17, 18] due to leaching of the active nickel into the reaction media [19], sintering of the active metal [18, 20] and poisoning of metallic nickel surface attributed to organic byproducts of the reaction [21]. The current trend consists on the preparation of ruthenium–based catalysts, which show catalytic activities per mass of active metal 20 – 50 times higher in comparison with nickel [13]. However, the high price of noble metals is the main drawback. Thus, the development of novel bimetallic nickel-based catalysts with comparable high activity to noble metal catalysts

still remains a technological challenge. Noteworthy efforts have been carried out to enhance catalytic activity of nickel-based catalysts in the catalytic conversion of D-Glucose into sorbitol. Hoffer et al. determined that the addition of Mo and Cr had a positive effect promoting Raney - Nickel catalysts activity and stability in the hydrolytic hydrogenation of D-Glucose [17]. Bizhanov et al. studied the influence of noble metals such as Pt, Ru, Rh and Pd on Raney nickel catalysts and they observed that Ni/Ru was the most promising option [22]. In that case the catalytic material was an unsupported catalyst; however, to the best of our knowledge, supported Ni-Ru-based catalysts have never been tested in the hydrogenation of D-Glucose. With this aim, we present the hydrogenation of D-Glucose over bimetallic Ru:Ni catalysts, using MCM-48 as porous support, which has shown an excellent catalytic behavior in previous works [23, 24].

In the present work, we report the catalytic behavior of Ru:Ni-based bimetallic MCM-48 catalysts in comparison with monometallic Ni/MCM-48 for the selective hydrogenation of D-Glucose into sorbitol. The influence of the addition of small amounts of ruthenium over Ni/MCM-48 in the catalytic activity is reported in this work.

2. MATERIALS AND METHODS

2.1. MCM-48 PREPARATION

MCM-48 has been prepared using a conventional hydrothermal synthesis, according to the procedure described by Schumacher et al. [25]. 2 g of n-Hexadecyltrimethylammonium bromide template ($CH_3(CH_2)_{15}N(Br)(CH_3)_3$ ≥ 98%, Sigma – Aldrich) was dissolved in 42 cm^3 of deionized water, 13 cm^3 of ammonium hydroxide (20% as NH_3, Panreac), and 18 cm^3 of absolute ethanol (partially denaturated QP, Panreac). The resulting solution was stirred for 15 min and 4 cm^3 of tetraethyl orthosilicate (TEOS, purity ≥ 99% GC, Sigma – Aldrich), were added dropwise during 1 minute approximately. The solution was further stirred for 18 h in a water bath at 30 ºC; the white precipitate was then collected by filtration, washed with distilled water and dried at 60 ºC overnight. Template was removed from dried samples by calcination with a heating rate of 2 $ºC \cdot min^{-1}$ from 80 ºC to 550 ºC and maintained at 550 ºC overnight.

2.2. CATALYST PREPARATION

Monometallic Ni/MCM-48 with a metal loading close to 3 % by weight was prepared by the conventional wet impregnation (WI) method using the so prepared MCM-48 as carrier. For this synthesis, nickel (II) nitrate hexahydrate ($Ni(NO_3)_2.6{\cdot}H_2O$, 99.999% trace metal basis Sigma Aldrich) and MCM-48 were sonicated in water previously to their mixture during ten minutes. Then, nickel nitrate solution and the dispersion containing MCM-48 were mixed and heated with a rate of 1 $^oC{\cdot}min^{-1}$ from room temperature to 105 ^oC using a Stuart model SD162 heating plate. The impregnation finished when the solvent was completely evaporated. Then, it was dried overnight at 105 ^oC. Bimetallic Ru:Ni/MCM-48 with a total metal loading around 3 %, were prepared by consecutive wet impregnations over MCM-48. Ruthenium (III) chloride anhydrous ($RuCl_3$.anhydrous, Strem Chemicals Inc.) and nickel nitrate were used as ruthenium and nickel precursors, respectively. In this case, the metal with the highest loading in the final catalyst was deposited first. An example of the nomenclature of bimetallic catalysts is presented: M_1:M_2/S (M_1/M_2), where M_1 is ruthenium, M_2 is nickel, S is MCM-48 support and M_1/M_2 is the mass ratio of ruthenium to nickel. Finally, both monometallic and bimetallic catalytic systems were reduced under H_2 atmosphere at 250 ^oC according to TPR-H_2 conditions.

2.3. SUPPORT AND CATALYST CHARACTERIZATION

Small Angle X-Ray Scattering (SAXS) and X-Ray Diffraction (XRD) were performed in a Bruker Discover D8 diffractometer using the Cu Kα radiation (λ = 0.15406 nm). The diffraction intensities were measured, for XRD, over an angular range of $5° < 2\theta < 80°$ with a step size of 0.03° and a count time of 2 s per step. In case of SAXS, $2° < 2\theta < 6^o$ was selected as angular range with a step size of 0.02° and a count time of 1 s per step. Nitrogen adsorption / desorption isotherms were performed with ASAP 2020 (Micromeritics, USA) to obtain surface and pore properties of the support and the catalyst. Prior to analysis, the samples were outgassed overnight at 350 ^oC. Total specific surface areas were determined by the multipoint BET method at $P/P_0 \leq 0.3$, total specific pore volumes were evaluated by single point adsorption from N_2 uptake at $P/P_0 \geq 0.99$. Pore diameter was obtained by BJH (adsorption average, $4{\cdot}V{\cdot}A^{-1}$). Pore size distribution was derived from the adsorption branch of the isotherm by BJH (dV/dD) Halsey:Faas correction. Temperature Programmed Reduction (TPR) profiles were recorded using the commercial Micromeritics TPD/TPR 2900 unit. The samples

were loaded into a U-shaped quartz cell, ramped (10 ºC·min^{-1}) from room temperature to 800 ºC under a flow of H_2/N_2 (5% v/v; 50 cm^3·min^{-1}, Air Liquide) and kept at the final temperature until the signal returned to the baseline. Hydrogen consumption was monitored by a thermal conductivity detector (TCD) with data acquisition/manipulation using the ChemiSoft TPX V1.03™ software. TPD-NH_3 experiments were performed in the same analyzer. In this case, the samples were activated under TPR-H_2 conditions (250 ºC) for 60 min. Prior to the analysis, the samples were outgassed at 105 ºC using pure He during 60 min. Then they were saturated with ammonia at 100 ºC during 30 min. Chemisorbed NH_3 was purged using pure He during 60 min and then samples were heated from 100 ºC to 600 ºC (ramped 15 ºC·min^{-1}) and kept at the final temperature until the signal returned to the baseline. The amount of chemisorbed ammonia was calculated according to calibrated volumes of this compound. Transmission electron microscopy (TEM) analyses used a JEOL 2100 unit with an accelerating voltage of 200 kV. Samples were prepared by ultrasonic dispersion in acetone with a drop of the resultant suspension evaporated onto a holey carbon-supported grid. A counting of nickel nanoparticles were carried out from TEM images of the different catalysts. At least 100 nickel nanoparticles were counted in each case and the mean Ni particle sizes were calculated as number average diameter ($\bar{d}_n$), surface area-weighted diameter ($\bar{d}_s$), volume-weighted diameter ($\bar{d}_V$), according to equations 1, 2 and 3, respectively [26],

$$\bar{d}_n = \frac{\sum_i n_i \cdot d_i}{\sum_i n_i} \quad (1)$$

$$\bar{d}_s = \frac{\sum_i n_i \cdot d_i^3}{\sum_i n_i \cdot d_i^2} \quad (2)$$

$$\bar{d}_v = \frac{\sum_i n_i \cdot d_i^4}{\sum_i n_i \cdot d_i^3} \quad (3)$$

where n_i is the number of nickel particles with a diameter d_i. Since chemical reactions occur on catalyst surface, surface-area weighted diameter is selected as the most meaningful parameter to obtain mean Ni particles sizes for catalysis purposes. In order to determine how closely the observed distribution approaches the true population, the standard deviation of the number diameter (σ_m) is be calculated as described in Eq. 4.

$$\sigma_m = \frac{\sum_i d_i^2 - n \cdot \bar{d}_n^2}{n^2} \quad (4)$$

EDS microanalysis (Oxford Instruments Inca X-Ray microanalysis system TEM 250) provided elemental and chemical identification of nickel and ruthenium in all cases. In addition, energy dispersive X-Ray spectroscopy mapping was performed in STEM mode for Ni/MCM-48. Metal loadings of ruthenium and nickel were determined by atomic absorption (AA) using a VARIAN SPECTRA 220FS analyzer. Digestion of the samples was performed with HCl, H_2O_2 and HF using microwave at 250 ºC.

2.4. CATALYTIC HYDROGENATION OF D-GLUCOSE

Catalytic tests were performed in a stainless-steel high pressure reactor with an internal volume of 25 cm^3 (Berghof BR-25), agitated with a magnetic stirring bar and PID controlled. Hydrogenation experiments were carried out in the temperature range 120–140 ºC at 2.5 MPa H_2 using a stirring rate of 1400 rpm. Prior to reaction catalysts were activated *in situ* by reducing under H_2 atmosphere at 250ºC during 60 minutes. Mole of carbon in feedstock to mole of total metal ratio (C:Ru) was kept at 142 in all the experiments. The reactor was flushed with N_2 for 10 minutes and subsequently fed with H_2, and then the reactor was heated up to the desired reaction temperature. Once the set point was reached, 5 cm^3 of a solution of 7.35 $g \cdot dm^{-3}$ D-Glucose was pumped (intelligent HPLC pump, Jasco PU-2080 Plus) and the reactor was pressurized up to 2.5 MPa of H_2. At the end of the experiments, recovery of the catalyst was made by filtering the product solution using a vacuum pump. Hydrogenation products were analyzed by HPLC. The HPLC column used was a SUGAR SC-1011 from Shodex at 80 °C and a flow of 0.8 $cm^3 \cdot min^{-1}$ using water Milli-Q as the mobile phase. A Waters IR detector 2414 was used to identify sugars, polyols and their derivatives. The error related to the concentrations so obtained by HPLC was lower than 0.08 %. D-Glucose conversion, yields and selectivities to sorbitol and mannitol were calculated using equations 5, 6 and 7.

$$X_{D-Glucose}(\%) = \frac{mole\ (D\text{-}Glucose_0) - mole\ (D\text{-}Glucose_f)}{mole\ (D\text{-}Glucose_0)} \cdot 100 \quad (5)$$

$$S_{product}(\%) = \frac{mole\ (product)}{mole\ (D\text{-}Glucose_0) - mole\ (D\text{-}Glucose_f)} \cdot 100 \quad (6)$$

$$Y_{product}(\%) = \frac{mole\ (product)}{mole\ (D\text{-}Glucose_0)} \cdot 100 = \frac{X \cdot S}{100} \quad (7)$$

$$Reaction\ rate\ (g_{sorbitol} \cdot g_{metal}^{-1} \cdot min^{-1}) = \frac{mass\ (Sorbitol)}{mass\ (metal) \cdot time} \quad (8)$$

$$Specific\ reaction\ rate = \frac{mol_{Sorbitol}}{S_{Ni} \cdot t} \quad (9)$$

$$S_{Ni} = \frac{6}{\rho_{Ni} \cdot \bar{d}_s} \quad (10)$$

Catalytic activity was expressed as reaction rate (Eq. 8) in Table 2 to be compared with those reported previously by other authors. In addition, catalytic activity was also stated as specific reaction rate (Eq. 9) in Table 2. In order to test catalyst reusability, after its recovery from reaction media, the solid catalyst was washed several times with deionized water and dried at 105 ºC overnight. Then, the catalyst was reactivated under TPR conditions and tested again in D-Glucose hydrogenation.

3. RESULTS AND DISCUSSION

3.1. SUPPORT CHARACTERIZATION

Figure 1(A) shows Small Angle X-Ray Scattering (SAXS) pattern of MCM-48. Calcined MCM-48 exhibits three main Bragg diffraction peaks in the 2θ range from 2-5 º, that can be assigned to (211), (220) and (332) planes. These results are in good agreement with the high quality of mesoporous MCM-48, where the cubic phase belongs to a Ia3d space group symmetry [25, 27].

To study adsorption properties of calcined MCM-48 material, typical adsorption / desorption isotherms of N_2 at -196 ºC were determined and results are illustrated in Figure 1(B). This isotherm shows the typical features of a mesoporous silica material, and it can be classified as a type IV according to the IUPAC [28]. First, a sharp nitrogen uptake at P/P_0 in the range of 0 – 0.02 due to a monolayer adsorption on the walls of MCM-48 is observed. This step is followed by an abrupt increase in the volume of nitrogen adsorbed at P/P_0 in the range of 0.2 – 0.3 associated to capillary condensation of N_2 in the channels of MCM-48, suggesting uniformity of the channels and a narrow pore size distribution [29]. No hysteresis was observed between adsorption and desorption branches, therefore MCM-48 shows a reversible type IV isotherm, comparable to those reported by Morey et al. [29]. Absence of hysteresis is attributed to the presence of small-sized mesopores. Materials such as MCM-48 usually shows type

H1 hysteresis, where the width of the hysteresis loop slightly increases with increasing the pore size [30]. Figure 1(C) illustrates the pore volume ($cm^3 \cdot g^{-1} \cdot Å^{-1}$) as a function of pore diameter (Å) for MCM-48. A unimodal pore size distribution with a well-defined peak centered at 20.3 Å was observed. This small mesopore size, in the limit between meso and micropores, is in good agreement with the shape of the isotherm. Textural properties for MCM-48 are described in Table 1, where it can be observed that BET surface area and pore volume values were 1289 $m^2 \cdot g^{-1}$ and 0.87 $cm^3 \cdot g^{-1}$, respectively, characteristic of these materials.

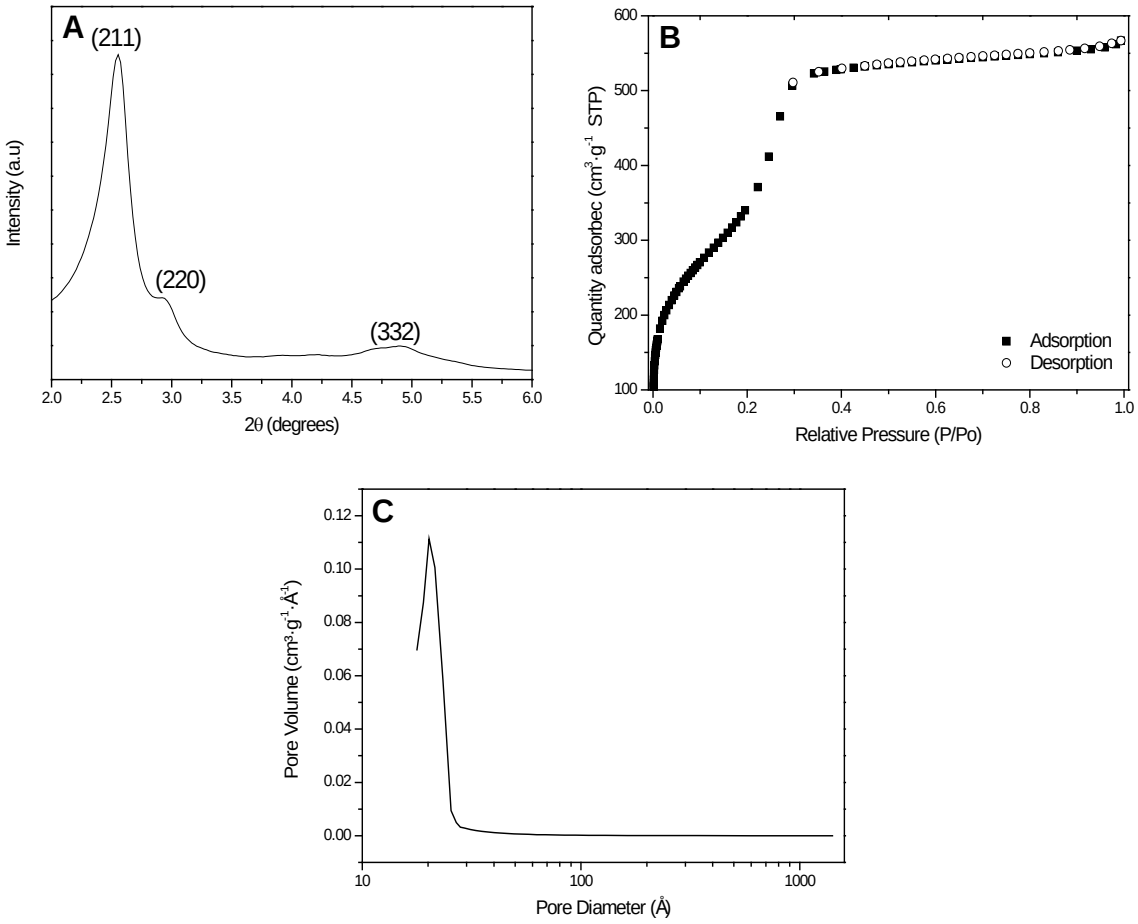

Figure 1. (A) SAXS diffraction pattern, **(B)** adsorption-desorption isotherm of N_2 and **(C)** pore size distribution of MCM-48**.**

Table 1. Textural properties, metal loading, Ru: Ni ratio, nickel particle size and acidic properties of Ni/MCM-48, Ru:Ni/MCM-48 bimetallic catalysts and bare MCM-48 support.

Catalyst	Ru (%)	Ni (%)	Ru:Ni	S_{BET} ($m^2 \cdot g^{-1}$)	V_{pore} ($cm^3 \cdot g^{-1}$)	$Ø_{pore}$ (nm)	$\bar{d}_{n\,Ni}$ (nm)	$\bar{d}_{s\,Ni}$ (nm)	$\bar{d}_{v\,Ni}$ (nm)	σ_m	Acidity ($mmol \cdot g^{-1}$)		
											I[a]	II[b]	Total
MCM-48	-	-	-	1289	0.87	2.2	-	-	-	-	0.157	0.343	0.500
Ni/MCM-48	-	2.95	-	572	0.44	4.4	2.1	2.3	2.4 (2.7[c])	0.5	0.546	0.462	1.007
Ru:Ni/MCM-48 (0.15)	0.38	2.48	0.15	931	0.59	2.2	17.5	20.6	21.6	5.9	0.396	0.756	1.152
Ru:Ni/MCM-48 (0.45)	0.76	1.67	0.45	1112	0.69	2.2	16.3	19.2	20.5	5.6	0.320	0.882	1.202
Ru:Ni/MCM-48 (1.39)	1.63	1.17	1.39	1184	0.74	2.2	10.5	10.9	11.3	1.9	0.334	0.918	1.253

[a] T = 170 -250 ºC.

[b] T = 520-590 ºC.

[c] Derived from XRD-Scherrer

3.2. CHARACTERIZATION OF NI AND RU-NI-BASED CATALYSTS

A monometallic Ni/MCM-48 and three bimetallic Ru:Ni/MCM-48 catalysts were prepared with a metal loading around 3 %, according to atomic absorption results (Table 1). The bimetallic catalysts presented Ru:Ni ratios in the range of 0.15-1.39

Figure 2 shows the temperature programmed reduction (TPR-H_2) profiles of the monometallic Ni/MCM-48 and bimetallic Ru:Ni/MCM-48 catalysts between 25 ºC and 400 ºC, since at temperatures higher than 400 ºC other reduction peaks were not recorded. For Ni/MCM-48, one reduction peak centered at 255 ºC is observed. This profile can be attributed to reduction of nickel nitrate species with two displaced ligands of water by terminal silanol groups ($Ni(NO_3)_2 \cdot 4H_2O \cdot 2(SiOH)$) from MCM-48. A smaller and broader peak was also observed from 275 ºC to 350 ºC corresponding to smaller amounts of $Ni(NO_3)_2 \cdot 5H_2O \cdot (SiOH)$ with higher interaction with the silica MCM-48 framework [31]. Ru/MCM-48 was characterized in terms of H_2-TPR in previous works showing a unique reduction peak at ca. 125 ºC corresponding to the reduction of Ru^{3+} to Ru^0 [23, 24]. The reduction patterns of Ru:Ni/MCM-48 bimetallic catalysts are clearly different from those obtained from the monometallic Ni/MCM-48 and Ru/MCM-48 catalysts, showing complex H_2-TPR profiles consisting on three overlapped peaks where reduction starts at 100 ºC and finishes at 260 ºC, approximately. In the case of Ru:Ni/MCM-48 (0.15), which presented the highest nickel loading in comparison with the other bimetallic systems, a low-intense peak centered at 122 ºC was observed attributed to the reduction of $RuCl_3$. Then, a broader peak was detected at 182 ºC suggesting the presence of Ru/Ni alloys formed during the impregnation process, as it was reported by other authors [32-34] and a narrow peak at 258 ºC corresponding to the reduction of $Ni(NO_3)_2.4H_2O.2(SiOH)$ to Ni^0 was observed. Similar behavior was detected for Ru:Ni/MCM-48 (0.45) and Ru:Ni/MCM-48 (1.39), though a decrease in the reduction temperature of ruthenium was observed when Ru:Ni ratio increased suggesting the presence of bigger ruthenium nanoparticles, with lower interaction with the MCM-48 framework. Also, the addition of different amounts of ruthenium over Ni/MCM-48 catalyst enhanced the reducibility of nickel species due to chemisorption of H_2 molecules on Ru^0 and subsequent spillover. According to the above results, 250 ºC was selected as an adequate common reduction temperature.

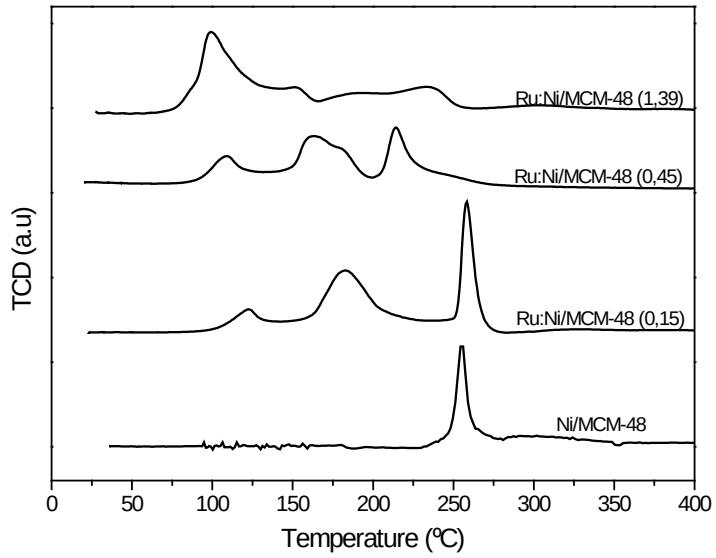

Figure 2. H_2-TPR profiles.

XRD patterns for Ni/MCM-48 and Ru:Ni/MCM-48 catalysts, after reduction under H_2-TPR conditions, are shown in Figure 3(A). Monometallic Ni/MCM-48 showed a broad characteristic metallic diffraction peak at $2\theta = 44.5^o$ (JCPDS card No. 4-850), corresponding to (111) crystallographic plane of Face-Centered Cubic (FCC) nickel. The position, shape and size of this peak suggests the presence of very small Ni^0 nanoparticles and it indicates the successful reduction of nickel species into Ni^0. Calculations based on the Scherrer equation and Ni (111) diffraction, determined a nickel crystallite diameter around 2.7 nm. Comparing monometallic Ni/MCM-48 and bimetallic Ru:Ni/MCM-48 XRD patterns, significant differences were observed as a result of the addition of small amounts of ruthenium over nickel catalysts. In the case of bimetallic Ru:Ni/MCM-48 catalysts, characteristic diffraction peaks corresponding to FCC Ni^0 reflections were observed at $2\theta = 44.5^o$, 51.7^o and 76.1^o (JCPDS card No. 4-850) related to (111), (200), and (220) crystallographic planes, respectively. Bimetallic catalysts showed Ni^0 diffraction peaks with higher intensity than in the case of the monometallic catalyst, which is indicative of the presence of bigger metallic nickel nanoparticles. This fact can be attributed to the additional drying and coprecipitation steps employed for bimetallic materials compared to the monometallic catalyst. In addition, Ru^0 reflections were detected at $2\theta = 38.8^o$, 42.2^o, 43.8^o, 58.2^o, 69.6^o and 78.4^o (JCPDS No. 06–0663), indicating the presence of Hexagonal Close Packing (HCP) Ru^0 nanoparticles. Thus, the most intense diffraction peaks of Ru^0 at $2\theta = 43.8^o$ and Ni^0 at $2\theta = 44.5^o$ overlapped. A expanded region of XRD analysis for Ru:Ni/MCM-48 is shown in Figure 3(B). A shift of the resulting peak was observed towards lower angles as the

atomic percentage of Ru increased. Similar behavior has been reported by different authors in the literature [35, 36]. In the case of Ru:Ni/MCM-48 (0.15), overlapped peak is close to $2\Theta = 44.5^{o}$ since this catalysts had the highest nickel metal loading. However, this peak moved around $2\Theta = 43.8^{o}$ for Ru:Ni/MCM-48 (1.39) because in this case Ru:Ni ratio was the highest one in comparison with the other bimetallic catalysts. This fact makes more inaccurate the application of Scherer equation for crystallite size determination. Therefore, shape and particle sizes of metallic species were evaluated by TEM.

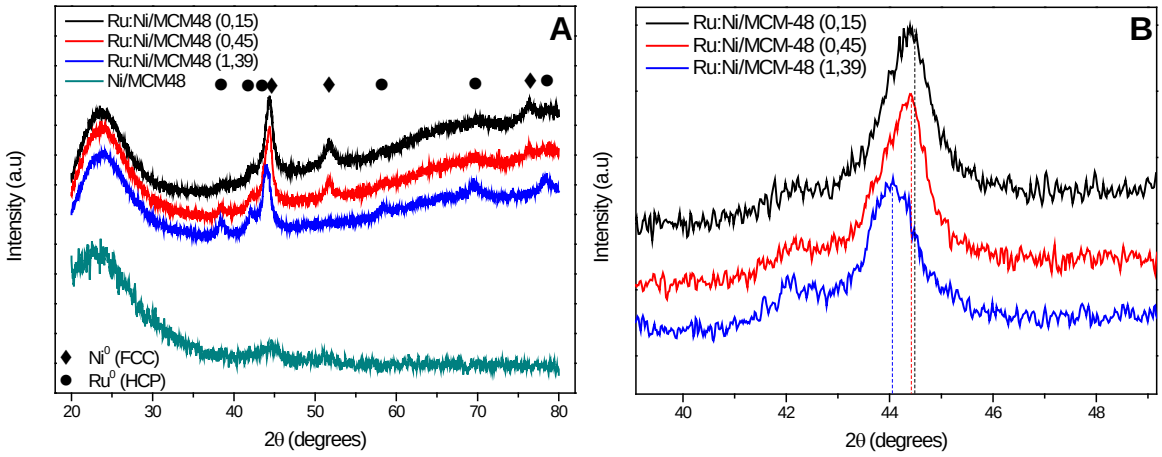

Figure 3. (A) XRD patterns of Ni/MCM-48, Ru:Ni/MCM-48 (0.15), Ru:Ni/MCM-48 (0.45) and Ru:Ni/MCM-48 (1.39) and **(B)** expanded region for bimetallic catalysts.

Textural properties of the catalysts are summarized in Table 1. A sharp decrease of BET surface area for MCM-48 from 1289 to 572 $m^2 \cdot g^{-1}$ upon nickel introduction was observed, and pore volume was reduced from 0.87 to 0.44 $cm^3 \cdot g^{-1}$, suggesting a high pore blockage for Ni/MCM-48 due to the deposition of metallic particles into the mesoporous network. This is consistent with TEM image for Ni/MCM-48 (Figure 4(A)), where Ni nanoparticles where located in the mesoporous network of MCM-48. It must be noted that nickel nanoparticle size was comparable to the average pore diameter of MCM-48. Therefore, the location of Ni nanoparticles in the porous network can lead to a forced increase of pore diameter, indicating a slight alteration of the structure after nickel deposition. According to these facts, some differences in the adsorption/desorption isotherms of Ni/MCM-48 (Figure 5(A)) and pore size distribution (Figure 5B) were observed in comparison with that from MCM-48. After the deposition of nickel into the pores of the support, the shape of the adsorption/desorption isotherm changes and a hysteresis loop appears between P/P_0 0.4 – 0.9. The presence of the

hysteresis loop in the case of Ni/MCM-48 is due to the observed modification in pore diameter. It is in good agreement with the results reported by other authors, where the increase of pore diameter promoted small increases in the width of the hysteresis loop [30]. The pore size distribution (dV/dD) did not show a clear maximum, exhibiting a wider diameter distribution and lower associated pore volumes than the corresponding MCM-48. In the case of bimetallic catalysts, the decrease of BET surface and pore volume after the introduction of ruthenium and nickel was smaller, being this decrease sharper at higher nickel loadings. Significant differences in adsorption/desorption isotherms and pore size distribution of bimetallic samples (not shown) were not observed in comparison with that obtained for MCM-48. TEM images, EDS analysis and Ni particle size distributions for all the samples are presented in Figure 4, 6, 7 and 8. TEM micrograph of the monometallic Ni/MCM-48 (Figure 4(A)) shows pseudospherical MCM-48 particles where small nickel nanoparticles with low contrast are detected, which could be distributed into the mesoporous network of MCM-48. X-Ray maps coupled to TEM images for Ni/MCM-48 demonstrated the homogeneous distribution of nickel nanoparticles in pore structure of MCM-48 (Figure 4(C), left side for Ni and right side for Si). A counting of nickel nanoparticles (> 100 nanoparticles) from TEM images was carried out for Ni/MCM-48 (Figure 4(B)). The histogram shows a nickel nanoparticle size distribution in the range 0.91-3.20 nm. Calculations based on equation 2 determined a surface-area weighted diameter of 2.3 nm, in the range of that obtained from XRD analysis. The small size of nickel nanoparticles can be related to the small size of MCM-48 channels where metallic nanoparticles were deposited during the synthesis [32]. Comparing TEM images from bimetallic Ru:Ni/MCM-48 with Ni/MCM-48, very different results were observed (Figures 6-8). In the case of Ru:Ni/MCM-48 (0.15) which presented the lower amount of ruthenium, two types of images were observed. Most of the pictures are similar to that presented in Figure 6(A), where EDS only detected the presence of nickel. Other images presented irregular agglomerates of ruthenium particles (Figure 6(B)). Due to the irregular geometry of the areas where ruthenium was identified and the impossibility of visually difference each metal, counting of nanoparticles (> 100) was only done for nickel. The distinction of Ni and Ru areas was carried out by EDS analysis. In this case, a broader nickel nanoparticle size distribution was obtained with a surface-area weighted diameter of 20.6 nm. Increasing Ru:Ni ratio up to 0.45, a heterogeneous distribution of the metallic particles was observed, where three different type of regions were identified: a)

irregular agglomerates, where EDS analysis determined the main presence of ruthenium (Figure 7(A)), b) better dispersed particles, where EDS only could identified nickel (Figure 7(B)) and c) the combination of the two previous morphologies, where both ruthenium and nickel were observed (Figure 7(C)). The counting of nickel nanoparticles resulted in a narrower nickel particle size distribution than the previous one. Surface-area weighted diameter of 19.2 nm was determined for Ru:Ni/MCM-48 (0.45). Finally, Ru:Ni/MCM-48 (1.39) showed a similar morphology to Ru:Ni/MCM-48 (0.45). This sample showed nickel regions (Figure 8(A)), ruthenium regions (Figure 8(B)) and other areas with presence of both (Figure 8(C)). The narrowest nickel nanoparticle size distribution was obtained for this catalyst, with a surface area-weighted diameter of 10.9 nm. Nickel nanoparticles were not detected into the pores of MCM-48 in the case of bimetallic catalysts by TEM; however, this fact cannot be discarded according to the reduction peaks observed at temperatures higher than 200 ºC, which can be attributed to small nickel nanoparticles deposited into the pores, as in the case of the monometallic catalyst.

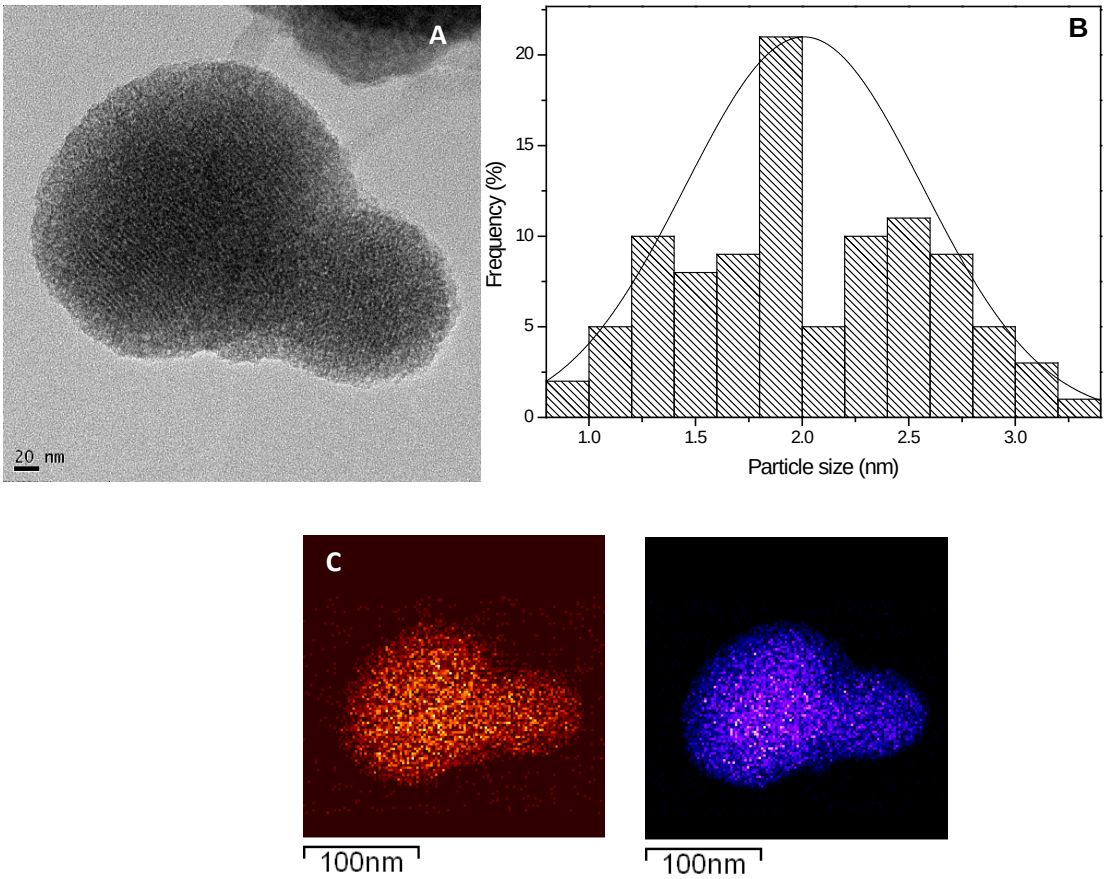

Figure 4. (A) Transmission Electron Microscopy (TEM) micrographs, **(B)** Ni particle size distribution and **(C)** Mapping images of Ni/MCM-48**.**

Derived number, surface and volume weighted diameters, as well as the standard deviation related to number diameter are given in Table 1. Standard deviations in number diameter were in the range 18 – 34 %. According to the additional drying and coprecipitation steps in the case of bimetallic catalysts, wider particle size distributions were obtained compared to Ni/MCM-48, in line with greater values of standard deviation.

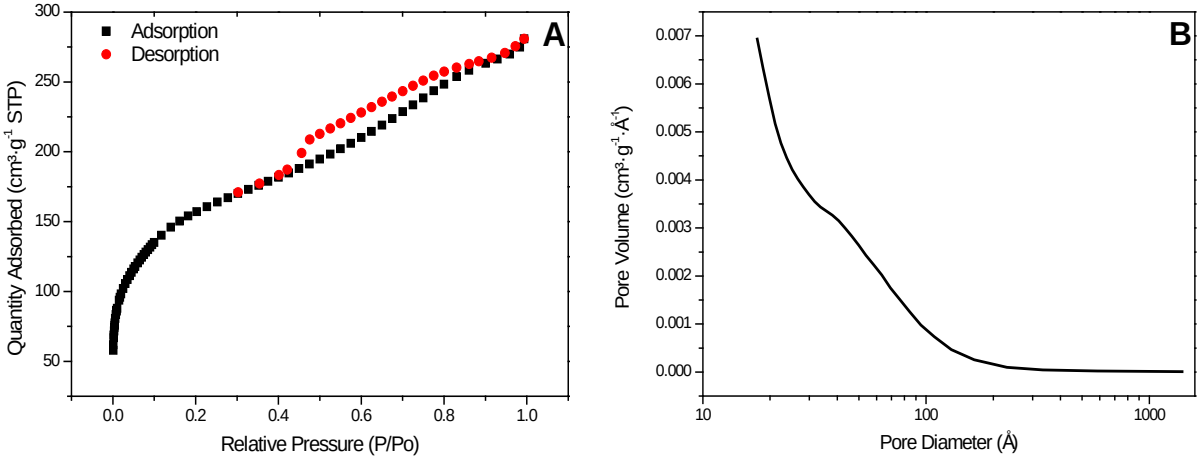

Figure 5. (A) Adsorption/desorption isotherm of N_2 and **(B)** pore size distribution of Ni/MCM-48.

Acidic properties are critical for the use of these catalysts in one-pot applications, which is the ultimate goal of our research [23, 24]. Acidic features from NH_3-TPD of the support and the reduced catalysts are presented in Table 1 and Figure 9. In general terms, all the samples showed two ammonia desorption peaks in the temperature range of 170 – 250 ºC and 520 – 590 ºC, which are related to weak and strong acid sites, respectively. Total amount of acid sites ($mmol_{NH3} \cdot g^{-1}_{catalyst}$) is consistent with the following sequence of increasing acidity: MCM-48 < Ni/MCM-48 < Ru:Ni/MCM-48. Compared to MCM-48 sample, an increase of acid sites was observed after the deposition of nickel into the framework of the support in the case of Ni/MCM-48 catalyst. In the case of bimetallic Ru:Ni/MCM-48 catalysts, the presence of ruthenium resulted in a slight increase of acidity in comparison with the monometallic catalyst. This fact is attributed to the higher trend of ruthenium atoms to adsorb ammonia molecules [37], while the influence of chlorine atoms cannot be discarded.

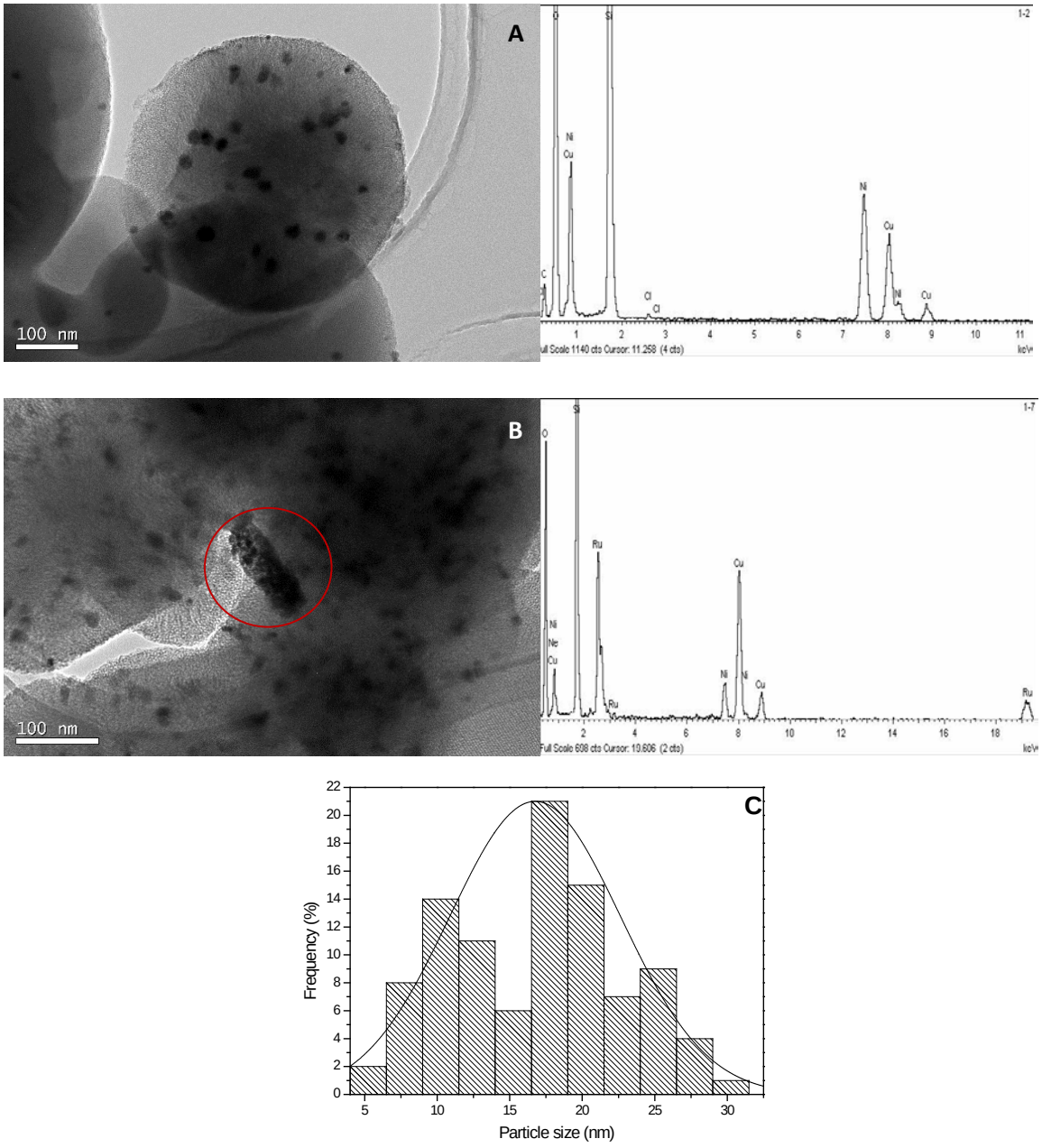

Figure 6. Transmission Electron Microscopy (TEM) micrographs and EDS of **(A)** nickel area and **(B)** bimetallic area of Ru:Ni/MCM-48 (0.15), **(C)** Ni particle size distributions from TEM images of Ru:Ni/MCM-48 (0.15).

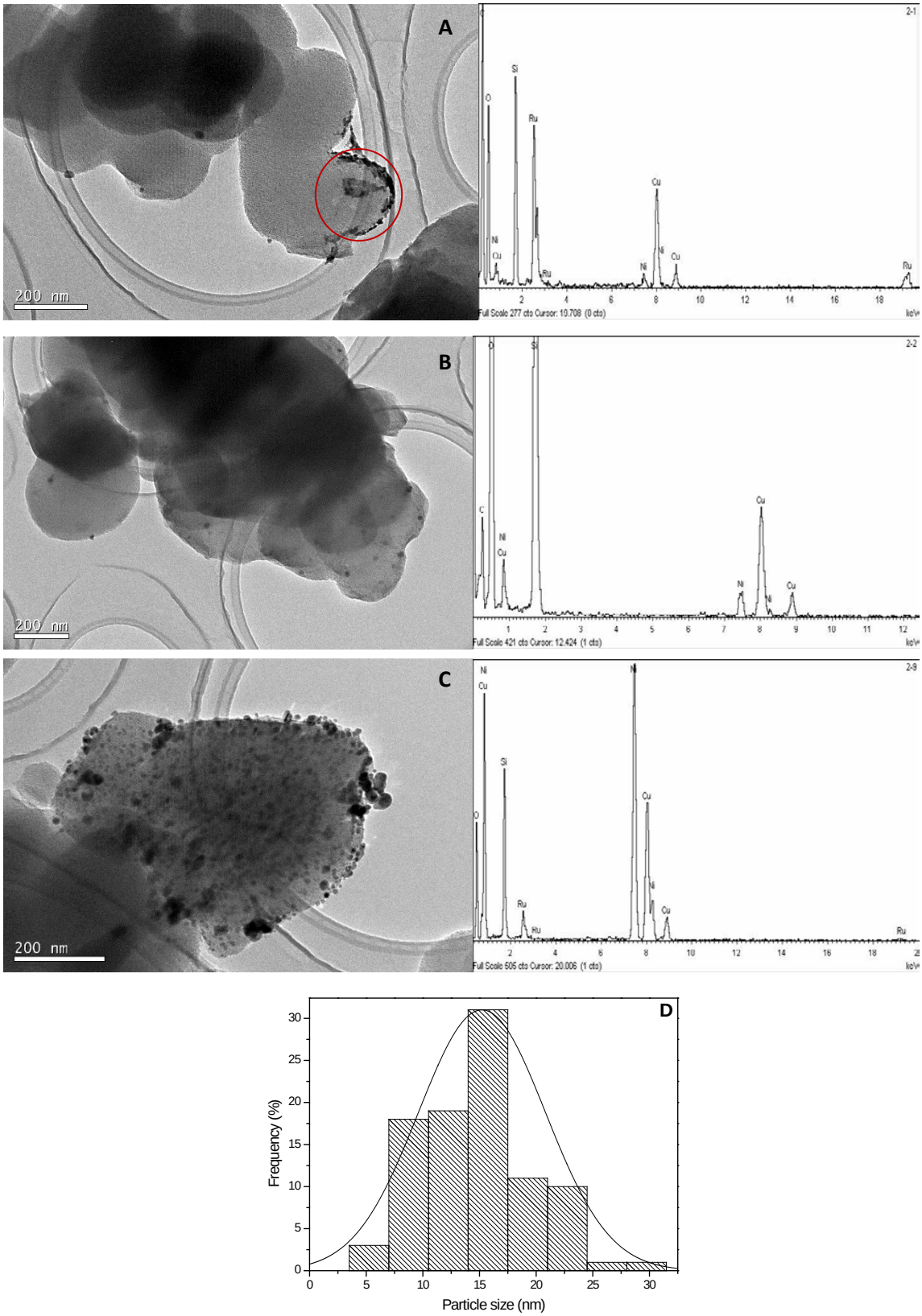

Figure 7. (A,B,C) Transmission Electron Microscopy (TEM) micrographs and EDS of Ru:Ni/MCM-48 (0.45). **(D)** Ni particle size distributions from TEM images.

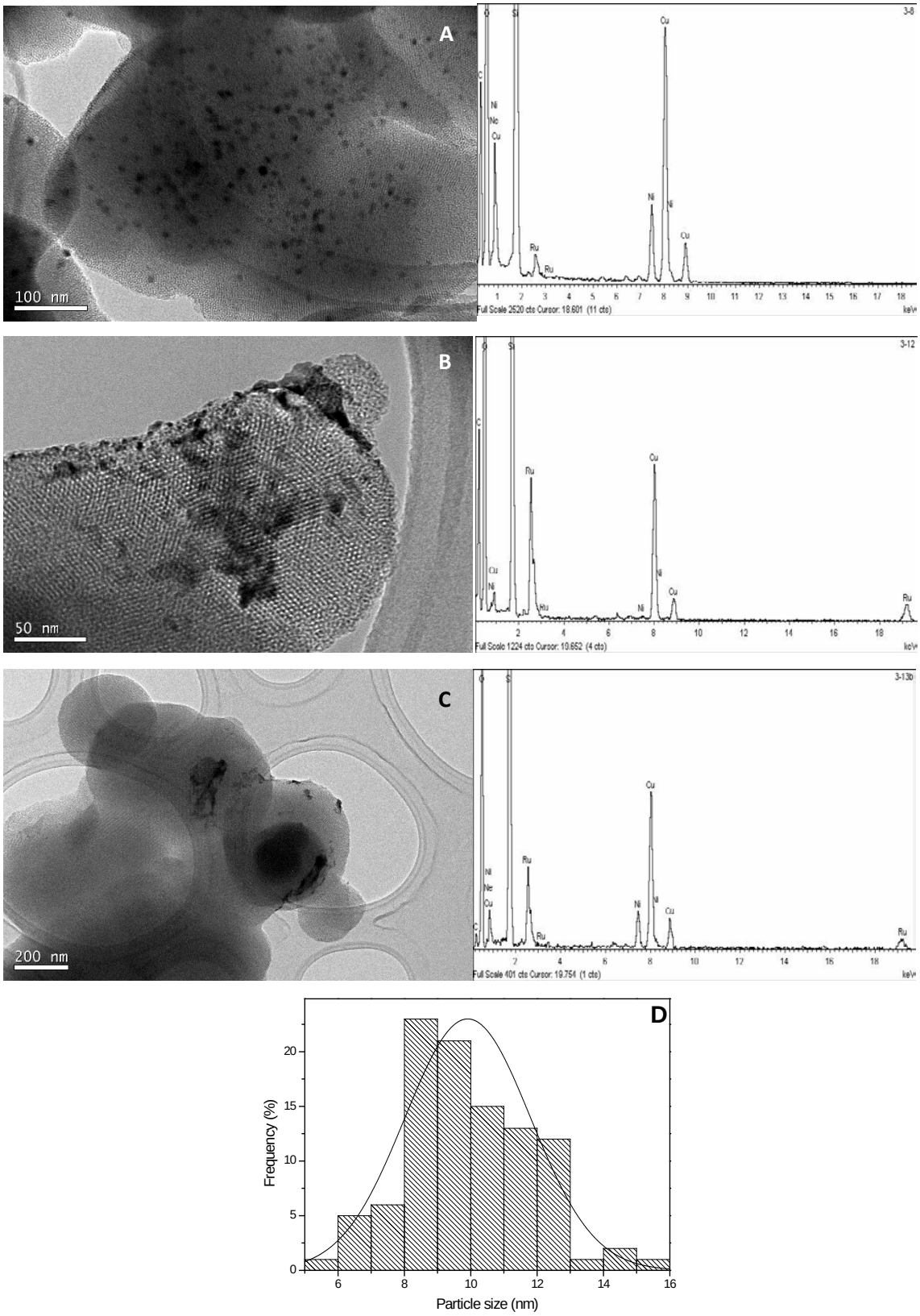

Figure 8. (A,B,C) Transmission Electron Microscopy (TEM) micrographs and EDS of Ru:Ni/MCM-48 (1.39). **(D)** Ni particle size distributions from TEM images.

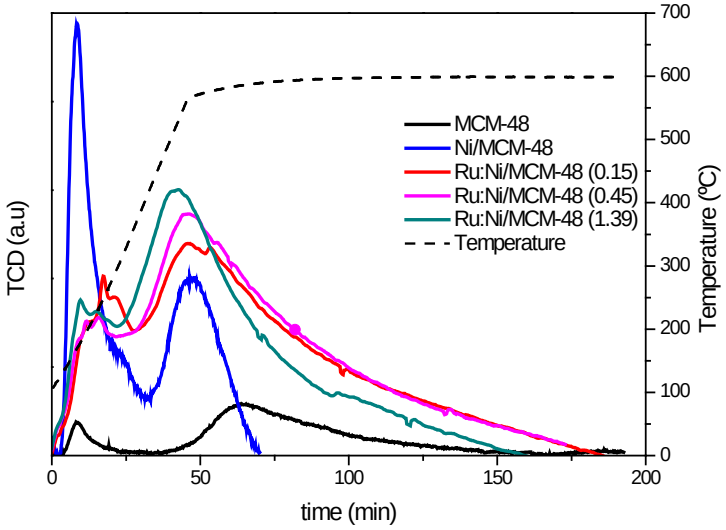

Figure 7. NH_3-TPD patterns for reduced catalysts.

3.3.ACTIVITY TEST: D-GLUCOSE HYDROGENATION

Hydrogenation of model compounds into sorbitol such as D-Glucose seems a very easy reaction pathway, but experimentally it is not as simple, since a decrease in the selectivity into sorbitol can be observed because of D-Glucose conversion into different byproducts by different ways. D-Glucose transformation into D-Mannose and D-Fructose can be obtained by Lobry de Bruyn–Alberda van Ekenstein rearrangements [14]. Subsequent hydrogenation of D-Mannose and D-Fructose produces mannitol and mixtures of sorbitol/mannitol, respectively. In addition, 5-HMF can be detected from dehydration of D-Glucose, as well as other derivatives, such as aldehydes [38]. In general terms, sorbitol is the major product in the catalytic hydrogenation of D-Glucose in hot compressed water, though sorbitol isomerizes into mannitol, which is the most important by-product of this reaction as well. Both the features of the carrier as the selected active metal play a very important role in D-Glucose hydrogenation reactions. In this sense, the monometallic Ni/MCM-48 and bimetallic Ru:Ni/MCM-48 catalysts were tested in the hydrogenation of D-Glucose at 120 ºC and 2.5 MPa H_2 at different reaction times. Then, Ni/MCM-48 and Ru:Ni/MCM-48 (0.45) were used at 130 ºC and 140 ºC in order to check the influence of temperature in the reaction. Preliminary experiments were carried out in the high pressure reactor, in order to confirm that the hydrogenation of D-Glucose was not mass transfer limited when stirring rate was 1400

rpm and catalyst particles presented a particle size smaller than 70 μm, neither limited by H_2 diffusion when pressure was adjusted to 2.5 MPa.

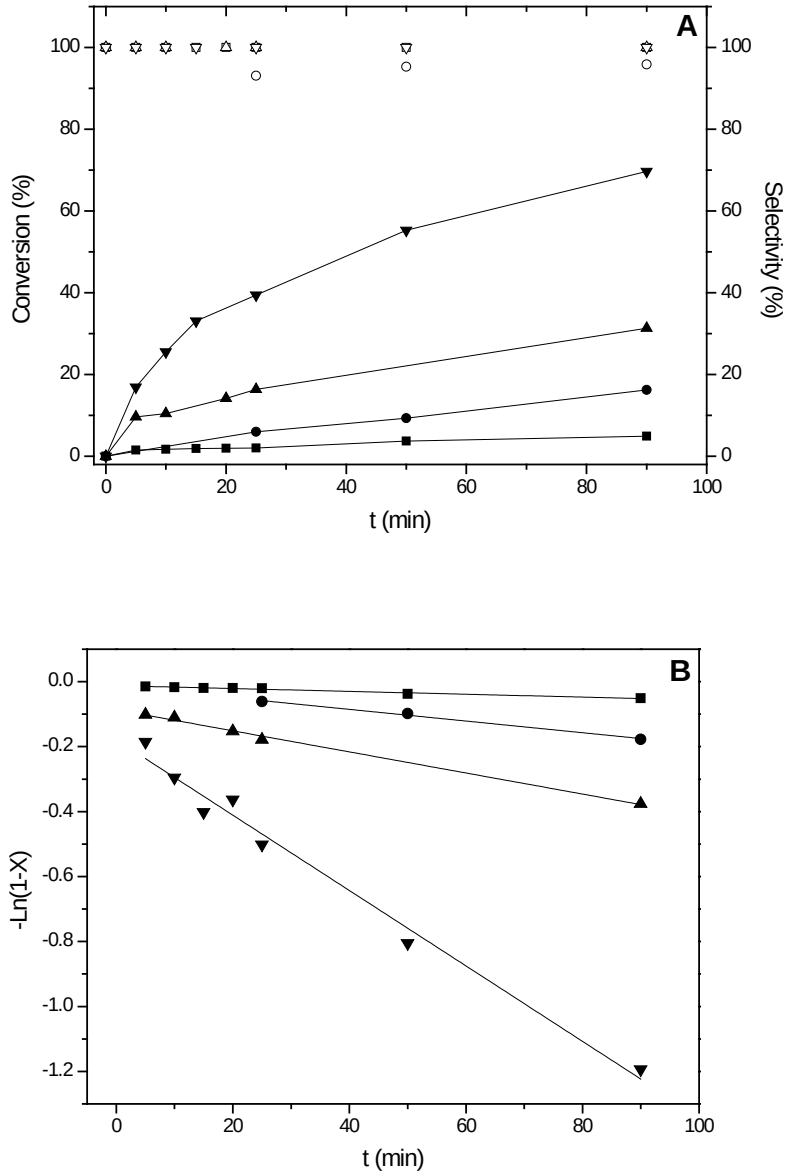

Figure 10. (A) Evolution of D-Glucose conversion (line + symbol) and selectivity (open symbol) as a function of reaction time and **(B)** pseudo-first fitting at C:Ru = 142, 120 ºC, 2.5 MPa H_2 and 1400 rpm for ● Ni/MCM-48, ■ Ru:Ni/MCM-48 (0.15), ▲ Ru:Ni/MCM-48 (0.45) and ▼Ru:Ni/MCM-48 (1.39).

According to the experimental data presented in Figure 10(A) and plotting -Ln (1 - *X*) versus reaction time in Figure 10(B), where *X* is conversion of D-Glucose, it was observed a linear fitting in all the cases. Given the excess of H_2 employed, a pseudo-first order dependence respect to D-Glucose was detected, which is consistent with previous data reported by other authors. Wisniak and Simon [39] found a first order dependency respect to D-Glucose concentration using Raney-Nickel catalysts. Mishra et al. proved that the hydrogenation of D-Glucose over Ru/HYZ followed a first order

dependence respect to D-Glucose as well [38]. In this sense, a pseudo-first order dependence respect to D-Glucose concentration was observed during the hydrolytic hydrogenation (Figure 10(B)). Figure 10(A) shows the catalytic behavior of the different catalysts during the hydrogenation process. A clear difference was observed between monometallic and bimetallic catalysts, since D-glucose was efficiently hydrogenated into sorbitol over bimetallic catalysts (100 % selective to sorbitol), while Ni/MCM-48 showed selectivities to sorbitol in the range of 93-95%. The slight decrease in sorbitol selectivity was attributed to the isomerization of sorbitol into mannitol, thus the addition of small amounts of ruthenium improved sorbitol selectivity being 100 % in all cases. The highest conversion of D-Glucose, around 70 %, was achieved over Ru:Ni/MCM-48 (1.39) after 90 min at 120 ºC and 2.5 MPa H_2. Experimental data presented in Table 2 provides further information about the behavior of the catalysts. Monometallic Ni/MCM-48 showed a kinetic constant of 9.7 $dm^3 \cdot g^{-1} \cdot min^{-1}$, which corresponds to a slower reaction rate in comparison with Ru:Ni/MCM-48 (0.45) and Ru:Ni/MCM-48 (1.39), although kinetic constant for Ni/MCM-48 is around 4.2 times higher than the obtained for Ru:Ni/MCM-48 (0.15). This catalytic behavior is in good agreement with TEM results, where smaller and better distributed nickel nanoparticles were observed in the monometallic catalyst than in Ru:Ni/MCM-48 (0.15). Both this fact and the small amount of ruthenium present in Ru:Ni/MCM-48 (0.15) could be not enough to overcome the catalytic behavior of Ni/MCM-48. In the case of Ru:Ni/MCM-48 (0.45) and (1.39), reaction rates were around 1.9 and 6.8 times higher than monometallic nickel-based catalyst, respectively, indicating that larger amounts of ruthenium conducted to more active catalysts even with less disperse nickel. Monometallic Ni/MCM-48 demonstrated higher catalytic activity in terms of reaction rate ($1.2 \cdot 10^{-3}$ $g_{sorbitol} \cdot g_{metal}^{-1} \cdot s^{-1}$) than other nickel-based catalyst reported in the literature under similar experimental conditions. Zhang et al. used Alumel catalyst (Ni/Al, 47% nickel metal loading) (Aladdin Reagent Limited Company. A. P. reagents) and nickel powder (Tianjin Kermel Chemical Reagents Limited Company) for the hydrogenation of D-Glucose at 120ºC, 3 MPa H_2 and 120 min obtaining reaction rates of $1.2 \cdot 10^{-4}$ $g_{sorbitol} \cdot g_{metal}^{-1} \cdot s^{-1}$ and $9.8 \cdot 10^{-5}$ $g_{sorbitol} \cdot g_{metal}^{-1} \cdot s^{-1}$, respectively [40]. However, Schimpf et al. working at higher pressure, longer time-on-stream (120 ºC, 12 MPa and 5 h) and using a Ni/SiO_2 achieved a reaction rate of $9.9 \cdot 10^{-3}$ $g_{sorbitol} \cdot g_{metal}^{-1} \cdot s^{-1}$. Ni/MCM-48 presented a catalytic activity 8.3 times smaller than those obtained by Schimpf et al [38]. There is not many information about the hydrogenation of D-Glucose over Ru:Ni-

based catalysts in the literature, but Bizhanov et al. reported the promoting effect of small amounts of ruthenium (0.1 – 0.5 %) and Palladium (5 %) over unsupported Raney-Nickel catalysts [22] which can raise its activity by as much as 30 %. In the case of Ru:Ni/MCM-48 (0.45), the addition of a 0.76 % of ruthenium over Ni/MCM-48 catalyst improved catalytic activity in a 100 %, approximately. In addition, catalytic activity of all the samples was calculated as specific reaction rate based on nickel surface area, which was calculated from the equation 9, where S_{Ni} is the specific Ni surface area calculated from equation 10 and t the reaction time. In equation 10, 6 is a shape factor that assumes a spherical geometry, whose its use is valid based on calculations from TEM analysis, $\bar{d}_s$ is surface-area weighted diameter of Ni from equation 2 and ρ_{Ni} is nickel density (8.9 $g \cdot cm^{-3}$) [41]. Specific reaction rate given in Table 2, are consistent with the following sequence of increasing activity: Ni/MCM-48 < Ru:Ni/MCM-48 (0.15) < Ru:Ni/MCM-48 (0.45) < Ru:Ni/MCM-48 (1.39). This sequence illustrates the impact of ruthenium addition per specific surface of nickel. Moreover, Ru/MCM-48 with a ruthenium loading around 4% reported in a previous work [23], showed a reaction rate of $3.2 \cdot 10^{-2}$ $g_{sorbitol} \cdot g_{metal}^{-1} \cdot s^{-1}$ for D-Glucose hydrogenation at the same experimental conditions, which was 5.8 times higher than that obtained by Ru:Ni/MCM-48 (1.39). Therefore, activity of bimetallic catalyst remarkably improved compared to that obtained by Ni/MCM-48, but it was not possible to achieve similar catalytic activity to that presented by Ru/MCM-48.

Table 2. Comparison of reaction rate ($g_{sorbitol} \cdot g_{metal}^{-1} \cdot s^{-1}$), specific reaction rate ($mol_{sorbitol} \cdot cm^{-2}_{Ni} \cdot s^{-1}$) and pseudo-first order kinetic constants of Ni/MCM-48 and Ru:Ni/MCM-48 catalysts in D-Glucose hydrogenation at 120 ºC, 2.5 MPa H_2 and 90 min.

Catalyst	**Specific reaction rate $\cdot 10^{13}$ ($mol_{sorbitol} \cdot cm^{-2}_{Ni} \cdot s^{-1}$)**	**Reaction rate $\cdot 10^{3}$ ($g_{sorbitol} \cdot g_{metal}^{-1} \cdot s^{-1}$)**	**k$\cdot 10^{3}$ ($dm^3 \cdot g^{-1} \cdot min^{-1}$)**	**R^2**
Ni/MCM-48	2.24	1.2	9.7	0.998
Ru:Ni/MCM-48 (0,15)	3.35	0.39	2.3	0.976
Ru:Ni/MCM-48 (0,45)	19.8	2.5	18.3	0.996
Ru:Ni/MCM-48 (1,39)	24.9	5.5	66.3	0.985

Ru:Ni/MCM-48 (0.45) was selected to study the influence of temperature in the conversion of D-Glucose, yield and selectivity to sorbitol. The so obtained results were compared with those acquired over Ni/MCM-48 (Figure 11) in the same range of temperatures (120 – 140 ºC). Kinetic constants at each temperature for both catalyst are

given in the caption for Figure 11. An increase of the hydrogenation temperature produced a slight improvement of the reaction rate using Ni/MCM-48. In addition, a clear decrease in the selectivity to D-Sorbitol from 95 to 86 % was detected as a result of its isomerization into mannitol by raising temperature. However, the influence of temperature had a major effect in the reaction rate for Ru:Ni/MCM-48 (0.45). In this case, the conversion to sorbitol was significantly increased with temperature from 31 to 59 %, while the selectivity to sorbitol remained constant (Figure 11).

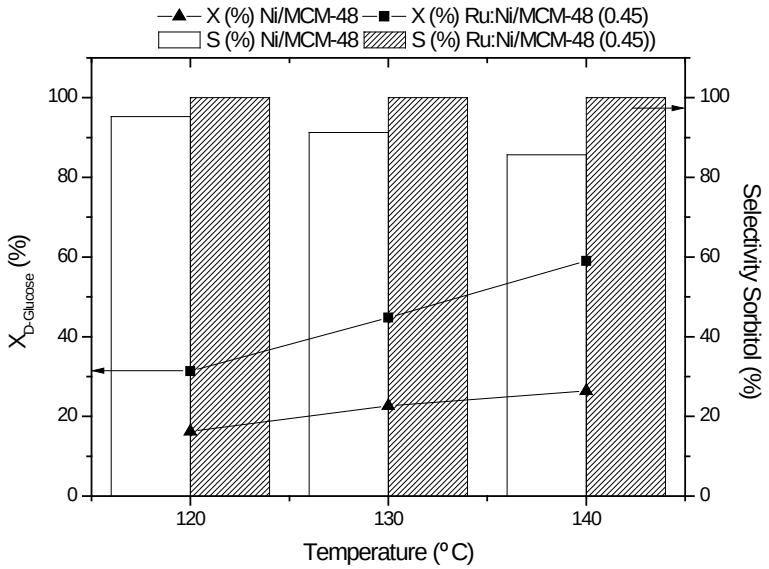

Figure 11. Effect of reaction temperature (120, 130, 140 ºC) in conversion of D-Glucose and selectivity to sorbitol over ▲ Ni/MCM-48 ($k_{120ºC} = 9.7 \cdot 10^{-3}$, $k_{130ºC} = 1.3 \cdot 10^{-2}$ and $k_{140ºC} = 1.7 \cdot 10^{-2}$ $dm^3 \cdot g^{-1} \cdot min^{-1}$) and ■ Ru:Ni/MCM-48 (0.45) ($k_{120ºC} = 1.8 \cdot 10^{-2}$, $k_{130ºC} = 3.4 \cdot 10^{-2}$ and $k_{140ºC} = 5.1 \cdot 10^{-2}$ $dm^3 \cdot g^{-1} \cdot min^{-1}$) at C:Ru = 142, 2.5 MPa H_2, 1400 rpm and 90 min.

Arrhenius plots for Ni/MCM-48 and Ru:Ni/MCM-48 (0.45) given in Figure 12(A). It can be observed that the activation energy value (E_a) for the hydrogenation of D-Glucose over Ni/MCM-48 was 36 $KJ \cdot mol^{-1}$, which is comparable to the values reported in the literature. Déchamp et al. carried out the hydrogenation of D-Glucose in a trickle bed reactor in the temperature range 70 – 130 ºC and 8 MPa of H_2 pressure over a commercial Silica-Alumina supported nickel catalyst (purchased from Harshaw, ref. Ni-3266E 1/16 in.) and the authors reported an activation energy around 67 $KJ \cdot mol^{-1}$ [16]. Brahme et al. studied the hydrogenation of D-Glucose in the temperature ranges of 77 – 100 ºC and 77 – 146 ºC over a Raney – Nickel catalyst and activation energies of 6 $KJ \cdot mol^{-1}$ and 44 $KJ \cdot mol^{-1}$ were obtained, respectively [42]. Ru:Ni/MCM-48 (0.45) was more sensitive to temperatures changes in comparison with Ni/MCM-48 during the hydrogenation of D-Glucose, showing a higher activation energy (70 $KJ \cdot mol^{-1}$). It is not

possible to make a relationship between reaction rates and activation energies for both catalysts due to the observed differences in terms of pre-exponential factors (Figure 12(A)). It should be noted that the bimetallic catalyst showed pre-exponential factor five orders of magnitude higher than the monometallic, pointing out a compensation effect. Bizhanov et al. reported activation energy values for bimetallic Ni-Pt (0.1 wt % Pt) (50 – 54 KJ·mol^{-1}) and Ni-Rh (38 – 42 KJ·mol^{-1} Rh) catalysts in the hydrogenation of D-Glucose at temperatures between 80 – 130 ºC [22]. Activation energy values obtained for Ni/MCM-48 (36 KJ·mol^{-1}) and Ru:Ni/MCM-48 (0.45) (70 KJ·mol^{-1}) are larger than those obtained for mass transfer limited processes (12 – 21 KJ·mol^{-1}), which indicates that the reaction rate was controlled by the kinetics on the metal surface.

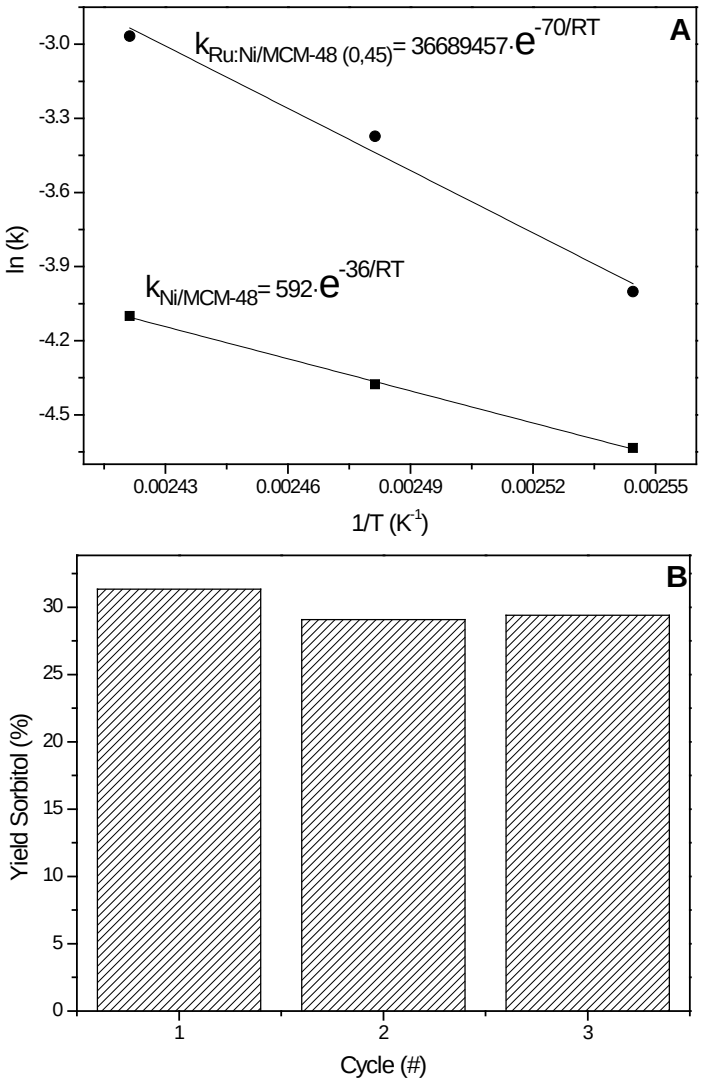

Figure 10. (A) Arrhenius plots of D-Glucose hydrogenation over ■ Ni/MCM-48 and ● Ru:Ni/MCM-48 (0.45) and **(B)** Stability test of Ru:Ni/MCM-48 (0.45) at C:Ru = 142, 120 ºC, 2.5 MPa H_2, 1400 rpm and 90 min.

In order to check catalyst stability, RuNi/MCM-48 (0.45) was recovered after each experiment and tested in D-Glucose hydrogenation at 120 ºC after three cycles. Results shown in Figure 12(B) confirmed that catalytic activity of Ru:Ni/MCM-48 (0.45) was not affected by the reusing of the catalyst. It was observed a slight decrease in the yield of sorbitol from 31 % to 29 % after three reaction cycles, probably due to the formation of impurities over the active surface of the catalyst, while the selectivity to sorbitol was 100 % in all cases, demonstrating the good stability of Ru:Ni/MCM-48 (0.45) under the experimental conditions.

4. Conclusions

As a result of the deposition of different amounts of Ru over Ni/MCM-48, significant differences were observed related to catalyst properties and thus in their behavior during hydrogenation of D-Glucose in comparison with monometallic Ni/MCM-48. According to the results presented above, the following conclusions were obtained:

i) The addition of different amounts of ruthenium over monometallic Ni/MCM-48 improved the reducibility of nickel and ruthenium species into their metallic state, respectively.

ii) Calculation from TEM images demonstrated that the preparation of bimetallic Ru:Ni catalyst by consecutive wet impregnation caused an increase of the nickel crystallite size in comparison with the monometallic catalyst. However, the higher Ru:Ni ratio, the smaller the nanoparticle size of nickel.

iii) The presence of Ru:Ni ratios higher than 0.45 in the materials improved the catalytic behavior of the monometallic system in the catalytic hydrogenation of D-Glucose, increasing the reaction rate and showing complete selectivity to sorbitol.

iv) Hydrogenation of D-Glucose into sorbitol was also carried out at different temperatures over Ni/MCM-48 and Ru:Ni/MCM-48 and activation energies of ca. 36 $KJ \cdot mol^{-1}$ and 70 $KJ \cdot mol^{-1}$ were obtained. Ru:Ni/MCM-48 (0.45) showed a good catalytic behavior at higher temperatures than 120 ºC, enhancing the reaction rate but maintaining a stable selectivity to sorbitol.

v) A good stability after three reaction cycles was observed for Ru:Ni/MCM-48 (0.45).

vi) In accordance with the results here presented, Ru:Ni/MCM-48 (0.45) stands as a good option for the efficient hydrogenation of carbohydrate sugars into sugar alcohols.

Acknowledgements

The authors gratefully acknowledge the Spanish Governement (MINECO) and FEDER founds for the financial support of this project CTQ2015-64892-R (MINECO/FEDER). A. Romero thanks to the program of predoctoral scholarships from Junta de Castilla y León Government for his grant (E-47-2015-0062773).

References

1. Xi, J., et al., *Direct conversion of cellulose into sorbitol with high yield by a novel mesoporous niobium phosphate supported Ruthenium bifunctional catalyst.* Applied Catalysis A: General, 2013. **459**(0): p. 52-58.

2. Lazaridis, P.A., et al., *d-Glucose hydrogenation/hydrogenolysis reactions on noble metal (Ru, Pt)/activated carbon supported catalysts.* Catalysis Today, (0).

3. Rogalinski, T., T. Ingram, and G. Brunner, *Hydrolysis of lignocellulosic biomass in water under elevated temperatures and pressures.* The Journal of Supercritical Fluids, 2008. **47**(1): p. 54-63.

4. Bobleter, O., *Hydrothermal degradation of polymers derived from plants.* Progress in Polymer Science, 1994. **19**(5): p. 797-841.

5. Kobayashi, H., et al., *Synthesis of sugar alcohols by hydrolytic hydrogenation of cellulose over supported metal catalysts.* Green Chemistry, 2011. **13**(2): p. 326-333.

6. Cao, Y.-l., et al., *Hydrolytic hydrogenation of cellulose over Ni-WO_3/SBA-15 catalysts.* Journal of Fuel Chemistry and Technology, 2013. **41**(8): p. 943-949.

7. Negoi, A., et al., *The hydrolytic hydrogenation of cellulose to sorbitol over M (Ru, Ir, Pd, Rh)-BEA-zeolite catalysts.* Catalysis Today, 2014. **223**(0): p. 122-128.

8. Li, Y., et al., *Advances in hexitol and ethylene glycol production by one-pot hydrolytic hydrogenation and hydrogenolysis of cellulose.* Biomass and Bioenergy, 2015. **74**(0): p. 148-161.

9. De Wulf, P., W. Soetaert, and E.J. Vandamme, *Optimized synthesis of L-sorbose by C5-dehydrogenation of D-sorbitol with Gluconobacter oxydans.* Biotechnology and Bioengineering, 2000. **69**(3): p. 339-343.

10. Perrard, A., et al., *Highly efficient metal catalysts supported on activated carbon cloths: A catalytic application for the hydrogenation of d-glucose to d-sorbitol.* Applied Catalysis A: General, 2007. **331**(0): p. 100-104.

11. Corma, A., S. Iborra, and A. Velty, *Chemical Routes for the Transformation of Biomass into Chemicals.* Chemical Reviews, 2007. **107**(6): p. 2411-2502.

12. Besson, M., P. Gallezot, and C. Pinel, *Conversion of Biomass into Chemicals over Metal Catalysts.* Chemical Reviews, 2014. **114**(3): p. 1827-1870.

13. Gallezot, P., *Chapter 1 - Metal Catalysts for the Conversion of Biomass to Chemicals*, in *New and Future Developments in Catalysis*, S.L. Suib, Editor. 2013, Elsevier: Amsterdam. p. 1-27.

14. Schimpf, S., C. Louis, and P. Claus, *Ni/SiO_2 catalysts prepared with ethylenediamine nickel precursors: Influence of the pretreatment on the catalytic properties in glucose hydrogenation.* Applied Catalysis A: General, 2007. **318**(0): p. 45-53.

15. Hoffer, B.W., et al., *The role of the active phase of Raney-type Ni catalysts in the selective hydrogenation of d-glucose to d-sorbitol.* Applied Catalysis A: General, 2003. **253**(2): p. 437-452.

16. Déchamp, N., et al., *Kinetics of glucose hydrogenation in a trickle-bed reactor*. Catalysis Today, 1995. **24**(1–2): p. 29-34.

17. Hoffer, B.W., et al., *Carbon supported Ru catalysts as promising alternative for Raney-type Ni in the selective hydrogenation of d-glucose.* Catalysis Today, 2003. **79–80**(0): p. 35-41.

18. Kusserow, B., S. Schimpf, and P. Claus, *Hydrogenation of Glucose to Sorbitol over Nickel and Ruthenium Catalysts.* Advanced Synthesis & Catalysis, 2003. **345**(1-2): p. 289-299.

19. van Gorp, K., et al., *Catalytic hydrogenation of fine chemicals: sorbitol production.* Catalysis Today, 1999. **52**(2–3): p. 349-361.

20. Mikkola, J.-P., et al., *Deactivation kinetics of Mo-supported Raney Ni catalyst in the hydrogenation of xylose to xylitol.* Applied Catalysis A: General, 2000. **196**(1): p. 143-155.

21. Gallezot, P., et al., *Glucose hydrogenation on promoted raney-nickel catalysts.* Journal of Catalysis, 1994. **146**(1): p. 93-102.

22. Bizhanov, F.B., et al., *Hydrogenation of glucose on Raney nickel. I.* Journal of Catalysis, 1968. **10**(2): p. 206-207.

23. Romero, A., et al., *Conversion of biomass into sorbitol: Cellulose hydrolysis on MCM-48 and d-Glucose hydrogenation on Ru/MCM-48.* Microporous and Mesoporous Materials, 2016. **224**: p. 1-8.

24. Romero, A., et al., *Supercritical water hydrolysis of cellulosic biomass as effective pretreatment to catalytic production of hexitols and ethylene glycol over Ru/MCM-48.* Green Chemistry, 2016.

25. Schumacher, K., M. Grün, and K.K. Unger, *Novel synthesis of spherical MCM-48.* Microporous and Mesoporous Materials, 1999. **27**(2–3): p. 201-206.

26. Amorim, C. and M.A. Keane, *Palladium supported on structured and nonstructured carbon: A consideration of Pd particle size and the nature of reactive hydrogen.* Journal of Colloid and Interface Science, 2008. **322**(1): p. 196-208.

27. Romero, A.A., et al., *Synthesis and Characterization of the Mesoporous Silicate Molecular Sieve MCM-48.* The Journal of Physical Chemistry B, 1997. **101**(27): p. 5294-5300.

28. Brunauer, S., et al., *On a Theory of the van der Waals Adsorption of Gases.* Journal of the American Chemical Society, 1940. **62**(7): p. 1723-1732.

29. Morey, M., et al., *Pseudotetrahedral O3/2VO Centers Immobilized on the Walls of a Mesoporous, Cubic MCM-48 Support: Preparation, Characterization, and Reactivity toward Water As Investigated by 51V NMR and UV−Vis Spectroscopies.* Chemistry of Materials, 1996. **8**(2): p. 486-492.

30. Thommes, M., R. Köhn, and M. Fröba, *Systematic Sorption Studies on Surfce and Pore Size Characteristics of Different MCM - 48 Silica Materials,* in *Studies in Surface Science and Catalysis*, G.K. K.K. Unger and J.P. Baselt, Editors. 2000, Elsevier. p. 259-268.

31. Arteaga, G., et al., *Effects of the Sn/Ni ratio and the oxidative treatments on properties of Ni-Sn/SiO_2 catalysts.* Revista Técnica de la Facultad de Ingeniería Universidad del Zulia, 2007. **30**: p. 494-503.

32. Braos-García, P., et al., *Bimetallic Ru/Ni supported catalysts for the gas phase hydrogenation of acetonitrile.* Applied Catalysis A: General, 2010. **381**(1–2): p. 132-144.

33. Cerro-Alarcón, M., A. Guerrero-Ruíz, and I. Rodríguez-Ramos, *Stereoselective hydrogenation of Paracetamol to trans-4-acetamidocyclohexanol on carbon-supported Ru□M (M = Co, Ni) bimetallic catalysts.* Catalysis Today, 2004. **93–95**(0): p. 395-403.

34. Crisafulli, C., et al., *CO2 reforming of methane over Ni–Ru and Ni–Pd bimetallic catalysts.* Catalysis Letters, 1999. **59**(1): p. 21-26.

35. Chen, G., et al., *Synthesis of Ni–Ru Alloy Nanoparticles and Their High Catalytic Activity in Dehydrogenation of Ammonia Borane.* Chemistry – A European Journal, 2012. **18**(25): p. 7925-7930.

36. Zhu, L., et al., *Synthesis of Different Ruthenium Nickel Bimetallic Nanostructures and an Investigation of the Structure–Activity Relationship for Benzene Hydrogenation to Cyclohexane.* ChemCatChem, 2014. **6**(7): p. 2039-2046.

37. Eliche-Quesada, D., et al., *Ru, Os and Ru–Os supported on mesoporous silica doped with zirconium as mild thio-tolerant catalysts in the hydrogenation and hydrogenolysis/hydrocracking of tetralin.* Applied Catalysis A: General, 2005. **279**(1–2): p. 209-221.

38. Mishra, D.K., et al., *Selective hydrogenation of d-glucose to d-sorbitol over HY zeolite supported ruthenium nanoparticles catalysts.* Catalysis Today, 2014. **232**: p. 99-107.

39. Wisniak, J. and R. Simon, *Hydrogenation of glucose, fructose, and their mixtures.* Industrial and Engineering Chemistry Product Research and Development, 1979. **18**(1): p. 50-57.

40. Zhang, J., et al., *Efficient conversion of d-glucose into d-sorbitol over MCM-41 supported Ru catalyst prepared by a formaldehyde reduction process.* Carbohydrate Research, 2011. **346**(11): p. 1327-1332.

41. Nieto-Márquez, A., et al., *Impact of nitrogen doping of carbon nanospheres on the nickel-catalyzed hydrogenation of butyronitrile.* Journal of Catalysis, 2010. **269**(1): p. 242-251.

42. Brahme, P.H. and L.K. Doraiswamy, *Modelling of a Slurry Reaction. Hydrogenation of Glucose on Raney Nickel.* Industrial & Engineering Chemistry Process Design and Development, 1976. **15**(1): p. 130-137.

CHAPTER 4

ONE-POT CATALYTIC HYDROLYSIS/HYDROGENATION OF CELLOBIOSE INTO HEXITOLS OVER RU/AL-MCM-48

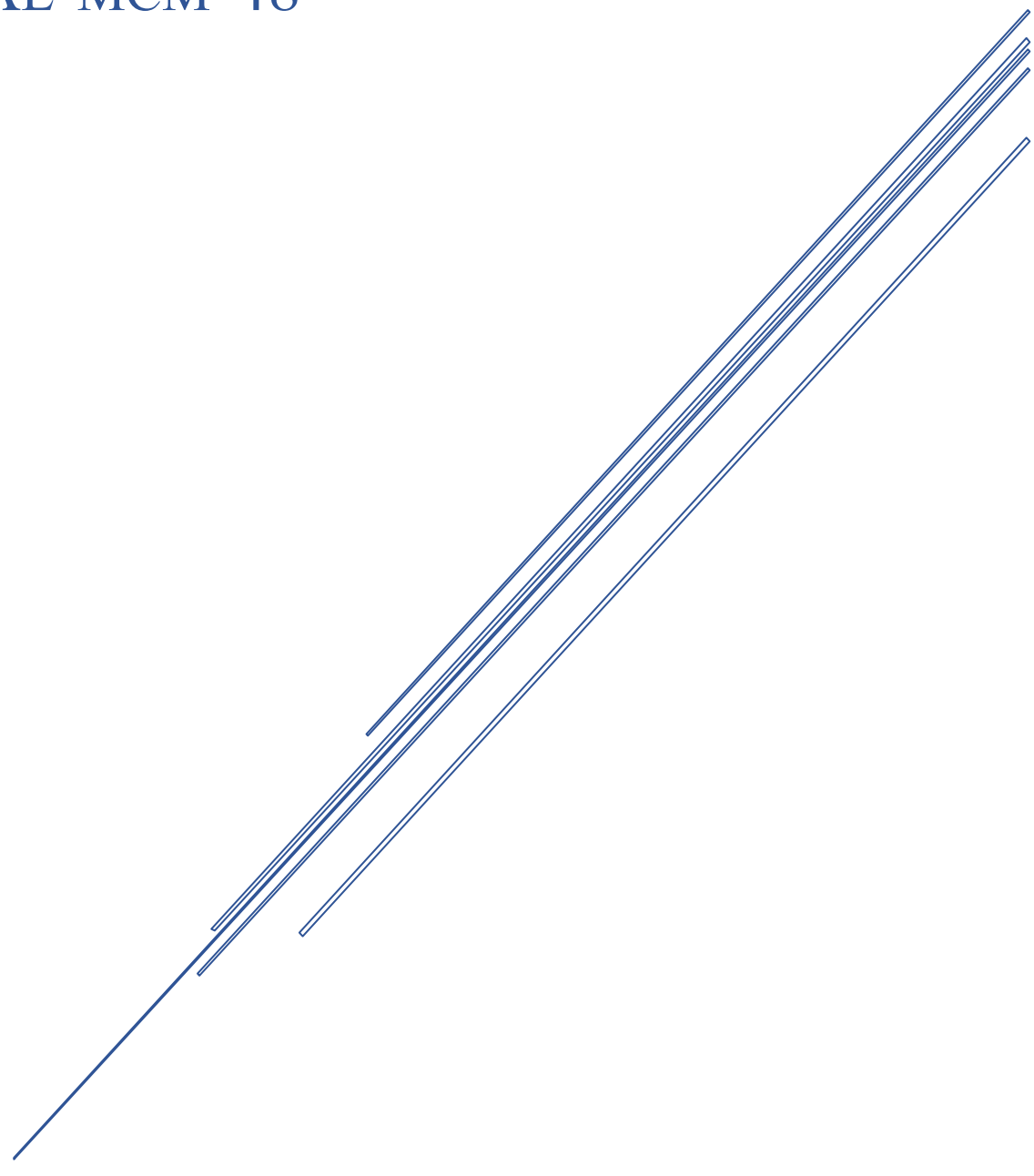

ONE-POT CATALYTIC HYDROLYSIS/HYDROGENATION OF CELLOBIOSE INTO HEXITOLS OVER RU/AL-MCM-48

Abstract

Ru/Al-MCM-48 as catalyst for the selective hydrolysis/hydrogenation of cellobiose to hexitols has been synthesized and characterized by means of adsorption-desorption isotherms of N_2, small angle X-Ray scattering (SAXS), reduction at programmed temperature (H_2-TPR), X-Ray Diffraction (XRD), transmission electron Mycroscopy (TEM) and desorption at programmed temperature of ammonia (NH_3-TPD). Additionally, possible reaction pathways and key intermediate compounds of conversion of cellobiose to hexitols were discussed. In the kinetic study the effects of pressure, temperature and time on the hydrogenolysis reaction were evaluated and a kinetic model covering different reaction temperatures was also developed. A maximum yield around 91 % of hexitols was achieved by catalytic hydrogenation of cellobiose over Ru/Al-MCM48 at 180 ºC, 5 MPa H_2 and 7 min, where sorbitol was the main compound in the final product with a yield of 82 %. Cellobitol was the main intermediate of the reaction over Ru/Al-MCM48. Temperatures in the range of 140 – 180 ºC and pressures in the range of 30 – 50 MPa H_2 were studied and it was concluded that higher temperatures and pressures had a positive effect in order to maximize the production of hexitols. The developed kinetic model predicted well the concentration of the different compounds involved in the proposed reaction pathway and calculated the specific reaction rate and activation energy values for the different steps of the catalytic process.

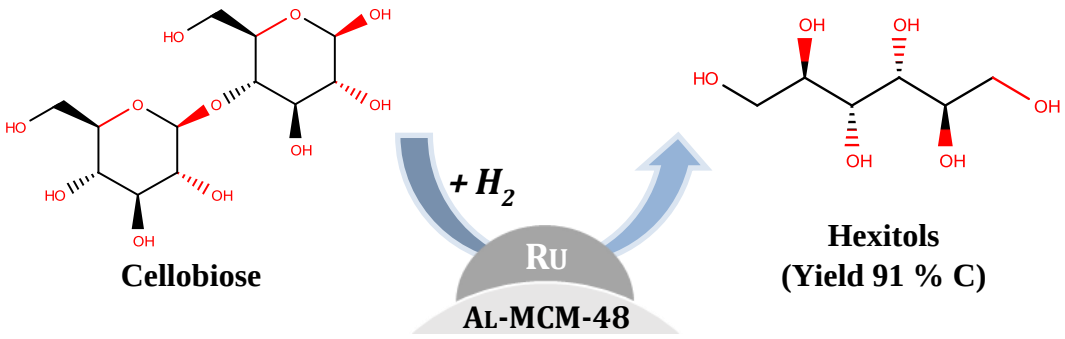

Cellobiose

Hexitols (Yield 91 % C)

Keywords:

Ru/Al-MCM-48, Cellobiose, Hexitols, Hydrolysis/Hydrogenation, Sorbitol

1. INTRODUCTION

Nowadays, different reasons such as the elevated energy demand, problems derived from global warming effects and the diminishing of fossil fuel reserves, have encouraged the scientific community to look for alternative raw materials for the production of fuels and chemicals, as well as the development of new renewable energy sources [1-4]. These alternatives should meet the two following requirements: a) to be renewable and b) to be potentially sustainable [5]. Lignocellulosic biomass is constituted by three structural polymers, namely cellulose (34 – 50 %), hemicelluloses (19 – 34 %) and lignin (11 – 30 %) [6]. Cellulose is the most abundant source of biomass on earth and it is currently considered as a potential alternative carbon source to fossil fuels in order to the sustainable production of chemicals and fuels [7]. Nevertheless, according to both complex crystalline structure composed by β-1,4-glycosidic bonds of D-Glucose and its insolubility in conventional solvents, cellulose conversion still remains a technological challenge. Thus, the development of bifunctional acid/redox catalysts for the efficient valorization of cellulose towards highly valuable chemicals such as sugar alcohols, glycols and alkanes, is extremely necessary [8-10].

Great attention have been paid to conversion of cellulosic biomass into hexitols such as sorbitol, which is a sugar alcohol with a wide range of uses in food, pharmaceutical, cosmetics and industrial applications [11]. Additionally, sorbitol is a platform chemical of considerable importance for the production of useful chemicals such as isosorbide, 1,4-sorbitan or alkanes [12]. Considering production of chemicals, polyols show some advantages over fossil sources: a) *High atom economy* since during conversion process most of the hydroxyl groups from cellulose are preserved in the desired polyol, b) *good economic viability* according to the high value of polyols and c) *market capacity* of polyols is noteworthy (30 – 40 million ton/year) but not too large [13]. In general terms, hydrolytic conversion of cellulose to sorbitol comprises two successive steps: a) Cellulose depolymerization into monosaccharides such as D-Glucose, which has been promoted by enzymes [14, 15], homogeneous acids [16], heterogeneous catalysts [17] and supercritical water [18] and b) further hydrogenation of so obtained soluble sugars to sorbitol in the presence of active metals under hydrogen atmosphere [19, 20]. In the recent years, one-pot catalytic hydrolysis/hydrogenation of cellulose to sorbitol has been develop, being the objective of several studies [1, 21, 22]. It is still a challenge to

develop kinetic studies from cellulose according to its complex structure. As an approach, simple model compounds such as cellobiose, which represents the basic repeating unit of cellulose consisting of two glucose monomers, has been used for this purpose [23].

Negahdar et al. carried out kinetic tests for the hydrolytic hydrogenation of cellobiose to sorbitol using a catalytic system consisting of silicotungstic acid and a supported ruthenium catalyst (5 wt.% Ru/C) [24]. They found two competitive reaction pathways for hydrolytic hydrogenation of cellobiose: a) First pathway consisting on the hydrolysis of cellobiose towards D-Glucose and the subsequently hydrogenation of D-Glucose to sorbitol and b) a secondary reaction route where cellobiose is hydrogenated to 3-D-glucopyranosyl-D-glucitol (also known as cellobitol), which is further hydrolyzed to sorbitol. In this second route D-Glucose can also be obtained as intermediate of cellobitol hydrolysis. Conversion of cellobiose to sorbitol was also studied over Ru/Zr-SBA-15 [25], Ru/CNT [23], a combination of H_3PO_4 + Ru/C [26] and combinations of molten salts hydrate $ZnCl_2.4H_2O$ + Ru/C [27]. Despite reaction rate constants and activation energy values are some of the most meaningful parameters in order to develop a kinetic model and to compare catalytic data, it is more common to observe in the literature data related to conversions and yields to the desired product. Thus, more detailed kinetic analysis of the reactions is required in order to achieve a higher understanding of the different mechanisms involved and to study the effect of the reaction parameters in the global process [24].

In the present work, we report the catalytic performance of bifunctional Ru/Al-MCM-48 in the hydrolytic hydrogenation of cellobiose into sorbitol. Up to our knowledge, other mesoporous Ru-based catalysts have been used, such as Ru/SBA-15 and Ru/Zr-SBA-15 [25], but it is the first time that Ru/Al-MCM-48 has been tested for the catalytic hydrolysis/hydrogenation of cellobiose. The interesting textural properties of Al-MCM-48 avoid diffusional limitations of large molecules [28]. The presence of aluminum in MCM-48 increases the number of acid sites compared to MCM-48 and these features play a significant role for hydrolysis steps involved in the conversion of cellobiose to sorbitol. Furthermore, ruthenium was selected as the active metal for hydrogenation steps. A screening of temperatures and H_2 pressures was done in order to study the effect of these parameters to maximize the production of hexitols (sorbitol and mannitol). In addition, a kinetic model covering different reaction temperatures was

developed and the possible reaction mechanisms, depending on the experimental conditions, are also discussed in this work.

2. MATERIALS AND METHODS

2.1. CATALYSTS PREPARATION

Synthesis of Al-MCM-48 has been done by the standard hydrothermal sol-gel method, as described in a previous work [9]. In a conventional synthesis, n-Hexadecyl-trimethylammonium bromide (CH3(CH2)15N(Br)(CH3)3 ≥ 98%, Sigma – Aldrich), which acts as template, was dissolved in the mixed solution of 42 cm3 of distilled water, 13 cm3 of aqueous ammonia (20% as NH3, Panreac), 18 cm3 of absolute ethanol (partially denaturated QP, Panreac) and 0.077 g of sodium aluminate (NaAlO2, Sigma - Aldrich), related to a ratio Si/Al = 20, by stirring for 15 min. After that, 4 cm3 of TEOS (≥ 99% GC, Sigma – Aldrich) were added dropwise. The final solution was stirred for 18 h in a hydrothermal bath; the white precipitates were collected by vacuum filtration and washed with distilled water until pH = 7. Then, precipitates were dried at 60 ºC overnight. Dried precipitates were calcined with air from 80 ºC to 550 ºC (heating rate of 2 ºC·min-1) and kept at the final temperature overnight.

Ruthenium was deposited on Al-MCM-48, with a metal loading around 4 %, by using the conventional wet impregnation method (WI). Ruthenium (III) chloride anhydrous (supplied by Strem Chemicals Inc.) was used as metal precursor for this preparation. The desired amounts of the metal salt and support were sonicated in water for 10 min, separately. Then, the resulting ruthenium trichloride solution and Al-MCM-48 dispersion in water were mixed and heated up from room temperature to 105 ºC (heating rate of 1 ºC·min-1) using a Stuart model SD162 heating plate. The impregnation process finishes when water is completely evaporated; then, the final product is dried at 105 ºC overnight. After that, the material is milled and reduced at 150 ºC under hydrogen atmosphere for 1 h.

2.2. CATALYSTS CHARACTERIZATION

Small Angle X-Ray Scattering (SAXS) and X-Ray Diffraction (XRD) were performed in a Bruker Discover D8 Focus diffractometer using the Cu Kα radiation (λ =

0.15406 nm). The diffraction intensities were measured, for XRD, over an angular range of $20° < 2\theta < 90°$ with a step size of 0.03° and a count time of 2 s per step. In case of SAXS, $2° < 2\theta < 6º$ was selected as angular range with a step size of 0.02° and a count time of 1 s per step.

Nitrogen adsorption-desorption of N_2 at -196 ºC was performed with ASAP 2020 (Micromeritics) to obtain surface and pore properties of Al-MCM-48 and Ru/Al-MCM-48. Prior to analysis, the samples were outgassed overnight at 350 ºC. Total specific surface areas were determined by the multipoint BET method at $P/P_0 \leq 0.3$, total specific pore volumes were evaluated by single point adsorption of N_2 $P/P_0 \geq 0.99$. Pore diameter was obtained by BJH adsorption average ($4 \cdot V \cdot A^{-1}$, nm). Pore size distribution was derived from the adsorption branch of the isotherm by BJH (dV/dD), Halsey: Faas correction.

Temperature Programmed Reduction (H_2-TPR) profile of Ru/Al-MCM-48 was recorded using the commercial Micromeritics TPD/TPR 2900 unit. The sample was loaded into a U-shaped quartz cell (100 mm × 3.76 mm i.d.), ramped (10 ºC·min^{-1}) from room temperature to 800 ºC under a flow of H_2/N_2 (5% v/v; 50 cm^3·min^{-1}, Air Liquide) and kept at the final temperature until the signal returned to the baseline. Hydrogen consumption was monitored by a thermal conductivity detector (TCD) with data acquisition/manipulation using the ChemiSoft TPX V1.03™ software.

NH_3-TPD experiments were performed in the same analyzer. In this case, the samples were activated under H_2-TPR conditions (150 ºC) for 60 min and then they were saturated with ammonia at 100 ºC during 30 min. NH_3 was purged using pure He during 60 min and then samples were heated from 100 ºC to 600 ºC (ramped 15 ºC·min^{-1}) and kept at the final temperature until the signal returned to the baseline. The amount of chemisorbed ammonia was calculated according to calibrated volumes of this compound.

Transmission electron microscopy (TEM) analyses used a JEOL 2100 unit with an accelerating voltage of 200 kV. Ru/Al-MCM-48 was prepared by ultrasonic dispersion in acetone with a drop of the resultant suspension, which was evaporated onto a holey carbon-supported grid. A counting of ruthenium nanoparticles was carried out from TEM images of Ru/Al-MCM-48. 175 ruthenium nanoparticles were counted and the

mean Ru particle size was expressed as surface-area weighted diameter ($\bar{d}_s$), which was calculated from the following equation (Eq. 1) [29].

$$\bar{d}_s = \frac{\sum_i n_i \cdot d_i^3}{\sum_i n_i \cdot d_i^2} \quad (1)$$

In equation 1, n_i is the number of ruthenium nanoparticles with a diameter d_i.

Ruthenium loading in Ru/Al-MCM-48 was determined by means of atomic absorption (AA) spectrophotometry, using a SPECTRA 220FS analyzer. Approximately, 0.05 g of the sample, 3 mL of HCl, 3 mL H_2O_2 and 3 mL HF were treated by microwave digestion at 250 ºC and the final solution was measured in the spectrophotometer.

2.3. CATALYTIC TESTS

In a typical catalytic experiment, 2 g of cellobiose (for microbiology, ≥99.0%, supplied by Sigma-Aldrich) were dissolved in 50 mL of distilled water. Then, the final solution of cellobiose (concentration of 40 $g \cdot l^{-1}$) and 0.5 g of catalyst were added into a 200 mL stainless steel batch reactor PID controlled. The internal wall of the reactor is protected by a Teflon vessel in order to prevent corrosion. The reactor was flushed with N_2 and pressurized with a low pressure of 0.5 MPa of N_2. The reaction mixture was stirred at 1200 rpm and heated up to the desired temperature at an average rate of 6 $ºC \cdot min^{-1}$. Temperature ranged from 140 ºC to 180 ºC. When the reactor reached the reaction temperature, it was pressurized at 5 MPa of H_2 and it was considered as t = 0 min. Lower pressures of hydrogen were also tested in this work (4 and 3 MPa). The reactor had a sampling valve in order to obtain samples from the aqueous phase at different reaction times. At the end of the experiment, the reactor was cooled down in an ice bath to rapidly stop the reaction. Then, it was depressurized and opened. Samples from aqueous phase were analyzed by means of total organic carbon (TOC, $mg \cdot l^{-1}$ C) using a Shimadzu TOC-VCSH analyzer and High Performance Liquid Chromatography (HPLC). The HPLC column used was a SUPELCO Ca^{2+} from Supelco at 60 °C and a flow of 0.4 $cm^3 \cdot min^{-1}$ using water Milli-Q as the mobile phase. A Shimadzu refractive index detector (IR) was used to identify sugars, polyols and their derivatives. Cellobiose conversion and yield to the reaction products were calculated using equations 2 and 3.

Concentrations of all the compounds involved in the calculation are expressed in carbon basis.

$$X_{Cellobiose}(\%) = \frac{[Cellobiose]_0 - [Cellobiose]_f}{[Cellobiose]_0} \cdot 100 \quad (2)$$

$$Y_{product}(\%) = \frac{[Product]}{[Cellobiose]_0} \cdot 100 \quad (3)$$

$$Specific\ reaction\ rate = \frac{n_{sorbitol}}{n_{Ru} \cdot t} \quad (4)$$

3. RESULTS AND DISCUSSION

3.1. CHARACTERIZATION OF THE CATALYTIC MATERIALS

Figure 1 shows Small Angle X-Ray Scattering (SAXS) pattern of Al-MCM-48. Calcined Al-MCM-48 shown four main Bragg diffraction peaks in the 2θ range from 2-5 º, that can be assigned to (211), (220), (420) and (332) planes. These results demonstrated the high quality of mesoporous Al-MCM-48, where the cubic phase belongs to a Ia3d space group symmetry [30, 31]. The d_{220} and d_{211} reflections were observed at approximately 2θ values of 2.6 and 3, respectively. The calculation of the ratio d_{220}/d_{211} for Al-MCM-48 was 0.86, which is typical of cubic symmetry [30-32].

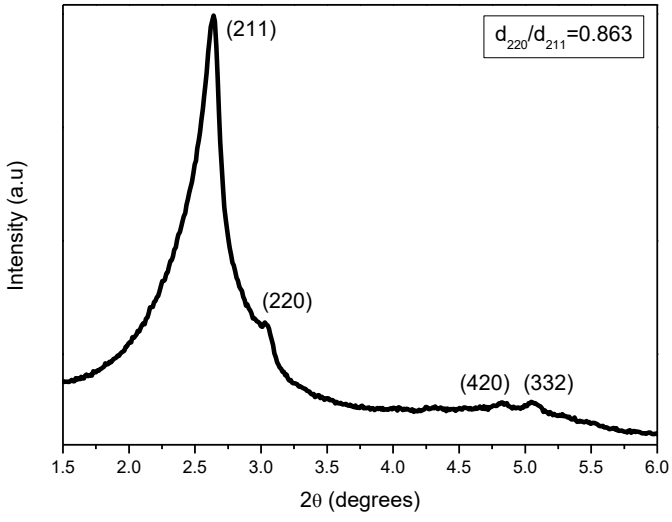

Figure1. SAXS pattern of Al-MCM-48 support

Adsorption-desorption isotherms of N_2 at -196 ºC were determined in order to study textural properties of Al-MCM-48 and Ru/Al-MCM-48 and results are presented in Figure 2 and Table 1. It is observed that in both cases, the materials presented isotherms

which have the typical features of the mesoporous silica materials and can be ascribed to type IV consistent with the IUPAC classification [33], with a sharp increase in quantity adsorbed at approximately relative pressures (P/P_0) between 0.15 and 0.3. This fact is associated with capillary condensation in the mesostructured channels of Al-MCM-48. Capillary condensation phenomenon is typical from mesoporous materials and it is indicative of the uniformity of the porous structure [34]. This was confirmed in pore size distribution in Figure 2, where both Al-MCM-48 and Ru/Al-MCM-48 shown unimodal and narrow pore size distributions centered at approximately 20 Å. Moreover, it was observed that both samples exhibit a type-H3 hysteresis loop at P/P_0 = 0.45 – 0.9, which can be associated to the particular and three-dimensional pore structure of this kind of materials [35].

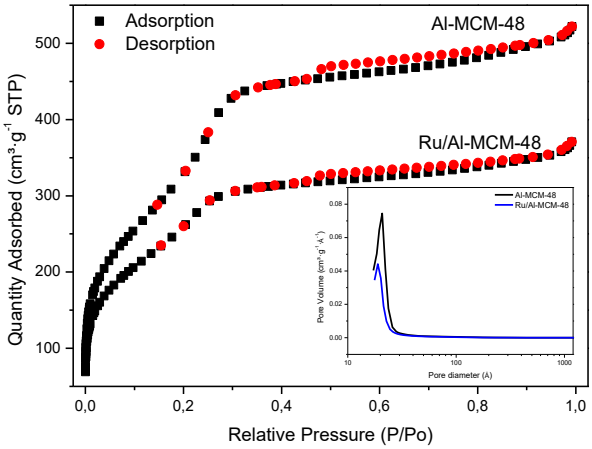

Figure 2. N_2 adsorption – desorption isotherms and pore size distributions of Al-MCM-48 and Ru/Al-MCM-48.

Bet surface area and total pore volume of Al-MCM-48 were 1352 $m^2 \cdot g^{-1}$ and 0.81 $cm^3 \cdot g^{-1}$, respectively. Similar results were obtained for Al-MCM-48 by Meng et al [36]. A slight decrease in the specific surface area and pore volume of Ru/Al-MCM-48 are noticed after the deposition of ruthenium into the pores of Al-MCM-48, from 1352 to 1028 $m^2 \cdot g^{-1}$ and from 0.81 to 0.57 $cm^3 \cdot g^{-1}$, respectively. This fact is associated to the partial blocking of the mesoporous network of the Al-MCM-48. The partial blockage of the porous network resulted in a slight alteration of the pore diameter from 2.5 to 2.7 nm. The ruthenium metal loading of Ru/Al-MCM-48 was 3.5 %, determined by AA. Regarding acidity of the prepared materials, Al-MCM-48 and Ru/Al-MCM-48 shown 0.842 and 1.219 $mmol_{NH3} \cdot g^{-1}$, determined by TPD-NH_3. Acidity value of Al-MCM-48 is attributed to the presence of weak acid hydroxyl groups and tri-coordinated aluminum

in the mesoporous framework [36]. Then, after the deposition of ruthenium into the pores of Al-MCM-48, a noticeable increase of acidity value was detected in Ru/Al-MCM-48, due to the high tendency of ruthenium atoms to adsorb ammonia[37].

Table 1. Textural properties, ruthenium loading, ruthenium particle size and acidity of Al-MCM-48 and Ru/Al-MCM-48.

Catalyst	Ru (%)	S_{BET} ($m^2 \cdot g^{-1}$)	V_{pore} ($cm^3 \cdot g^{-1}$)	$Ø_{pore}$ (nm)	Ru (nm)	Acidity ($mmol_{NH3} \cdot g^{-1}$)
Al-MCM-48	-	1352	0.81	2.5	-	0.84
Ru/Al-MCM-48	3.5	1028	0.57	2.7	2.0[a] / 1.9[b]	1.22

[a] Ru surface-area weighted diameter from TEM images.[b]Ru crystallite size from XRD analysis.

H_2-TPR profile for Ru/Al-MCM-48 is shown in Figure 3(A) in order to discuss the reducibility of the different ruthenium species present on Al-MCM-48. H_2-TPR profile exhibits two reduction peaks at ca. 135 ºC and 175 ºC for Ru/Al-MCM-48, suggesting the existence of two different types of ruthenium nanoparticles. The narrower and more intense peak at ca. 135 ºC can be ascribed to the reduction of agglomerates or not well-distributed crystallites of $RuCl_3$ over Al-MCM-48 to Ru^0. The second peak at ca. 173 ºC can be attributed to the reduction of small-sized $RuCl_3$ crystallites, which are well-distributed into the porous structure of Al-MCM-48. The existence of smaller crystallites, which have higher metal-support interaction is associated to higher reduction temperatures. According to the H_2-TPR profile, Ru/Al-MCM-48 was activated at 150 ºC under hydrogen atmosphere for 1 h in order to assure the proper reduction of all the ruthenium species. In previous works, ruthenium was deposited over MCM-48 and a single reduction peak centered at ca. 125 ºC was obtained, attributed to the reduction of well-dispersed Ru^{3+} to Ru^0 [8, 9]. Vanama et al. reported H_2-profiles of Ru/MCM-41 for different ruthenium metal loadings (1-6 wt.%). Ru/MCM-41 with a 4 wt.% of Ru showed a main reduction peak at ca. 200 ºC related to the complete reduction of $RuCl_3$ species [38].

XRD patterns for the bare support, Ru/Al-MCM-48 before reduction and Ru/Al-MCM-48 after reduction are shown in Figure 3(B). No diffraction peaks were observed at the range of 2θ from 30 º to 80 º for Al-MCM-48 and Ru/Al-MCM-48 before

reduction, as it was expected. After the reduction under hydrogen atmosphere, a broad metallic diffraction peak related to Ru^0 (101) was observed at $2\theta = 43.8\ ^o$ for Ru/Al-MCM-48, corresponding to the presence of Hexagonal Close Packing (HCP) Ru^0 nanoparticles. This fact confirms the correct reduction of Ru/Al-MCM-48 (Figure 3(B)). In addition, the small and wide metallic ruthenium peak suggests the existence of small Ru^0 nanoparticles well-distributed into the porous structure of Al-MCM-48. This fact is in good agreement with the calculations based on Scherrer equation, which determined the presence of Ru^0 nanoparticles with a crystallite size of 1.9 nm.

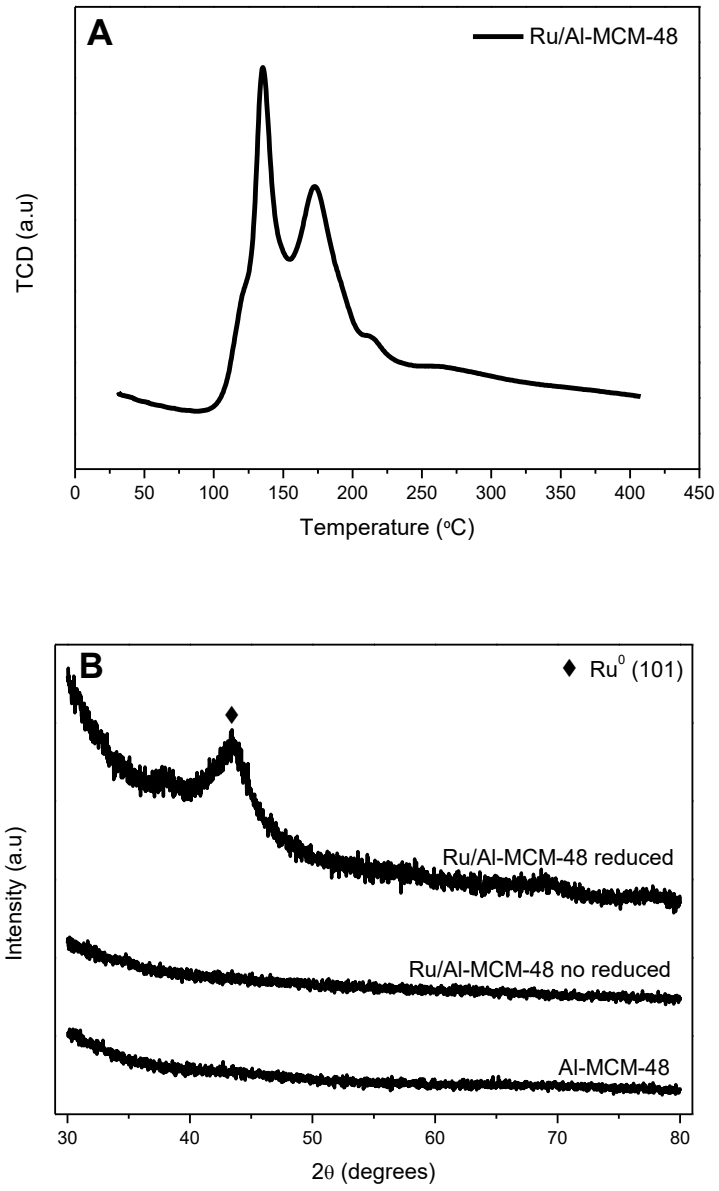

Figure 3. (A) H_2-TPR of Ru/Al-MCM-48 and **(B)** XRD patterns of Al-MCM-48, Ru/Al-MCM-48 and activated Ru/Al-MCM-48.

TEM-images and ruthenium nanoparticle size distribution for Ru/Al-MCM-48 are presented in Figure 4. Two different areas were observed by TEM for Ru/Al-MCM-48: a) Regions where ruthenium nanoparticles are finely distributed into the pores of Al-MCM-48 (Figure 4(A)) and b) other areas where agglomerates of ruthenium nanoparticles were detected in the outer surface of the support. This fact confirms a correlation between TEM images and reduction peaks from H_2-TPR, where the ruthenium agglomerates presented in the outer surface of Al-MCM-48 are related to the reduction peak at lower temperature in H_2-TPR, while the well-distributed ruthenium nanoparticles are associated to the second reduction peak observed at higher temperatures. In addition, a counting of ruthenium nanoparticles from TEM-images was developed and the ruthenium nanoparticle size distribution is presented in Figure 4(C). The histogram showed a narrow ruthenium nanoparticle size distribution in the range 1.2 – 2.5 nm, which is related to isolated ruthenium nanoparticles. Surface-area weighted diameter of 2.0 nm was obtained from calculations based on equation 1, which is similar to that obtained for Ru/Al-MCM-48 by Scherrer equation (Table 1).

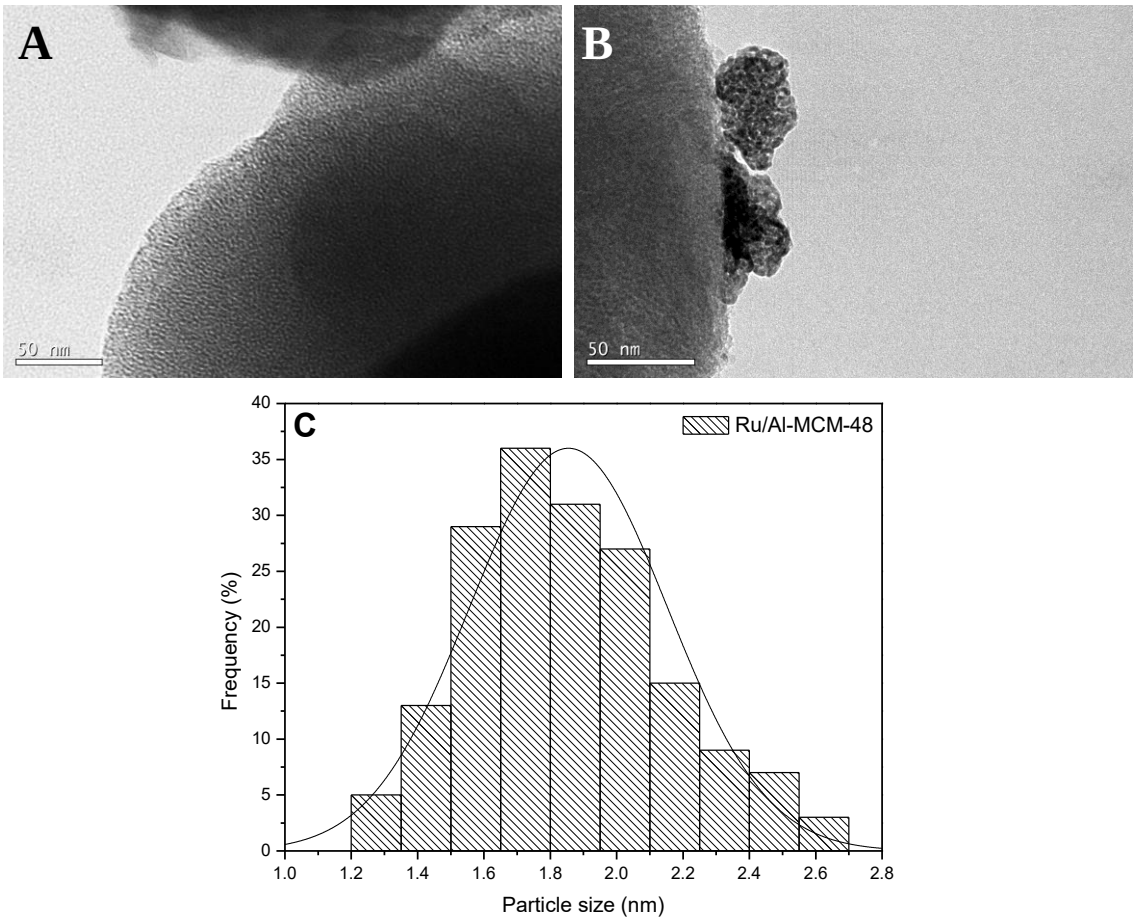

Figure 4. (A) (B) TEM images and **(C)** ruthenium particle size distribution of Ru/Al-MCM-48.

3.2. CATALYTIC HYDROGENOLYSIS OF CELLOBIOSE

The catalytic performance of Ru/Al-MCM-48 to convert cellobiose towards hexitols is presented. Different experimental parameters such as temperature, pressure and reaction time were studied in order to maximize the production of hexitols.

Kinetic tests using Ru/Al-MCM-48 were carried out under 5 MPa of H_2 at temperatures between 140 and 180 ºC and the main results are presented in Figure 5. Conversions of cellobiose were 22 %, 41 % and 73 % at 140 ºC, 160 ºC and 180 ºC and 1 min of reaction time, respectively. Thus, the increase of reaction temperature from 140 ºC to 180 ºC resulted in an important increase of the conversion of cellobiose at the initial reaction stage, as expected. Total conversion of cellobiose was achieved after 20, 10 and 5 min, at 140 ºC, 160 ºC, 180 ºC, respectively. In general terms, according to the results presented in Figure 5, cellobiose is rapidly hydrogenated to cellobitol which is further hydrolyzed into sorbitol. Therefore, cellobitol was the main reaction intermediate during cellobiose hydrolysis/hydrogenation over Ru/Al-MCM-48. No glucose issued from hydrolysis of cellobiose could be detected in any case. Nevertheless, hydrolysis of cellobiose into D-glucose cannot be discarded. Low amounts of D-glucose can be obtained, which are rapidly hydrogenated into sorbitol and due to this fact, D-glucose cannot be observed in the chromatograms. This fact was also reported by Deng et al [23], where only traces of D-glucose could be observed at the initial reaction stage using Ru/CNT as catalyst with lower ruthenium nanoparticle sizes than 12 nm. The highest yields to cellobitol were reached around 82 %, 48 % and 34 % at 140 ºC, 160 ºC and 180 ºC, respectively. Therefore, a decreased in the maximum yield to cellobitol was observed when temperature is increasing, since cellobitol is less stable at higher temperatures and it is faster converted to sorbitol by hydrolysis process as clearly observed on the figures [24]. Moreover, once that maximum in yield to cellobitol was achieved at each temperature, yield to cellobitol decreased as a result of the conversion of cellobitol to sorbitol. Then, consecutive isomerization processes of the so obtained sorbitol enhanced the production of mannitol and iditol. Other byproducts from sorbitol dehydration such as 1,4-sorbitan and isosorbide were also detected in very low concentrations at temperatures higher than 140 ºC (Figure 5B and 5C) [39]. Regardless, the temperature, the mass balance was higher than 98 %.

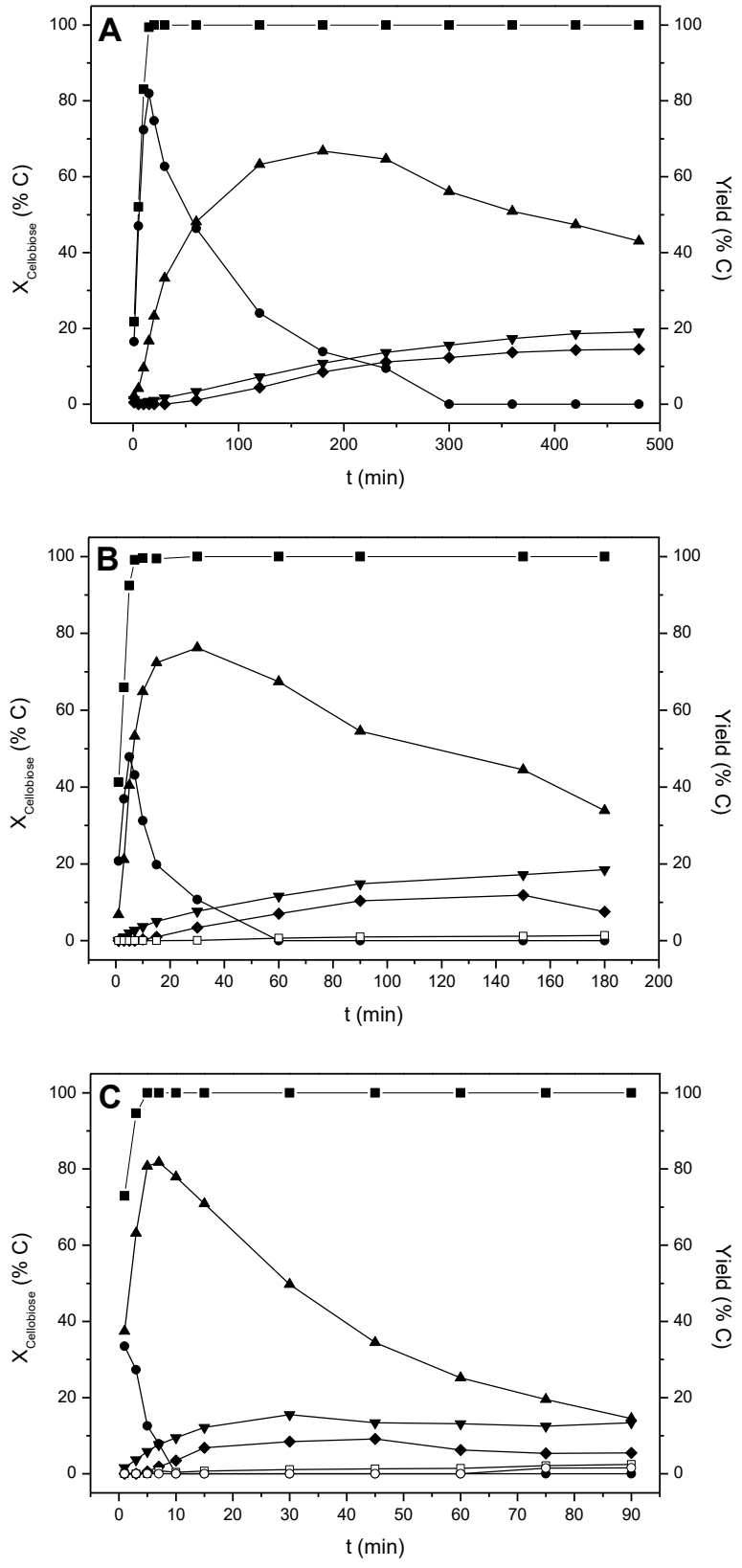

Figure 5. Kinetics of hydrogenolysis of cellobiose at **(A)** 140 ºC, **(B)** 160 ºC, **(C)** 180 ºC and 5 MPa H_2.■ Cellobiose, ● Cellobitol, ▲ Sorbitol, ▼ Mannitol, ♦ Iditol, □ 1,4 – Sorbitan and ○ Isosorbide.

Table 2. Maximum of yield to hexitols, composition of the final product and mass balances at different temperatures.

			Yield (% C)						
T (ºC)	**t (min)**	**X_C [a] (% C)**	**Cellobitol**	**Sorbitol**	**Mannitol**	**Iditol**	**Hexitols**	**1,4-Sorbitan**	**MB (% C)**
140	240	100	9.5	64.7	13.6	11.1	89.4	0	98.9
160	30	100	10.7	76.3	7.7	3.5	87.5	0.1	98.3
180	7	100	7.9	81.8	7.7	1.9	91.4	0.7	100

The influence of the temperature at 5 MPa of H_2 and after 5 min of reaction on the conversion of cellobiose and selectivity to hexitols is presented in Figure 6A. Conversion of cellobiose was around 52 % at 140 ºC, achieving a yield to hexitols around 5 %. A yield of cellobitol around 47 % was detected in the final product. Thus, low yield to hexitols at 140 ºC, 5 MPa of H_2 and 5 min is attributed to the high stability of the intermediate cellobitol at low temperatures. Conversion of cellobiose improved up to 92 % by increasing the temperature at 160 ºC. After 5 min of reaction time, at 5 MPa of H_2 and 160 ºC around 42 % of hexitols were observed as a result of the hydrolysis of cellobitol, however an important yield to cellobitol around 48 % was detected yet in the final product. Finally, total conversion of cellobiose was achieved after 5 min, at 5 MPa of H_2 and 180 ºC. A significant yield to hexitols of 87 % was reached and 12.5 % of cellobitol remained in the final product. According to all these results given in Figure 6A, it is possible to conclude that higher temperatures have a positive effect in order to maximize the yield to hexitols at a certain time, since more cellobitol can be hydrolyzed at higher temperatures. In all the cases, sorbitol was the main product of hexitols fraction in the final product, however; other products such as mannitol and iditol were observed in lower concentrations. Isomerization of sorbitol was favored at higher temperatures, thus higher yields to mannitol and iditol were observed when temperature was increasing. This fact was also observed comparing the data at similar conversions. The maximum yield to hexitols, which was calculated as the sum of the yields of sorbitol, mannitol and iditol was around 89 % at 140 ºC and 240 min, 88 % at 160 ºC and 30 min and 91 % at 180 ºC and 7 min (Table 2).In spite of obtaining a similar maximum of hexitols between 88 % and 91 % at different

temperatures, the composition of the final product was changing. When temperature increases from 140 ºC to 180 ºC, the maximum in the yield of hexitols was reached at lower reaction times (Table 2). The greater conversion of cellobitol at higher temperatures allowed to obtain higher yields to sorbitol and low reaction times avoided further degradation reactions of sorbitol. Thus, at higher temperatures and lower reaction times, the yield to sorbitol increased and the yield to mannitol and iditol decreased.

The influence of pressure of hydrogen in the range between 3 and 5 MPa was also studied in the present work and the main results are presented in Figure 6B. Working under higher pressures did not demonstrate an important influence in the conversion of cellobiose. Conversion of cellobiose was around 99 % at 3 MPa, while it was 100 % at higher pressures. Nevertheless, pressure had a big influence in the reaction pathway converting cellobiose to hexitols. At 3 MPa of H_2, glucose was the unique intermediate of the reaction, while cellobitol was not detected (Figure 7A). At 4 MPa H_2, glucose was the main intermediate of the reaction, while only low amounts of cellobitol were detected (Figure 7B). However, working at 5 MPa of H_2 cellobitol was the main intermediate and glucose was not detected in the final product (Figure 7C). Therefore, it can be concluded that at pressures lower than 5 MPa, concentration of hydrogen is limiting hydrogenation of cellobiose to cellobitol enhancing hydrolysis of cellobiose to glucose, while at 5 MPa of H_2 hydrogenation of cellobiose to cellobitol is favored, avoiding hydrolysis of cellobiose to glucose. In general, higher hydrogen pressures demonstrated a significant influence promoting greater yields to hexitols. Yield to hexitols was 76 % at 3 MPa of H_2, 90 % at 4 MPa of H_2 and 91 % at 5 MPa of H_2 after 7 min of reaction time. The lower yield to hexitols obtained at 3 MPa compared to those obtained at higher pressures, can be attributed to mass transfer limitations from gas to liquid phase. At lower pressures the availability of hydrogen in the reaction media is influencing the reaction mechanism. This fact is in good agreement with the experimental results reported by Negahdar et al [24]. They stated the effect of pressure in the catalytic conversion of cellobiose to sorbitol and according to their experimental results the authors concluded that a kinetic control of the reaction can be surely assumed at a stirring rate above 750 rpm and pressure of hydrogen above 3.5 MPa and low concentrations of cellobiose in the solution. Therefore, working at higher hydrogen pressures than 3.5 MPa under the presented experimental conditions in this work,

hydrolysis/hydrogenation of cellobiose is not limited. Moreover, higher hydrogen pressures favored isomerization reactions of sorbitol to mannitol and iditol, increasing their yield in the final product. According to the aforementioned experimental results the optimal conditions for conversion of cellobiose to maximize the yield to hexitols (91 %) were selected at 180 ºC, 7 min and 5 MPa of H_2.

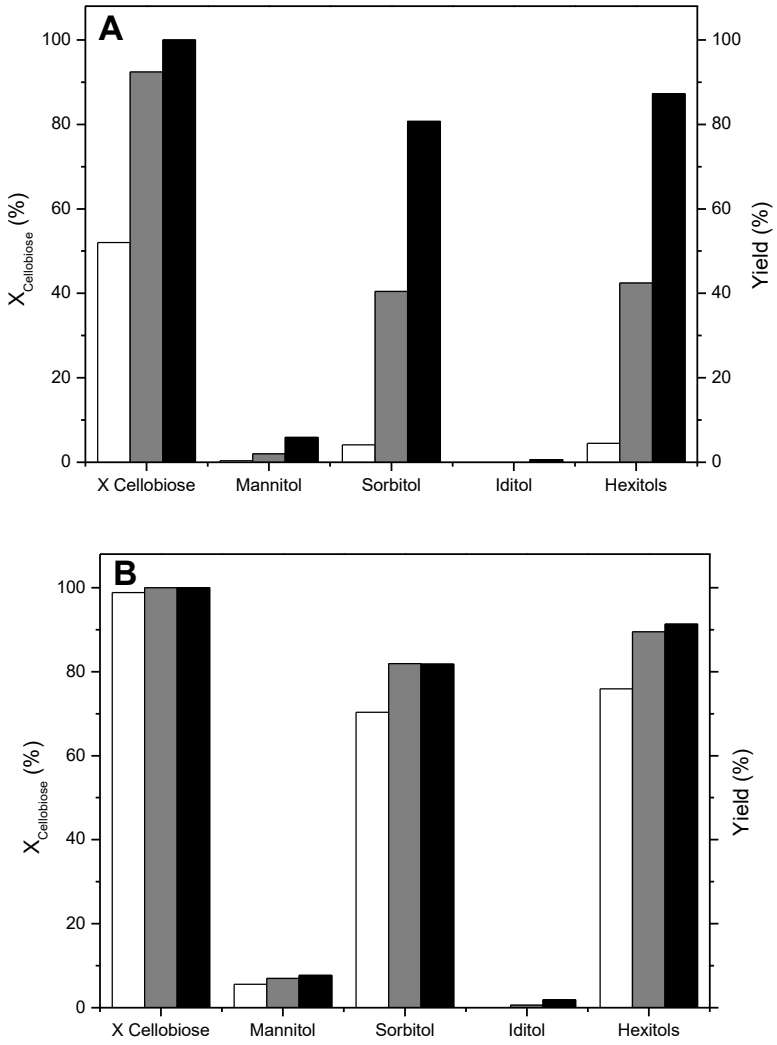

Figure 6. Effect of temperature **(A)** and pressure **(B)** in the conversion of cellobiose and yield to hexitols over Ru/Al-MCM-48. **(A)** T = 140 ºC, T = 160 ºC, T = 180 ºC, 5 MPa H_2 and 5 min. **(B)** P = 3 MPa H_2, P = 4 MPa H_2, P = 5 MPa H_2, 180 ºC and 7 min.

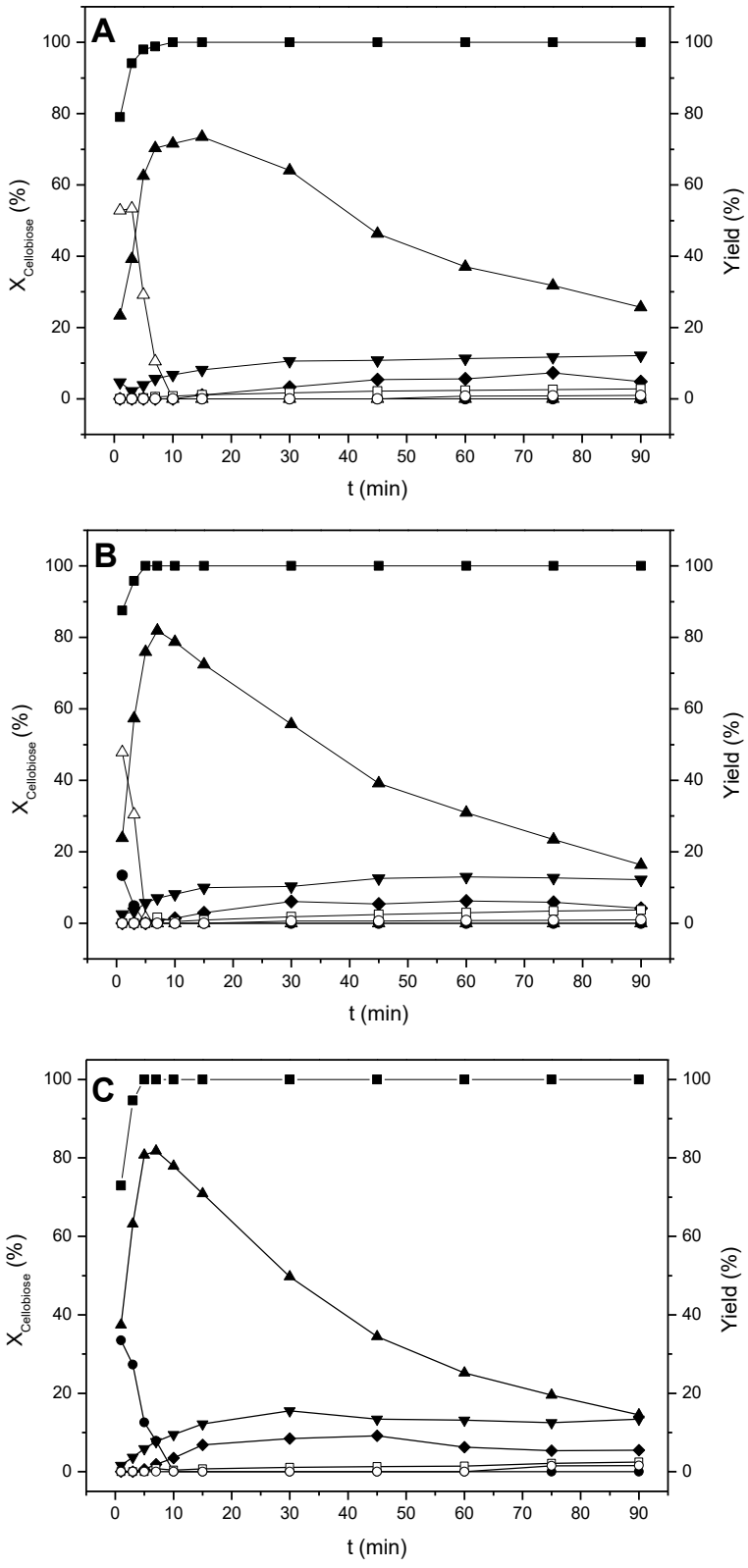

Figure 7. Kinetics of hydrogenolysis of cellobiose at **(A)** 3 MPa of H_2, **(B)** 4 MPa of H_2, **(C)** 5 MPa of H_2 and 180 ºC. ■ Cellobiose, ● Cellobitol, ∆ Glucose, ▲ Sorbitol, ▼ Mannitol, ♦ Iditol, □ 1,4 – Sorbitan and ○ Isosorbide.

Activity results obtained in this work are compared with those previously reported by other authors (Table 3). In this research field, it is typical to find many catalytic data in the literature in terms of yield to sorbitol. However, since the specific reaction rate is the most meaningful parameter in order to compare the catalytic activity of different materials, in addition to consider yield to sorbitol, specific reaction rate was also calculated in Table 3. Niu et al. reported the one-pot conversion of cellobiose to hexitols over zirconia-modified Ru on SBA-15 [25]. In that work, a yield to sorbitol of 4 % was achieved at 140 ºC, 5 MPa and 15 min over Ru/SBA-15 (1.7 wt.%). Under the same experimental conditions Ru/Al-MCM-48 demonstrated a highest yield to sorbitol around 17 %. In addition, the specific reaction rate of Ru/Al-MCM-48 at 140 ºC, 5 MPa and 15 min was a 29 % higher than that obtained by Ru/SBA-15. In the same research work, Niu et al. tested a Ru on zirconia-modified SBA-15 (1.8 wt.%), which showed a good catalytic behavior, achieving a yield to sorbitol of 15 % at 140 ºC, 5 MPa and 15 min, comparable to that obtained in this work under similar experimental conditions. Modification with Zr on SBA-15 improved the number of acid sites enhancing the production of sorbitol in comparison with Ru/SBA-15. Ru/Zr-SBA-15 revealed a specific reaction rate of 1.59 $mol_{Sorbitol} \cdot mol_{Ru}^{-1} \cdot min^{-1}$, which is around 2.1 times higher than that obtained for Ru/Al-MCM-48 at 140 ºC, 5 MPa of H_2 and 15 min. Deng et al. tested Ru/CNT (1 wt.%) at 185 ºC, 5 MPa and 180 min achieved a yield to sorbitol of 87 % [23]. At comparable experimental conditions of pressure and temperature (180 ºC and 5 MPa), Ru/Al-MCM-48 showed a slightly lower yield to sorbitol of 82 % after 7 min of reaction time. Ru/Al-MCM-48 showed a specific reaction rate of 7.89 $mol_{Sorbitol} \cdot mol_{Ru}^{-1} \cdot min^{-1}$, while it was 0.98 $mol_{Sorbitol} \cdot mol_{Ru}^{-1} \cdot min^{-1}$ for Ru/CNT. Comparing the catalytic activity of both materials, the results demonstrated that Ru/Al-MCM-48 outperformed the reaction rate obtained by Ru/CNT around 8 times. Moreover, other authors reported catalytic systems combining homogeneous or heteropolyacids with supported Ru-based catalysts with this purpose. Negahdar et al. studied the conversion of cellobiose to sorbitol with a catalytic system consisting of silicotungstic acid (HPA) and a supported ruthenium catalyst (Ru/C, 5 wt.%, Sigma Aldrich). At 160 ºC, 5 MPa and 70 min a yield to sorbitol of 68 % was obtained. Ru/Al-MCM-48 presented in this work demonstrated approximately 3.7 times higher specific reaction rate under comparable reaction conditions (160 ºC, 5 MPa and 30 min). In addition, the combination of Ru/C + HPA was not enough to improve the conversion rate of cellobiose compare to that obtained in the present work. Ru/Al-MCM-48 was

able to achieved total conversion of cellobiose after 15 min of reaction time at 160 ºC and 5 MPa, while Ru/C + HPA reached 100 % of cellobiose conversion after 70 min under similar reaction conditions. Zhang et al. examined Ru/C catalyst (3.6 wt.% Ru) for the direct conversion of cellobiose to sorbitol in 0.05 wt.% H_3PO_4 solution [26]. In that work a yield to sorbitol around 87 % was reached, showing a specific reaction rate of 1.58 $mol_{Sorbitol} \cdot mol_{Ru}^{-1} \cdot min^{-1}$ at 170 ºC, 3 MPa of H_2 and 60 min. The specific reaction rate related to the combination of Ru/C + H_3PO_4 was sligthly lower than that obtained by Ru/Al-MCM-48 at lower temperature (160 ºC) in the present work.

Table 3. Conversion of cellobiose into sorbitol and specific reaction rate

Catalyst	Ru (%)	T (ºC)	t (min)	$Y_{Sorbitol}$ (%)	Activity ($mol_{Sorbitol} \cdot mol_{Ru}^{-1} \cdot min^{-1}$)	Ref.
Ru/Al-MCM-48	3.5	140	15	17	0.75	This work
		160	30	76	1.72	
		180	7	82	7.89	
Ru/C + HPA	5	160	70	68	0.46[a]	[24]
Ru/C + H_3PO_4	3.6	170	60	87	1.58[a]	[26]
Ru/SBA-15	1.7	140	15	4	0.46[a]	[25]
Ru/Zr-SBA-15	1.8	140	15	14.6	1.59[a]	[25]
Ru/CNT	1	185	180	87	0.98[a]	[23]

Ru/Al-MCM-48 was recovered after different experiments in order to study the recycling and reusability of the catalyst in the hydrolysis/hydrogenation of cellobiose at 180 ºC, 5 MPa and 7 min. After one cycle of reaction the conversion of cellobiose was around 92 %, while using the fresh catalyst (reduced) complete conversion for cellobiose was reached. In addition, the yield of hexitols presented in the final product after one cycle of reaction was much lower (25 % hexitols) than that achieved over the fresh catalyst (91 % hexitols). In addition, glucose was detected as intermediate (3 % yield of glucose), but cellobitol was the main intermediate presenting a yield around 60 % in the final product. According to all these experimental results, it is suggested that metal phase of the catalyst could be modified after one cycle of reaction. This fact was

confirmed by XRD (Figure 8), where an increase of the crystallite size of Ru increased from 1.9 to 5.5 nm due to sintering of ruthenium even after very short reaction time. The detected increase in ruthenium crystallites suggested a considerably decrease in the active surface of the metal [40], which is related to the worse catalytic behavior of Ru/Al-MCM-48 after one cycle of reaction.

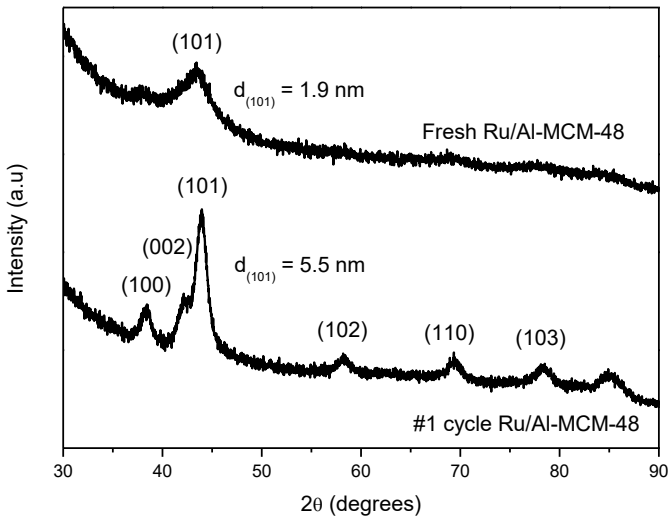

Figure 8. Recycling of the catalyst at 180 ºC, 5 MPa H_2 and 7 min (1 cycle). XRD of fresh Ru/Al-MCM-48 and 1 cycle Ru/Al-MCM-48.

3.3. KINETIC MODELLING

Scheme 1 shows the proposed reaction pathway for the hydrolytic hydrogenation of cellobiose into hexitols over Ru/Al-MCM-48. First, cellobiose is hydrogenated into cellobitol (k_1), which is subsequently hydrolyzed into sorbitol (k_2). The so obtained sorbitol can be isomerized into mannitol (k_3) and iditol (k_4) and both of them can be further converted into degradation products (k_5 and k_6). Other by-products from dehydration reaction of sorbitol, such as isosorbide and 1,4 – sorbitan, are not included in the proposed model since they were only detected in very low concentrations in some of the presented experiments under the applied experimental conditions.

A homogeneous catalytic kinetic model was proposed, by considering carbon mass balance close to 100% (as observed in Table 2)., Given the large excess of hydrogen and the low concentration of cellobiose fed in the initial solution, all reaction pathways were considered to be pseudo-first order. Some assumptions were taken into account in the development of the proposed model: a) catalyst deactivation is not taking place during the catalytic tests and b) reaction products are weakly adsorbed on the active

surface of the catalyst. Negahdar et al. assumed similar statements for their kinetic models for hydrogenation reactions of cellobiose [24]. The model includes the effect of reaction temperature (140 ºC, 160 ºC and 180 ºC).

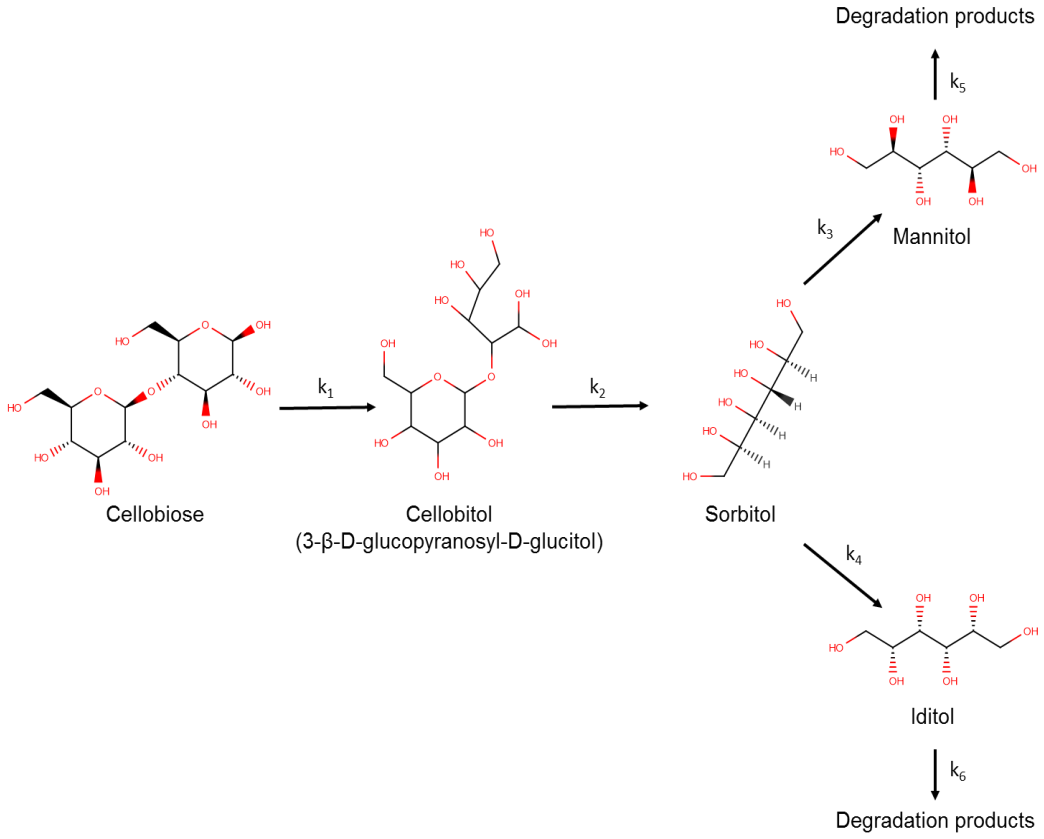

Scheme 1. Proposed reaction network for the catalytic conversion of cellobiose towards hexitols over Ru/Al-MCM-48

Diffusional constrains were evaluated to ensure that all reactions were conducted in the kinetic regime. Firstly, as it was demonstrated in the preliminary experiments (not shown) and stated by other authors [24], a stirring rate of 1200 rpm prevents reactions from external diffusional constrains. Then, the Weisz-Prater criterion was used for the evaluation of internal diffusional constrains. The Weisz-Prater number ($N_{W\text{-}P}$) should meet the following equation (5):

$$N_{W-P} = r \cdot \frac{R_p^2}{D_{eff} \cdot C_S} \leq 0.3 \qquad (5)$$

Being R_p the catalyst average particle size (35 μm), r the measured reaction rate and C_S the surface concentration (equal to the concentration in the reaction medium as there were no external diffusion limitations) [41]. The initial cellobiose concentration and

consumption rate were respectively set as C_S and r. On the other hand, the effective diffusivity was calculated as follows in equation 6:

$$D_{eff} = D \cdot \frac{\varepsilon}{\tau} \quad (6)$$

being D the bulk diffusivity of cellobiose-water and hydrogen-water in each case. The tortuosity (τ) and porosity (ε) values were not available, so they were set as 4 and 0.5, respectively [42]. Bearing in mind all these points and the calculated data in Table 4, the most restrictive $N_{W\text{-}P}$ value (for the mixture hydrogen-water and the reaction at 180 ºC) was 0.19, so internal diffusional constrains could be considered negligible.

According to the proposed reaction network presented in Scheme 1, the following differential equations (Eq. 7 – Eq. 11) are proposed for the different compounds as a function of time.

$$\frac{dC_{Cellobiose}}{dt} = -k_1 \cdot C_{Cellobiose} \quad (7)$$

$$\frac{dC_{Cellobitol}}{dt} = k_1 \cdot C_{Cellobiose} - k_2 \cdot C_{Cellobitol} \quad (8)$$

$$\frac{dC_{Sorbitol}}{dt} = 2 \cdot k_2 \cdot C_{Cellobitol} - k_3 \cdot C_{Sorbitol} - k_4 \cdot C_{Sorbitol} \quad (9)$$

$$\frac{dC_{Mannitol}}{dt} = k_3 \cdot C_{Sorbitol} - k_5 \cdot C_{Mannitol} \quad (10)$$

$$\frac{dC_{Iditol}}{dt} = k_4 \cdot C_{Sorbitol} - k_6 \cdot C_{Iditol} \quad (11)$$

Moreover, reaction rate constants in the present work are given by the orthogonalised Arrhenius equation as follow in equation 12:

$$k_j = \overline{A_j} \cdot \exp\left(-\frac{E_{aj}}{R} \cdot \left(\frac{1}{\theta}\right)\right) \quad (12)$$

$$\overline{A_j} = A_j \cdot exp\left(-\frac{E_{aj}}{R} \cdot \left(\frac{1}{\overline{T}}\right)\right) = \overline{k_j} \quad (13)$$

$$\frac{1}{\theta} = \frac{1}{T_j} - \frac{1}{\overline{T}} \quad (14)$$

Table 4. Derived calculations from the evaluation of internal diffusional constrains by the Weisz-Prater criterion.

Parameter	T = 140 ºC	T = 160 ºC	T = 180 ºC
Nw-p H_2-water	$7.2\cdot10^{-2}$	$1.4\cdot10^{-1}$	$1.9\cdot10^{-1}$
Nw-p cellobiose-water	$9.4\cdot10^{-3}$	$2.4\cdot10^{-2}$	$6.7\cdot10^{-2}$
D H_2-water ($m^2\cdot s^{-1}$)	$1.7\cdot10^{-9}$	$2.1\cdot10^{-9}$	$2.5\cdot10^{-9}$
D cellobiose-water ($m^2\cdot s^{-1}$)	$3.6\cdot10^{-9}$	$4.2\cdot10^{-9}$	$4.8\cdot10^{-9}$
D_{eff} H_2-water ($m^2\cdot s^{-1}$)	$2.2\cdot10^{-10}$	$2.6\cdot10^{-10}$	$3.1\cdot10^{-10}$
D_{eff} cellobiose-water ($m^2\cdot s^{-1}$)	$4.4\cdot10^{-10}$	$5.2\cdot10^{-10}$	$5.9\cdot10^{-10}$
Henry constant ($mol\cdot l^{-1}\cdot bar^{-1}$)	$4.9\cdot10^{-4}$	$4.6\cdot10^{-4}$	$4.4\cdot10^{-4}$

Table 5. Estimated kinetic parameter, standard deviation percentages and t-test

Parameter[a]	Estimate	|σ| (%)	t-test[b] / Meaningful?
$k_1(\bar{T})$	$4.80\cdot10^{-1}$	19.31	5.18 / YES
Ea_1	68.05	17.85	5.60 / YES
$k_2(\bar{T})$	$1.20\cdot10^{-1}$	2.14	46.69 / YES
Ea_2	136.37	0.14	722.29 / YES
$k_3(\bar{T})$	$4.30\cdot10^{-3}$	1.04	95.83 / YES
Ea_3	100.50	5.46	18.33 / YES
$k_4(\bar{T})$	$2.40\cdot10^{-3}$	1.11	90.48 / YES
Ea_4	88.25	2.39	41.87 / YES
$k_5(\bar{T})$	$9.50\cdot10^{-3}$	2.48	40.30 / YES
Ea_5	110.03	10.36	9.65 / YES
$k_6(\bar{T})$	$9.50\cdot10^{-3}$	2.48	40.30 / YES
Ea_6	110.03	10.36	9.65 / YES

[a] *$\bar{T}$=160 ºC, k_j ($\bar{T}$) / (min^{-1}) and Ea_j ($KJ\cdot mol^{-1}$).*

[b] *t (n-p, 1-α/2) = t (170, 0.95) = 1.98.*

Therefore, in the presented model; 12 parameters were estimated: 6 kinetic constants at the average temperature k_j (T = 160 ºC) and 6 activation energy values Ea_j. MATLAB was used for the numerical integration of the differential equations and for the estimation of the parameters by using non-linear regression. The experimental data was compared to those calculated with the kinetic model and the Residual Sum of Squares (RSS) to reach the optimal kinetic parameters. RSS was calculated as follows in equation 15:

$$RSS = \sum_{i=1}^{n} \left(C_{exp,i} - C_{calc,i}\right)^2 \qquad (15)$$

where n was related to the considered data set. The estimation of the parameter was carried out by means of a built-in option, i.e., by using the last estimation result as a starting point for the next one [43].

A comparison of calculated and experimental data versus reaction time profiles of cellobiose conversion to hexitols is presented in Figure 9(A, B, C) at 140, 160 and 180 ºC, respectively. The results so obtained, demonstrated that the model predicted fairly well the concentrations of the different components involved in the general reaction mechanism. The kinetic model fits better at higher reaction temperatures to the experimental data than at lower temperatures, where small deviations can be observed. Estimated reaction rate constants at the average temperature and the corresponding activation energy values are summarized in Table 5, as well as the standard deviation percentages and the results from Student's t-test (α = 0.1) for each parameter. At the average temperature ($\bar{T}$), the reaction rate constant (min^{-1}) for the catalytic hydrogenation of cellobiose into cellobitol is higher than that obtained for the subsequently hydrolysis of cellobitol towards sorbitol. This fact indicates that hydrolysis of cellobitol to sorbitol is the rate-determining step of the proposed reaction pathway. Negahdar et al. in their kinetic investigation of the hydrogenation of cellobiose over Ru/C + HPA also observed that hydrolysis steps showed lower reaction rates than those reached for the hydrogenation processes [24]. The rate constants related to further isomerization processes of sorbitol to mannitol (k_3) and iditol (k_4) and the subsequent degradation of both mannitol and iditol (k_5, k_6), respectively, are smaller compared to k_1 and k_2. Regarding activation energy values, hydrogenation of cellobiose to cellobitol was determined to be around Ea_1 = 68 $KJ \cdot mol^{-1}$.This activation energy

value compares well with that reported by Tan et al. for the hydrogenation of cellobiose to cellobitol over Ru/CNT (71 KJ·mol^{-1}) [44]. In addition, the activation energy of Ru/Al-MCM-48 was also lower than that reached by Ru/C in the research work of Negahdar et al. (76 KJ·mol^{-1})[24].Then, the activation energy value for the hydrolysis of cellobitol to sorbitol was Ea_2 = 136 KJ·mol^{-1}, which was higher than Ea_1. This fact is pointing out that hydrolysis of cellobitol to sorbitol is more complicated than the previous hydrogenation of cellobiose to cellobitol. Ea_2 achieved over Ru/Al-MCM-48 is in the same range of activation energies reported in the literature for the same reaction step (103 KJ·mol^{-1}) [24]. Activation energy presented by Negahdar et al. was lower than that presented in this work for the hydrolysis of cellobiose to sorbitol since the used HPA combined with Ru/C enhancing hydrolysis processes. The corresponding activation energies for isomerization of sorbitol were Ea_3 = 101 KJ·mol^{-1} and Ea_4 = 88 KJ·mol^{-1}, respectively. The highest activation energy for sorbitol isomerization into mannitol suggested a higher temperature sensitivity of this step compared to isomerization of sorbitol to iditol. Furthermore, the same activation energy values were obtained in both cases for the final conversion of mannitol and iditol to other degradation products (110 KJ·mol^{-1}). The Student's t-test results, lets the validation of the statistical significance of the different parameters estimated with the proposed model as it was previously reported by Lopez-González et al. [45]. Figure 9D shows the parity plot between estimated and experimental concentration of the different compounds involved in the proposed model. The so obtained results suggested that there were no correlation issues in the proposed kinetic model, whereas all the estimated parameters were statistically significant.

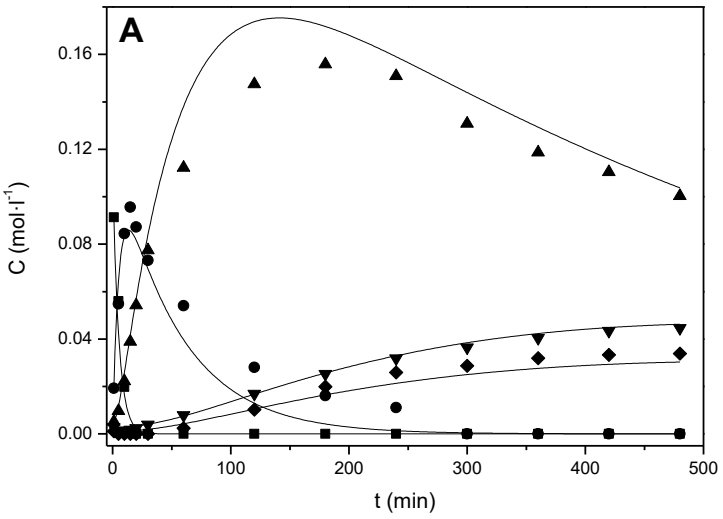

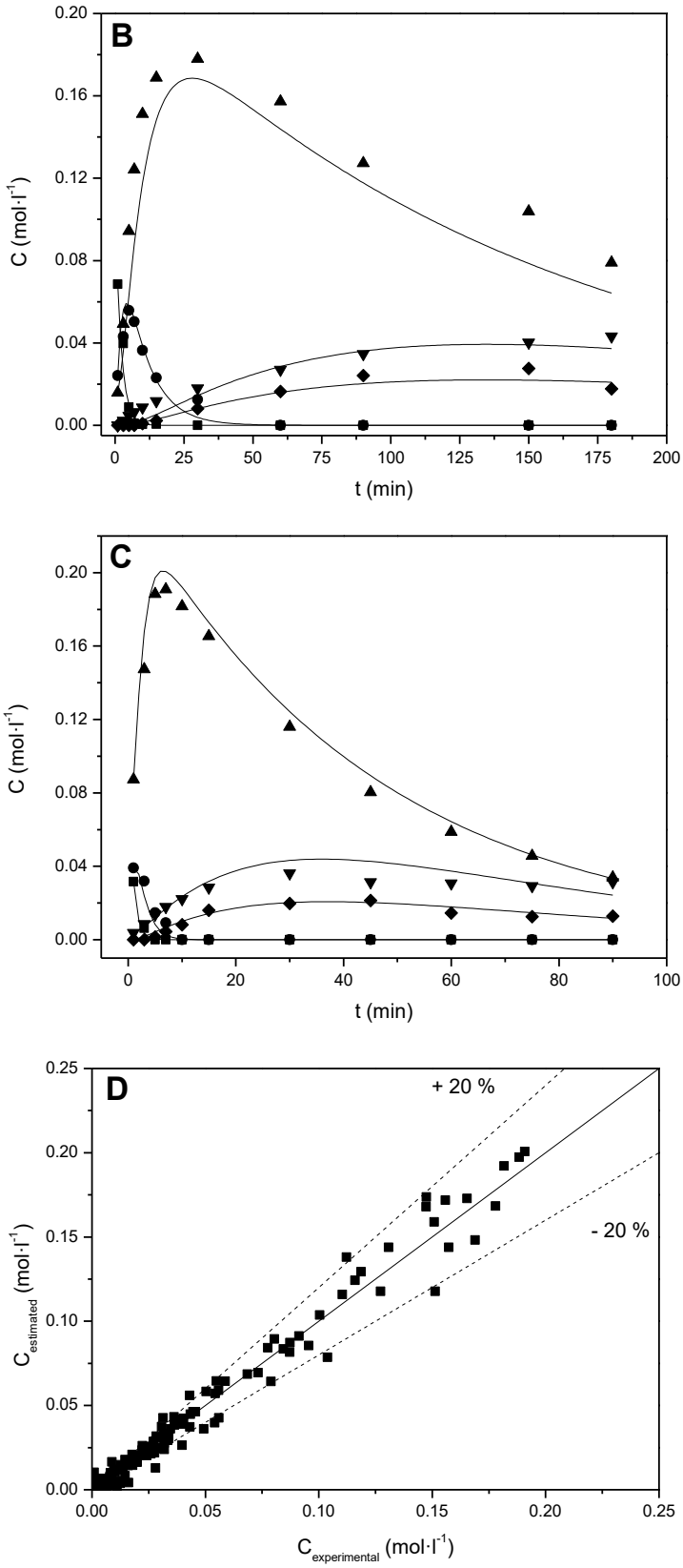

Figure 9. Experimental and calculated concentration vs. time profiles of cellobiose hydrogenolysis into hexitols. **(A)** T = 140 ºC**(B)** T = 160 ºC (**C)** 180 ºC and 5 MPa H_2.■ Cellobiose, ● Cellobitol, ▲ Sorbitol, ▼ Mannitol, ♦ Iditol and model. **(D)** Parity plot between experimental and estimated considerations.

4. CONCLUSIONS

The experimental results presented above support the following conclusions:

i) Ru/Al-MCM-48 with a 3.5 wt. % of Ru was prepared, showing a very narrow ruthenium nanoparticle size distribution with ruthenium nanoparticles around 2 nm. Ruthenium was properly reduced under H_2-TPR conditions.

ii) Cellobitol was the main intermediate in the conversion of cellobiose to hexitols. In addition, glucose was not detected as intermediate in any of the kinetic tests.

iii) A meaningful improvement of the final yield to hexitols was detected by increasing temperature from 140 ºC to 180 ºC. In addition, an important influence of hydrogen pressures in the yield to hexitols and the reaction mechanism was also noticed.

iv) Longer reaction times promoted further sorbitol hydrolysis/hydrogenation to isosorbide or 1,4-sorbitan and isomerization to mannitol and iditol.

v) Maximum yield to hexitol around 91 % was obtained at 180 ºC, 7 min and 5 MPa of H_2 over Ru/Al-MCM-48.

vi) Ru/Al-MCM-48 demonstrated higher activity in the one-pot catalytic conversion of cellobiose than other catalytic systems reported in the literature such as Ru/C + HPA, Ru/CNT, Ru/SBA-15 and Ru/C + H_3PO_4.

vii) A homogeneous catalytic kinetic model was developed for the hydrolysis/hydrogenation of cellobiose towards hexitols which predicted well the concentration of the different reactants and products involved in the proposed reaction pathway.

viii) Sintering of ruthenium was detected after one cycle of reaction, promoting a worse catalytic behavior than that observed for the fresh catalyst.

Acknowledgements

The authors gratefully acknowledge the Spanish Ministry, MINECO, and FEDER founds for the financial support of this project CTQ2015-64892-R (MINECO/FEDER). A. Romero thanks to the program of predoctoral scholarships from Junta de Castilla y León Government for his grant (E-47-2015-0062773).

References

1. Fukuoka, A. and P.L. Dhepe, *Catalytic Conversion of Cellulose into Sugar Alcohols.* Angewandte Chemie, 2006. **118**(31): p. 5285-5287.

2. Roman-Leshkov, Y., et al., *Production of dimethylfuran for liquid fuels from biomass-derived carbohydrates.* Nature, 2007. **447**(7147): p. 982-985.

3. Cortright, R.D., R.R. Davda, and J.A. Dumesic, *Hydrogen from catalytic reforming of biomass-derived hydrocarbons in liquid water.* Nature, 2002. **418**(6901): p. 964-967.

4. Xi, J., et al., *Direct conversion of cellulose into sorbitol with high yield by a novel mesoporous niobium phosphate supported Ruthenium bifunctional catalyst.* Applied Catalysis A: General, 2013. **459**: p. 52-58.

5. Serrano-Ruiz, J.C. and J.A. Dumesic, *Catalytic routes for the conversion of biomass into liquid hydrocarbon transportation fuels.* Energy & Environmental Science, 2011. **4**(1): p. 83-99.

6. Rogalinski, T., T. Ingram, and G. Brunner, *Hydrolysis of lignocellulosic biomass in water under elevated temperatures and pressures.* The Journal of Supercritical Fluids, 2008. **47**(1): p. 54-63.

7. Liang, G., et al., *Selective conversion of concentrated microcrystalline cellulose to isosorbide over Ru/C catalyst.* Green Chemistry, 2011. **13**(4): p. 839-842.

8. Romero, A., et al., *Supercritical water hydrolysis of cellulosic biomass as effective pretreatment to catalytic production of hexitols and ethylene glycol over Ru/MCM-48.* Green Chemistry, 2016. **18**(14): p. 4051-4062.

9. Romero, A., et al., *Conversion of biomass into sorbitol: Cellulose hydrolysis on MCM-48 and d-Glucose hydrogenation on Ru/MCM-48.* Microporous and Mesoporous Materials, 2016. **224**: p. 1-8.

10. Palkovits, R., et al., *Heteropoly acids as efficient acid catalysts in the one-step conversion of cellulose to sugar alcohols.* Chemical Communications, 2011. **47**(1): p. 576-578.

11. Chen, J., et al., *Conversion of Cellulose and Cellobiose into Sorbitol Catalyzed by Ruthenium Supported on a Polyoxometalate/Metal–Organic Framework Hybrid.* ChemSusChem, 2013. **6**(8): p. 1545-1555.

12. Kobayashi, H., H. Ohta, and A. Fukuoka, *Conversion of lignocellulose into renewable chemicals by heterogeneous catalysis.* Catalysis Science & Technology, 2012. **2**(5): p. 869-883.

13. Schlaf, M. and Z.C. Zhang. *Reaction Pathways and Mechanisms in Thermocatalytic Biomass Conversion I : Cellulose Structure, Depolymerization and Conversion by Heterogeneous Catalysts*. 2016.

14. Walker, L.P. and D.B. Wilson, *Enzymatic Hydrolysis of Cellulose Enzymatic hydrolysis of cellulose: An overview.* Bioresource Technology, 1991. **36**(1): p. 3-14.

15. Kassaye, S., K.K. Pant, and S. Jain, *Synergistic effect of ionic liquid and dilute sulphuric acid in the hydrolysis of microcrystalline cellulose.* Fuel Processing Technology, 2016. **148**: p. 289-294.

16. Jacobsen, S.E. and C.E. Wyman, *Cellulose and Hemicellulose Hydrolysis Models for Application to Current and Novel Pretreatment Processes*, in *Twenty-First Symposium on Biotechnology for Fuels and Chemicals: Proceedings of the Twenty-First Symposium on Biotechnology for Fuels and Chemicals Held May 2–6, 1999, in Fort Collins, Colorado*, M. Finkelstein and B.H. Davison, Editors. 2000, Humana Press: Totowa, NJ. p. 81-96.

17. Onda, A., T. Ochi, and K. Yanagisawa, *Selective hydrolysis of cellulose into glucose over solid acid catalysts.* Green Chemistry, 2008. **10**(10): p. 1033-1037.

18. Cantero, D.A., M. Dolores Bermejo, and M. José Cocero, *High glucose selectivity in pressurized water hydrolysis of cellulose using ultra-fast reactors.* Bioresource Technology, 2013. **135**: p. 697-703.

19. Dabbawala, A.A., D.K. Mishra, and J.-S. Hwang, *Selective hydrogenation of D-glucose using amine functionalized nanoporous polymer supported Ru nanoparticles based catalyst.* Catalysis Today, 2016. **265**: p. 163-173.

20. Lazaridis, P.A., et al., *d-Glucose hydrogenation/hydrogenolysis reactions on noble metal (Ru, Pt)/activated carbon supported catalysts.* Catalysis Today, 2015. **257, Part 2**: p. 281-290.

21. Ding, L.-N., et al., *Selective Transformation of Cellulose into Sorbitol by Using a Bifunctional Nickel Phosphide Catalyst.* ChemSusChem, 2010. **3**(7): p. 818-821.

22. Kobayashi, H., et al., *Synthesis of sugar alcohols by hydrolytic hydrogenation of cellulose over supported metal catalysts.* Green Chemistry, 2011. **13**(2): p. 326-333.

23. Deng, W., et al., *Conversion of cellobiose into sorbitol in neutral water medium over carbon nanotube-supported ruthenium catalysts.* Journal of Catalysis, 2010. **271**(1): p. 22-32.

24. Negahdar, L., et al., *Kinetic investigation of the catalytic conversion of cellobiose to sorbitol.* Applied Catalysis B: Environmental, 2014. **147**: p. 677-683.

25. Niu, Y., et al., *Ru supported on zirconia-modified SBA-15 for selective conversion of cellobiose to hexitols.* Microporous and Mesoporous Materials, 2014. **198**: p. 215-222.

26. Zhang, J., et al., *Direct conversion of cellobiose into sorbitol and catalyst deactivation mechanism.* Catalysis Communications, 2012. **29**: p. 180-184.

27. Li, J., et al., *Simultaneous hydrolysis and hydrogenation of cellobiose to sorbitol in molten salt hydrate media.* Catalysis Science & Technology, 2013. **3**(6): p. 1565-1572.

28. Kusema, B.T., et al., *Hydrolytic hydrogenation of hemicellulose over metal modified mesoporous catalyst.* Catalysis Today, 2012. **196**(1): p. 26-33.

29. Amorim, C. and M.A. Keane, *Palladium supported on structured and nonstructured carbon: A consideration of Pd particle size and the nature of reactive hydrogen.* Journal of Colloid and Interface Science, 2008. **322**(1): p. 196-208.

30. Kosslick, H., et al., *Acidity and Catalytic Behavior of Substituted MCM-48.* Journal of Catalysis, 1998. **176**(1): p. 102-114.

31. Danumah, C., et al., *Synthesis of macrostructured MCM-48 molecular sieves.* Microporous and Mesoporous Materials, 2001. **44–45**: p. 241-247.

32. Seshadri, S.K. and Y.S. Lin, *Synthesis and water vapor separation properties of pure silica and aluminosilicate MCM-48 membranes.* Separation and Purification Technology, 2011. **76**(3): p. 261-267.

33. Brunauer, S., et al., *On a Theory of the van der Waals Adsorption of Gases.* Journal of the American Chemical Society, 1940. **62**(7): p. 1723-1732.

34. Schumacher, K., et al., *Characterization of MCM-48 Materials.* Langmuir, 2000. **16**(10): p. 4648-4654.

35. Van Steen, E., L.H. Callanan, and M. Claeys, *Recent advances in the science and technology of zeolites and related materials: proceedings of the 14th International Zeolite Conference, Cape Town, South Africa, 25-30th April 2004*. Vol. 154. 2004: Elsevier.

36. Meng, J., et al., *Assembling of Al-MCM-48 supported H3PW12O40 mesoporous materials and their catalytic performances in the green synthesis of benzoic acid.* Materials Research Bulletin, 2014. **60**: p. 20-27.

37. Eliche-Quesada, D., et al., *Influence of the incorporation of palladium on Ru/MCM hydrotreating catalysts.* Applied Catalysis B: Environmental, 2006. **65**(1): p. 118-126.

38. Vanama, P.K., et al., *Vapor-phase hydrogenolysis of glycerol over nanostructured Ru/MCM-41 catalysts.* Catalysis Today, 2015. **250**: p. 226-238.

39. Li, J., et al., *Sorbitol dehydration into isosorbide in a molten salt hydrate medium.* Catalysis Science & Technology, 2013. **3**(6): p. 1540-1546.

40. Manyar, H.G., et al., *Deactivation and regeneration of ruthenium on silica in the liquid-phase hydrogenation of butan-2-one.* Journal of Catalysis, 2009. **265**(1): p. 80-88.

41. Vannice, M.A., *Kinetics of Catalytic Reactions*. 2005: Springer US.

42. M. E. Davis, R.J.D., *Fundamentals of Chemical Reaction Engineering*. 2002: McGraw-Hill.

43. Díaz, J.A., et al., *Kinetic modeling of the quasi-homogeneous oxidation of glycerol over unsupported gold particles in the liquid phase.* European Journal of Lipid Science and Technology, 2016. **118**(1): p. 72-79.

44. TAN, X., et al., *Mechanism and kinetics of cellobiose hydrogenation catalyzed by Ru/CNT.* CIESC Journal, 2010. **10**: p. 015.

45. López-González, D., et al., *Pyrolysis of three different types of microalgae: Kinetic and evolved gas analysis.* Energy, 2014. **73**: p. 33-43.

CHAPTER 5

CATALYTIC CONVERSION OF D-GLUCOSE INTO SHORT-CHAIN ALKANES OVER RU-BASED CATALYSTS

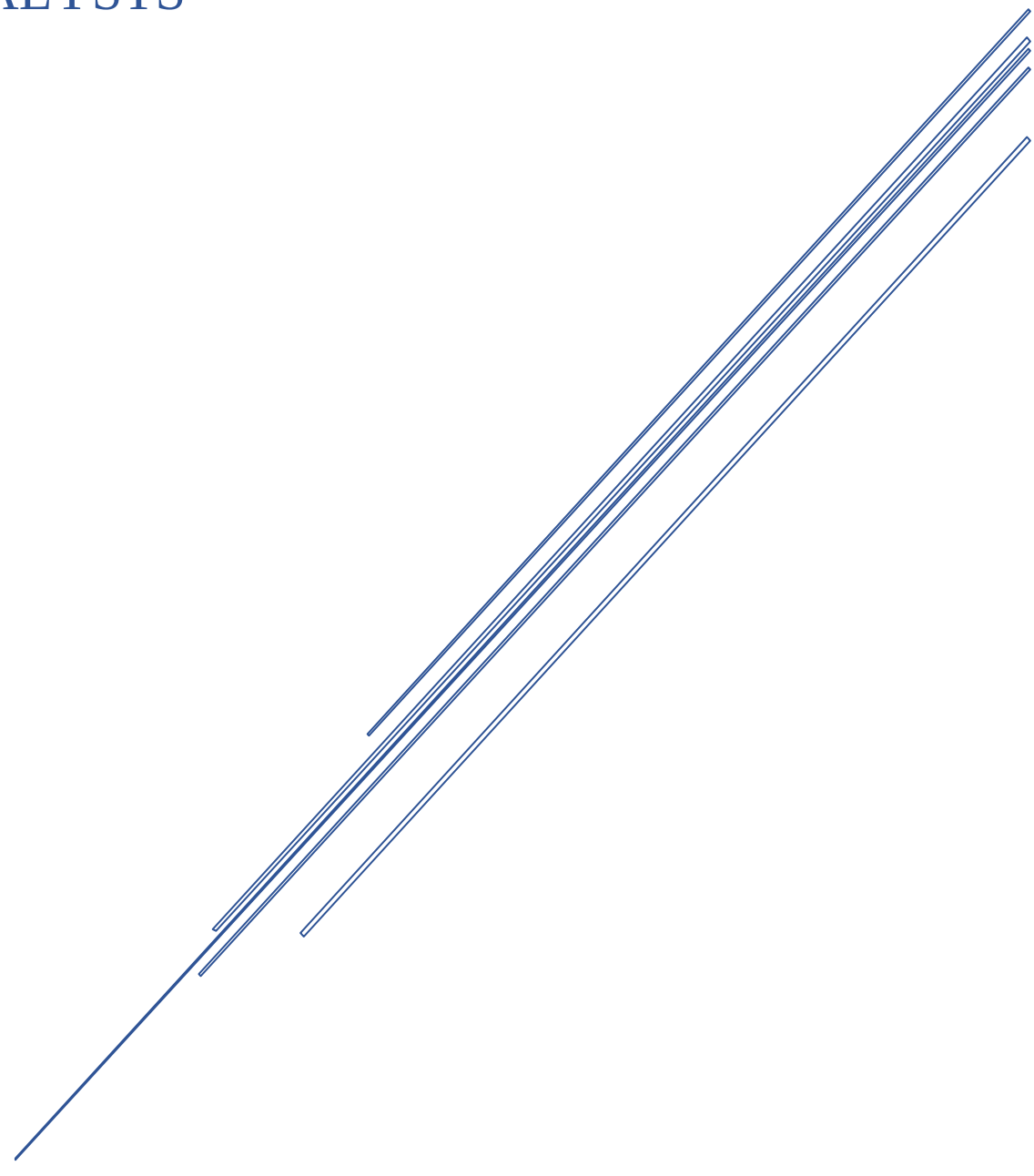

CATALYTIC CONVERSION OF D-GLUCOSE INTO SHORT-CHAIN ALKANES OVER RU-BASED CATALYSTS

Abstract

Liquid alkanes generated by conversion of renewable feedstocks such as biomass has attracted a good piece of attention in order to decrease the dependence of fossil fuels. Herein, we report the conversion of D-Glucose into short-chain alkanes (mainly n-butane, n-pentane, n-hexane) in a one-pot biphasic catalytic system. The reaction was carried out at 190 ºC under 5 MPa of hydrogen pressure in a biphasic n-decane – water system using different catalytic materials for this purpose. Catalytic behavior of supported Ru/Al-MCM-48 and acidified Ru/MCM-48 with tungstophosphoric acid (TPA) was compared with that for a commercial Ru/C. Mesoporous catalytic materials were characterized by means of adsorption / desorption of N_2, X-Ray Diffraction, Transmission Electron Microscopy, Temperature Programmed Reduction (TPR), Temperature Programmed Desorption of ammonia (NH_3 – TPD) and Atomic Absorption (AA). Ru/Al-MCM-48 demonstrated better catalytic behavior in the conversion of D-Glucose to alkanes than Ru/C. Moreover, the addition of Al-MCM-48 combined with Ru/C resulted in an important improvement in the production of alkanes compared to that achieved by Ru/C. The influence of TPA as homogeneous catalyst was also studied with Ru/Al-MCM-48 and commercial Ru/C. The highest yield of alkanes, around 81.9 % (n-butane 7.1 %, n-pentane 29.3 % and n-hexane 45.4 %) was achieved using Ru/C + Al-MCM-48 system.

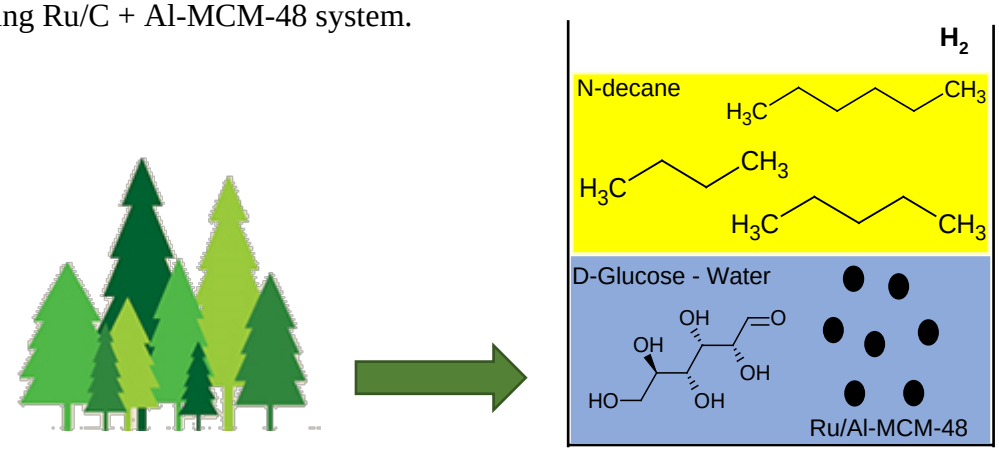

Keywords:

Alkanes, ruthenium, Al-MCM-48, biomass, TPA.

1. INTRODUCTION

Nowadays, the sustainable production of fuels, energy and chemicals from biomass have attracted a great deal of attention [1]. Depletion of fossil fuels and global warming issue have motivated different research efforts in order to develop new reaction routes to transform biomass into valuable products [2]. One of the most promising alternatives is the conversion of lignocellulosic biomass into fuels. Many approaches have been done in order to achieve this purpose, such as catalytic conversion of carbohydrates (cellulose, sugars) [3-6], sugar alcohols (sorbitol and xilytol) [7], furan derivatives [8] and hydropyrolysis processes. In general terms, the products obtained from these processes are based on aromatics compounds, long-chain hydrocarbons (C_{7+}) and gasoline alkanes [9]. In this sense, deoxygenation of carbohydrates and their related alcohols essentially produces liquid straight-chain alkanes such as n-hexane, n-pentane and their isomers which are also commonly known as gasolines alkanes [3, 4, 6, 9].

Cellulosic biomass is one of the most promising alternatives to produce chemicals according to its high oxygen/carbon ratio. Since cellulose is the most common source of biomass and it shows an uniform chemical structure by repeating C_6 units linked by ether bonds, it is a very interesting precursor for the production of liquid straight-chain alkanes by hydrodeoxygenation [10]. The most important reaction routes for the production of alkanes from biomass are a) *Gasification of biomass to produce synthesis gas (H_2/CO) and the subsequently production of methanol and alkanes by Fischer-Tropsch synthesis*, and b) *Aqueous phase reforming of biomass-derived oxygenates* such as sorbitol [3, 6, 11] and glucose [11-13].

In general terms, the production of light straight-chain alkanes from biomass is conducted by a bifunctional reaction route including hydrolysis, hydrogenation, dehydration and hydrodeoxygenation steps [6]. Two different reaction pathways have been reported for the efficient conversion of cellulose into n-hexane as it can be observed in Scheme 1. Tomishige reported the one-pot conversion of cellulose into n-hexane over Ir-ReO_x/SiO_2 combined with H-ZSM-5 as cocatalyst and using n-dodecane as cosolvent [4]. In that work a yield of n-hexane around 83 % was achieved by hydrolytic hydrogenation of cellulose into sorbitol, followed by the subsequently hydrodeoxygenation step to obtain n-hexane (left hand side, Scheme 1). Moreover, Op de Beck et al. described the selective conversion of cellulose into alkanes, mainly n-hexane, over a modification of a commercial Ru/C with silicotungstic acid (TSA)

developing a novel reaction route through 5-hydroxymethylfurfural (HMF) intermediate (right hand-side, Scheme 1) [6].

According to the above explanation, bifunctional acid/redox catalysts are required for this purpose, where hydrolysis and dehydration processes are carried out on solid acid sites and dehydrogenation/hydrogenation on active metal sites of the catalyst [11]. On the one hand, zeolites such as H-ZSM-5 have been used as support for this purpose but their strong acidity, related to Brønsted acid sites, promotes the formation of coke over the catalyst. This fact combined with the poor stability of zeolites under the extreme experimental conditions achieved during the aqueous phase reforming of biomass, motivated the modification of zeolites with pure silica MCM-41 in order to adjust Brønsted acidity from zeolites [13]. MCM-41 belongs to the family of mesoporous silica materials (MSM), which present very interesting catalytic properties such as high hydrothermal stability, high surface area and pore volume and adjustable pore size. MCM-48 shows similar properties than MCM-41 but there are important differences related to their pore structures. While MCM-41 has a hexagonal array of unidirectional pores, MCM-48 has an ordered cubic structure based on a narrow tridimensional pore network which is beneficial for the diffusion of large molecules [14]. MCM-48 has demonstrated to be a good candidate for the selective hydrolysis of cellulose and oligosaccharides into glucose [14, 15] On the other hand, different kind of metals have been used for the conversion of lignocellulosic biomass into alkanes such as Pt, Pd, Ir, Ni, Ru and Rh. and Ru deposited over MCM-48 was an efficient metallic catalyst for the conversion of hemicellulose and carbohydrates into sugar alcohols [14-17].

This paper reports the preparation of solid bifunctional catalysts based on MCM-48 as the support and ruthenium as the metal phase. Severe acidity conditions are required for dehydration steps. MCM-48 provides weak acidity from terminal silanol groups and it has been improved by the introduction of aluminum into the matrix of the support (Al-MCM-48) and by the deposition of tungstophosphoric acid (TPA) on the surface of MCM-48. Ru, as hydrogenating active metal, has been deposited over TPA-modified MCM-48 and Al-MCM-48. Both catalysts have been tested and compared with a standard commercial Ru/C in the conversion of D-Glucose into alkanes using n-decane as cosolvent. The influence of adding Al-MCM-48 and TPA as cocatalyst combined with Ru-based catalysts was also studied.

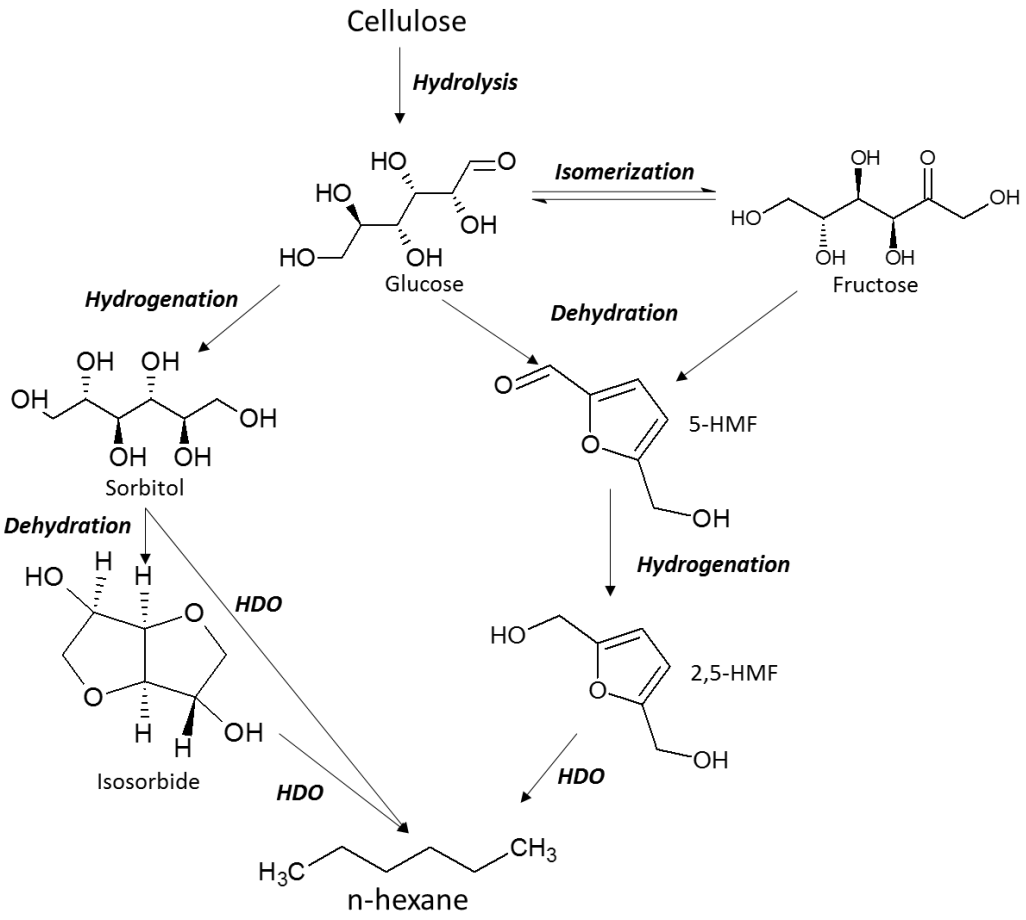

Scheme 1. Proposed reaction pathways for conversion of cellulose into alkanes over bifunctional catalysts with acidic and metal components

2. MATERIALS AND METHODS

2.1. SUPPORTS AND CATALYSTS PREPARATION

Preparation of mesoporous silica MCM-48 has been developed by a conventional hydrothermal procedure as described by Schumacher et al [18, 19]. Firstly, n-hexadecyltrimethylammonium bromide template ($CH_3(CH_2)_{15}N(Br)(CH_3)_3$ ≥ 98%, Sigma – Aldrich) was dissolved in 42 cm^3 of distilled water, 13 cm^3 of aqueous ammonia (20% as NH_3, Panreac), and 18 cm^3 of absolute ethanol (partially denaturated QP, Panreac) by stirring for 15 min; then 4 cm^3 of TEOS (≥ 99% GC, Sigma – Aldrich), were added dropwise. The solution was further stirred for 18 h; the white precipitate was then collected by filtration and washed with distilled water. After that, the precipitate was dried at 60 ºC overnight. Dried samples were calcined with a heating rate of 2 ºC·min^{-1} from 80 ºC to 550 ºC and maintained at 550 ºC overnight. Synthesis

of Al-MCM-48 was carried out with the same procedure as that used for MCM-48, with a modification consisting in the addition of 0.077 g of sodium aluminate ($NaAlO_2$, Sigma - Aldrich) related to a Si/Al = 20, just before the addition of TEOS.

Preparation of MCM-48/TPA was performed by dispersing 1 g of MCM-48 in TPA aqueous solution (1 g of TPA in 25 mL of distilled water). TPA was supplied by Sigma Aldrich. The suspension was stirred for 1 h and kept static at room temperature for 12 h. The final product was dried at 110 ºC overnight and then calcined in air with a heating rate of 2 ºC·min^{-1} from room temperature to 400 ºC and kept at this temperature for 3 h [20].

Two ruthenium catalysts, with a metal loading around 3.5 – 5 %, were synthesized by the wet impregnation (WI) technique using the so-prepared Al-MCM-48 and MCM-48/TPA as supports. For this preparation, ruthenium (III) chloride anhydrous ($RuCl_3$.anhydrous, Strem Chemicals Inc.) is used. The corresponding support was sonicated in water, previously to the addition of the metallic solution. Then, ruthenium trichloride solution and a dispersion containing the support were mixed and heated with a rate of 1 ºC·min^{-1} from room temperature to 105 ºC using a Stuart model SD162 heating plate. The impregnation finished when the solvent was completely evaporated. Then, catalysts were dried overnight at 105 ºC. Finally, the samples were activated under H_2 atmosphere at 150 ºC. A commercial Ru/C catalyst (Ruthenium, 5% on activated carbon, reduced, (Alfa Aesar, lot. M11068)) and Ru/MCM-48 have been used as reference catalysts.

2.2. SUPPORTS AND CATALYSTS CHARACTERIZATION

Small Angle X-Ray Scattering (SAXS) and X-Ray Diffraction (XRD) were performed with a Bruker Discover D8 Focus diffractometer using the Cu Kα radiation (λ = 0.15406 nm). The diffraction intensities were measured, for XRD, over an angular range of 20° < 2θ < 90° with a step size of 0.03° and a count time of 2 s per step. In the case of SAXS, 2° < 2θ < 6º was selected as angular range with a step size of 0.02° and a count time of 1 s per step. Nitrogen adsorption-desorption isotherms were performed with ASAP 2020 (Micromeritics, USA) to obtain surface and pore properties of supports and catalysts. Prior to analysis, the samples were outgassed overnight at 350 ºC. Total specific surface areas were determined by the multipoint BET method at $P/P_0 \leq 0.3$, total specific pore volumes were evaluated from N_2 uptake at $P/P_0 \geq 0.99$. Pore

diameter was obtained by BJH adsorption average ($4 \cdot V \cdot A^{-1}$, nm). Pore size distribution was derived from adsorption branch of the isotherm by BJH desorption pore volume (dV/dD) Halsey: Faas correction. Temperature Programmed Reduction (TPR) profiles of Ru/Al-MCM-48 and Ru/MCM-48/TPA were recorded using the commercial Micromeritics TPD/TPR 2900 unit. The samples were loaded into a U-shaped quartz cell (100 mm × 3.76 mm i.d.), ramped (10 ºC·min^{-1}) from room temperature to 800 ºC under a flow of H_2/N_2 (5% v/v; 50 cm^3·min^{-1}, Air Liquide) and kept at the final temperature until the signal returned to the baseline. Hydrogen consumption was monitored by a thermal conductivity detector (TCD) with data acquisition/manipulation using the ChemiSoft TPX V1.03™ software. NH_3-TPD experiments were performed in the same analyzer. In this case, the samples were activated under H_2-TPR conditions (150 ºC) for 60 min and then they were saturated with ammonia at 100 ºC during 30 min. NH_3 was purged using pure He during 60 min and then samples were heated from 100 ºC to 600 ºC (ramped 15 ºC·min^{-1}) and kept at the final temperature until the signal returned to the baseline. The amount of chemisorbed ammonia was calculated according to calibrated volumes of this compound. Transmission electron microscopy (TEM) analyses used a JEOL 2100 unit with an accelerating voltage of 200 kV. Ruthenium samples were prepared by ultrasonic dispersion in acetone with a drop of the resultant suspension, which was evaporated onto a holey carbon-supported grid. A counting of ruthenium nanoparticles were carried out from TEM images of the different catalysts. At least 170 ruthenium nanoparticles were counted in each case and the mean Ru particle sizes were expressed as surface-area weighted diameter ($\bar{d}_s$),which was calculated from the following expression (Eq. 1) [21].

$$\bar{d}_s = \frac{\sum_i n_i \cdot d_i^3}{\sum_i n_i \cdot d_i^2} \quad (1)$$

where n_i is the number of ruthenium nanoparticles with a diameter d_i. Since chemical reactions occurs on catalyst surface, surface-area weighted diameter is selected as the most meaningful parameter to obtain mean Ru particles sizes for catalysis purposes. Ruthenium loading in the catalysts was determined by means of atomic absorption (AA) spectrophotometry, using a SPECTRA 220FS analyzer. Approximately, 0.05 g of the sample, 3 mL of HCl, 3 mL H_2O_2 and 3 mL HF were treated by microwave digestion at 250 ºC and the final solution was measured in the spectrophotometer.

2.3. CATALYTIC TESTS

In a typical catalytic experiment, 2 g of D-Glucose (supplied by Sigma-Aldrich) were dissolved in 50 mL of distilled water. The aqueous sugar solution, 50 mL of n-decane supplied by TCI (purity > 99.5 % for GC) and 0.5 g of activated catalyst were added into a Teflon vessel, which was put into a 200 mL stainless steel batch reactor PID controlled. In the tests where TPA and Al-MCM-48 were used as additive, 1 g and 0.5 g were added, respectively. The reactor was flushed with N_2 and pressurized with a low pressure of 0.5 MPa of N_2. The reaction mixture was stirred at 1200 rpm and heated up to 190 ºC at an average rate of 6 $ºC \cdot min^{-1}$. When the reactor reached the reaction temperature, it was pressurized at 5 MPa of H_2 and it was considered as t = 0. The reactor had a sampling valve in order to obtain samples from the aqueous phase at different reaction times. At the end of the experiment, the reactor was cooled down in an ice bath to rapidly stop the reaction. Then, it was depressurized and opened. Sample from n-decane phase was only taken at the end of the reaction. Samples from aqueous phase were analyzed by means of total organic carbon (TOC, $mg_c \cdot l^{-1}$) using a Shimadzu TOC-VCSH analyzer and High Performance Liquid Chromatography (HPLC). The HPLC column used was SUPELCO Ca^{2+} from Supelco at 60 °C and a flow of 0.4 $cm^3 \cdot min^{-1}$ using water Milli-Q as the mobile phase. A Shimadzu refractive index detector (IR) was used to identify sugars, polyols and their derivatives. Samples from the organic phase were analyzed by Gas chromatography (Shimadzu GC-MS QP202S) and 1-heptanal was used as standard reference. The yield of each product based on carbon was calculated according to equation 2, where [P] is the concentration of the product analyzed by HPLC and GC-MS ($mg \cdot l^{-1}$), x_c is the mass fraction of carbon related to each product and TOC ($mg_c \cdot l^{-1}$) is the total organic carbon value from the starting D-Glucose solution.

$$Y\ (C\ \%) = \frac{[P] \cdot x_C}{TOC} \cdot 100 \quad (2)$$

3. RESULTS AND DISCUSSION

3.1. CHARACTERIZATION OF SUPPORTS

Figure 1A shows Small Angle X-Ray Scattering (SAXS) pattern of MCM-48, Al-MCM-48 and MCM-48/TPA. MCM-48 exhibits four main Bragg diffraction peaks in

the 2θ range from 2-5 º, that can be assigned to (211), (220), (321) and (332) planes, which can be indexed to cubic mesophase belonging to a Ia3d symmetry [19, 22]. These results are in good agreement with the high quality of mesoporous phase. However, in the case of Al-MCM-48 only the peaks attributed to (211), (220) and (332) are clearly detected with lower intensity than in the case of the bare MCM-48. This fact can be due to the introduction of Al into the walls of MCM-48, which decreases the quality of the mesoporous structure of Al-MCM-48. Similar behavior was observed by Meng et al for Al-MCM-48 [23]. In the case of MCM-48/TPA, only the peaks ascribed to (211) and (220) and a higher decrease of the intensity of these peaks in comparison with those for MCM-48 and Al-MCM-48 were observed. According to these results, the mesoporous order of MCM-48/TPA remained upon the deposition of TPA into the pores of MCM-48, but TPA damaged porous structure causing a noticeably decrease of the long-range order of the material as it was reported by Wu et al [24].

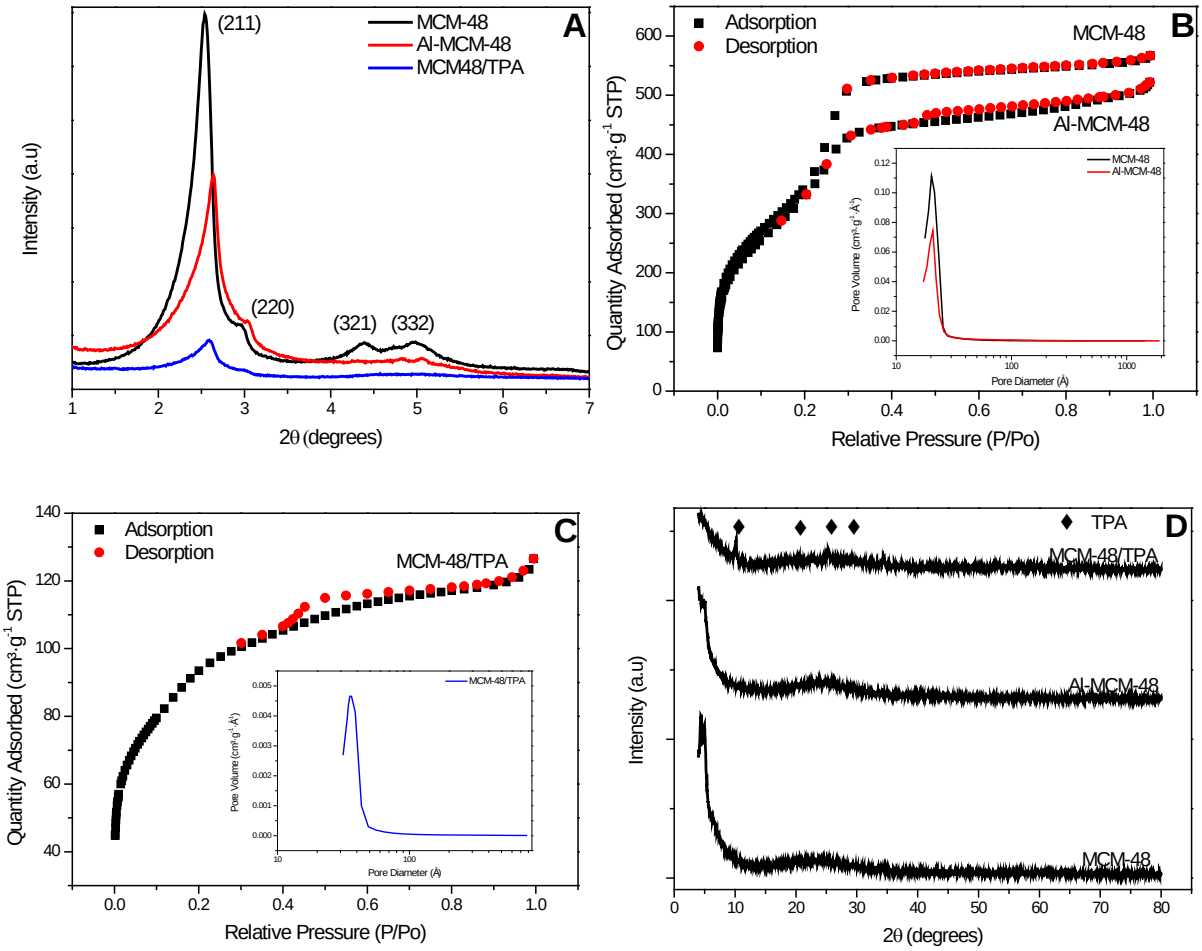

Figure 1. (A) SAXS diffraction patterns **(B, C)** adsorption-desorption isotherms of N_2 and pore size distribution and **(D)** XRD diffraction patterns of MCM-48, Al-MCM-48 and MCM-48/TPA.

Adsorption / desorption isotherms of N_2 at -196 ºC were determined in order to study textural properties of MCM-48, Al-MCM-48 and MCM-48/TPA and results are illustrated in Figure 1B and C. MCM-48 was only used for comparison purposes not as catalytic material in this work, since its weakly acidity related to terminal Si-OH groups, was not enough in order to promote dehydration steps involved in the tested process. In general terms, it was observed that in all the cases the materials presented typical isotherms of the mesoporous silica materials, classified as type IV according to the IUPAC classification [25]. In this sense, this kind of adsorption isotherm displays an abrupt increase in the quantity of adsorbed nitrogen in the relative pressure (P/P_0) range of 0.2 – 0.3 which is typically associated to capillary condensation of N_2 into the mesopores of the materials. This fact is clearly observed for MCM-48, then a lower increase of the quantity adsorbed of nitrogen in that range of relative pressures were detected for Al-MCM-48 and it was not detected for MCM-48/TPA. Pore condensation without hysteresis at $P/P_0 < 0.4$, as observed for MCM-48, has been reported before for this material according to the presence of pores in the limit of small mesopores [26]. The sharpness of the capillary condensation step is indicative of the uniformity of pore channels, with a narrow distribution [19]. However, Al-MCM-48 and MCM-48/TPA presented hysteresis loops (type H_3), which are indicative of a secondary pore structure upon modification of MCM-48 with aluminum or TPA. The pore volume ($cm^3 \cdot g^{-1} \cdot Å^{-1}$) as a function of pore diameter (Å) were depicted in Figure 1B for MCM-48 and Al-MCM-48 and in Figure 1C for MCM-48/TPA. Unimodal pore size distributions with well-defined peaks centered at around 20 Å were observed for MCM-48 and Al-MCM-48, while the peak was shifted up to 36 Å in the case of MCM-48/TPA. Textural properties for MCM-48, Al-MCM-48 and MCM-48/TPA are presented in Table 1. BET surface area and pore volume for MCM-48 were 1289 $m^2 \cdot g^{-1}$ and 0.87 $cm^3 \cdot g^{-1}$, respectively. No significantly changes in BET surface and pore volume were detected in Al-MCM-48 compared to MCM-48. However, an important decrease of BET surface and pore volume was observed after the deposition of TPA, showing 335 $m^2 \cdot g^{-1}$ and 0.20 $cm^3 \cdot g^{-1}$, respectively. Therefore, there is a big influence of TPA in the textural properties of the MCM-48, since the heteropolyacid is strongly adsorbed to the surface of the channels and inside the pores of MCM-48 [27]. Pore diameter was not affected after the introduction of Al into the walls of MCM-48. However, after the adsorption of TPA over MCM-48, a noticeably increase in pore diameter was observed. Thus,

according to the former results, the addition of TPA resulted in a higher modification of the porous structure of MCM-48 in comparison with the introduction of aluminum.

Table 1. Textural properties, ruthenium loading, ruthenium particle size of the catalysts and textural properties of the bare supports.

Catalyst	Ru (%)	S_{BET} ($m^2 \cdot g^{-1}$)	V_{pore} ($cm^3 \cdot g^{-1}$)	Ø $_{pore}$ (nm)	Ru (nm)	Ref.
MCM-48	-	1289	0.87	2.2	-	[17]
Al-MCM-48	-	1352	0.81	2.5	-	This work
MCM-48/TPA	-	335	0.20	3.1	-	This work
Ru/Al-MCM-48	3.5	1028	0.57	2.7	2.0[a] / 1.9[b]	This work
Ru/MCM-48/TPA	4.9	504	0.29	2.5	2.0[a]	This work
Ru/C	5	815	-	-	1.1	[28]

[a] Ru surface-area weighted diameter from TEM images. [b]Ru crystallite size from XRD analysis.

Figure 1D shows XRD patterns of MCM-48, Al-MCM-48 and MCM-48/TPA. Comparing XRD patterns of MCM-48 and MCM-48/TPA, diffraction peaks related to the impregnation of TPA over MCM-48 were observed. The characteristic diffraction peaks for bulk $H_3PW_{12}O_{40}$ are detected at $2\Theta = 10.36^o, 21.35^o, 25.44^o, 29.46^o$ (JCPDS 50-0657) and also Keggin types peaks as it was reported by Zhang et al [20]. In that work, the authors did not observed any diffraction peak of TPA over MCM-48 matrix suggesting that the heteropolyacid was preferably impregnated on the surface of MCM-48. In this work, the main peaks of the crystalline phase of TPA over MCM-48 are detected. In addition, no significantly changes were observed in XRD pattern of Al-MCM-48 after the introduction of aluminum in the pore network of MCM-48.

3.2. CHARACTERIZATION OF RU-BASED CATALYSTS

Textural properties for Ru/Al-MCM-48 and Ru/MCM-48/TPA are presented in Table 1. A slight decrease in the specific surface area and pore volume of Ru/Al-MCM-48 are noticed after the introduction of active metal into the pores, from 1352 to 1028 $m^2 \cdot g^{-1}$ and from 0.81 to 0.57 $cm^3 \cdot g^{-1,}$ respectively. This phenomenon is attributed to the partial blocking of the porous network of the support. However, specific surface area

and pore volume slightly increased from 335 to 504 $m^2 \cdot g^{-1}$ and from 0.20 to 0.29 $cm^3 \cdot g^{-1,}$ respectively for Ru/MCM-48/TPA. This effect could be due to removal of certain amounts of TPA presented into the pores upon ruthenium deposition. Ru/C from Alfa Aesar with a 5% of active metal loading was also used by other authors, who reported BET surface areas of 815 m^2/g for this material [28].

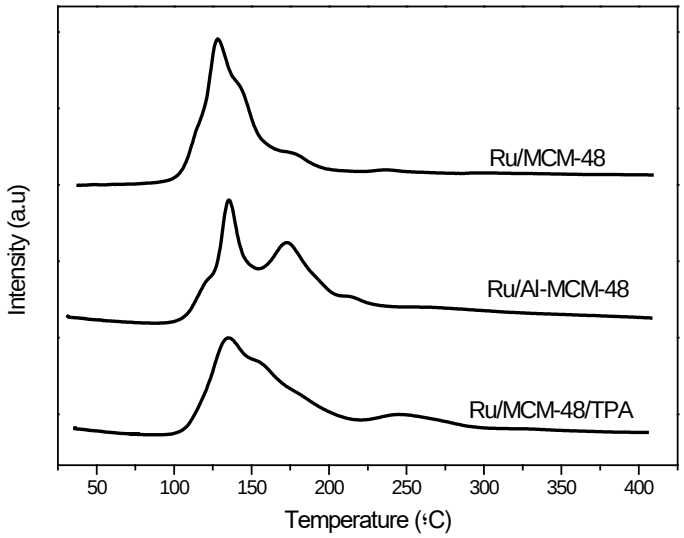

Figure 2. H_2-TPR profiles of Ru-based catalysts

H_2-TPR profiles of Ru/Al-MCM-48 and Ru/MCM-48/TPA are presented in Figure 2 in order to check the reducibility of the ruthenium species deposited over the supports. In previous works, ruthenium was deposited over MCM-48 and a single reduction peak at ca. 125 ºC was measured, related to the reduction of well-dispersed Ru^{3+} to Ru^0 [14, 15]. Ru/MCM-48/TPA showed a similar reduction peak centered at ca. 135 ºC, which is also related to the reduction of Ru^3 species to Ru^0 and a second less intense reduction peak at ca. 250 ºC that can be ascribed to the same ruthenium species with higher interaction with the support. First reduction peak of Ru/MCM-48/TPA is broader than that obtained for Ru/MCM-48, suggesting that the deposition of the heteropolyacid in the mesoporous matrix resulted in the formation of ruthenium species with a higher range of metal-support interactions. Two reduction peaks also exist at ca. 135 ºC and 175 ºC respectively in the case of Ru/Al-MCM-48, suggesting the presence of two different types of ruthenium nanoparticles. The narrower and most intense peak at ca. 135 ºC can be ascribed to the reduction of agglomerates or bad-distributed crystallites of $RuCl_3$ over Al-MCM-48 towards metallic ruthenium. Nevertheless, the second peak at higher temperature can be attributed to the reduction of well-dispersed

$RuCl_3$ with small crystallite size. In general terms, smaller nanoparticles have higher metal-support interaction, thus they are reduced at higher temperatures. According to the former results, catalysts were activated at 150 ºC under hydrogen atmosphere for 1 h and an additional time at 200 ºC in order to assure the proper reduction of ruthenium species in all cases. Reduction temperature of 300 ºC was also evaluated. Ru/C is a commercial catalyst and it was purchased in its reduced form, thus TPR analysis were not conducted.

XRD patterns for activated Ru-based catalysts are shown in Figure 3. A broad characteristic metallic diffraction peak corresponding to Ru^0 (101) was observed at $2\theta = 43.8^{o}$ for Ru/Al-MCM-48, indicative of the presence of Hexagonal Close Packing (HCP) Ru^0 nanoparticles. It indicates the correct reduction of Ru/Al-MCM-48 (Figure 3 A). The small and broad metallic ruthenium peak suggests the presence of very small Ru^0 nanoparticles well-distributed into the Al-MCM-48. This fact was confirmed by calculations based on Scherrer equation and Ru^0 (101) diffraction peak, which determined the existence of Ru^0 nanoparticles with a crystallite size of 1.9 nm. It is usual to find in the literature higher activation temperature for similar Ru-based catalysts in comparison with that reported in the present work [16]. Kusema et al. obtained a ruthenium crystallite size from Scherrer equation around 16 nm for modified Ru-MCM-48 after its activation under H_2 atmosphere at 300 ºC. We checked the influence of a higher activation temperature in the crystallite size of ruthenium in Ru/Al-MCM-48. After the reduction of Ru/Al-MCM-48 at 300 ºC under H_2 atmosphere, different Ru^0 reflections were detected at $2\theta = 38.8^{o}, 42.2^{o}, 43.8^{o}, 58.2^{o}, 69.6^{o}$ and 78.4^{o} corresponding to the presence of Hexagonal Close Packing Ru^0 nanoparticles. The observed differences between Ru/Al-MCM-48 reduced at 150 ºC and 300 ºC related to shape and sizes of the peaks suggest the formation of bigger Ru^0 nanoparticles at higher activation temperature. Calculations based on Scherrer equation and Ru^0 (101) confirmed the existence of ruthenium nanoparticles with a crystallite size of 5.3 nm. This fact can be attributed to sintering of ruthenium, which considerably decrease the active surface area of the metal [29]. XRD pattern of activated Ru/MCM-48/TPA at 150 ºC is shown in Figure 3B. Given the presence of high intensity diffraction peaks from crystalline tungstophosphoric acid, the corresponding to Ru^0 nanoparticles could not be detected into MCM-48/TPA [30]. A XRD analysis was

carried out for this sample in the range 2θ = 40 - 50 º (not shown) and related diffractions peaks to Ru^0 were not observed.

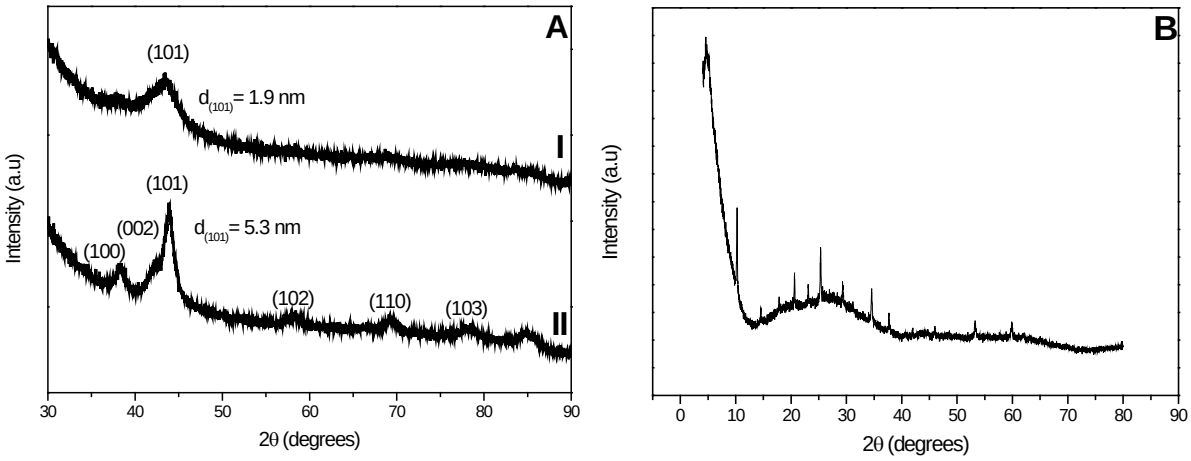

Figure 3. XRD patterns of **(A)** Ru/Al-MCM-48 reduced at 150 ºC (I) and 300 ºC (II) and **(B)** Ru/MCM-48/TPA at 150 ºC.

TEM-images of Ru/Al-MCM-48 and Ru/MCM-48/TPA are presented in Figure 4 and 5, respectively. Different regions were observed for the Ru/Al-MCM-48 as it is presented in Figure 4 A, B and C. First, pseudo spherical particles of Al-MCM-48 were detected where ruthenium nanoparticles with low contrast are deposited in the central areas of Al-MCM-48 particles (Figure 4A). Then, there are some areas where agglomerates of ruthenium nanoparticles deposited in the outer surface of support particles were observed. This fact is in accordance with the lower reduction peak obtained for Ru/Al-MCM-48 in Figure 2. Finally, most of the regions demonstrated the presence of well-distributed ruthenium nanoparticles into the mesoporous network of the support (Figure 4C). A counting of at least 170 ruthenium particles was carried out for Ru/Al-MCM-48 from TEM-images (Figure 4D). The obtained histogram showed a narrow ruthenium nanoparticle size distribution in the range 1.2 – 2.5 nm and a surface-area weighted diameter of 2 nm was obtained as a result of calculations based on equation 1. In the case of Ru/MCM-48/TPA, different areas were also observed. As it is showed in Figure 5A, big agglomerates of ruthenium are detected in the outer surface of the support particles (Figure 5A). Even in some cases, they were covering a big part of MCM-48/TPA particles. Then, homogeneous ruthenium nanoparticles were observed in other regions, which are deposited into the pores of MCM-48/TPA (Figure 5B). Finally, big ruthenium aggregates were detected close to the border of the support particles in some cases. Figure 5D shows a broader ruthenium nanoparticle size distribution for

Ru/MCM-48/TPA than that achieved for Ru/Al-MCM-48. In this case, ruthenium particles were in the range 1.0 – 3.1 nm, showing a surface-area weighted diameter of 2 nm. Both values of surface-area weighted diameter calculated for Ru/Al-MCM-48 and Ru/MCM-48/TPA are slightly lower than that obtained in a previous work for Ru/MCM-48 (2.3 nm). The observed differences in terms of ruthenium nanoparticle size are in good agreement with those from H_2-TPR, where Ru/MCM-48 showed a reduction peak centered at 125 ºC and Ru/MCM-48/TPA and Ru/Al-MCM-48 presented the main reduction peak at 135 ºC. Therefore, the biggest ruthenium nanoparticles presented in Ru/MCM-48 with lower interaction with MCM-48, demonstrated to be reducible at lower temperatures than those deposited in Ru/Al-MCM48 and Ru/MCM-48/TPA. According to TEM images, Choi et al reported that the commercial catalyst from Alfa-Aesar presented a narrow ruthenium nanoparticle size distribution were the mean ruthenium particle size was 1.1 nm [28].

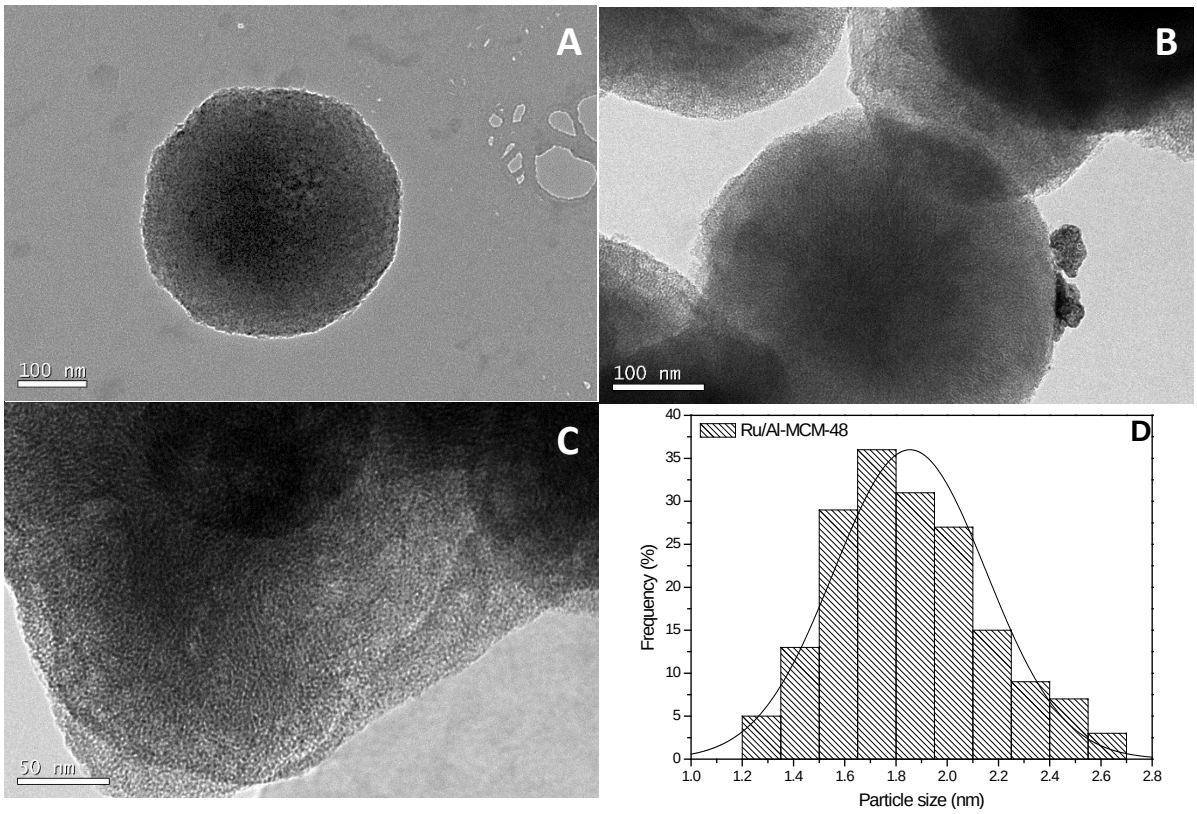

Figure 4. (A, B, C) Transmission Electron Microscopy (TEM) micrographs, **(D)** Ru particle size distribution of Ru/Al-MCM-48**.**

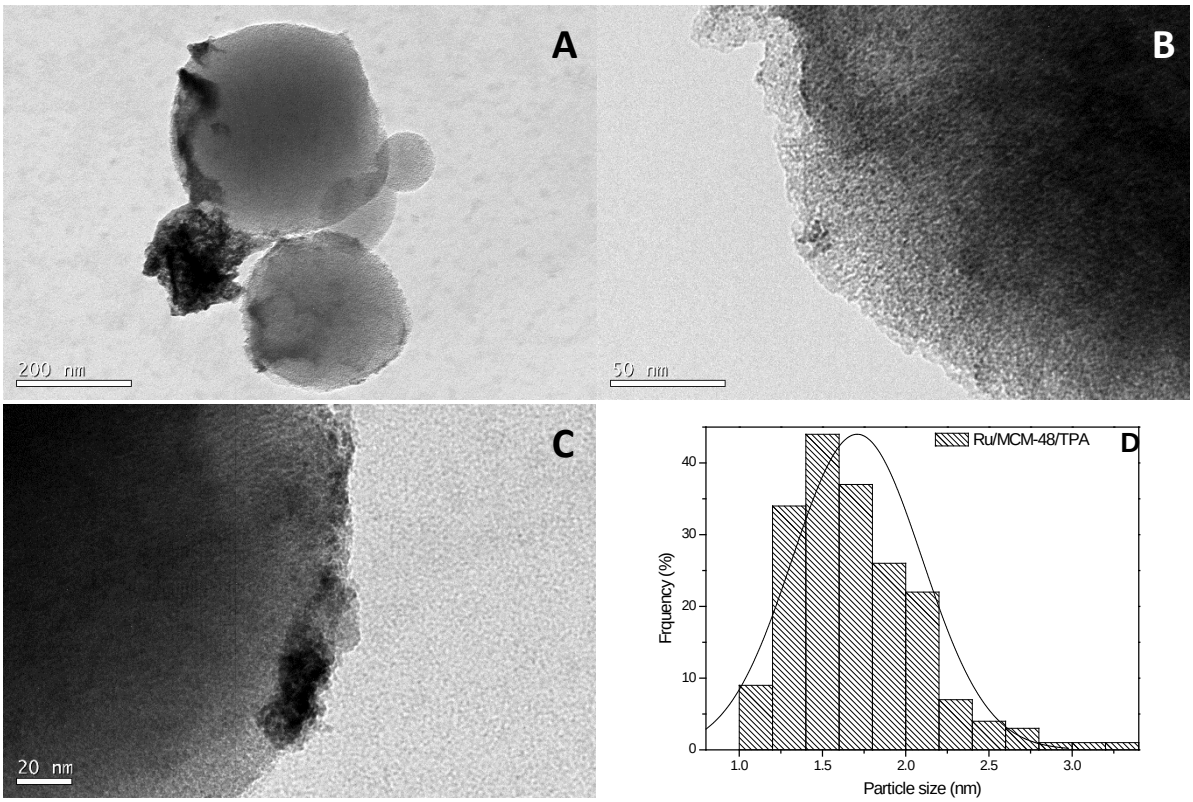

Figure 5. (A, B, C) Transmission Electron Microscopy (TEM) micrographs, **(D)** Ru particle size distribution of Ru/MCM-48/TPA**.**

Acidity is a key factor for the application of these catalysts in one-pot processes such as conversion of cellulosic biomass into alkanes, where hydrolysis and dehydratation processes are carried out on the acid sites of the materials. The NH_3-TPD profiles of the supports and the reduced catalysts are presented in Figure 6. Amount of acid sites and temperatures of the different peaks detected in the NH_3-TPD are shown in Table 2. In general terms, the strength of the acid sites could be determined according to desorption temperature of each peak. Low temperature ammonia desorption peaks are associated to weak acid sites and high temperature peaks are attributed to strong acid sites, respectively. All the samples presented a main peak at low temperatures (130 – 300 ºC) and one or two desorption peaks at higher temperatures (300 – 600 ºC). The incorporation of Al into MCM-48 increased acidity of Al-MCM-48 in comparison with MCM-48, as expected. The addition of Al caused that weak acidity peak shifted to higher temperature, which is attributed to the existence of trivalent aluminum species in the MCM-48 framework [23]. In addition, this peak was broader than that obtained for MCM-48, which results in an increase of the number of weak acid sites. MCM-48/TPA presented three desorption peaks at ca. 200 ºC, 430 ºC and 590 ºC. The peak at 200 ºC is associated to weak acid sites corresponding to surface hydroxyl groups (Si-OH), while

430 ºC and 590 ºC peaks are related to TPA deposited over MCM-48 [23]. After the introduction of Ru into Al-MCM-48, an important increase in terms of acidity was detected in comparison with bare Al-MCM-48. This fact is ascribed to the noticeable tendency of ruthenium atoms to adsorb ammonia [31], while the influence of residual chlorine atoms cannot be discarded [17]. However, Ru/MCM-48/TPA acidity slightly decrease compared to MCM-48/TPA. As it was suggested for the increase of BET surface after ruthenium deposition in Ru/MCM-48/TPA, the slight decrease in acidity can be also due to removing of certain amounts of TPA presented into the pores when ruthenium is deposited there. In addition this fact is in good agreement with the decrease of $mmol_{NH3} \cdot g^{-1}$ of Ru/MCM-48/TPA compared to MCM-48/TPA, related to the peaks between 300 – 600 ºC ascribed to TPA. Total amount of acid sites (Table 2) is consistent with the following sequence of increasing acidity: MCM-48 < Al-MCM-48 < Ru/MCM-48/TPA < MCM-48/TPA < Ru/Al-MCM-48.

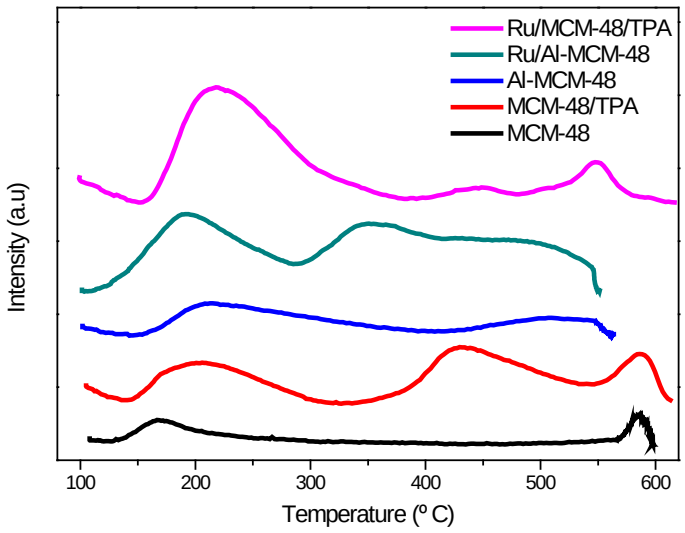

Figure 6. NH_3-TPD patterns for supports and ruthenium reduced catalysts.

Table 2. Acidic properties from NH_3-TPD for the reduced catalysts.

	Acidity ($mmol_{NH3} \cdot g^{-1}$)		
	I (130 - 300 ºC)	**II and III (300 - 600 ºC)**	**Total**
MCM-48	0.157	0.343	0.500
Al-MCM-48	0.454	0.388	0.842
MCM-48/TPA	0.358	0.683	1.041
Ru/Al-MCM-48	0.456	0.763	1.219
Ru /MCM-48/TPA	0.479	0.411	0.890

3.3. CONVERSION OF D-GLUCOSE INTO ALKANES

In the present work, D-Glucose was selected as raw material since it is a model compound that allows the achievement of a higher understanding of the fundamental steps of the catalytic process, before using a real biomass for the same purposes. Catalytic behavior of Ru/Al-MCM-48 and Ru/MCM-48/TPA in comparison with a commercial Ru/C as reference material, were tested in the conversion of D-Glucose into short-chain alkanes. In addition, other catalytic combinations including the addition of TPA and Al-MCM-48 to the reaction media were tested in order to enhance the production of alkanes. Results are shown both in Table 3 and Figure 7. Reaction media consists of a biphasic D-Glucose water solution – n-decane system, where the organic phase allowed the extraction of some intermediates from the aqueous phase, which can be degraded due to the acidic features of the reaction aqueous phase. Additionally, solubility of hydrogen is higher in the organic phase than in the aqueous phase, thus hydrogenation and dehydration steps are favored in this kind of environment [6]. Catalytic tests were conducted at 190 ºC, 5 MPa of H_2 pressure, 20 h of reaction time and a mechanical stirring of 1200 rpm. Several samples from the aqueous phase were taken in order to obtain a higher understanding of the different reaction mechanism that can be involved in the global process. However, organic phase where alkanes are dissolved is only analyzed after 20 h of reaction time.

Catalytic reactions started by testing Ru/Al-MCM-48 in D-Glucose conversion into straight-chain alkanes. Catalytic behavior of Ru/Al-MCM-48 in the aqueous phase is presented in Figure 7A. D-Glucose was totally converted following sorbitol reaction pathway. After 5 min of reaction time D-Glucose was not detected by HPLC. Sorbitol was the main intermediate that could be identified in the aqueous phase. Additionally, iditol and mannitol were also obtained as a result of sorbitol isomerization. Sorbitol was totally converted by dehydration to isosorbide and 1,4-sorbitan after 840 min. After 1200 min low amounts of sugar alcohols were detected in the aqueous phase, corresponding to a carbon basis yield of 1.4 %. A yield of 14.2 % related to other soluble compounds, which could not be identified by HPLC, was obtained by TOC measurements. Moreover, around 16 % of the initial carbon remained in the aqueous phase after 1200 min of reaction time. A total yield of 56.6 % alkanes were obtained as a result of the sum of partial yields of n-butane, n-pentane and n-hexane. In this case, similar yields to n-pentane and n-hexane were obtained, 25.9 % and 23.5 %,

respectively. Moreover, yield around 7 % of n-butane was measured. N-butane is obtained by the hydrogenolysis of erythritol as it was stated by Chen et al [3]. The presence of considerable amount of C4 and C5 alkanes in the final product can be due to the high activity of Ru for C—C bond cleavage in comparison with other active metals such as Pd or Pt, as it was reported by Palkovits et al. [32]. Finally, sum of the yields of presented carbon in organic and aqueous phase was around 72 %, suggesting the production of light alkanes in the gas phase. This fact is in good agreement with the presence of bubbles after the depressurization of the reactor and the slight increase in the reaction pressure after 20 h from 5 MPa to 5.2 MPa.

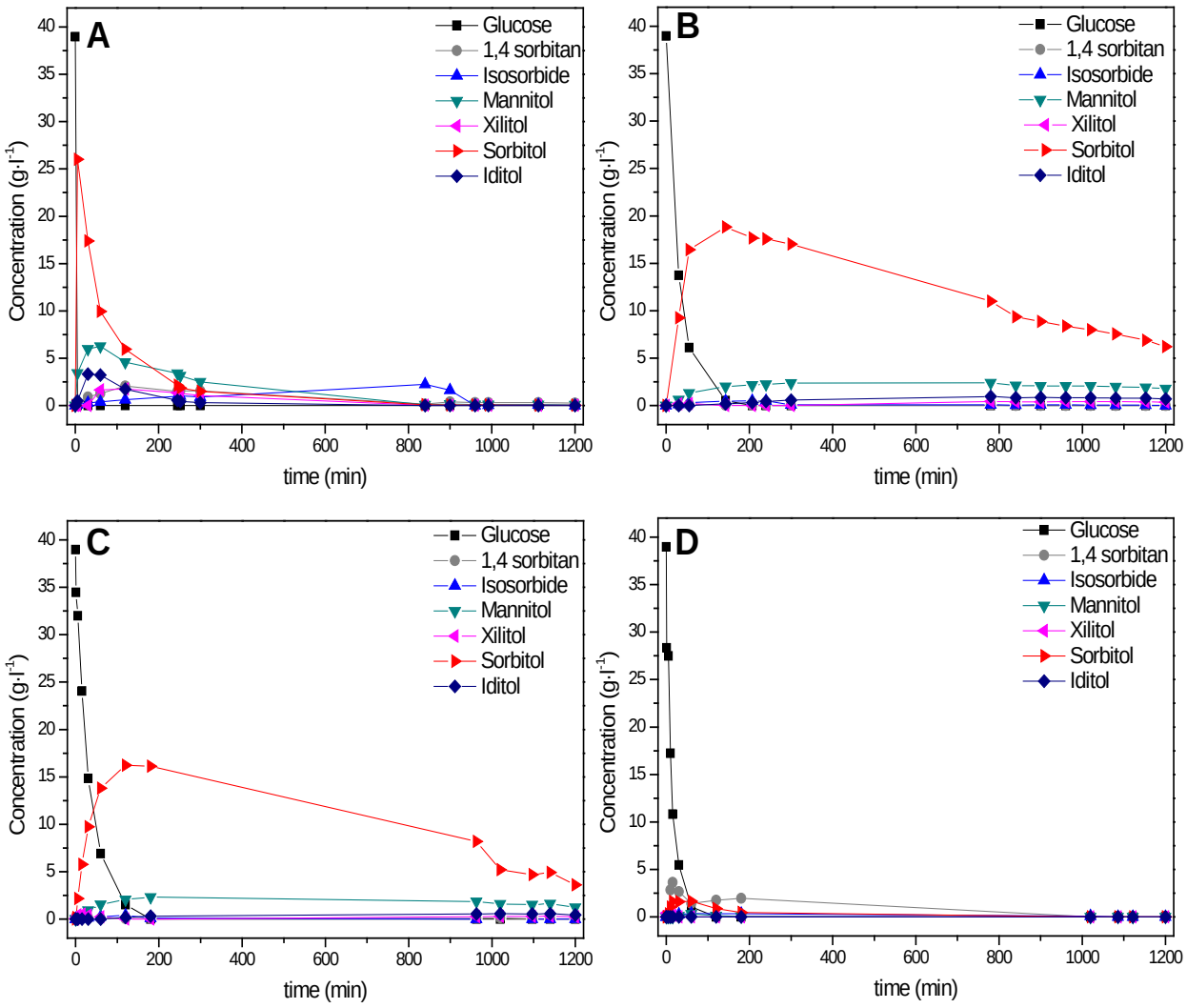

Figure 7. Concentration profiles in the aqueous phase for conversion of D-Glucose over **(A)** Ru/Al-MCM-48, **(B)** Ru/C, **(C)** Ru/C + Al-MCM-48 and **(D)** Ru/C + TPA.

Table 3. Conversion of D-Glucose using different catalytic systems (190 ºC, 5 MPa H_2 and 1200 min).

		Yield (C %)											
		n-decane								Water			
Entry	**Catalyst**	**But[a]**	**MCP[b]**	**Pen[c]**	**Hex[d]**	**DMTHF[e]**	**HexOH[f]**	**Other[g]**	**Sum**	**SA[h]**	**Other[i]**	**Sum**	**Carbon balance**
1	Ru/C	3.9	0	9.8	15.5	0	0	0	29.2	29.6	4.5	34.1	63.3
2	Ru/C + TPA	6.0	6.6	25.3	38.9	9.2	1.9	1.7	89.6	0	7.2	7.2	96.8
3	Ru/C + Al-MCM-48	7.1	0	29.3	45.4	0	0	0	81.8	18.2	3.3	21.5	>100
4	Ru/Al-MCM-48	7.2	0	25.9	23.5	0	0	0	56.6	1.4	14.2	15.6	72.2
5	Ru/Al-MCM-48 + TPA	0.5	0	2.6	7.5	18.7	8.2	17.4	54.9	2.7	40.9	43.6	98.5
6	Ru/MCM-48/TPA	0.8	1.4	2.5	4.2	2.2	0	0.5	11.6	64.8	26.9	91.7	>100

[a] Butane, [b] Methylcyclopentane, [c] Pentane, [d] Hexane, [e] 2,5-dimethyltetrahydrofuran [f] Sum of yields of 1- hexanol and 2-hexanol, [g] Sum of the yields to cyclopentane, cyclohexane and 2-hexanone, [h] Sum of the yield of the sugar alcohols (SA) , isosorbide and 1,4-sorbitan and [i] yield of the rest of soluble products calculated by diference between carbon obtained by HPLC and TOC measurements.

Ru/C was evaluated in the same reaction. In the absence of decane (not shown), the conversion of glucose was very fast and after 1h, only traces of polyols (mainly sorbitol) were analyzed in aqueous phase. After addition of decane, the reaction rate was much lower. After 20 h of reaction time around 34 % of the initial carbon still remained in the aqueous phase. Sugar alcohols were the major products in the aqueous phase with a carbon basis yield of 29.6 %. Regarding the concentration profiles in the aqueous phase for the reaction using Ru/C (Figure 7B), it is observed that D-Glucose is catalytically converted to alkanes through sorbitol pathway. D-Glucose was totally converted after 200 min and during this reaction time, different intermediates such as 1,4 - sorbitan, isosorbide, sorbitol, mannitol, xylitol and iditol were detected. As it was reported in a previous work, sorbitol is thermally more stable than D-Glucose, thus sorbitol hydrogenolysis looks like the slowest step of both [15]. Despite of this fact, after 20 h of reaction time, a considerable concentration of sorbitol around 6 $g \cdot l^{-1}$ (yield to sorbitol of 20.3 %) was detected in the aqueous phase, suggesting that Ru/C is not very active in this reaction media. On the one hand, after 20h, a total carbon basis yield of 29.2 % was obtained in the decane phase, where the major product of the process was n-hexane with a yield of 15.5 %. In addition, 9.8 % of pentane and 3.9 % of butane were also obtained in the organic phase. No other products were detected by GC-MS in the final product. During the loading of the reactor, it was observed that Ru/C was located in the n-decane phase. Carbon, which is acting as support in Ru/C, is not very functionalized and thus it is well-dispersed in a non-polar media. Therefore, the higher affinity of Ru/C for the organic phase limited further hydrogenolysis of sugar alcohols to alkanes. Sum of the yields from organic and aqueous phase was around 63 %, suggesting the production of gas phase alkanes such as methane or ethane, which were not analyzed in this experimental work [33, 34]. However, at the end of the experiment a slight increase in the reaction pressure from 5 MPa to 5.4 MPa. Liu et al. tested a Ru/C catalyst for the hydrogenolysis of D-Glucose in aqueous phase at 180 ºC and 4 MPa of H_2 achieving a carbon basis yield to hexane of 4.6 %, which is lower than that obtained in the present work [35]. However in that case, the major product of the process was methane with a yield around 67 %. Furthermore, Liu et al. reported the hydrolysis/hydrodeoxygenation of cellulose (230 ºC, 6 MPa H_2 and 24 h) over Ru/C reporting the outstanding catalytic behavior of this catalyst to cleavage C–O bonds and the C–C bonds, where 91 % carbon of cellulose was converted to C_1 – C_4 alkanes [36]. Only a 1.9 % of n-hexane and 2-methylpentane was produced in that case.

Comparing the catalytic activity of Ru/Al-MCM-48 and commercial Ru/C, the following partial conclusions were obtained:

i) According to the highest affinity of Al-MCM-48 for the aqueous phase, Ru/Al-MCM-48 allowed a higher conversion of the soluble carbon presented in the aqueous phase than Ru/C.

ii) Thus, the highest conversion of soluble carbon from the aqueous phase over Ru/Al-MCM-48 enhanced the production of a higher amount of alkanes than using Ru/C.

iii) The use of Ru/Al-MCM-48 improved approximately 1.9 times the yield to C4-C6 alkanes compared to that for Ru/C.

iv) Using Ru/Al-MCM-48 yield of n-pentane was slightly higher than that for n-hexane, while for Ru/C n- hexane was the major alkane detected in the final product. This fact can be attributed to the highest concentration of xylitol (around three times higher) obtained in the aqueous phase compared to that observed for Ru/C case. In general terms, hydrogenolysis of xylitol generates n-pentane [3].

Since different selectivities in C4-C6 alkanes were achieved in the presence of Ru/Al-MCM-48 compared to Ru/C, the influence of the presence of Al-MCM-48 together with Ru/C was evaluated.. In the selected combination of catalytic materials, Ru/C shows higher affinity for the organic phase and Al-MCM-48 for the aqueous phase. Looking at concentrations profiles for Ru/C + Al-MCM-48 (Figure 7C) D-Glucose was fully converted after 200 min following sorbitol reaction pathway. Thus, the addition of Al-MCM-48 did not improve the conversion rate of D-Glucose hydrogenation step. However, the presence of a solid acid catalyst in the aqueous phase plays an important role enhancing dehydrogenation of sugar alcohols. As it can be observed in Figure 7C and Table 3, a lower yield to sugar alcohols (carbon basis yield 18.2 %) in the aqueous phase was detected compared to that observed for Ru/C. Therefore, the addition of Al-MCM-48 allowed increasing conversion of soluble carbon in the aqueous phase in a 59 % in comparison with Ru/C case. An important yield of C4-C6 alkanes of 81.8 % was obtained by conversion of D-Glucose over Ru/C + Al-MCM-48, where n-hexane was the major product achieving a yield of 45.4 %. A yield of 29.3 of n-pentane and 7.1 % of n-butane were also obtained. Similar attempts for this purpose have been reported combining noble metal catalysts with other catalytic

materials. Ma et al. used a combined system comprising Ni/H-ZSM-5 catalyst modified with pure silica MCM-41 and they reported a production of liquid alkanes from sorbitol around 66 % [13]. Chen et al. combined different metal catalyst (Ru/C, Pt/C, skeletal Ni) with H-ZSM-5 in aqueous phase for the conversion of sorbitol [3]. In that work, if almost Ru/C + H-ZSM-5 were able to convert all sorbitol presented in the aqueous phase, a lower amount of n-hexane around 13 % was obtained than that achieve for Ru/C + Al-MCM-48 presented in this work. Ru/C + H-ZSM-5 demonstrated higher selectivity to produce $C_1 - C_5$ alkanes, with a yield of 35.1 %. Skeletal Ni and Pt/C combined with H-ZSM-5 shown very low and practically no activity for this purpose, respectively.

Different authors have tested the behavior of heteropolyacids such as tungstophosphoric acid in this kind of processes. In order to enhance the acidity of the reaction media (in terms of number of acid sites and strength), Ru/C, Ru/MCM-48 and Ru/Al-MCM-48 were tested for the conversion of D-Glucose into alkanes using TPA as additive. Figure 7 D shown the evolution of detected compounds in the water phase when Ru/C was used with TPA. It was observed that the formation of sugar alcohols is not favored with the combination of Ru/C and the tungstophosphoric acid, however, it allowed converting most of the carbon presented in the aqueous phase. Thus, the low concentration of sugar alcohols detected suggested that the presence of TPA, avoided isosorbide production, while sugars dehydratation is kinetically favored to furans derivatives formation (Table 3). Indeed, 9% DMTHF was analyzed in the decane phase together with 78.5% of C4-C6 alkanes including 8.3 % of cyclopentane, cyclohexane and methylcyclopentane [6, 12, 37].

Then, Ru/MCM-48/TPA was also tested showing poor results in terms of alkanes formation. Comparing the catalytic behavior of Ru/MCM-48/TPA with the rest of the catalysts employed in this work, it is clear that this catalytic system led to meaningfully less alkane production, while yield to sugar alcohols noticeably increased. In this case, yield to sugar alcohols was 64.8 %, where the main compound was 1,4-sorbitan (28.9 %), followed by sorbitol (21.5 %), mannitol (11.5 %) and isosorbide (2.9 %) This difference can be attributed to the higher ability of this catalyst for the hydrogenation of glucose than for further dehydratation/hydrodeoxygenation processes. Moreover, Ru/MCM-48/TPA showed a lower amount of total acid sites (Table 2) in comparison

with Ru/Al-MCM-48. Therefore, lower acidity values resulted in a high concentration of sugar alcohols in the aqueous phase, which were not converted to alkanes. Textural properties of mesoporous materials are an important factor for their employment in the conversion of organic molecules such as those derived from biomass feedstocks [38], avoiding diffusional problems. The presence of TPA in MCM-48 resulted in a significantly decrease of the long-range order of the final material. In addition, Ru/MCM-48/TPA presented lower surface area and pore volume compared to Ru/Al-MCM48. All these facts can be responsible of the poor catalytic behavior of Ru/MCM-48/TPA for the conversion of D-Glucose into alkanes. Blasco et al. reported the formation of clusters at high loadings of TPA, which can block the pores of the mesoporous silica catalyst and as a consequence the catalytic activity in the alkylation reaction decreased [39].

Similar behavior than that observed for Ru/C + TPA, was also detected for Ru/Al-MCM-48 + TPA. Although using Ru/Al-MCM-48 + TPA, 43.6% of carbon was still present in the aqueous phase where only a 2.7 % belongs to sugar alcohols. As observed with Ru/C + TPA, in the presence of Ru/Al-MCM-48 combined with TPA, 18.7 % of 2,5–dimethyltetrahydrofuran (DMTHF) produced by hydrogenation of 5-HMF was analyzed in the organic phase. DMTHF presented a high octane number and high energy content, thus it appears as a very interesting material for replacing gasoline directly [40]. This fact confirms that the combination of ruthenium-based catalyst and heteropolyacid conducted the reaction through 5-HMF. Therefore, the high yield of soluble products detected in the aqueous phase can be attributed to furan derivatives when Ru/Al-MCM-48 + TPA were used. In addition, the formation of 1-hexanol and 2-hexanol was observed by using Ru/C and Ru/Al-MCM-48 combined with TPA. Just in case of Ru/Al-MCM-48 + TPA a yield of 3.5 % of 2 – hexanone was also identified. Ru/C + TPA demonstrated to be very effective for the conversion of D-Glucose into C4-C6 alkanes achieving a global yield of 78.5 %, while in the presence of of Ru/Al-MCM-48 + TPA 20.1 % of C4-C6 alkanes were produced. Ru/Al-MCM-48 demonstrated to be more active than Ru/C in order to produce alkanes, however, this tendency is inverted when TPA is added to the reaction media. As it was previously explained, Ru/C showed higher affinity for organic phase and Ru/Al-MCM-48 higher affinity for the aqueous phase. Thus, this fact join to the presence of TPA in the aqueous solution is a drawback for Ru/Al-MCM-48, which does not seem such an effective combination for the conversion of D-Glucose to alkanes through HMF pathway.

However, in the case of Ru/C its higher affinity for n-decane favored the production of higher yields of C4-C6 alkanes in the presence of TPA, since more of the carbon presented in the aqueous phase is converted than using Ru/Al-MCM-48. In addition, higher yields of intermediates presented in the organic phase such as DMTHF or hexanols were observed for Ru/Al-MCM-48 + TPA, suggesting lower activity of this system than Ru/C + TPA for their conversion to alkanes as well. Op de Beck et al used a combination of Ru/C and tungstosilicic acid (TSA) for the conversion of microcrystalline cellulose into liquid alkanes [6]. In that work, Ru/C showed a yield of 19 % to n-hexane and 13.1 % to n-pentane. Additionally, Liu et al. reported the conversion of cellulose over a combination of Ru/C and H_3PO_4 achieving a total yield of alkanes around 55%, where the major compound in the final product was n-hexane + i-hexane (yield 23.3 %). Yields of 12.4 % of n-pentane and 6.9 % of C_1-C_4 alkanes were also detected in that work [36].

4. CONCLUSIONS

In this work a one-pot approach for the catalytic conversion of D-Glucose into short-chain alkanes have been developed, where the partial goals achieved can be listed as follows:

i) Al-MCM-48 presented interesting textural properties for the diffusion of large molecules derived from biomass. Moreover, the introduction of Al into the silica matrix resulted in a noticeable improvement of the acidic properties of the material compared to MCM-48.

ii) Ru/Al-MCM-48 and Ru/MCM-48/TPA shown very narrow ruthenium nanoparticle size distributions with surface-area weighted diameter around 2 nm in both cases.

iii) Ru/Al-MCM-48 demonstrated better catalytic behavior than commercial Ru/C for the conversion of D-Glucose into short-chain alkanes such as n-butane, n-pentane and n-hexane (yields 56.6 % and 29.2 %, respectively). The use of Ru/Al-MCM-48 improved approximately 1.9 times the yield to alkanes compared to that obtained for Ru/C.

iv) Combination of Al-MCM-48 and Ru/C promoted a significant increase in conversion of soluble carbon in the aqueous phase in a 59 % compared to commercial Ru/C. An important improvement of the final yield to alkanes around 180 % was obtained by conversion of D-Glucose over Ru/C + Al-MCM-

48, where n-hexane (yield 45.4 %) and n-pentane (yield 29.3 %) where the main compounds.

v) The presence of TPA in the aqueous solution conducted the reaction through HMF pathway. Combination of Ru/C and TPA demonstrated a good catalytic behavior producing alkanes (yield 78.5 %).

vi) Combinations of TPA and Ru-based mesoporous materials did not result in an improvement of alkanes production.

The production of bio-derived naphtha fractions from renewable sources such as lignocellulosic biomass is a promising reaction route that helps to reduce the actual dependence of our society on fossil fuels and to mitigate problems derived from global warming issues. These naphtha fractions are very useful for their implementation as green raw materials in the production of gasolines, olefins and aromatics.

Acknowledgements

The authors gratefully acknowledge the Spanish Ministry, MINECO, and FEDER founds for the financial support of this project CTQ2015-64892-R (MINECO/FEDER). A. Romero thanks to the program of predoctoral scholarships from Junta de Castilla y León Government for his grant (E-47-2015-0062773).

References

1. Rinaldi, R. and F. Schuth, *Design of solid catalysts for the conversion of biomass.* Energy & Environmental Science, 2009. **2**(6): p. 610-626.

2. Huber, G.W., S. Iborra, and A. Corma, *Synthesis of Transportation Fuels from Biomass: Chemistry, Catalysts, and Engineering.* Chemical Reviews, 2006. **106**(9): p. 4044-4098.

3. Chen, K., et al., *One-Pot Conversion of Sugar and Sugar Polyols to n-Alkanes without C□C Dissociation over the Ir-ReOx/SiO2 Catalyst Combined with H-ZSM-5.* ChemSusChem, 2013. **6**(4): p. 613-621.

4. Liu, S., et al., *One-Pot Conversion of Cellulose into n-Hexane over the Ir-ReOx/SiO2 Catalyst Combined with HZSM-5.* ACS Sustainable Chemistry & Engineering, 2014. **2**(7): p. 1819-1827.

5. Matson, T.D., et al., *One-Pot Catalytic Conversion of Cellulose and of Woody Biomass Solids to Liquid Fuels.* Journal of the American Chemical Society, 2011. **133**(35): p. 14090-14097.

6. Op de Beeck, B., et al., *Direct catalytic conversion of cellulose to liquid straight-chain alkanes.* Energy & Environmental Science, 2015. **8**(1): p. 230-240.

7. Li, N., G.A. Tompsett, and G.W. Huber, *Renewable High-Octane Gasoline by Aqueous-Phase Hydrodeoxygenation of C5 and C6 Carbohydrates over Pt/Zirconium Phosphate Catalysts.* ChemSusChem, 2010. **3**(10): p. 1154-1157.

8. Chheda, J.N., G.W. Huber, and J.A. Dumesic, *Liquid-Phase Catalytic Processing of Biomass-Derived Oxygenated Hydrocarbons to Fuels and Chemicals.* Angewandte Chemie International Edition, 2007. **46**(38): p. 7164-7183.

9. Liu, Y., et al., *One-Pot Catalytic Conversion of Raw Lignocellulosic Biomass into Gasoline Alkanes and Chemicals over LiTaMoO6 and Ru/C in Aqueous Phosphoric Acid.* ACS Sustainable Chemistry & Engineering, 2015. **3**(8): p. 1745-1755.

10. Liao, Y., et al., *Promoting Hydrolytic Hydrogenation of Cellulose to Sugar Alcohols by Mixed Ball Milling of Cellulose and Solid Acid Catalyst.* Energy & Fuels, 2014. **28**(9): p. 5778-5784.

11. Huber, G.W., R.D. Cortright, and J.A. Dumesic, *Renewable Alkanes by Aqueous-Phase Reforming of Biomass-Derived Oxygenates.* Angewandte Chemie International Edition, 2004. **43**(12): p. 1549-1551.

12. Kunkes, E.L., et al., *Catalytic Conversion of Biomass to Monofunctional Hydrocarbons and Targeted Liquid-Fuel Classes.* Science, 2008. **322**(5900): p. 417-421.

13. Zhang, Q., et al., *Highly Selective Sorbitol Hydrogenolysis to Liquid Alkanes over Ni/HZSM-5 Catalysts Modified with Pure Silica MCM-41.* ChemCatChem, 2012. **4**(8): p. 1084-1087.

14. Romero, A., et al., *Conversion of biomass into sorbitol: Cellulose hydrolysis on MCM-48 and d-Glucose hydrogenation on Ru/MCM-48.* Microporous and Mesoporous Materials, 2016. **224**: p. 1-8.

15. Romero, A., et al., *Supercritical water hydrolysis of cellulosic biomass as effective pretreatment to catalytic production of hexitols and ethylene glycol over Ru/MCM-48.* Green Chemistry, 2016.

16. Kusema, B.T., et al., *Hydrolytic hydrogenation of hemicellulose over metal modified mesoporous catalyst.* Catalysis Today, 2012. **196**(1): p. 26-33.

17. Romero, A., A. Nieto-Márquez, and E. Alonso, *Bimetallic Ru:Ni/MCM-48 catalysts for the effective hydrogenation of d-glucose into sorbitol.* Applied Catalysis A: General, 2017. **529**: p. 49-59.

18. Schumacher, K., M. Grün, and K.K. Unger, *Novel synthesis of spherical MCM-48.* Microporous and Mesoporous Materials, 1999. **27**(2–3): p. 201-206.

19. Schumacher, K., et al., *Characterization of MCM-48 Materials.* Langmuir, 2000. **16**(10): p. 4648-4654.

20. Zhang, Y. and S. Yang, *Synthesis, characterization and catalytic application of H3PW12O40/MCM-48 in the esterification of methacrylic acid with n-butyl*

alcohol. Journal of Wuhan University of Technology-Mater. Sci. Ed., 2008. **23**(3): p. 346-349.

21. Amorim, C. and M.A. Keane, *Palladium supported on structured and nonstructured carbon: A consideration of Pd particle size and the nature of reactive hydrogen.* Journal of Colloid and Interface Science, 2008. **322**(1): p. 196-208.

22. Schmidt, R., et al., *High-resolution electron microscopy and X-ray diffraction studies of MCM-48.* Microporous Materials, 1995. **5**(1–2): p. 1-7.

23. Meng, J., et al., *Assembling of Al-MCM-48 supported H3PW12O40 mesoporous materials and their catalytic performances in the green synthesis of benzoic acid.* Materials Research Bulletin, 2014. **60**: p. 20-27.

24. Wu, H.-Y., et al., *Preparation, characterization and catalytic properties of MCM-48 supported tungstophosphoric acid mesoporous materials for green synthesis of benzoic acid.* Journal of Solid State Chemistry, 2014. **211**: p. 51-57.

25. Brunauer, S., et al., *On a Theory of the van der Waals Adsorption of Gases.* Journal of the American Chemical Society, 1940. **62**(7): p. 1723-1732.

26. Thommes, M., R. Köhn, and M. Fröba, *Systematic Sorption Studies on Surfce and Pore Size Characteristics of Different MCM - 48 Silica Materials*, in *Studies in Surface Science and Catalysis*, G.K. K.K. Unger and J.P. Baselt, Editors. 2000, Elsevier. p. 259-268.

27. Madhusudhan Rao, P., et al., *Immobilization of molecular H3PW12O40 heteropolyacid catalyst in alumina-grafted silica-gel and mesostructured SBA-15 silica matrices.* Journal of Catalysis, 2005. **232**(1): p. 210-225.

28. Jae-Soon Choi, V.S., Eduardo Santillan-Jimenez, Mark Crocker, Samuel A. Lewis Sr., Michael J. Lance, Harry M. Meyer and Karren L. More, *Structural Evolution of Molybdenum Carbides in Hot Aqueous Environments and Impact on Low-Temperature Hydroprocessing of Acetic Acid.* Catalysts, 2015. **5**.

29. Manyar, H.G., et al., *Deactivation and regeneration of ruthenium on silica in the liquid-phase hydrogenation of butan-2-one.* Journal of Catalysis, 2009. **265**(1): p. 80-88.

30. Hu, J., et al., *Highly effective Ru/CMK-3 catalyst for selective reduction of nitrobenzene derivatives with H2O as solvent at near ambient temperature.* RSC Advances, 2016. **6**(4): p. 3235-3242.

31. Eliche-Quesada, D., et al., *Influence of the incorporation of palladium on Ru/MCM hydrotreating catalysts.* Applied Catalysis B: Environmental, 2006. **65**(1–2): p. 118-126.

32. Palkovits, R., et al., *Hydrogenolysis of cellulose combining mineral acids and hydrogenation catalysts.* Green Chemistry, 2010. **12**(6): p. 972-978.

33. Li, N., et al., *Renewable gasoline from aqueous phase hydrodeoxygenation of aqueous sugar solutions prepared by hydrolysis of maple wood.* Green Chemistry, 2011. **13**(1): p. 91-101.

34. Fabicovicova, K., et al., *Hydrogenolysis of cellulose to valuable chemicals over activated carbon supported mono- and bimetallic nickel/tungsten catalysts.* Green Chemistry, 2014. **16**(7): p. 3580-3588.

35. Liu, C., et al., *Aqueous-phase hydrogenolysis of glucose to value-added chemicals and biofuels: A comparative study of active metals.* Biomass and Bioenergy, 2015. **72**: p. 189-199.

36. Liu, Y., et al., *High yield of renewable hexanes by direct hydrolysis-hydrodeoxygenation of cellulose in an aqueous phase catalytic system.* RSC Advances, 2015. **5**(15): p. 11649-11657.

37. Rosatella, A.A., et al., *5-Hydroxymethylfurfural (HMF) as a building block platform: Biological properties, synthesis and synthetic applications.* Green Chemistry, 2011. **13**(4): p. 754-793.

38. Stöcker, M., *Biofuels and Biomass-To-Liquid Fuels in the Biorefinery: Catalytic Conversion of Lignocellulosic Biomass using Porous Materials.* Angewandte Chemie International Edition, 2008. **47**(48): p. 9200-9211.

39. Blasco, T., et al., *Supported heteropolyacid (HPW) catalysts for the continuous alkylation of isobutane with 2-butene: The benefit of using MCM-41 with larger pore diameters.* Journal of Catalysis, 1998. **177**(2): p. 306-313.

40. Jiang, Y., et al., *Chemical Conversion of Biomass to Green Chemicals*, in *Sustainable Production of Bulk Chemicals: Integration of Bio-Chemo-Resources and Processes*, M. Xian, Editor. 2015, Springer Netherlands: Dordrecht. p. 19-49.

CONCLUSIONS

CONVERSION OF CELLULOSIC BIOMASS TOWARDS ADDED VALUE PRODUCTS OVER BIFUNCTIONAL CATALYSTS.

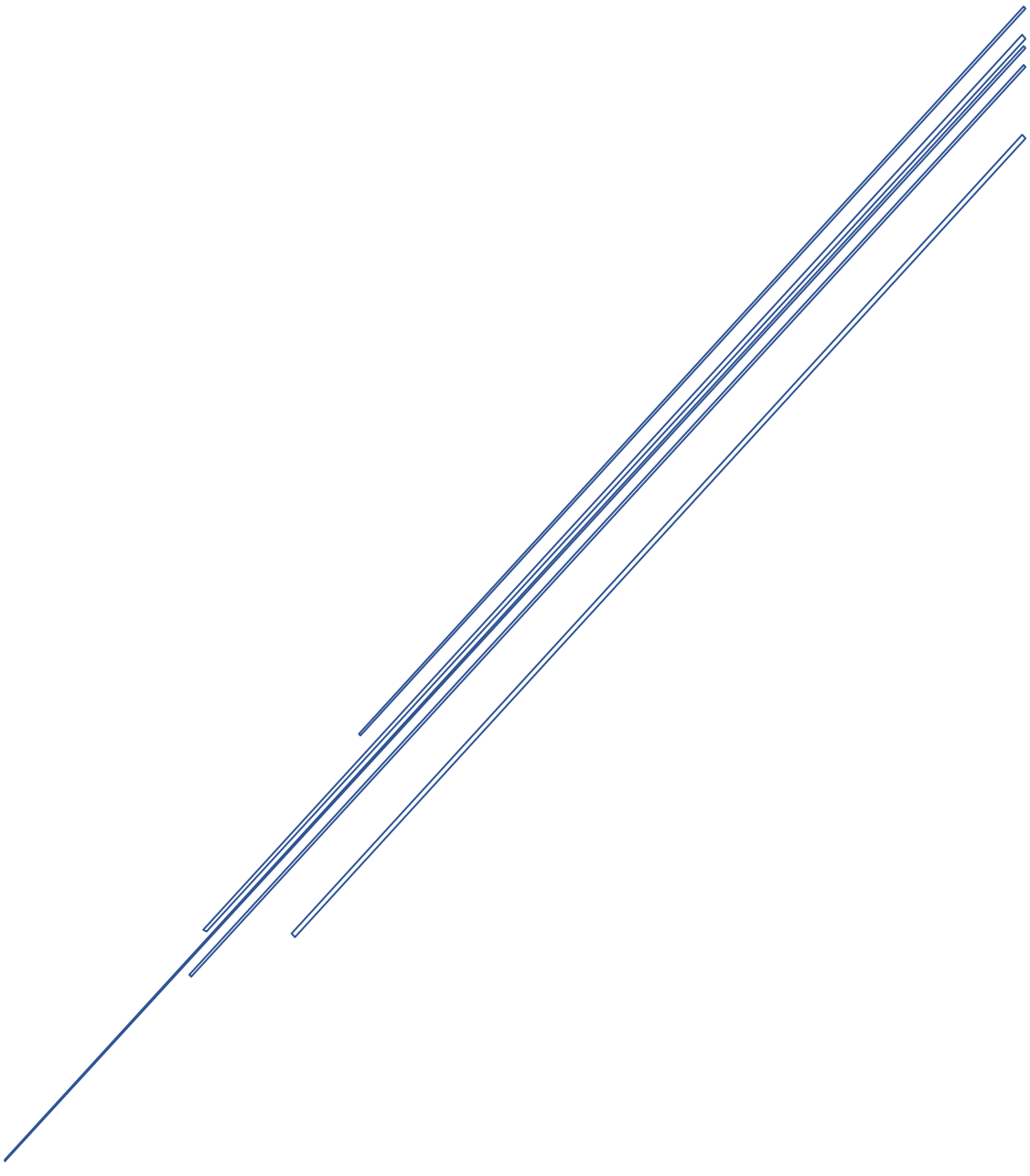

The present PhD thesis is a contribution to the development of novel supported Ru and Ni mesoporous catalysts for their application in the conversion of cellulosic biomass into a wide range of products such as hexitols, ethylene glycol and short-chain alkanes. Moreover, this work has meant the start-up of a new research topic in the High Pressure processes Group at the University of Valladolid.

The main conclusions of the overall work are presented below:

- Synthesis and characterization of mesoporous catalysts based on Ru and Ni.
  - Correct preparation of the following catalysts: MCM-48, Al-MCM-48, MCM-48/TPA, Ru/MCM-48, Ru/Al-MCM-48, Ru/MCM-48/TPA, Ni/MCM-48 and Ru:Ni/MCM-48.
  - The aforementioned catalytic materials were characterized by means of different techniques such as adsorption / desorption isotherms of N_2, SAXS, XRD, H_2-TPR, NH_3-TPD, SEM, TEM and AA.
  - In general terms, all the catalysts presented relatively high specific surface area and pore volume, pore size in the mesoporous range, which are very interesting properties in order to avoid diffusional problems in the valorization of biomass. The so prepared catalysts shown bifunctionality, presenting acid sites where hydrolysis and dehydration processes take place, while hydrogenation steps are developed in the active metal sites of the catalyst.
- An experimental set-up for the catalytic hydrogenolysis of cellulosic biomass has been developed and starting-up.

- Catalytic activity tests of the synthesised catalyst.
  - MCM-48 promoted selective hydrolysis of cellulose towards D-Glucose due to to its weakly acidity related to terminal silanol groups (-SiOH). MCM-48 outperformed the catalytic behaviour of commercial TiO_2 and Ru/C for the hydrolysis of cellulose, achieving around 4- and 47-folds higher yields to D-Glucose, respectively.
  - Ru/MCM-48 demonstrated to be a potential alternative to classical catalytic materials used in the hydrogenation of D-Glucose such as Ru/C or Ru/TiO_2, showing high comparable specific activity to those materials. Ru/MCM-48 showed complete selectivity to sorbitol working at temperatures in between 80 and 120 ºC and pseudo-first order dependency was observed respect to D-

Glucose. Ru/MCM-48 showed lower activation energy value (45 KJ·mol^{-1}) in comparison with commercial Ru/C and prepared Ru over commercial TiO_2 (52 and 86 KJ·mol^{-1}, respectively). In addition, recycling test of Ru/MCM-48 confirmed the good stability of the catalyst after three reaction cycles.

- A low specific activity of monometallic Ni/MCM-48 was noticed in the hydrogenation of D-Glucose, showing selectivities to sorbitol in the range of 93-95 %. However, the presence of bimetallic Ru:Ni ratios higher than 0.45 over MCM-48 significantly improved the specific activity of Ni/MCM-48, efficiently converting D-Glucose to sorbitol (100 % selectivity). Pseudo-first order dependency respect to D-Glucose was also observed when Ni/MCM-48 and Ru:Ni/MCM-48 were used as catalysts. Activation energies of 36 and 70 KJ·mol^{-1} were obtained for Ni/MCM-48 and Ru:Ni/MCM-48 (0.45), respectively. As well as Ru/MCM-48, Ru:Ni/MCM-48 demonstrated a good stability after three reaction cycles under the experimental conditions.
- Ru/Al-MCM-48 was successfully tested in the hydrogenolysis of cellobiose, achieving a high yield of hexitols around 91 % at 180 ºC, 5 MPa of H_2 and 7 min. A significantly effect of increasing temperature and pressure, from 140 to 180 ºC and 3 to 5 MPa H_2, was noticed in order to maximize final yield to hexitols, respectively. The developed catalytic kinetic model predicted well the concentration of all the compounds involved in the proposed overall reaction pathway.
- Better textural properties and acid features of Ru/MCM-48 compared to commercial Ru/C, promoted hydrolysis step in one-pot hydrogenation of cellulose, enhancing final yield to hexitols. A yield of hexitols around 21 % was obtained over Ru/MCM-48 in one-pot hydrogenation of cellulose at 240 ºC, 5 MPa H_2 and 10 min, while under comparable experimental conditions commercial Ru/C achieved a yield to hexitols around 6 %A novel valorization scheme for plant combining both, the ability of SCW hydrolysis to depolymerize cellulose selectively and the hydrogenation process using the synthesized catalyst Ru/MCM-48 was proposed as an alternative to one-pot process. SCW hydrolysis demonstrated to be an excellent hydrolysis stage for using cellulosic material to produce polyols. Final yield to hexitols increased almost 2.3 times compared to one-pot hydrogenation of cellulose. The use of Ru/MCM-48 is highly beneficial, promoting the hydrolysis of the obtained oligosaccharides

from SCW step to D-Glucose selectively increasing the glucose production from 8.6 % to 55.7 %. Moreover, this catalyst demonstrated a high selectivity converting D-Glucose into hexitols, obtaining a yield to hexitols of 48.5 %, which represents a sugar to hexitols conversion yield around 88 %.In addition, when the proposed two-steps process was checked for Sugar Beet Pulp valorization. glycolaldehyde was produced with high yields from SCW hydrolysis of biomass, and it was selectively converted into ethylene glycol (yield of 21 %).

- Ru/Al-MCM-48 outperformed catalytic behaviour of commercial Ru/C for the conversion of D-Glucose into short-chain alkanes, achieving around 1.9-folds higher yields to alkanes (57 and 29 %, respectively). Ru/MCM-48/TPA demonstrated a good catalytic response to produce sugar alcohols, while its activity for further dehydration and hydrodeoxygenation steps was limited. The presence of TPA in the aqueous medium conducted the reaction through the formation of HMF pathway. Combination of Ru/C + TPA enhanced final yield to alkanes up to 79 %. In addition, combination of Al-MCM-48 + Ru/C promoted conversion of soluble carbon in the aqueous phase in comparison with Ru/C, resulting in an important enhancement of the final yield to alkanes (82 %).

FUTURE WORK

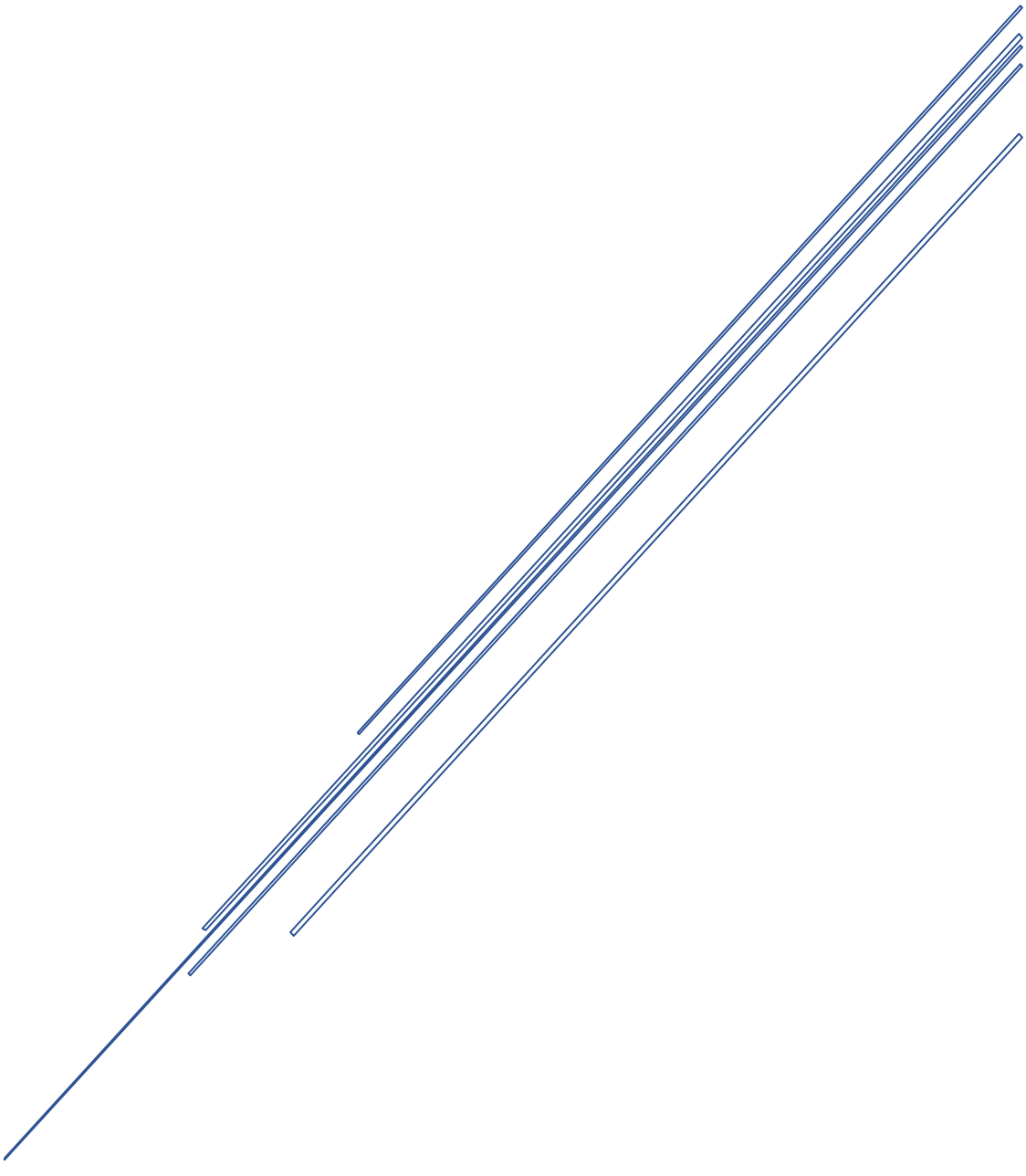

Further studies could be conducted following the work developed in this thesis. Different catalysts were prepared in this work, but only Ru/MCM-48 was tested in the conversion of cellulose or real biomass. Thus, Ru:Ni/MCM-48 and Ru/Al-MCM-48 could be used for the catalytic hydrogenation of cellulose, oligosaccharides from cellulosic biomass or real biomass towards sugar alcohols. In order to carry out these tasks, the implementation of a gas sampling system could be very helpful in order to close in a better way the mass balances of the overall process.

In addition, according to the good catalytic behaviour of the materials prepared in this thesis for the production of sugar alcohols from cellulosic biomass, they will be also tested for the hydrogenation of hemicelluloses to produce mainly arabitol, galactitol and xylitol. Regarding the interesting properties of mesoporous silica materials, they could be used as catalyst to promote the extraction and hydrolysis of arabinoxylans from destarched wheat bran by hydrothermal methods. These tasks have been scheduled in the PhD theis of *Gianluca Gallina and Nuria Sánchez*.

Apart from the research developed during the last years related to catalytic conversion of biomass into chemicals, it could be very interesting to take into account polysaccharides from different sources as excellent precursor for the preparation of polymer cryo-, xero- and aerogels and porous carbon. In their native form, polysaccharides have a low specific surface area and porosity. Therefore, the enhancement of the textural properties of these polymers seems vital for the preparation of materials for applications where surface interactions (catalytic liquid phase reactions) and mass transfer limitations (i.e. chromatography) are critical. This idea have been motivated by the interesting results obtained by *Dr. Luis Miguel Sanz, Dr. Ana Najwa and Dr. Marta Salgado* in previous research work developed in this field in the High Pressure Research Group of University of Valladolid. Therefore, the idea will be to developed porous materials based on cellulose and sugar beet pulp oligosaccharides and their transformation to carbonaceous materials by pyrolysis. In this sense, the so obtained carbon-based materials could be an interesting alternative for many applications such as catalysis, separation chromatography of complex mixtures, purification of water or recovery of precious metals. This approach could also act to valorise low value polysaccharides.

RESUMEN

CONVERSIÓN DE BIOMASA LIGNOCELULÓSICA EN COMPUESTOS DE ALTO VALOR AÑADIDO MEDIANTE CATALIZADORES BIFUNCIONALES.

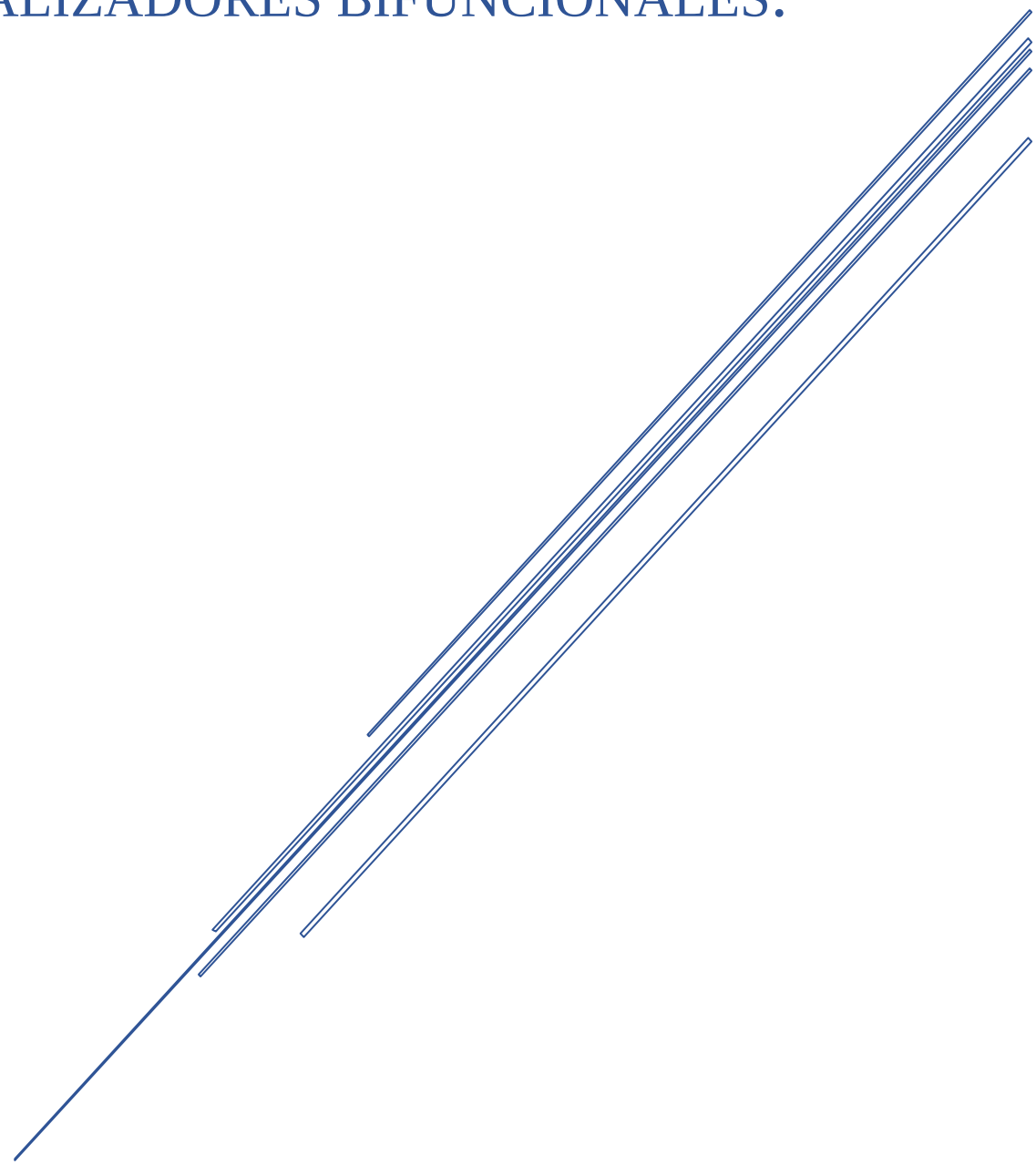

Durante los últimos años, la utilización de biomasa como materia prima para la obtención de combustibles, energía y compuestos químicos está atrayendo mucha atención y cada vez hay más ejemplos de procesos de biorefinería implantados a escala industrial. La utilización de biomasa contribuiría a la reducción del calentamiento global y a la construcción de una sociedad menos dependiente de los combustibles fósiles integrándose además dentro del concepto de economía circular de recurso-producto-reciclado. Se estima que en un futuro próximo alcanzaremos el pico de petróleo (máxima producción de combustibles fósiles), y por tanto, hay una demanda urgente de utilización de otras fuentes de carbón para sintetizar productos químicos sin aumentar las emisiones de CO_2. La biomasa es una de estas fuentes alternativas a los combustibles fósiles. El avance de los procesos de conversión de biomasa, pasa por desarrollar procesos selectivos y competitivos en los que la catálisis heterogénea juega un papel fundamental. Un adecuado diseño del catalizador puede ser la base del proceso desde el punto de vista económico y medioambiental. Todos los costes de producción (costes variables como el de materias primas, energía y tratamiento de residuos, así como los costes fijos, como la depreciación, el personal y los costes de mantenimiento) se reducen con la mejora del catalizador. Parámetros como el tamaño de partícula, porosidad, área específica, y propiedades superficiales del mismo son clave para el desarrollo de estos procesos.

Para lograr una sociedad sostenible, el diseño de los procesos químicos necesita cambiar desde las producciones masivas a gran escala actuales, a procesos descentralizados de menor escala de producción donde tanto las materias primas como la energía puedan ser suministradas por biomasa y otras fuentes renovables. La industria química basada en biomasa puede ser capaz de producir, utilizando energías renovables como la solar y medios de reacción amables con el medio ambiente, tanto energía como compuestos químicos base “building blocks“ tales como glucosa, etilenglicol, o polioles en general, ácido láctico, glutárico, o succínico, etc. Estas moléculas pueden transformarse fácilmente en productos de alto valor añadido. Este proceso es conocido como “biorrefino”.

Los principales constituyentes de la biomasa lignocelulósica son la celulosa, las hemicelulosas y la lignina, y este proyecto de tesis se centra en la conversión de celulosa y sus derivados. Una alternativa tecnológica para el desarrollo de una sociedad sostenible que utilice celulosa como materia prima, pasa por el desarrollo del proceso de

conversión selectiva de celulosa utilizando condiciones suaves hidrotermales y catalizadores selectivos. El proceso global objeto de estudio se divide fundamentalmente en dos etapas consecutivas. En primer lugar, la celulosa se tiene que depolimerizar mediante hidrólisis para obtener glucosa como molécula plataforma. Se han observado diferentes alternativas para esta etapa en la literatura, como enzimas, ácidos homogéneos o agua supercrítica. En segundo lugar, la glucosa y azúcares obtenidos de la etapa de hidrólisis son hidrogenados mediante un metal activo para la obtención de alcoholes de azúcares. En esta segunda etapa, la elección del metal es crucial en términos de actividad y selectividad hacia los productos de interés.

De acuerdo con las necesidades requeridas en los procesos a estudiar, se propone como objetivo general de la tesis el estudio del comportamiento de catalizadores metálicos soportados en sílices mesoporosas para la conversión efectiva de celulosa y de sus compuestos modelo derivados en alcoholes. Un esquema de las etapas involucradas se recoge en el Esquema 1. Los materiales mesoporosos de sílice se eligieron como soporte debido a que presentan una estructura porosa con propiedades muy interesantes para evitar problemas difusionales de moléculas grandes en aplicaciones catalíticas, además de presentar buena estabilidad térmica. Debido a su remarcable actividad en reacciones de hidrogenación, el rutenio y el níquel fueron seleccionados como metales activos.

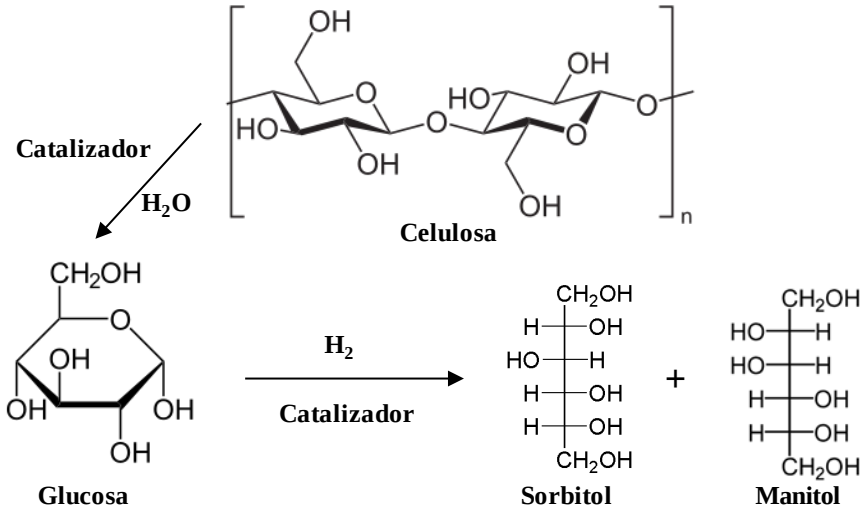

Esquema 1. Etapas del proceso de obtención de alcoholes a partir de celulosa

Este objetivo general, se lleva a cabo mediante la consecución de los siguientes objetivos parciales:

- Sintetizar materiales de sílice mesoporosa como soportes de catalizador utilizando la metodología sol-gel.

  Se sintetizaron diferentes soportes mediante la metodología sol-gel. Por lo tanto, se sintetizaron los soportes MCM-48 y Al-MCM-48. Además, la MCM-48 se modificó con ácido tungstofosfórico (TPA) obteniéndose el soporte MCM-48/TPA.

- Sintetizar catalizadores monometálicos de rutenio y níquel.

  Tanto rutenio como níquel fueron depositados sobre MCM-48 mediante el método de impregnación húmeda. El rutenio también se depositó sobre Al-MCM-48 y MCM-48/TPA mediante el mismo método de preparación.

- Síntesis de catalizadores bimetálicos basados en rutenio y níquel.

  Rutenio y níquel fueron depositados de manera conjunta sobre la MCM-48, mediante impregnaciones húmedas consecutivas.

- Caracterizar los soportes y catalizadores sintetizados, desde el punto de vista químico, estructural y morfológico.

  Los materiales desarrollados fueron caracterizados para estudiar las diferentes características de los mismos. Se analizaron propiedades texturales, morfología, dispersión del metal sobre el soporte. Interacciones entre metal y soporte, estado metálico, acidez y carga metálica.

- Diseñar y construir una planta experimental para desarrollar estudios de hidrogenación de biomasa en medio hidrotermal.

- Estudiar el comportamiento catalítico de los materiales sintetizados en las reacciones de:
  - Hidrólisis de celulosa sobre diferentes materiales catalíticos. Estudio sobre la influencia de la acidez de dos soportes como son la MCM-48 y el TiO_2 comparándolo con un catalizador comercial de Ru/C de referencia en bibliografía.

- Hidrogenación de D-Glucosa en hexitoles. Comparación del comportamiento catalítico del Ru/MCM-48, con respecto a Ru/C comercial y Ru depositado sobre un soporte comercial de TiO_2. Comparación de la actividad del catalizador monometálico de níquel Ni/MCM-48, frente a la de diferentes catalizadores bimetálicos de rutenio y níquel Ru:Ni/MCM-48. Cálculo de la actividad específica y energías de activación. Reutilización de los catalizadores sintetizados.
- Hidrólisis/hidrogenación de celobiosa sobre Ru/Al-MCM-48. Estudio del efecto de la temperatura y la presión de H_2 para maximizar el rendimiento final en hexitoles. Desarrollo de un modelo cinético y del mecanismo de reacción, cubriendo las condiciones experimentales estudiadas.
- Hidrólisis/hidrogenación de celulosa para la obtención de hexitoles en una sola etapa ("One-pot"). Evaluación del comportamiento catalítico del Ru/MCM-48 en comparación con un Ru/C comercial.
- Hidrólisis de celulosa en medio supercrítico + hidrogenación de los productos obtenidos (proceso en dos etapas). Utilización de la hidrolisis de celulosa en agua supercrítica como etapa previa a la de hidrogenación de azúcares para mejorar la producción de hexitoles. Comparación entre el proceso en una etapa y el de dos etapas. Prueba del proceso en dos etapas para una biomasa real (pulpa de remolacha).
- Conversión de D-Glucosa en alcanos lineales sobre Ru/Al-MCM-48, Ru/MCM-48/TPA y Ru/C comercial. Estudio de la influencia del TPA combinado con los catalizadores en la reacción. Influencia del Al-MCM-48 mejorando la actividad catalítica del catalizador comercial de Ru/C.

La presente tesis ha sido estructurada en cinco capítulos experimentales. En cada uno de ellos se realiza una revisión bibliográfica que permite conocer los principales logros conseguidos en el campo de investigación seleccionado. Además, se presentan los objetivos parciales de cada uno de los capítulos y los resultados correspondientes. Los contenidos más relevantes de cada capítulo se presentan a continuación.

En el **Capítulo 1** titulado "*Conversion of biomass into sorbitol: Cellulose hydrolysis on MCM-48 and D-Glucose hydrogenation on Ru/MCM-48"*, se desarrolla la

síntesis y caracterización de un catalizador bifuncional que tiene como soporte MCM-48 y rutenio como fase metálica, para estudiar la hidrogenación de glucosa y la hidrólisis de celulosa sobre MCM-48. El soporte MCM-48 presenta una superficie específica elevada y acidez débil, las cuales son propiedades interesantes para favorecer la etapa de hidrólisis de celulosa en glucosa, incrementando el acceso a sitios ácidos de los oligómeros intermedios. Por otro lado, el rutenio actúa como metal activo para la hidrogenación de D-Glucosa. Por lo tanto, en este capítulo se han estudiado las etapas individuales de la conversión de celulosa en sorbitol, de modo que se pueda alcanzar un mayor entendimiento del rol que juegan la acidez del soporte y la actividad del rutenio en la hidrólisis de celulosa y la hidrogenación de D-Glucosa, respectivamente. La actividad del catalizador Ru/MCM-48 ha sido evaluada en comparación con un catalizador de Ru impregnado sobre TiO_2 comercial y un catalizador comercial de Ru/C.

En una primera etapa se realizó el estudio preliminar del comportamiento en hidrólisis de celulosa de las sílices mesopororas que de forma general se iban a utilizar de soporte catalítico en la tesis. Se evaluó el comportamiento catalítico de la MCM-48 en comparación con el de un TiO_2 comercial y con Ru/C comercial que otros autores estaban utilizando como referencia en bibliografía. En el caso del Ru/C no se ha encontrado el soporte de carbón equivalente, por lo tanto el catalizador se usó en su lugar. En la Tabla 1 se muestran los resultados referentes a la etapa de hidrólisis de celulosa a 230ºC y 2 MPa de N_2. En primer lugar, se ha realizado un experimento sin catalizador (blanco), observándose que tras 30 min de hidrólisis, tan solo se ha obtenido un rendimiento del 5,6 % en glucosa. Cuando se usa el soporte MCM-48 (1594 $m^2 \cdot g^{-1}$), se observa un claro incremento del 60 % en rendimiento en glucosa (rendimiento en glucosa 14,1 %) bajo las mismas condiciones de reacción. El soporte TiO_2, ha demostrado un rendimiento máximo en glucosa del 3,2 %. Este pobre rendimiento en glucosa unido a que el 5-HMF ha sido el producto principal, indica que el soporte de titanio no es selectivo hacia la producción de glucosa. El catalizador de Ru/C ha demostrado una actividad muy baja en esta etapa, donde se observa un rendimiento máximo en glucosa del 0,3 % tras 5 min de reacción disminuyendo hasta 0,2% a los 30 min y detectándose subproductos como fructosa, gliceraldehido, glicolaldehido, ácido láctico y fórmico a tiempos de reacción más elevados. Por lo tanto, la MCM-48 ha demostrado ser un buen soporte de catalizadores para reacciones de hidrólisis de

celulosa, donde la acidez débil de la MCM-48, atribuible a los grupos terminales silanol (-Si-OH), juega un rol muy importante en la producción selectiva de glucosa.

Table 1. Experimentos hidrólisis de celulosa. [a] Tiempo de reacción (t (min)).[b] Rendimiento Glucosa (%).

	t (min)[a]	D-Glucosa (ppm)	$Y_{D\text{-}Glucosa}$ (%)[b]
Blanco	0	184	2,2
	5	277	3,3
	15	328	3,9
	30	474	5.6
MCM-48	0	819	9,8
	5	971	11,6
	15	1159	13,8
	30	1182	14,1
TiO_2	0	89	1,1
	5	198	2,4
	15	175	2,1
	30	270	3,2
Ru/C	0	19	0,2
	5	25	0,3
	15	9	0,1
	30	5	0,2

En cuanto a los catalizadores metálicos, el Ru/MCM-48 presenta mejores propiedades texturales (A_{BET} = 1453 $m^2 \cdot g^{-1}$ y V_p = 0,47 $cm^3 \cdot g^{-1}$) que Ru/TiO_2 (A_{BET} = 43 $m^2 \cdot g^{-1}$ y V_p = 0,11 $cm^3 \cdot g^{-1}$) y que Ru/C comercial (A_{BET} = 759 $m^2 \cdot g^{-1}$ y V_p = 0,5 $cm^3 \cdot g^{-1}$). Estos materiales se han probado en la hidrogenación catalítica de D-Glucosa entre 80 - 120 ºC, con una presión de 2,5 MPa H_2. Se observa una dependencia de pseudo primer orden con respecto a la D-Glucosa en todos los casos. En la Figura 1A, se muestran los ajustes de pseudo primer orden a 100 ºC, 2,5 MPa H_2 usando Ru/MCM-48, Ru/TiO_2 y Ru /C, con coeficientes de correlación $R^2 \geq 0{,}989$. En la Figura 1B, se observa la evolución de conversión de D-Glucosa con el tiempo a 100 ºC, 2,5 MPa H_2 usando Ru/MCM-48, Ru/TiO_2 y Ru /C. La conversión de D-Glucosa aumenta hasta alcanzar prácticamente la conversión total después de 40 min. En todos los casos, la selectividad hacia sorbitol es del 100 %. El catalizador Ru/MCM-48 demostró una elevada actividad

en hidrogenación de glucosa, sin embargo los catalizadores Ru/C y Ru/TiO_2 presentaron cinéticas de conversión de D-Glucosa en sorbitol más rápidas (Figura 1).

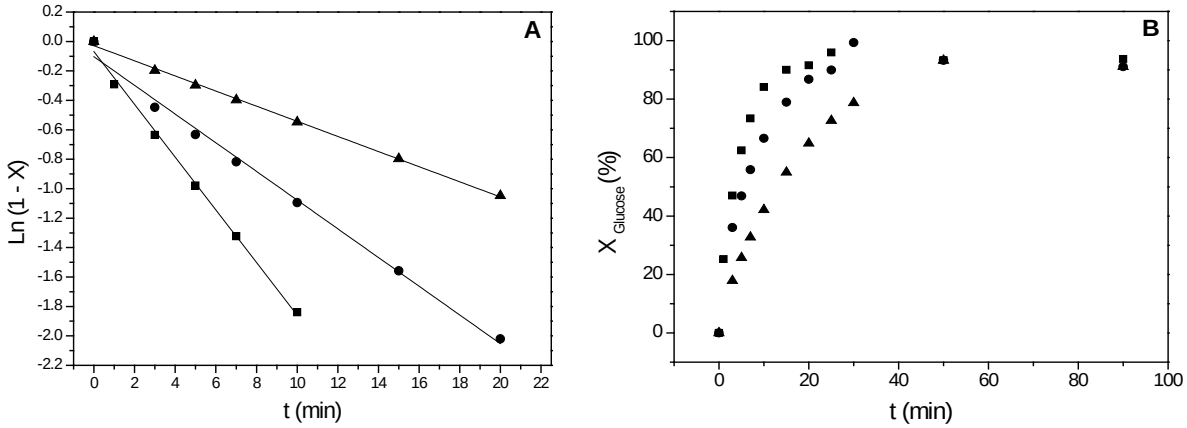

Figure 1. (A) Ajuste cinético de pseudo-primer orden y **(B)** evolución de la conversion de D-Glucosa con el tiempo de reacción a 100 ºC y 2.5 MPa H_2. ▲Ru/MCM-48, ■ Ru/C and ● Ru/TiO_2.

La energía de activación del catalizador Ru/MCM-48 es de 45 KJ·mol^{-1}, 86 KJ·mol^{-1} la del Ru/TiO_2 y 52 KJ•mol^{-1}la del Ru/C comercial. No es posible establecer una relación entre la actividad y la energía de activación de los catalizadores, debido a las diferencias existentes entre los valores del factor pre-exponencial. Ru/MCM-48 se ha recuperado después de cada experimento y se ha reutilizado durante tres ciclos de reacción. El catalizador sintetizado ha mostrado una excelente estabilidad tras tres ciclos de reacción, manteniendo el rendimiento y la selectividad hacia sorbitol con respecto al catalizador fresco.

En el **Capítulo 2** titulado *"Supercritical water hydrolysis of cellulosic biomass as effective pretreatment to catalytic production of hexitols and ethylene glycol over Ru/MCM-48"*, se ha estudiado el comportamiento catalítico del catalizador bifuncional Ru/MCM-48 en la hidrogenación catalítica de celulosa, comparando el proceso "one-pot", con un proceso en dos etapas combinando hidrólisis en agua supercrítica seguido de la hidrogenación del hidrolizado obtenido. El comportamiento catalítico del Ru/MCM-48 se compara con el del Ru/C comercial. La elevada superficie específica y volumen de poro de la MCM-48 evitan problemas difusionales de moléculas grandes, mientras que las funciones ácidas del soporte juegan un rol importante durante la etapa de hidrólisis. Por otro lado, el rutenio actúa como fase activa durante la hidrogenación de azúcares para producir hexitoles. Controlar la degradación de glucosa durante la etapa de hidrólisis es clave a la hora de maximizar la producción de hexitoles. Por lo

tanto en este capítulo, el agua supercrítica se ha usado para depolimerizar parcialmente la celulosa en la etapa de hidrólisis, ya que ha demostrado ser un medio de reacción excelente para lograr la solubilización de la celulosa evitando la degradación de la glucosa producida, mediante el control del tiempo de reacción (en el rango de los milisegundos). En este sentido, es posible alcanzar mayores rendimientos en hexitoles usando la hidrólisis ultrarrápida en agua supercrítica previamente al proceso de hidrogenación, que mediante el proceso de hidrólisis/hidrogenació ("one-pot") partiendo de celulosa microcristalina. En este capítulo, además, se ha evaluado el proceso en dos etapas con una biomasa real como es la pulpa de remolacha.

En cuanto a la hidrogenación de celulosa en una etapa a 240ºC y 5 MPa H_2, se ha obtenido una conversión máxima de celulosa del 31,4 % usando Ru/MCM-48 en un tiempo de reacción de 30 min. Cuando la reacción se llevó cabo bajo las mismas condiciones con el catalizador Ru/C comercial, la conversión ha sido del 14,4 %. En términos de selectividad, el catalizador Ru/MCM-48 ha alcanzado un rendimiento del 20,7 % en hexitoles en 10 min, siendo más selectivo hacia sorbitol. Sin embargo, el Ru/C ha demostrado un rendimiento pobre en hexitoles en torno al 6 %, siendo más selectivo hacia manitol. En general, a pesar de que el Ru/MCM-48 ha obtenido mejores rendimientos en hexitoles que el Ru/C (3,5 veces mayores, aproximadamente), sería deseable mejorar dicho resultado. En el proceso en una etapa, la hidrólisis de la celulosa y la hidrogenación de los azúcares tienen lugar de manera simultánea, siendo la hidrólisis la etapa limitante. Por lo tanto, una eficiencia baja en la primera etapa limita el rendimiento final en sorbitol y manitol. En este caso, la acidez débil que presenta Ru/MCM-48 unida a la baja reactividad de la celulosa microcristalina debido a la elevada cristalinidad (76 %), hacen que la etapa de hidrólisis sea aún más compleja.

Por lo tanto, para mejorar la baja reactividad de la celulosa microcristalina, en este capítulo se propone utilizar el proceso de hidrólisis ultrarrápida en agua supercrítica, desarrollado en el grupo de Ingeniería de Procesos a Presión, como etapa previa a la de hidrogenación, con objeto de depolimerizar e hidrolizar parcialmente la celulosa, controlando la degradación de azúcares monoméricos. De la hidrólisis de celulosa en agua supercrítica (0,2 s, 400 ºC y 25 MPa) se ha obtenido un producto con 5940 $mg \cdot l^{-1}$ de carbono orgánico total, siendo el 14,6 % celobiosa, 8,6 % glucosa, 1,3 % gliceraldehido y 10,2 % glicolaldehido. Además, el 50% del TOC corresponde a oligosacáridos de glucosa, susceptibles de someterse a hidrogenación hidrolítica para

obtención de hexitoles. Los catalizadores de Ru/MCM-48 y Ru/C se han probado en la hidrogenación de los hidrolizados procedentes de la hidrólisis de celulosa en agua supercrítica a 180 ºC, 5 MPa H_2 durante 90 min. Además, se han llevado a cabo experimentos sin catalizador y con MCM-48 (Figura 2).

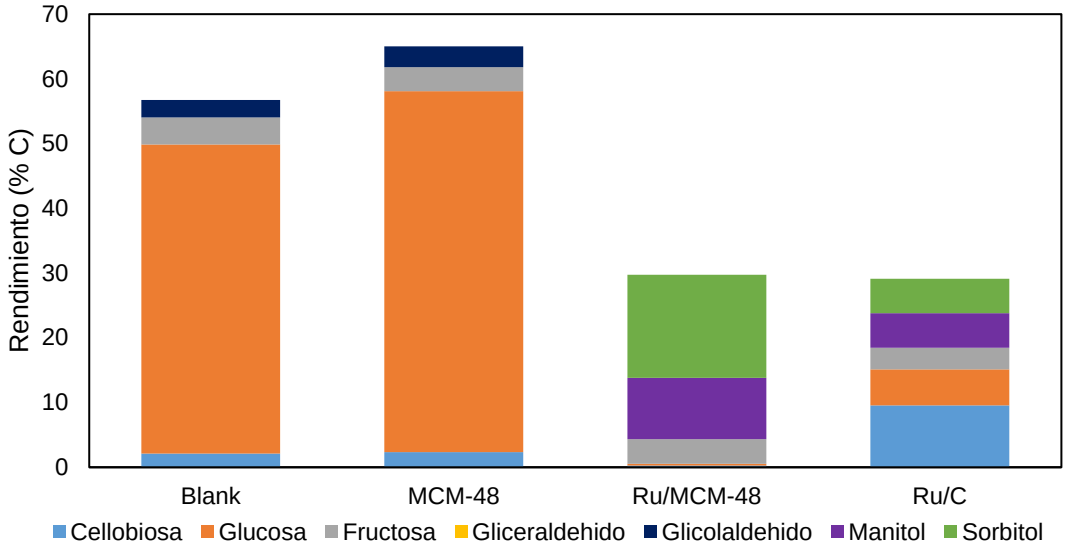

Figura 2. Hidrogenación de hidrolizados procedentes de la hidrólisis de celulosa en agua supercritica usando MCM-48, Ru/MCM-48 and Ru/C a 180 ºC, 5 MPa H_2 durante 90 min.

En el experimento sin catalizador en atmósfera de hidrógeno, se ha observado que la celobiosa y los oligosacáridos se hidrolizan en glucosa a temperaturas en torno a 180 ºC. El rendimiento en glucosa aumentó desde un 8,6 % en los hidrolizados iniciales hasta un 47,7 % en el producto final. Usando MCM-48 se ha observado un comportamiento similar al anterior, sin embargo, el rendimiento en glucosa en el producto final se ha incrementado en un 8 %, alcanzándose un rendimiento en glucosa del 55,7 %. Este incremento en el rendimiento final en glucosa se ha atribuido a la acidez del soporte debida a los grupos terminales silanol. Como en los experimentos en una sola etapa, el Ru/MCM-48 también ha demostrado un mejor comportamiento catalítico en comparación con el catalizador comercial de Ru/C, cuando se combinan las etapas de hidrólisis con agua supercrítica e hidrogenación de los hidrolizados obtenidos. Ru/MCM-48 ha obtenido un rendimiento en hexitoles del 25,4 %, mientras que el catalizador comercial Ru/C tan solo ha obtenido un 10,7 % de hexitoles. El producto obtenido por Ru/MCM-48 fundamentalmente se compone de sorbitol y manitol, mientras que el obtenido por Ru/C aún presenta porcentajes importantes de celobiosa y

glucosa que no se han hidrogenado. Estos resultados muestran de nuevo, el mejor comportamiento del Ru/MCM-48 frente al Ru/C. Sin embargo, los rendimientos en hexitoles siguen sin ser elevados, debido a que en las condiciones de reacción seleccionadas para estos primeros experimentos se produce la hidrogenólisis del sorbitol, disminuyendo el rendimiento final en los productos de interés. De acuerdo con los resultados obtenidos, la influencia de la temperatura y tiempo se han estudiado para maximizar la producción de hexitoles mediante la hidrogenación de los hidrolizados obtenidos de la hidrólisis de celulosa en agua supercrítica. Tras realizar la optimización de ambas variables, se ha obtenido que el mayor rendimiento en hexitoles sobre Ru/MCM-48 (48,5 % hexitoles, 41,8 % sorbitol y 6,7 % manitol) se ha dado a 200 ºC, 5 MPa H_2 y 6 min. En la Figura 3, se observa la evolución de los máximos en rendimiento en hexitoles a diferentes temperaturas usando Ru/MCM-48 como catalizador. En general, se obtienen mayores rendimientos en hexitoles cuanto mayor es la temperatura ya que a temperaturas mayores es posible hidrolizar mayor cantidad de oligosacáridos de glucosa y por tanto se aumenta el rendimiento en hexitoles. Entre 120 y 165 ºC, se observa un aumento en el rendimiento en manitol, sin embargo, el rendimiento en sorbitol permanece más o menos constante. A temperaturas entre 165 y 200 ºC, se observa un aumento significativo en el rendimiento hacia sorbitol ya que es posible hidrolizar un mayor número de oligosacáridos, disponiendo por lo tanto un mayor número de azúcares que podrían hidrogenarse en sorbitol.

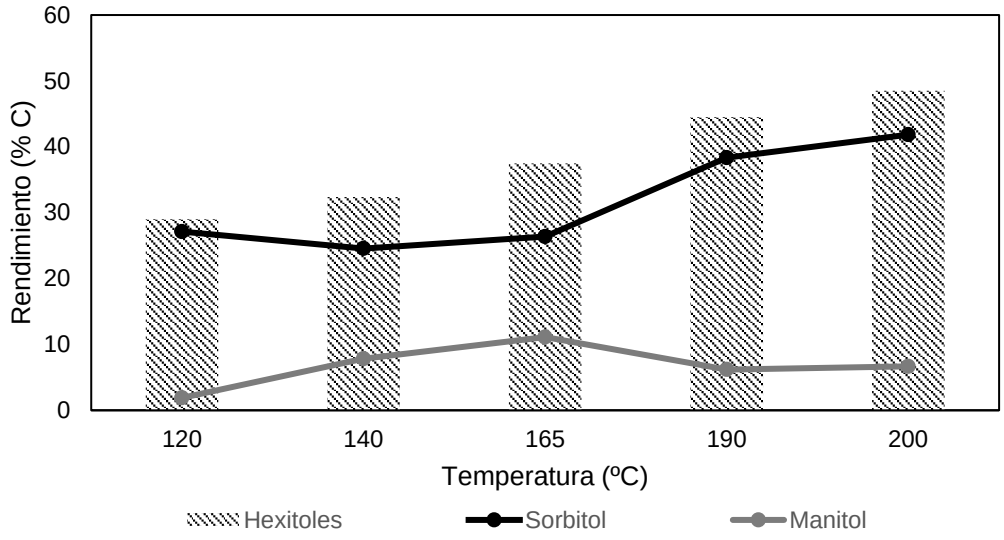

Figura 3. Producción máxima de hexitoles a cada temperatura sobre Ru/MCM-48. (T = 120 ºC y t = 1440 min, T = 140 ºC y t = 175 min, T = 165 ºC y t = 90 min, T = 190 ºC y t = 10 min, T = 200 ºC y t = 6 min).

Finalmente, se ha usado el proceso en dos etapas con una biomasa real como la pulpa de remolacha. Tras la hidrólisis de pulpa de remolacha en agua supercrítica, se ha obtenido un producto con 4854 $mg \cdot l^{-1}$ de carbono orgánico total, compuesto por un 7,1 % de celobiosa, 11,7 % de glucosa, 7,9 % de fructosa, 4,8 % gliceraldehido y 21,2 % de glicolaldehido. Además, el 16 % del carbono orgánico total corresponde a oligosacáridos de glucosa. Tras la hidrogenación del producto de la hidrólisis de pulpa de remolacha en agua supercrítica a 200 ºC, 5 MPa H_2 y 6 min, se ha obtenido un producto donde el compuesto mayoritario ha sido el etilenglicol con un rendimiento del 21,5 % y un 15 % de hexitoles.

En el **Capítulo 3** titulado *"Bimetallic Ru:Ni/MCM-48 catalysts for the effective hydrogenation of D-Glucose into sorbitol"*, se ha estudiado la preparación de catalizadores bimetálicos basados en rutenio y níquel sobre MCM-48, como alternativa a sus homólogos monometálicos de níquel. Los catalizadores sintetizados se han probado experimentalmente en la hidrogenación catalítica de D-Glucosa para la obtención de sorbitol y se ha realizado una comparación de la actividad catalítica del catalizador Ni/MCM-48 con respecto a los catalizadores bimetálicos Ru:Ni/MCM-48. Por lo tanto, en este capítulo se ha evaluado la influencia de diferentes cargas de rutenio sobre el catalizador Ni/MCM-48 en la actividad catalítica durante la hidrogenación de D-Glucosa.

En este capítulo se han preparado un catalizador monometálico de níquel Ni/MCM-48 y tres bimetálicos Ru:Ni/MCM-48 con una carga metálica total en torno al 3 %. Los catalizadores bimetálicos se han preparado con diferentes ratios de Ru:Ni comprendidas entre 0,15 y 1,39. El efecto de la adición de diferentes cargas de rutenio sobre el catalizador Ni/MCM-48 se observa claramente en la reducibilidad de las especies de Ni y Ru en la Figura 4. El catalizador monometálico de Ni fundamentalmente ha mostrado un pico de reducción centrado a 255 ºC, que se atribuye a la reducción de especies $Ni(NO_3)_2 \cdot 4H_2O \cdot 2(SiOH)$. Además, el perfil correspondiente al Ni/MCM-48 muestra un pico de poca intensidad y ancho que se atribuye a la reducción de pequeñas cantidades de especies $Ni(NO_3)_2 \cdot 5H_2O \cdot (SiOH)$, que tienen mayor interacción con el soporte MCM-48. Los perfiles de reducción de los catalizadores bimetálicos Ru:Ni/MCM-48 son diferentes de los obtenidos para el Ni/MCM-48 y Ru/MCM-48 (perfiles TPR-H_2 Ru/MCM-48, capítulos 1 y 2). En este caso se han obtenido perfiles complejos de TPR-H_2, compuestos fundamentalmente por tres picos de reducción entre 100 y 260 ºC,

aproximadamente. El primer pico, en torno a 100 – 125 ºC corresponde a la reducción de $RuCl_3$ a Ru^0. El pico intermedio observado entre 150 – 175 ºC, se atribuye a la presencia de aleaciones de Ru:Ni formadas durante el proceso de impregnación, como reportan otros autores en trabajos similares. Finalmente, el pico a mayores temperaturas, corresponde a la reducción de $Ni(NO_3)_2 \cdot 4H_2O \cdot 2(SiOH)$ a Ni^0. En general, se ha observado que mayores concentraciones de Ru favorecen la reducibilidad de especies de Ni y Ru a menores temperaturas, ya que las especies de Ru^0 son capaces de quimisorber moléculas de hidrógeno que sirven para reducir otras especies de rutenio y níquel. De acuerdo, con los resultados obtenidos en el TPR-H_2, los catalizadores se activaron a 250 ºC en atmósfera de hidrógeno. La reducción de los catalizadores se ha comprobado mediante XRD, observándose la correcta reducción de ambos metales. En cuanto a las propiedades texturales, el catalizador monometálico Ni/MCM-48 ha mostrado un área específica de 572 $m^2 \cdot g^{-1}$ y un volumen de poro de 0,44 $cm^3 \cdot g^{-1}$, mientras que los catalizadores bimetálicos han mostrado áreas específicas entre 900 – 1200 $m^2 \cdot g^{-1}$ y volúmenes de poro en torno a 0,6 – 0,7 $cm^3 \cdot g^{-1}$.

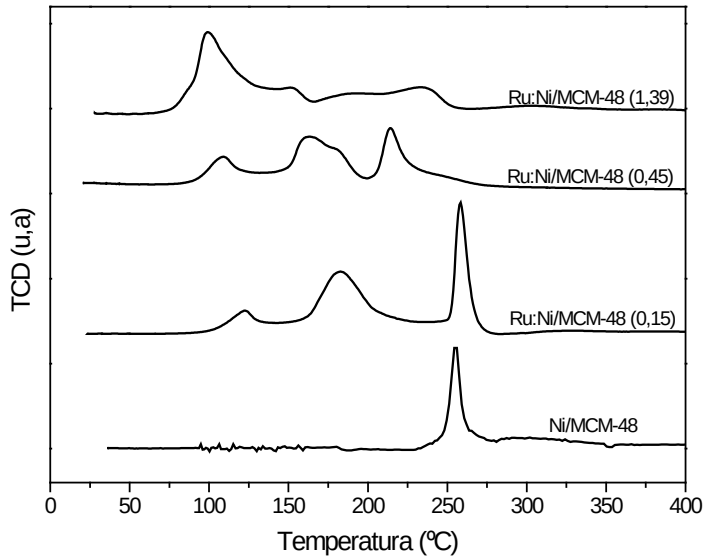

Figura 4. Perfiles TPR-H_2 de los catalizadores sintetizados.

El catalizador Ni/MCM-48 y los bimetálicos Ru:Ni/MCM-48 han demostrado una dependencia de pseudo primer orden con respecto a la D-Glucosa, durante las reacciones de hidrogenación. Se ha observado una clara diferencia en el comportamiento catalítico entre los catalizadores monometálico y bimetálicos en términos de selectividad. Los catalizadores bimetálicos han mostrado selectividad completa hacia sorbitol, mientras el catalizador Ni/MCM-48 ha demostrado una

selectividad hacia sorbitol en torno al 93 – 95 %, obteniéndose manitol como subproducto. En general, usando ratios de Ru:Ni iguales o superiores a 0,45, los catalizadores bimetálicos mejoran la actividad catalítica del Ni/MCM-48 en la hidrogenación de D-Glucosa, incrementando la velocidad de reacción y la selectividad hacia sorbitol.

Se ha evaluado el efecto de la temperatura en la conversión de D-Glucosa y en la selectividad a sorbitol usando Ni/MCM-48 y Ru:Ni/MCM-48 como se muestra en la Figura 5. En el caso del Ni/MCM-48, un aumento de la temperatura entre 120 – 140 ºC ha producido un ligero incremento en la velocidad de reacción, mientras que se ha observado una disminución de la selectividad a sorbitol desde el 95 % al 86 %. En el caso del Ru:Ni/MCM-48, el efecto de la temperatura ha producido un claro incremento de la conversión desde un 31 % hasta un 59 % entre 120 ºC y 140 ºC, manteniendo la selectividad hacia sorbitol en un 100 %.

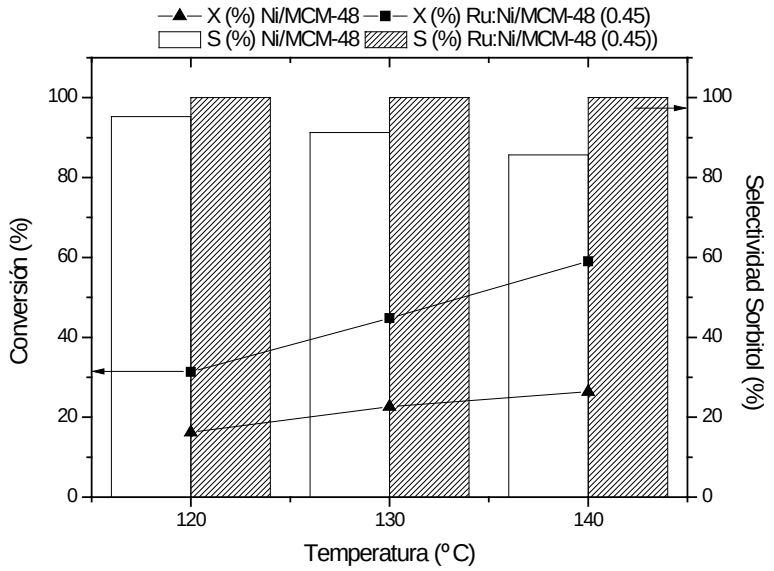

Figure 5. Efecto de la temperatura de reacción (120, 130, 140 ºC) en la conversión de D-Glucosa y en la selectividad a sorbitol usando ▲ Ni/MCM-48 ($k_{120ºC} = 9.7 \cdot 10^{-3}$, $k_{130ºC} = 1.3 \cdot 10^{-2}$ y $k_{140ºC} = 1.7 \cdot 10^{-2}$ $dm^3 \cdot g^{-1} \cdot min^{-1}$) y ■ Ru:Ni/MCM-48 (0.45) ($k_{120ºC} = 1.8 \cdot 10^{-2}$, $k_{130ºC} = 3.4 \cdot 10^{-2}$ y $k_{140ºC} = 5.1 \cdot 10^{-2}$ $dm^3 \cdot g^{-1} \cdot min^{-1}$) a C:Ru = 142, 2.5 MPa H_2, 1400 rpm y 90 min.

La energía de activación con Ni/MCM-48 es de 36 $KJ \cdot mol^{-1}$, mientras que con el catalizor bimetálico Ru:Ni/MCM-48 (0,45) es de 70 $KJ \cdot mol^{-1}$. No es posible establecer una relación entre la actividad y la energía de activación de los catalizadores, debido a las diferencias existentes entre los valores del factor pre-exponencial. Tras la reutilización del catalizador Ru:Ni/MCM-48 (0,45), se ha observado la estabilidad del catalizador, donde el rendimiento en sorbitol durante la hidrogenación de D-Glucosa tan

solo ha disminuido desde un 31 % a un 29 % tras tres ciclos de reacción, manteniendo la selectividad hacia sorbitol constante en un 100 %.

En el **Capítulo 4** titulado *"Catalytic hydrogenolysis of cellobiose into hexitols over Ru/Al-MCM-48"*, se ha estudiado el comportamiento catalítico del catalizador Ru/Al-MCM-48 en la reacción de hidrólisis/hidrogenación de celobiosa para la obtención de hexitoles. La adición de Al al soporte incrementa el número total de centros ácidos, los cuales juegan un rol importante en las etapas de hidrólisis dentro del proceso global de conversión de celobiosa en hexitoles, que como ocurre con la celulosa es la etapa limitante. En este capítulo se ha realizado un estudio del efecto de latemperatura y la presión de H_2, para ver el efecto de estos dos parámetros para maximizar la producción de hexitoles a partir de celobiosa. Finalmente, se ha desarrollado un modelo cinético teniendo en cuenta el diferente comportamiento observado en función de las diferentes temperaturas de reacción.

El estudio cinético de la hidrólisis/hidrogenación de celobiosa para la obtención de hexitoles usando Ru/Al-MCM-48 como catalizador, se ha desarrollado a 140 ºC, 160 ºC y 180 ºC, a 5 MPa H_2. En general, la celobiosa se hidrogena rápidamente (100 % conversión después de 20, 10 y 5 min a 140 ºC, 160 ºC y 180 ºC, respectivamente) en celobitol, que posteriormente se hidroliza en sorbitol. Por tanto, el celobitol es el principal intermedio de reacción en la hidrólisis/hidrogenación de celobiosa cuando se utiliza Ru/Al-MCM-48 como catalizador. No se ha detectado glucosa en ninguno de los experimentos llevados a cabo, por lo que, de producirse como intermedio, se estaría hidrogenando rápidamente en sorbitol y no se detectaría en el producto. En la Figura 6A se muestra el efecto de la temperatura en la producción de hexitoles. Como se observa en en esta figura, temperaturas más altas tienen un efecto positivo a la hora de maximizar el rendimiento en hexitoles a un determinado tiempo de reacción, ya que más celobitol se puede hidrolizar cuanto mayor es la temperatura. En todos los casos, el sorbitol es el producto mayoritario, sin embargo, manitol e iditol también aparecen en concentraciones menores como subproductos. La isomerización de sorbitol a manitol e iditol se ve favorecida a temperaturas elevadas, por lo tanto, se obtienen mayores rendimientos en los isómeros cuando la temperatura se incrementa. Los rendimientos máximos en hexitoles que se han obtenido a cada temperatura, han sido los siguientes: 9 % a 140 ºC y 240 min, 87 % a 160 ºC y 30 min y 91 % a 180 ºC y 7 min. A pesar de obtener máximos en los rendimientos en hexitoles similares a diferentes temperaturas

(87 – 91 % C), la composición en el producto final varía. Cuando la temperatura se incrementa de 140 a 180 ºC, el máximo en el rendimiento en hexitoles se alcanza a menores tiempos de reacción. La mayor conversión de celobitol a mayores temperaturas, favorece la obtención de concentraciones mayores de sorbitol y los tiempos de reacción cortos evitan las reacciones de isomerización de sorbitol. Por lo tanto, las temperaturas elevadas y los tiempos cortos de reacción, favorecen la obtención de rendimientos mayores de sorbitol, disminuyendo aquellos de manitol e iditol.

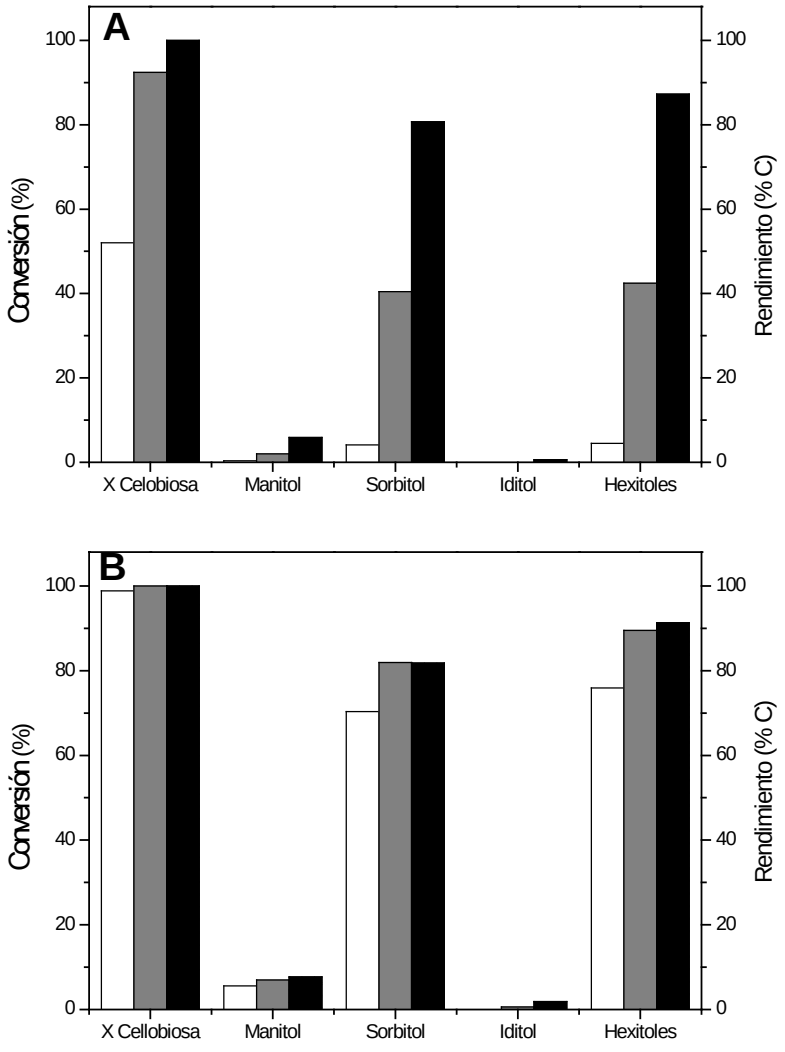

Figura 6. Efecto de la temperatura **(A)** y la presión **(B)** en la conversión de celobiosa y en el rendimiento en hexitoles sobre Ru/Al-MCM-48. **(A)** T = 140 ºC, T = 160 ºC, T = 180 ºC, 5 MPa H_2 y 5 min. **(B)** P = 3 MPa H_2, P = 4 MPa H_2, P = 5 MPa H_2, 180 ºC y 7 min.

La influencia de la presión de H_2 se ha estudiado en el intervalo comprendido entre 3 y 5 MPa H_2 (Figura 6B). El aumento de la presión no tiene un efecto significativo en la conversión de celobiosa, sin embargo, sí que tiene gran influencia en el mecanismo de reacción por el cual la celobiosa se convierte en sorbitol. A presiones inferiores a 5

MPa H_2, la glucosa es el principal intermedio de reacción, observándose pequeñas concentraciones de celobitol. Sin embargo, a 5 MPa H_2 el celobitol es el único intermedio de reacción y la glucosa no se detecta en el producto final. Por lo tanto, trabajando a presiones inferiores a 5 MPa H_2, la concentración de hidrógeno en el medio de reacción limita la hidrogenación de celobiosa a celobitol, favoreciendo la hidrólisis de celobiosa en glucosa. En general, se ha observado que presiones de hidrógeno mayores tienen una importancia significativa a la hora de maximizar el rendimiento en hexitoles. Se han obtenido los siguientes resultados a diferentes presiones: 76 % a 3 MPa H_2, 90 % a 4 MPa H_2 y 92 % a 5 MPa H_2.

Finalmente, en este capítulo se ha desarrollado un modelo cinético homogéneo que tiene en cuenta el efecto de la temperatura entre 140 ºC y 180 ºC para la hidrólisis/hidrogenación de celobiosa en hexitoles. El modelo consiste Dicho modelo permite predecir las velocidades de reacción de las diferentes etapas involucradas en el proceso global, así como sus energías de activación. El modelo cinético propuesto reproduce fielmente los datos experimentales obtenidos para la hidrólisis/hidrogenación de celobiosa (R^2 = 0.97). Además, a partir de los resultados estadísticos obtenidos, se ha concluido que todos los parámetros calculados a partir del modelo son estadísticamente significativos.

En el **Capítulo 5** titulado *"Catalytic conversion of D-Glucose into short-chain alkanes over Ru-based catalysts"*, se ha estudiado el comportamiento catalítico de catalizadores de Ru soportados en sílices mesoporosas en la obtención de alcanos a partir de glucosa. El esquema de reacción se recoge en el Esquema 2. Para las etapas de deshidratación, englobadas dentro del proceso de conversión de glucosa en alcanos, se requieren condiciones de acidez fuertes. La MCM-48 presenta acidez de tipo débil, por lo tanto ésta se ha mejorado mediante la introducción de aluminio en la matriz del soporte (Al-MCM-48) y mediante la deposición de ácido tungstofosfórico (TPA) sobre la superficie de la MCM-48 (MCM-48/TPA). Se ha depositado rutenio que actúa como metal hidrogenante, sobre MCM-48/TPA y sobre la Al-MCM-48. Ambos catalizadores se han probado en la conversión catalítica de glucosa para la obtención de alcanos de cadena corta, comparando su actividad catalítica con respecto a la de un catalizador comercial de Ru/C. En este capítulo también se ha evaluado la influencia del Al-MCM-48 y TPA como cocatalizador en combinación con el Ru/C comercial para mejorar la producción de alcanos.

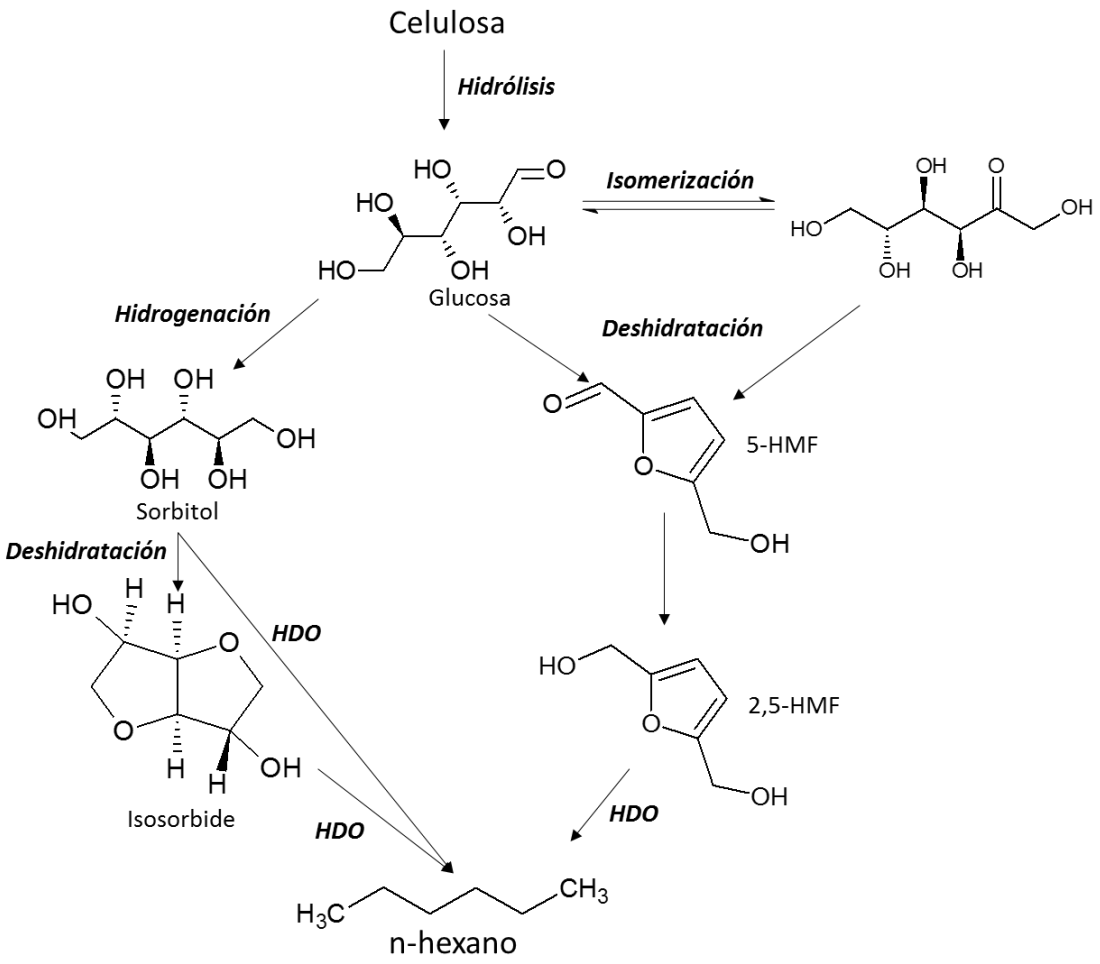

Esquema 2. Etapas de reacción en la producción de alcanos a partir de glucosa.

Tras la deposición de Ru mediante impregnación húmeda sobre los soportes Al-MCM-48 y MCM-48/TPA, se obtuvieron catalizadores con una carga metálica en rutenio del 3,5 % y del 4,9 %, respectivamente. El catalizador Ru/Al-MCM-48 ha demostrado poseer mejores propiedades texturales (A_{BET} = 1028 $m^2 \cdot g^{-1}$ y V_p = 0,57 $cm^3 \cdot g^{-1}$) que el Ru/MCM-48/TPA (A_{BET} = 504 $m^2 \cdot g^{-1}$ y V_p = 0,29 $cm^3 \cdot g^{-1}$) y además un mayor número de centros ácidos. Tras realizar TPR-H_2 a los catalizadores sintetizados se concluye que la activación de los mismos se realizará a 150 ºC durante 1 h en atmósfera de hidrógeno más un tiempo adicional a 200 ºC para asegurar la correcta reducción de todas las especies de rutenio presentes en los catalizadores. Después de la activación, se ha comprobado la correcta reducción de las especies de rutenio en el Ru/Al-MCM-48 y Ru/MCM-48/TPA.

En cuanto a los test de actividad catalítica, la conversión de D-Glucosa para la obtención de alcanos se ha llevado a cabo en un reactor de hidrogenación donde el

sistema de reacción se compone de una fase acuosa y de una fase orgánica (n-decano), a 190 ºC, 5 MPA H_2 y 1200 min. La D-glucosa se encuentra solubilizada en la fase acuosa y el n-decano sirve para extraer los productos de reacción. El catalizador Ru/Al-MCM-48 ha demostrado una mejor actividad en comparación con el catalizador Ru/C comercial. El Ru/Al-MCM-48 ha conseguido convertir en torno a un 20 % más de carbono soluble presente en la fase acuosa en comparación con el catalizador Ru/C comercial, siendo también superior el rendimiento en alcanos. Por lo tanto esta mayor conversión de carbono soluble de la fase acuosa por parte del Ru/Al-MCM-48, ha resultado en unos rendimiento en alcanos mayores en comparación con el Ru/C. Ru/Al-MCM-48 ha obtenido un rendimiento final en alcanos en torno al 57 %, correspondiendo el 7 % a n-butano, el 26 % a n-pentano y el 24 % a n-hexano. En el caso del Ru/C, se ha obtenido un rendimiento en alcanos del 29 %, donde un 4 % corresponde a n- butano, el 10 % a n-pentano y el 15 % a n-hexano. Debido al mejor comportamiento catalítico del Ru/Al-MCM-48 con respecto al Ru/C para producir alcanos, se ha usado Al-MCM-48 y TPA como cocatalizadores ácidos para mejorar los rendimientos en los productos deseados cuando se utiliza Ru/C. La combinación de Ru/C + Al-MCM-48 ha dado lugar a un elevado rendimiento en alcanos en torno al 82 %, donde un 7 % ha sido n-butano, un 29 % n-pentano y un 46 % n-hexano. La presencia del Al-MCM-48 ha producido conversiones mayores de carbono soluble en la fase acuosa que en el caso en el que solo se usaba Ru/C. Por lo tanto, esa mayor conversión de carbono soluble en la fase acusa se ha traducido en un mayor rendimiento en alcanos. Por otro lado, la combinación de Ru/C + TPA, a pesar de convertir mayor carbono soluble presente en la fase acuosa en comparación con la combinación anterior, ha obtenido un rendimiento en alcanos ligeramente inferior en torno al 70 %. La adición de TPA al medio de reacción ha provocado que la reacción transcurriera a través de un mecanismo de reacción diferente, a través de la deshidratación de glucosa hacia 5-HMF, mientras que sin TPA la reacción sigue una ruta de reacción a través de la hidrogenación de glucosa hacia sorbitol.

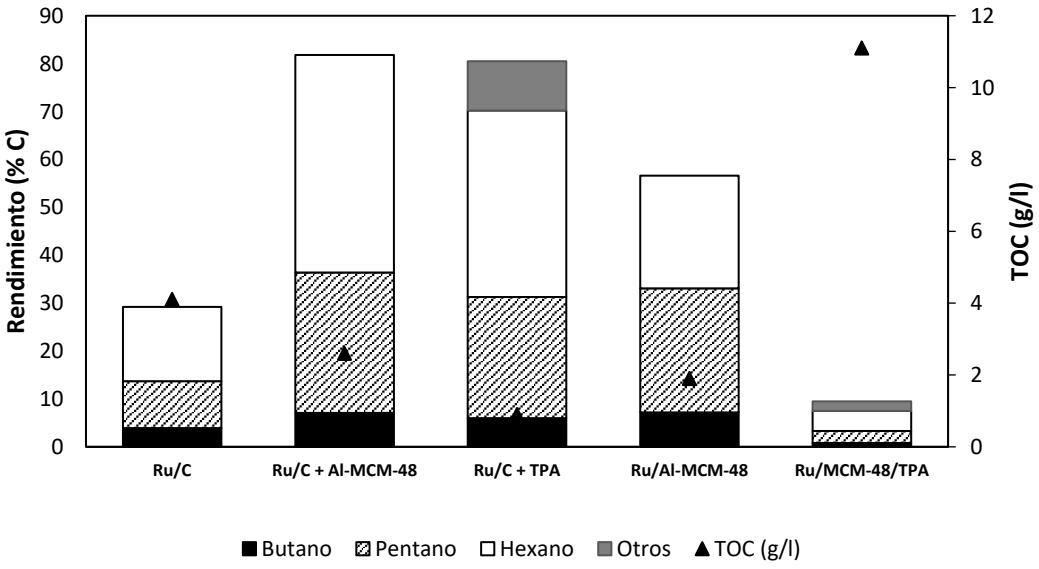

Figura 7. Rendimiento en alcanos de cadena corta usando diferentes catalizadores de rutenio.

Finalmente, se ha probado Ru/MCM-48/TPA en la conversión de D-Glucosa para producir alcanos mostrando unos rendimientos muy pobres en los productos de interés en comparación con el resto de sistemas catalíticos empleados en este trabajo. El catalizador Ru/MCM-48/TPA ha mostrado mayor capacidad para hidrogenar glucosa que para llevar a cabo las siguientes etapas de deshidratación y dehidrodeoxigenación.

CONCLUSIONES

La presente tesis es una contribución al desarrollo de nuevos materiales mesoporosos de rutenio y níquel para su aplicación en la conversión de biomasa lignocelulósica para la obtención de un amplio intervalo de productos, como hexitoles, etilenglicol y alcanos de cadena corta. Además, este trabajo ha significado el comienzo de una nueva línea de investigación en el Grupo de Ingeniería de Procesos a Presión de la Universidad de Valladolid.

Las principales conclusiones de esta tesis se presentan a continuación:

- Síntesis y caracterización de catalizadores mesoporosos de rutenio y níquel.
  - Los siguientes catalizadores se sintetizaron correctamente: MCM-48, Al-MCM-48, MCM-48/TPA, Ru/MCM-48, Ru/Al-MCM-48, Ru/MCM-48/TPA, Ni/MCM-48 and Ru:Ni/MCM-48.

- Estos catalizadores se han caracterizado por medio de diferentes técnicas, isotermas de adsorción / desorción de N_2, SAXS, XRD, TPR-H_2, TPD-NH_3, SEM, TEM y AA.
- En general, todos los catalizadores presentados en esta tesis, han mostrado una elevada área específica y volumen y tamaño de poro en el intervalo de los mesoporos, que son propiedades muy interesantes para evitar problemas difusionales durante la valorización de biomasa. Los catalizadores preparados han demostrado ser bifuncionales, presentando sitios ácidos capaces de promover las etapas de hidrólisis y deshidratación, y sitios metálicos que son los responsables de llevar a cabo las reacciones de hidrogenación.

- Se ha puesto en marcha un montaje experimental para la hidrogenación catalítica de biomasa lignocelulósica.

- Pruebas catalíticas con los catalizadores preparados.
  - La MCM-48 es más activa y mejora la selectividad en la hidrólisis de celulosa hacia D-Glucosa, en comparación con TiO_2 o con un catalizador comercial Ru/C. Los rendimientos en D-Glucosa son 4 y 47 veces mayores, respectivamente, y esto puede ser debido a la acidez débil de la MCM-48 atribuida a los grupos superficiales silanol (-SiOH).
  - Se ha demostrado que el catalizador Ru/MCM-48 es una alternativa potencial a los catalizadores convencionales, como el Ru/C y el Ru/TiO_2, usados para la hidrogenación en fase líquida de D-Glucosa con H_2 gaseoso, mostrando una actividad alta comparable a la de esos materiales. El Ru/MCM-48 ha demostrado ser totalmente selectivo hacia sorbitol entre 80 ºC y 120 ºC durante la hidrogenación de D-Glucosa. Además, se propone una cinética de pseudo primer orden respecto a la concentración de D-Glucosa en dicha reacción cuando se utiliza el Ru/MCM-48 como catalizador. . La energía de activación con dicho catalizador es de 45 $KJ \cdot mol^{-1}$, que es menor que la obtenida con el Ru/C comercial y con el catalizador de Ru depositado sobre TiO_2 comercial Ru/TiO_2 (52 y 86 $KJ \cdot mol^{-1}$, respectivamente). Además, el Ru/MCM-48 ha demostrado ser muy estable tras tres ciclos de reacción.
  - Se ha observado una baja actividad específica del catalizador monometálico Ni/MCM-48 en la hidrogenación de D-Glucosa en comparación con la obtenida

por el catalizador monometálico Ru/MCM-48, mostrando selectividades hacia sorbitol entre 93 – 95 %. Sin embargo, la presencia de ratios de Ru:Ni superiores o iguales a 0,45 sobre la MCM-48, mejoran notablemente la actividad del catalizador monometálico, convirtiendo eficientemente la D-Glucosa en sorbitol (selectividad del 100 %). Tanto con el catalizador Ni/MCM-48 como con los bimetálicos Ru:Ni/MCM-48 la cinética presenta una dependencia de pseudo primer orden con respecto a la concentración de D-Glucosa. Con los catalizadores Ni/MCM-48 y Ru:Ni/MCM-48 (0,45) se han obtenido energías de activación de 36 y 70 $KJ \cdot mol^{-1}$, respectivamente. De la misma manera que el Ru/MCM-48, el catalizador Ru:Ni/MCM-48 ha mostrado una excelente estabilidad tras tres ciclos de reacción.

- El Ru/Al-MCM-48 se ha evaluado satisfactoriamente en la hidrólisis/hidrogenación de celobiosa, alcanzando un 91 % de rendimiento en hexitoles a 180 ºC, 5 MPa H_2 y 7 min. Se ha observado un efecto significativo tanto de la presión de hidrógeno (3 – 5 MPa H_2), como de la temperatura (140 – 180 ºC) a la hora de maximizar la el rendimiento en hexitoles. El modelo cinético desarrollado en esta tesis, predice bien las concentraciones de los compuestos involucrados en el mecanismo de reacción de hidrólisis/hidrogenación de celobiosa para la obtención de hexitoles.
- Las mejores propiedades ácidas y texturales del Ru/MCM-48 en comparación con las del catalizador comercial Ru/C, mejoran la etapa de hidrólisis de celulosa durante la hidrogenación de celulosa en un proceso "one pot", incrementando así el rendimiento final en hexitoles. Se ha alcanzado un rendimiento en hexitoles del 21 % usando Ru/MCM-48 durante la hidrogenación de celulosa en proceso “one-pot" a 240 ºC, 5 MPa H_2 y 10 min, mientras que en las mismas condiciones experimentales el catalizador comercial Ru/C ha obtenido un 6 % de rendimiento en hexitoles.
- Se ha propuesto una alternativa interesante al proceso “one-pot”, combinando las buenas propiedades del agua supercrítica para depolimerizar celulosa selectivamente durante la etapa de hidrólisis y el buen comportamiento del Ru/MCM-48 para llevar a cabo la hidrogenación de azúcares. La hidrólisis en agua supercrítica ha demostrado ser una excelente etapa previa a la producción de hexitoles. El rendimiento final en hexitoles usando el proceso en dos etapas se ha incrementado en 2,3 veces en comparación con el proceso de

hidrogenación de celulosa en "one pot". El uso de Ru/MCM-48 ha sido altamente beneficioso, ya que la utilización de MCM-48 como soporte mejora la hidrólisis de oligosacáridos de glucosa obtenidos en la etapa de hidrólisis en agua supercrítica, incrementando así el rendimiento en glucosa de un 8,6 % a un 55,7 % en el producto final. Además este catalizador, ha demostrado una elevada selectividad convirtiendo glucosa en hexitoles, obteniendo un rendimiento máximo en hexitoles del 48,5 %, que representa un rendimiento en la conversión de azúcares en torno al 88 %.

- Además, cuando se ha evaluado el proceso propuesto en dos etapas en la hidrólisis e hidrogenación de pulpa de remolacha, se ha observado que el glicolaldehido obtenido a partir de la hidrólisis en agua supercrítica de la pulpa de remolacha, se ha convertido con una selectividad del 100% en etilenglicol (rendimiento del 21 %).
- EL Ru/Al-MCM-48 ha mostrado un mejor comportamiento catalítico que el catalizador comercial Ru/C para la conversión de D-Glucosa en alcanos de cadena corta, alcanzando rendimientos en alcanos alrededor de 1,9 veces mayores (57 y 29 %, respectivamente). El Ru/MCM-48/TPA ha demostrado una buena actividad a la hora de hidrogenar D-Glucosa en alcoholes de azúcares, sin embargo, su actividad para llevar a cabo las etapas posteriores de deshidratación y deshidrodesoxigenación ha sido limitada. La presencia de TPA en el medio de reacción hace que el mecanismo sea a través de la formación de 5-HMF. La combinación de Ru/C + TPA mejora el rendimiento final en alcanos, obteniéndose un 79 % de rendimiento. Además, la combinación de Ru/C + Al-MCM-48 mejora la conversión de carbono soluble en la fase acuosa en comparación con Ru/C, resultando en una mejora importante del rendimiento hacia alcanos (82 %).

TRABAJO FUTURO

El trabajo desarrollado en la presente tesis podría ser ampliado en un futuro mediante la realización de diferentes trabajos de investigación. En esta tesis, se han preparado diferentes catalizadores, pero solo Ru/MCM-48 ha sido probado en la conversión de celulosa microcristalina o biomasa real. Por tanto, se propone el uso de Ru:Ni/MCM-48 y Ru/Al-MCM-48 como alternativas para ser usadas en la hidrogenación de celulosa, oligosacáridos de biomasa lignocelulósica o biomasas reales,

para la obtención de alcoholes de azúcares. Para llevar a cabo estas tareas, el desarrollo de un sistema de muestreo para la fase gaseosa sería de gran ayuda a la hora de cerrar mejor los balances de materia del proceso global.

Además, de acuerdo con el buen comportamiento catalítico de los materiales preparados en esta tesis para la obtención de alcoholes de azúcares a partir de biomasa lignocelulósica, estos se podrían probar en la hidrogenación de hemicelulosas para producir principalmente arabitol, galactitol y xilitol. Debido a las interesantes propiedades de los materiales de sílice, estos también se podrían usar para mejorar los rendimientos de hidrólisis de arabinoxilanos a partir de salvado de trigo mediante métodos hidrotermales. Ambas tareas se han iniciado en las tesis de *Gianluca Gallina y Nuria Sánchez*.

Aparte de la investigación realizada durante estos años en torno a la conversión catalítica de biomasa en productos químicos, sería muy interesante tener en cuenta a los polisacáridos como un excelente precursor para la síntesis de crio-, xero- y aerogeles, así como carbonos porosos. En su forma natural, los polisacáridos presentan áreas específicas y porosidades bajas. Por lo tanto, parece interesante investigar la mejora de las propiedades de los polisacáridos para producir materiales. Esta idea ha sido motivada por el excelente trabajo previo realizado en este campo de investigación dentro del Grupo de Ingeniería de Procesos a Presión de la Universidad de Valladolid por el *Dr. Luis Miguel Sanz*, la *Dra. Ana Najwa y* la *Dra. Marta Salgado*. Por lo tanto, la idea sería desarrollar materiales porosos basados en oligosacáridos de celulosa y pulpa de remolacha, así como la transformación de los mismos en compuestos porosos de carbono mediante pirolisis. En este marco, los materiales carbonosos obtenidos podrían ser utilizados en diferentes aplicaciones como cromatografía de mezclas complejas, purificación de agua o recuperación de metales preciosos. Además, con este objetivo se conseguiría valorizar los polisacáridos de bajo coste obteniendo materiales de alto valor añadido.

APPENDIX

BUSINESS PLAN

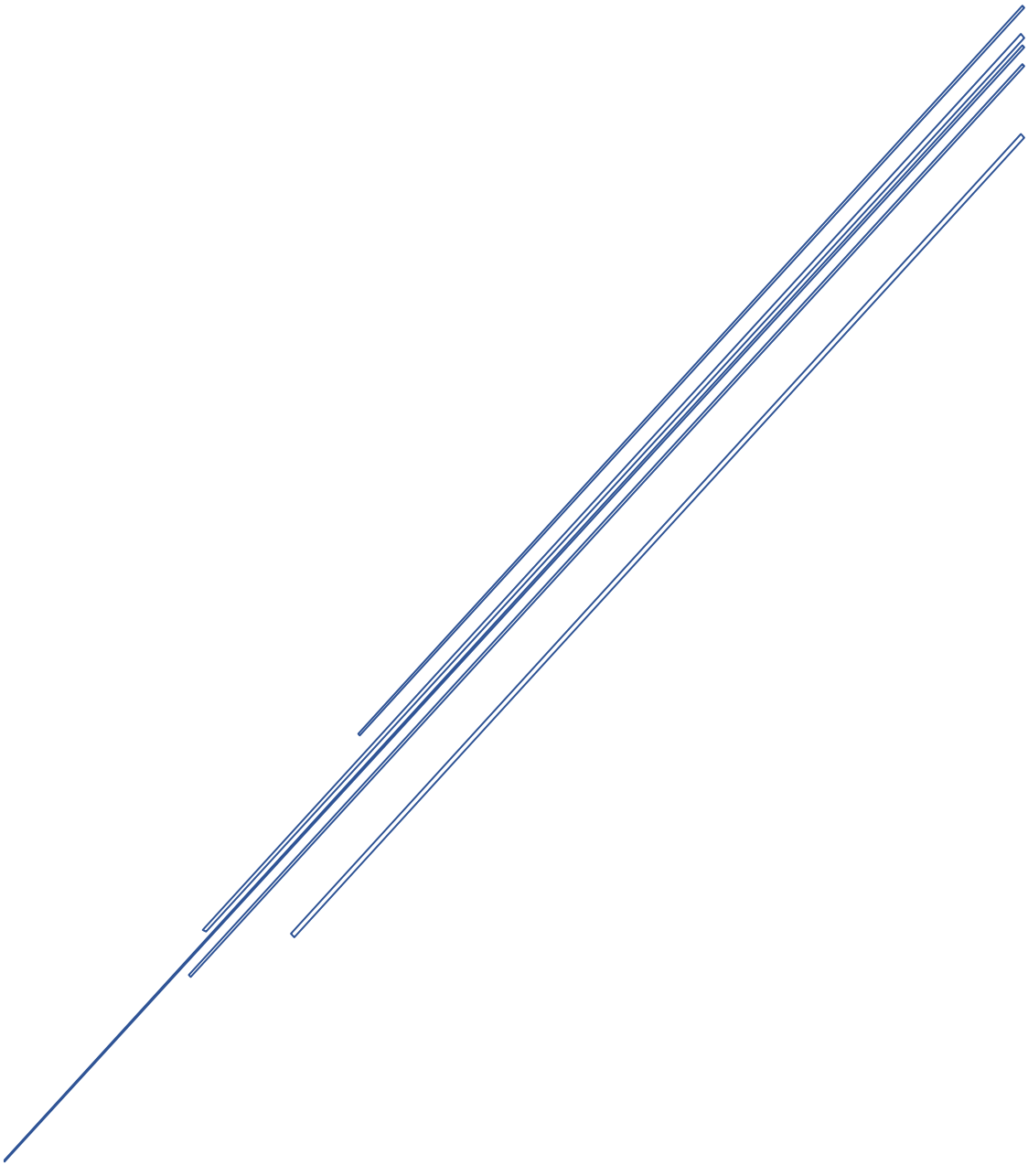

RESUMEN EJECUTIVO

LOGO:

CONTACTO:
Nombre y Apellidos
Alberto Romero Camacho
Tfno: 687016401
Em@il:
albertoromeroiq@gmail.com

SECTOR: Biorefinerías, azúcar y químico.

EQUIPO:
Gloria Esther Alonso Sánchez
Antonio Nieto-Márquez B.
Alberto Romero Camacho

ALIANZAS/PARTNES:
Sociedad Cooperativa General Agropecuaria ACOR

INVERSIONES:
Inversión inicial:
200.000 €
Inversión a corto plazo:
30.000 €

USO DE LOS FONDOS
Se usan para pagar a los empleados, mejoras en el proceso productivo, pagar a la azucarera por materia prima y alquiler, marketing, I+D+i.

Descripción de la empresa
Biorefinería que se encarga de valorizar residuos de la industria azucarera como la pulpa de remolacha para la obtención de un producto de alto valor añadido llamado sorbitol. Cathycel también realiza labores de consultoría de I+D+i

Problema que resuelve
Las azucareras producen un gran tonelaje de residuos de pulpa de remolacha que venden a 25 €/tn, sin darle ningún valor adicional. Además, la producción de sorbitol actual es poco sostenible, ya que usa disolventes perjudiciales para el medio ambiente.

Solución
Cathycel propone dar un valor añadido a la pulpa de remolacha convirtiéndola en sorbitol, que es un compuesto fundamental para la actividad diaria de industrias tan importantes como la alimentaria, cosmética y farmacéutica. Esto se hace usando una metodología mucho más sostenible basada en el uso de agua presurizada a alta temperatura, gracias a la cual se reducen los tiempos de reacción y más económica.

Mercado al que te diriges
Biorefinerías, azúcares y químicos.

Competencia
Actuales productores de sorbitol, alcoholes de azúcares y otros edulcorantes de bajo poder calórico.

Ventaja Competititva
La ventaja competitiva fundamentalmente radica en el proceso productivo, ya que es mucho más sostenible, más rápido y por tanto más económico que el que se realiza actualmente en la industria.

Modelo de Negocio. Tipo de modelo
Modelo de negocio de fabricante

Hitos conseguidos y futuros
Cathycel se encuentra en pleno desarrollo, consiguiendo durante esta etapa el primer premio en la I Greenweekend Valladolid organizada por Enviroo por ser la mejor idea de negocio verde. Este plan de negocio será presentado a inversores para conseguir financiación. Además se seguirá trabajando sobre la alianza con la azucarera ACOR de Olmedo que será nuestro principal socio clave.

	Año 1	Año 2	Año 3
INGRESOS (€)	60.000	95.000	145.000
GASTOS (€)	50.000	75.000	76.000
EBITDA (%)	17 %	21 %	48 %

CATHYCEL: UN VALOR AÑADIDO AL USO DE BIOMASA

1. Identificación del proyecto.

La biomasa ha sido la principal materia prima para la producción de energía, productos químicos y combustibles hasta el siglo XIX, sin embargo, su uso con la revolución industrial disminuyó progresivamente comenzando la era de los combustibles fósiles. Actualmente, el aumento de su precio, los problemas medioambientales ocasionados por su uso y el agotamiento de los mismos, han desencadenado una nueva actividad económica más sostenible emergiendo así una economía basada en la biomasa (bioeconomía). La síntesis de bioproductos es una actividad cuyo mercado se encuentra en constante expansión, con aplicaciones en la industria farmacéutica, química, papelera y alimentaria. Sin embargo, aún es necesario un mayor desarrollo tecnológico que permita obtener estos productos a un coste menor y de una manera más eficiente. Íntimamente ligado a este mercado, se encuentra el concepto de biorrefinería, el cual engloba la integración de procesos y tecnologías para un uso eficaz de las materias primas y así lograr instalaciones que operen de una manera sostenible con el medio ambiente [1].

A continuación se incluyen algunas definiciones encontradas en la bibliografía para el concepto de biorefinería:

- La biorefinería es una estructura que integra procesos de conversión de biomasa y equipamiento para producir combustibles, energía y productos químicos a partir de la biomasa. El concepto de biorefinería es análogo al de refinerías de petróleo, los cuales producen productos y combustibles múltiples derivados del petróleo [2].
- Es la combinación óptima de procesos biológicos, termoquímicos y químicos para la obtención de una variada gama de productos, que posibilita el empleo de numerosas materias primas gracias a las sinergias establecidas entre las tecnologías [3].

1.1. Descripción de la idea y la propuesta de valor

En este contexto surge CATHYCEL dentro del Grupo de Procesos a Alta Presión de la Universidad de Valladolid dirigido por la catedrática de universidad Dña. María José Cocero Alonso. El equipo investigador lleva trabajando sobre la utilización de biomasa

de tipo lignocelulósico para la obtención de productos de valor añadido (alcoholes de azúcares y alcanos) desde enero de 2012. Como resultado del trabajo de investigación desarrollado en este campo nace Cathycel, una novedosa propuesta de biorefinería capaz de convertir residuos de la industria azucarera como la pulpa de remolacha en un compuesto de alto valor añadido llamado sorbitol. El sorbitol es un compuesto fundamental para la actividad diaria de industrias tan importantes como la farmaceútica, cosmética y alimentaria. Normalmente, las azucareras no dan ninguna aplicación a la pulpa de remolacha, más allá de venderla (25 €/tn). Por lo tanto, Cathycel se presenta como una excelente opción para dar valor al residuo de las azucareras mediante su conversión en sorbitol.

La producción actual de sorbitol se lleva a cabo mediante la hidrogenación del azúcar común, obtenido a partir de procesos enzimáticos. Estos procesos previos a la obtención del azúcar, implican tiempos de operación elevados, donde se utilizan compuestos contaminantes y además las enzimas requieren un elevado control. Por lo tanto, todo ello se traduce en elevados costes de producción. Además la pureza del sorbitol que se obtiene en este tipo de procesos suele estar en torno al 70 %.

Nosotros hemos desarrollado un proceso de obtención de sorbitol en dos etapas que combinan un proceso de hidrólisis llevado a cabo en agua caliente presurizada y un proceso de hidrogenación también realizado en medio acuoso en presencia de hidrógeno y un catalizador metálico. De esta manera se obtiene un sorbitol de elevada pureza (>95 %) mediante una metodología más sostenible, con tiempos de producción hasta 200 veces menores a los empleados actualmente y por lo tanto con menores costes.

1.2. Descripción del modelo de negocio.

Cathycel es un modelo de negocio que compite en el sector de las biorefinerías, edulcorantes e industria química, valorizando un residuo de la industria azucarera para la producción de sorbitol de elevada calidad, a un menor coste y usando una metodología sostenible. Además, debido a la formación del equipo promotor, Cathycel también da soluciones de I+D+i a las empresas, universidades o centros de investigación interesados en este tipo de servicios de consultoría. En el momento inicial, en el que Cathycel arranque, la actividad clave será realizar una importante labor de consultoría. De esta manera, se establecerán numerosas colaboraciones con clientes y se

conseguirán los ingresos necesarios para la financiación de la propia empresa mediante la redacción de proyectos y aportando soluciones de I+D+i. Al mismo tiempo, se irá construyendo la planta para la valorización de la biomasa en sorbitol. Una vez acabado el montaje de la planta de conversión de biomasa, la actividad de producción de sorbitol a partir del residuo de pulpa de remolacha irá incrementando su peso como actividad clave dentro de la empresa de manera gradual, manteniendo las labores de consultoría como claves. Por lo tanto en esta segunda etapa se obtendrán ingresos tanto de la venta de proyectos de I+D+i y labores de consultoría, como de la producción y distribución del sorbitol.

1.3. Descripción del equipo promotor

En una primera etapa inicial, Cathycel estará constituida por tres socios principales (Gloria Esther Alonso Sánchez, Antonio Nieto-Márquez Ballesteros y Alberto Romero Camacho), los cuales han sido los encargados de desarrollar el presente modelo de negocio. Cathycel es una empresa que nace en el Grupo de procesos de Alta Presión, que forma parte del Departamento de Ingeniería Química de la Universidad de Valladolid, liderado por la catedrática de universidad Dña. María José Cocero Alonso. A pesar de que el grueso de este ambicioso proyecto se ha desarrollado en Valladolid, la constante colaboración con la Escuela Técnica Superior de Ingeniería y Diseño Industrial de la Universidad Politécnica de Madrid ha resultado fundamental para llegar hasta aquí.

A continuación se presenta el resumen del CV de cada uno de los fundadores de la empresa:

Gloria Esther Alonso Sánchez (Asesora de I+D+i). Profesora Titular de Ingeniería Química en la Universidad de Valladolid, con experiencia docente e investigadora de más de 20 años. Ha trabajado en desarrollo de procesos y productos utilizando fluidos supercríticos y fluidos presurizados en general. Preocupada por el medio ambiente y por contribuir al desarrollo de su entorno social, ha desarrollado proyectos relacionados con la descontaminación de suelos, el tratamiento de efluentes, y la revalorización de residuos y subproductos de la industria

agroalimentaria. Su mayor logro en transferencia de tecnología es la realización del desarrollo del proceso de extracción de beta-glucanos de hongos y levadura para la Biofactoría Naturae en Pradoluengo, Burgos.

Antonio Nieto-Márquez Ballesteros (Asesor I+D+i). Antonio Nieto-Márquez Ballesteros (Manzanares, Ciudad Real, 1982) es Ingeniero Químico (2005) y Doctor Ingeniero Químico (2010) por la Universidad de Castilla-La Mancha, donde ha sido becario FPI y profesor ayudante. En el año 2004 recibió una beca para realizar su Proyecto fin de Carrera en el Departamento de Ingeniería Química y de los Materiales, en la Universidad de Kentucky (EEUU), donde empezó a trabajar en la síntesis de nanoestructuras de carbono, tema que posteriormente desarrollaría en mayor profundidad durante su tesis doctoral, ahondando en su caracterización y aplicaciones catalíticas. En el año 2010 se incorporó como profesor Titular de Universidad interino a la Escuela Técnica Superior de Ingeniería y Diseño Industrial, donde desarrolla su investigación en las áreas de catálisis y adsorción con aplicaciones ambientales y energéticas, e imparte docencia en el Grado de Ingeniería Química. Es autor de 26 publicaciones indexadas en JCR (h = 13), un capítulo de libro y una patente en fase de comercialización, así como de numerosas contribuciones a congresos. Ha realizado estancias predoctorales en la Universidad Heriot-Watt, de Edimburgo, y ha sido investigador invitado en la Universidad de Limoges (Francia) y en Pontificia Universidad Católica del Perú. Es evaluador independiente de proyectos de investigación (EQA, Academia Polaca de Ciencias) y censor habitual de revistas del área de Ingeniería Química. También ha participado activamente en el reconocimiento de la profesión de Ingeniero Químico, impulsando la creación del Colegio Oficial de Profesionales en Ingeniería Química de Castilla-La Mancha, del que fue decano fundador.

Alberto Romero Camacho (Desarrollo Proceso y producto). Alberto Romero Camacho (Madrid, 1988). Ingeniero químico (2006-2011) por la Universidad de Castilla La Mancha. Recibió el I Premio COPIQCLM al mejor trabajo fin de carrera en Ingeniería Química. En 2010 fue becario de la oficina técnica de Repsol Química en Puertollano dentro del

área de ingeniería, desarrollando sus tareas dentro de las plantas de producción de polietileno de alta y baja densidad. En 2012, se marchó a Valladolid para continuar su formación, realizando un máster de investigación en ingeniería termodinámica de fluidos en la Universidad de Valladolid, recibiendo el premio al mejor estudiante de su promoción. En 2013, comenzó a desarrollar su tesis doctoral en torno a la conversión de biomasa lignocelulósica con catalizadores mesoporosos de níquel y rutenio. En 2015, realizó una estancia de investigación de tres meses en el Institut de recherches sur la catalyse et l'environement de Lyon (Lyon, Francia). Durante estos tres meses desarrolló tareas relacionadas con la conversión de biomasa en biocombustibles. Actualmente se encuentra finalizando su tesis doctoral que espera defender a lo largo de 2017. Alberto es una persona proactiva, responsable y que siempre está en continuo aprendizaje. Destaca por su carácter emprendedor en diferentes facetas de la vida, por trabajar eficientemente en grupos y por su capacidad de adaptarse a diferentes ambientes de trabajo. Interesado en todos aquellos temas relacionados con la ingeniería de procesos, sostenibilidad y química verde.

Los fundadores de Cathycel aportan tres perfiles técnicos diferentes, con amplia experiencia en el desarrollo de procesos y materiales. Es un equipo multidisciplinar capaz de aportar soluciones novedosas a diferentes problemas dentro del ámbito de la industria química, que demuestra un gran afán de superación, altamente motivado para llevar a buen puerto todos los proyectos que se proponen y en busca de un planeta más limpio y sostenible para nuestra sociedad. En este contexto, los emprendedores involucrados en Cathycel tienen como misión la implantación de un nuevo modelo de biorefinería capaz de producir productos químicos de alto valor añadido a partir de residuos usando una tecnología sostenible.

2. Proceso de validación del plan de negocio

Como ya se ha comentado en el apartado anterior, Cathycel es una novedosa propuesta de biorefinería capaz de valorizar residuos de la industria azucarera, como la pulpa de remolacha, para la obtención de un producto de alto valor añadido conocido como sorbitol. Además, Cathycel también da soluciones de I+D+i tanto a universidades, empresas y pequeños productores.

2.1.Hipótesis planteadas

Tras realizar el business model CANVAS sobre nuestra idea de negocio Cathycel, se han detectado numerosas hipótesis. Sin embargo no todas ellas presentan un elevado índice de incertidumbre y criticidad. Por lo tanto, para el proceso de validación de nuestra idea de negocio, se han tenido en cuenta aquellas hipótesis que se encuentran en el sector superior derecho de la Figura 1. Estas se corresponden con aquellas hipótesis decisivas para seguir adelante con nuestro modelo de negocio.

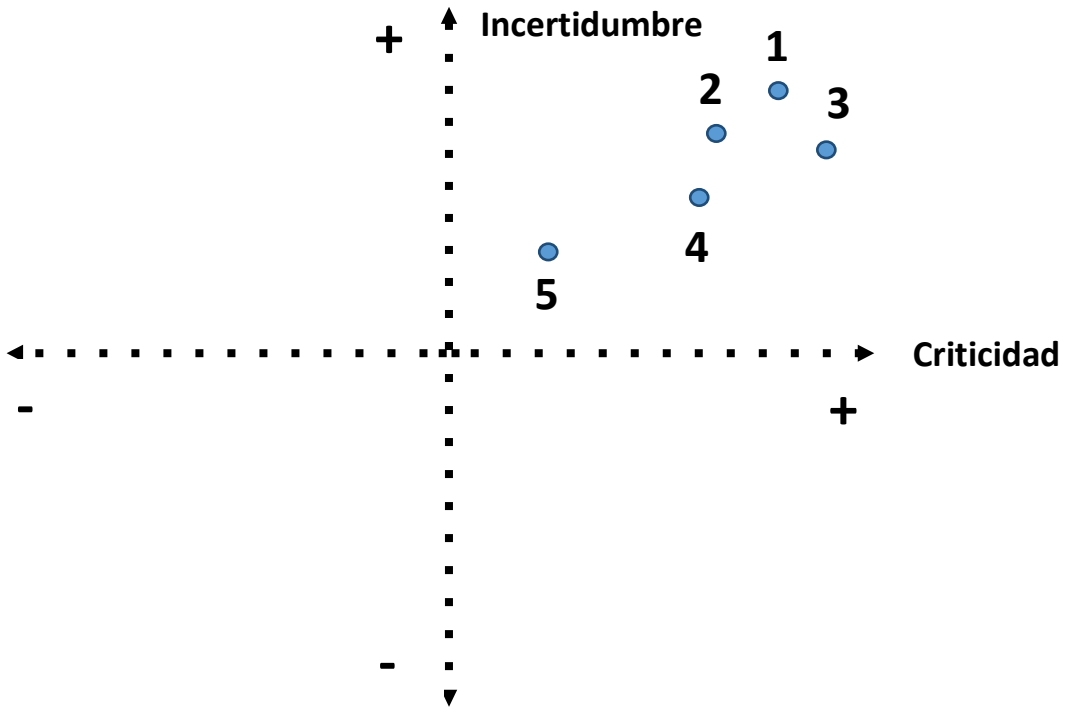

Figura 1. Priorización de hipótesis.

A continuación se enumeran las hipótesis representadas en la figura 1:

1. Creo que las azucareras estarían interesadas en este modelo de negocio, convirtiéndose en nuestro principal socio clave.
2. Creo que el embalaje del producto es algo importante para nuestro cliente final.
3. Creo que necesito conocer el nivel de residuos de pulpa de remolacha de la azucarera.
4. Creo que los clientes pagarán lo mismo o un poco más por nuestro producto en comparación con el de la competencia.

5. Creo que los clientes que quieran encontrar soluciones de I+D+i en Cathycel solicitarán pruebas en planta piloto para escalar su proceso.

2.2.Proceso de validación de hipótesis, métrica y criterios.

Para resolver las hipótesis planteadas en el apartado anterior se han llevado a cabo entrevistas de dos tipos: a) entrevistas con clientes y b) entrevistas con los socios claves y proveedores.

i. **Creo que las azucareras estarían interesadas en este modelo de negocio, convirtiéndose en nuestro principal socio clave.**

Tras la realización de diversas entrevistas, los entrevistados han validado esta hipótesis. Todos los entrevistados consideran que las azucareras están interesadas en este modelo de negocio, ya que actualmente están vendiendo su resido a 25 €/tn, mientras que con esta novedosa idea podría valorizarla en un producto de elevado valor añadido, obteniendo mayores beneficios de dicho residuo. Además, en muchos casos afirman que las azucareras se encuentran esperando ideas de negocio en esta línea para potenciar su actividad. La métrica empleada para validar esta hipótesis se basa en saber si los clientes están de acuerdo o no con la misma. Finalmente, como se comentaba con anterioridad, el 100 % de los encuestados validaron la hipótesis. Desde nuestro punto de vista, esta hipótesis era decisiva ya que si no se validaba, el modelo de negocio estaría en riesgo.

ii. **Creo que el embalaje del producto es algo importante para nuestro cliente final.**

Tras realizar numerosas entrevistas a clientes finales, hemos podido ver que realmente este punto era importante para ellos. En función de la actividad para la que los clientes vayan a utilizar el sorbitol, afirman que les serían más prácticos unos tipos de envases u otros. Por ejemplo bidones de plástico de diferentes volúmenes cuando necesitan sorbitol líquido (sirope) o sacos cuando necesitan sorbitol sólido. La métrica empleada para validar esta hipótesis se basa en saber si los clientes están de acuerdo o no con la misma. El 91 % de los entrevistados consideran importantísimos estos factores, sin embargo el 9 % restante lo consideran importante sin ser algo decisivo. Por

lo tanto, podemos concluir que el embalaje es un factor importante para nuestros clientes finales.

iii. **Creo que necesito conocer el nivel de residuos de pulpa de remolacha de la azucarera.**

Tras realizar entrevistas con proveedores y clientes, hemos podido observar que este punto es decisivo de cara al modelo de negocio. Los entrevistados consideran clave este factor ya que es algo que servirá para definir las dimensiones finales de la planta y producción total anual. Una vez conocido el nivel de residuos que se podrían tratar, se podría evaluar cuál sería la producción total de Cathycel por año. La métrica empleada para validar esta hipótesis se basa en saber si los clientes están de acuerdo o no con la misma. El 100 % de los encuestados validaron dicha la hipótesis. A pesar de que la hipótesis queda validada, hay que seguir trabajando sobre ella para hacernos con datos realistas sobre el número de toneladas de pulpa de remolacha que una azucarera produce por año.

iv. **Creo que los clientes pagarán lo mismo o un poco más por nuestro producto en comparación con el de la competencia.**

Tras la realización de las entrevistas se han obtenido diferentes resultados respecto a la presente hipótesis. Por un lado, gran parte de los clientes entrevistados pagarían un precio superior al sorbitol ofrecido por la competencia ya que lo consideran un producto más limpio desde el punto de vista medioambiental. Además el sorbitol de Cathycel presenta una pureza elevada, lo que debería repercutir en su precio final. Por otro lado, varios clientes consideran que el precio que pagarían por este producto sería similar al que ofrecen los competidores. La métrica empleada para validar esta hipótesis se basa en saber si los clientes están de acuerdo o no con la misma. El 95 % de los entrevistados pagarían lo mismo por nuestro producto que por el de la competencia, no consideran que haya que incrementar el precio final. El 5 % restante afirma que pagarían un precio mayor al del sorbitol ofrecido por la competencia. Por lo tanto la hipótesis quedaría validada.

v. **Creo que los clientes que quieran encontrar soluciones de I+D+i en Cathycel, solicitarán pruebas en planta piloto para escalar su proceso.**

La realización de las entrevistas con los futuros clientes nos han permitido obtener conclusiones muy interesantes respecto a este punto. Hay un tipo de cliente muy específico que considera que para ellos sería muy bueno contar con Cathycel para poder trasladar sus investigaciones desde el nivel de laboratorio a nivel piloto-industrial. Por otro lado, en estas entrevistas también hemos podido detectar que los clientes estarían interesados en que les demos alternativas de valorización para los diferentes residuos lignocelulósicos derivados de su actividad industrial. Además, los clientes querrían solicitar los servicios de I+D+i para llevar a cabo la redacción de proyectos europeos en colaboración con ellos. La métrica empleada para validar esta hipótesis se basa en saber si los clientes están de acuerdo o no con la misma. El 86 % de los entrevistados valoran positivamente el hecho de poder realizar pruebas de escalado de sus procesos desarrollados en laboratorio para llevarlos a escala piloto-industrial. El 14 % restante lo considera interesante, sin embargo valoraría más otras ofertas dentro del área de consultoría de I+D+i, debido a su actividad. Por lo tanto la hipótesis quedaría validada.

3. Plan de marketing

3.1. Descripción del producto / servicio y del mercado

En primer lugar, Cathycel produce sorbitol a partir de pulpa de remolacha (residuo de la industria azucarera), que es la actividad principal que da sentido al presente plan de negocio. Esencialmente, el sorbitol es un producto industrial que diferentes empresas pertenecientes a la industria farmacéutica, alimentaria y cosmética, necesitan incorporar a su stock para poder llevar a cabo su proceso productivo. El sorbitol generado presenta las siguientes características diferenciales con respecto al que se produce en la actualidad por la competencia:

i) **Elevada pureza (>95 %).** Es típico observar la producción de una corriente de sorbitol con una pureza en torno al 70 % denominada sirope de sorbitol.

ii) Es obtenido mediante una metodología **novedosa y sostenible** consistente en **dos etapas** (hidrólisis e hidrogenación) llevadas a cabo **en medio acuoso a**

elevada temperatura y presión. En el proceso de producción de sorbitol llevado a cabo por otras empresas se utilizan disolventes y compuestos químicos más perjudiciales para el medio ambiente. Además, se parte de materias primas puras y no de residuos para la producción del sorbitol.

iii) **Tiempos de producción.** Cathycel ha demostrado una importante intensificación del proceso global de producción de sorbitol a partir de biomasa. Es capaz de producir sorbitol con tiempos de producción hasta 200 veces menores que los de la competencia.

Además, desde el punto de vista de comercialización del sorbitol, Cathycel se dirige a un mercado real formado por los actuales demandantes de este tipo de compuesto, vital para la actividad productiva de los mismos. Inicialmente la oferta del producto se dirigirá hacia la zona de Castilla y León, que es una zona que cuenta con un sector agroalimentario potente, amplio y fuerte, pudiéndose ampliar la oferta del producto a otras zonas de España como País Vasco, Madrid y Cataluña en etapas posteriores.

En segundo lugar, Cathycel lleva a cabo labores de consultoría de I+D+i para satisfacer las necesidades de diferentes universidades, centros de investigación y pequeños empresarios que puedan estar interesados en dicho servicio. Dicho servicio es una actividad secundaria de Cathycel, pero que es necesaria para la creación y crecimiento de la empresa. El equipo de Cathycel tiene una amplia experiencia en labores de investigación y desarrollo, redacción de proyectos, así como dando soluciones a diferentes tipos de industrias, las cuales son características importantísimas para llevar a cabo de manera exitosa esta labor. Una característica diferenciadora de este servicio, sería que en determinados momentos de la actividad productiva, los clientes podrían solicitar servicios para llevar a cabo el escalado de sus procesos de conversión de biomasa y realizarlos en las facilidades experimentales de Cathycel. La oferta de estos servicios de consultoría sería tanto nacional como internacional, lo cual nos permitirá obtener a su vez una gran cantidad de colaboraciones importantes.

Cathycel es una empresa que compite como empresa en diferentes sectores como en el de las biorefinerías, edulcorantes y químico. En los siguientes apartados se dará una visión general sobre la situación de estos tres sectores.

3.2.Situación del sector de las biorefinerías

En general Cathycel es una empresa que compite dentro del sector de las biorefinerías, por lo tanto, a continuación se comenta brevemente cual es la situación actual de este sector. Actualmente, existe un amplio rango de alternativas para el aprovechamiento de biomasa lignocelulósica de acuerdo con la definición de biorefinería, sin embargo ninguna de ellas es una instalación donde se valorice biomasa de una manera integral. La tendencia actual consiste en avanzar en la investigación en este campo. Además, existe un importante número de plantas tipo demostración, donde lo que se hace es llevar a cabo la optimización de las variables de operación y del proceso y adecuar las tecnologías disponibles a la heterogeneidad de la biomasa. A nivel europeo, cabe destacar la trayectoria de los países nórdicos (Finlandia, Suecia y Noruega) en este sector. Estos países sobre todo se dedican al desarrollo de biorefinerías basadas en biomasa de tipo forestal. Por otro lado, en Estados Unidos los esfuerzos en el sector de las biorefinerías se han focalizado sobre la investigación hacia biorefinerías basadas en el uso del cereal o maíz para la obtención de ácido poliláctico (PLA). En el resto del mundo el PLA se obtiene a partir de la caña de azúcar. Finalmente, Brasil posee un gran desarrollo en plantas de bioetanol con caña de azúcar, lo que ha provocado que se encuentre desarrollando numerosas iniciativas para la mejora de la tecnología empleada en los procesos de valorización de la caña de azúcar [1].

Por lo tanto, el desarrollo comercial de las biorefinerías supondrá un gran avance en la industria, así como en el sector agrícola. Sin embargo, previamente, es necesario superar una serie de barreras que obstaculizan su implementación comercial. Estas se dividen en tres categorías:

i) Retos tecnológicos: integración de procesos de revalorización de los componentes de la biomasa y desarrollo de pretratamientos y mejora de enzimas que permitan el aprovechamiento de la biomasa lignocelulósica.
ii) Retos comerciales: establecimiento de la logística de materias primas y productos, dificultades de financiación e incertidumbre asociada a un sector novedoso como el de las biorefinerías.
iii) Retos sostenibles: al final se trata de poner en marcha instalaciones de aprovechamiento de biomasa que lo hagan de manera eficiente y que consigan aportar mejoras a la situación medioambiental actual.

Por tanto, Cathycel contribuye a este avance en el desarrollo comercial de las biorefinerías ya que aporta novedades muy interesantes para superar todas esas barreras que impiden la implementación de las mismas. En primer lugar, Cathycel revaloriza el residuo de la pulpa de remolacha, permitiendo el aprovechamiento integral de este tipo de biomasa. Además, esta novedosa idea de biorefinería no necesita mejorar los pretratamientos enzimáticos para aprovechar mejor la biomasa lignocelulósica, sino que propone una primera etapa de pretratamiento de la biomasa basada en el uso de agua presurizada a elevada temperatura. Esta permite obtener conversiones de la biomasa cercanas al 100%, obteniendo una corriente rica en azúcares en un tiempo de milisegundos. Todas estas novedades en el proceso de valorización de la pulpa de remolacha se traducen en una fuerte apuesta por la sostenibilidad de nuestro planeta en dos sentidos principalmente. Por un lado, se reduce el consumo energético durante la producción de sorbitol debido a la disminución de los tiempos de producción con respecto a los procesos convencionales. Por otro lado, los pretratamientos necesarios para el aprovechamiento integro de la biomasa lignocelulósica, implican la utilización de ácidos y compuestos poco amigables con el medioambiente, mientras que en nuestro proceso tan solo se usa agua con dicho objetivo.

3.3. Situación del sector del azúcar y edulcorantes

A su vez, Cathycel como productor de sorbitol de elevada calidad, compite en el sector de los edulcorantes. Los edulcorantes tienen una aplicación fundamental en industria alimentaria, por lo que a continuación se hace un análisis sobre este tipo de mercado.

3.3.1. Producción de azúcar en España y en el resto del mundo

En términos de producción mundial de azúcar, esta se situó en 172,8 millones de toneladas la campaña de 2015/2016, un volumen inferior en casi 2 millones de toneladas a la producción de la campaña anterior. Además, hay que tener en cuenta que la producción aumentó años atrás por la subida de los precios internacionales y la mayor demanda. A nivel mundial, los principales países productores de azúcar son Brasil, con un volumen estimado de 35 millones de toneladas en 2015/2016, 1,2 millones más que

la campaña 2014/2015. A Brasil le siguió India, con una producción cercana a los 26 millones de toneladas y la UE-28 en torno a los 14,8 millones de toneladas. En relación con el consumo, a nivel mundial se está comprobando de año en año el aumento progresivo del uso del azúcar (un 2% anual), especialmente en los países en vías de desarrollo. En el año 2015, el consumo fue superior a los 172 millones de toneladas.

En España se utilizan al año cerca de 1,3 millones de toneladas de azúcar. La producción de azúcar de remolacha de cultivo nacional sólo permite suministrar unas 500.000 toneladas. Hace ya años que el cultivo de caña se extinguió en la Península Ibérica y para hacer frente a la demanda anual, la industria tiene que importar azúcar procedente de la caña de otros países donde se dan las condiciones climatológicas para su cultivo. Asimismo, otros productores europeos también venden sus producciones en nuestro país para satisfacer la demanda. En la campaña 2014/15 la producción nacional de azúcar quedó en 606.000 toneladas, un 35% más que en la campaña precedente, según los datos manejados por la Comisión Europea. Igualmente, en la campaña 2015/2016 la previsión de la Comisión apunta a una producción de azúcar en España cercana a los 562.000 toneladas, un 7% menos que en la campaña anterior [4].

3.3.2. Estructura empresarial del sector del azúcar y edulcorantes en España

La reducción de la cuota de producción de edulcorantes a nuestro país ha provocado una difícil situación para los diferentes eslabones la cadena productiva. En la base productiva se encuentran unos 8.000 agricultores que se dedican al cultivo de la remolacha en Castilla y León, Andalucía, La Rioja, País Vasco y Navarra. Además, el sector genera unos 2.000 puestos de trabajo directos.

La producción de azúcar y edulcorantes se encuentra concentrada en dos grandes grupos. El principal tiene una cuota de producción de 378.000 toneladas y es propiedad de una gran compañía internacional de origen británico que opera en 46 países (AB Azucarera Iberia, S.L). En España tiene 6 centros de fabricación y suministro, dos sedes de oficinas, una delegación y un centro de I+D+i. Sus ventas rondan los 466 millones de euros anuales. El segundo operador es una cooperativa, asociada a una empresa francesa. Tiene 500 socios agricultores y una planta productora en Castilla y León. Su cuota de producción es de 160.000 toneladas y registra una facturación de 210 millones de euros anuales. Aparte del azúcar y edulcorantes, se dedica a la producción de biocarburantes (biodiesel) y a la energía solar fotovoltaica. Ambas empresas refinan

azúcar de caña, ya que la cuota asignada a nuestro país no es suficiente para cubrir las demandas internas. El resto de las empresas del sector deben trabajar con azúcares importados. La tercera empresa del sector alcanza unas ventas de 82 millones de euros, mientras que la cuarta ronda los 62 millones de euros y la quinta se queda en 21 millones de euros. El sector europeo del azúcar está compuesto por cerca de 160.000 agricultores y unas 55 compañías, básicamente francesas y alemanas. Todos estos datos se encuentran recogidos en la Tabla 1 y se han obtenido del informe anual de ALIMARKET 2015 [4].

Tabla 1. Principales empresas del sector del azúcar y edulcorantes en España y sus ventas.

PRINCIPALES EMPRESAS DEL SECTOR DE AZÚCAR Y EDULCORANTES	
EMPRESA	**VENTAS (Mill. €)**
AB Azucarera Iberia, S.L	465,81
Acor & Tereos Iberia, S.A	210,00
Zukan, S.L *	82,00
Jesus Navarro, S.A. *	61,74
Comercial Javier Casado, S.L. *	20,71
Comasucar, S.A. *	12,00
Cortes Bartolomé, S.L *	12,00
Beneo Ibérica, S.L. *	10,00
Promoción Mercantil Catalana, S.A *	8,60
Bara Ezquerra, S.A. *	5,80
* *Los datos incluyen actividades en otros sectores*	

3.3.3. Demanda y gasto de azúcar y edulcorantes

Durante el año 2015, los hogares españoles consumieron un total de 172,9 millones de kilos de azúcar y gastaron 146,5 millones de euros en este producto. En términos per cápita, se llegó a 3,9 kilos de consumo y 3,3 euros de gasto. En cuanto a los edulcorantes, el consumo total en hogares alcanzó los 3,7 millones de kilos y se gastaron 55,2 millones de euros en este producto. En términos per cápita, se llegó a 0,1 kilos de consumo y 1,2 euros de gasto. Durante los últimos cinco años, el consumo de azúcar se ha mantenido estable, con alguna pequeña variación, mientras que el gasto ha descendido 70 céntimos de euro per cápita. En el periodo 2011-2015, el consumo más

elevado se produjo en los años 2013 y 2014 (4,3 kilos), mientras que el mayor gasto tuvo lugar en el ejercicio 2013 (4,4 euros por consumidor) [4].

En la familia del azúcar y de los edulcorantes, la evolución del consumo per cápita durante el periodo 2011-2015 ha sido diferente para cada tipo de producto. Respecto a la demanda de 2011, el consumo de edulcorantes aumenta y, por el contrario, en el caso del azúcar se produce un descenso (Figura 3).

Este aumento en el consumo de edulcorantes con respecto al azúcar común está relacionado con el menor contenido calórico de los edulcorantes. Por todo ello, actualmente el mercado de los edulcorantes bajos en calorías es unas de las áreas más dinámicas dentro de los aditivos alimentarios. En general, la sacarina es el edulcorante más consumido en el mundo, sin embargo el aspartamo ha demostrado progresos importantes tanto en Europa como en Estados Unidos [5].

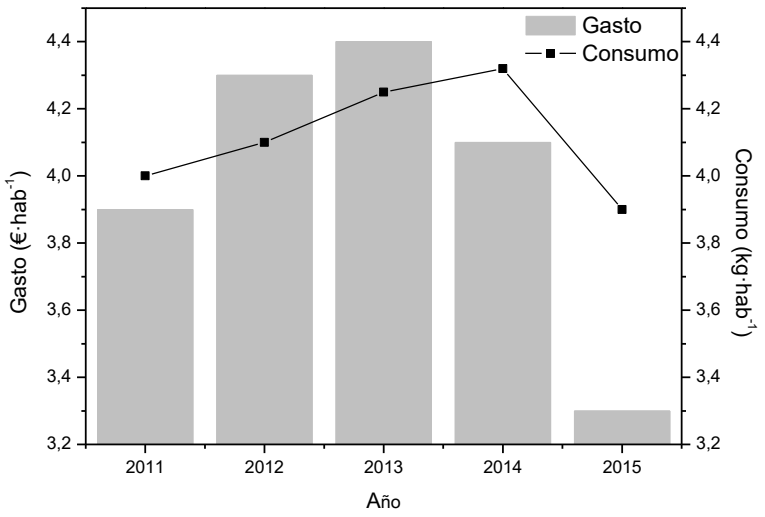

Figure 2. Evolución del consumo y del gasto de azúcar en España en el periodo 2011-2015.

Un estudio realizado por Calorie Control Council y la empresa Pfizer demuestra que el 18 % de la población en Reino Unido, el 19 % en Francia, 39 % en Alemania y el 31 % en Estados Unidos, sustituye el azúcar por un edulcorante bajo en calorías. Las expectativas de este mercado son que la demanda de edulcorantes con bajo nivel calórico continuará aumentando en los próximos años, siendo la principal alternativa a los azúcares convencionales. Dentro de los edulcorantes con bajo nivel calórico, los polioles (alcoholes de azúcares) están experimentando un importante incremento en su cuota de mercado. Los estudios realizados por Amylum Group han demostrado el uso

mayoritario de sorbitol (82 % consumo) como edulcorante frente a otros polioles (Figura 4) [5].

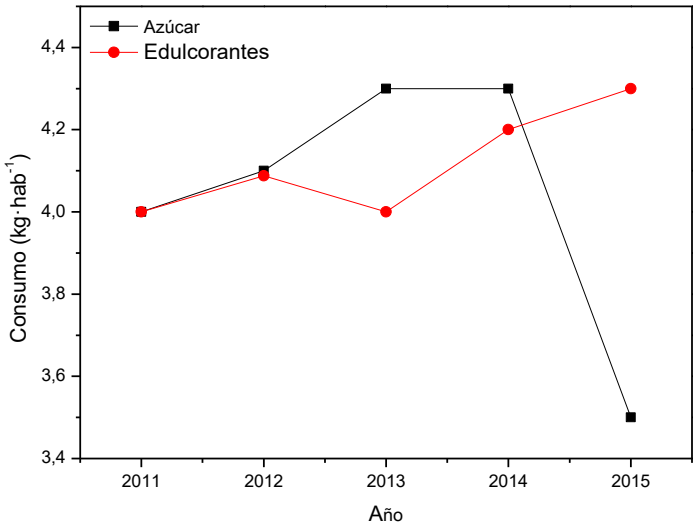

Figura 3. Evolución del consumo per cápita de azúcar y edulcorante entre 2011 y 2015.

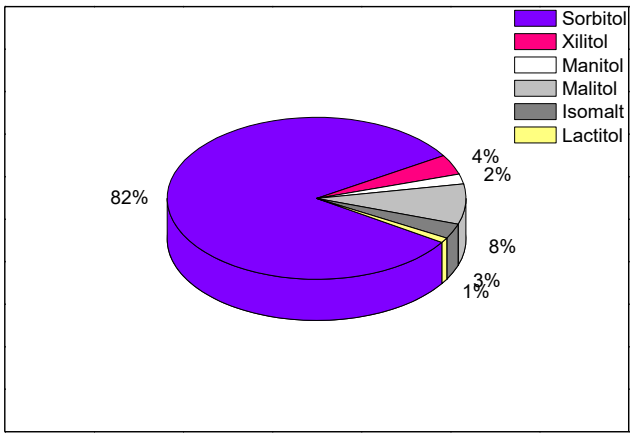

Figura 4. Distribución del consumo de polioles como edulcorantes según Amylum Group.

3.4. Situación del sector químico

Finalmente, Cathycel también compite en el sector químico. La Industria Química continúa consolidándose como uno de los sectores claves de la economía española. Sus más de 3.000 empresas, con una cifra de negocios con- junta de 59.000 millones de euros, generan el 12,6% del producto industrial bruto, y más de 540.000 empleos directos, indirectos e inducidos. Los datos aportados sobre este sector se han obtenido

de un informe reportado por la Federación Empresarial de Industria Química Española (FEIQUE).

3.4.1. Producción sector químico en España

El sector de la industria química española registró en 2016, un crecimiento en su producción en torno al 3%, además hay que tener en cuenta que la caída de los precios internacionales asociados al comportamiento del crudo limitó el incremento de la cifra de negocios al 1,7%, hasta superar los 59.000 M€.

Se observa un comportamiento similar en cuanto a las exportaciones. Pese al buen comportamiento en los mercados internacionales, que generó un incremento del volumen exportado del 1,4%, la facturación exterior quedó lastrada por la reducción de los precios, experimentando una caída del 2,1% hasta los 32.500 M€.

Tanto en el mercado interior como en el mercado exterior, el sector aumentó su volumen productivo, lo cual es un resultado muy positivo y que permite mantener un ritmo de crecimiento constante durante los últimos años, situándonos ya en una cifra de negocios un 19% superior a los niveles previos a la crisis económica de 2007 (Figura 5).

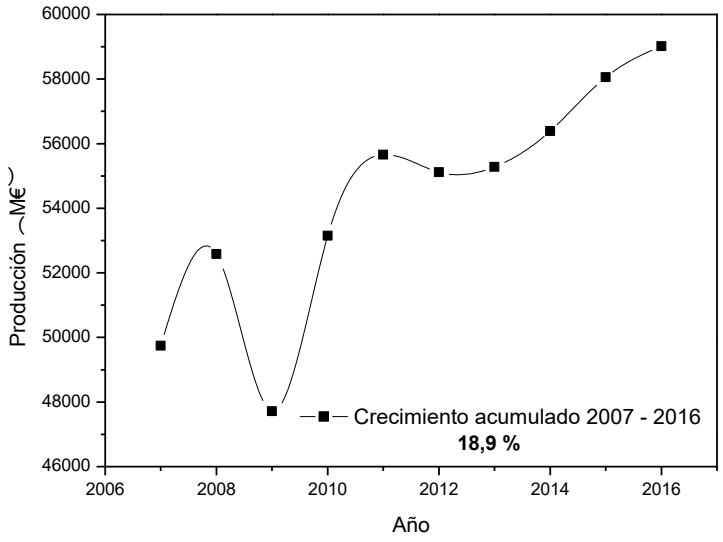

Figura 6. Evolución de la cifra de negocios del sector Químico entre 2007 – 2016.

En el mismo periodo, 2007-2016, las exportaciones han registrado un crecimiento acumulado del 40% y quizás lo que es más importante hemos mejorado nuestra posición en todos los mercados internacionales extracomunitarios, de modo que ya acogen el 41% de nuestras exportaciones frente al 29% que representaban en el año 2000. De

hecho, hoy somos ya capaces de exportar a más de 200 países y estados asociados. Actualmente, el buen comportamiento macro de nuestra economía desde 2014 y el previsto en los próximos años, en los que tanto el PIB como el consumo y las exportaciones están registrando las cifras de crecimiento más elevadas entre los principales países de la eurozona, permiten mirar con optimismo a medio y largo plazo, siempre con la premisa de que el precio del petróleo se mantenga en niveles próximos a los actuales.

Este hecho, unido a que el sector químico mantiene hasta 2030 previsiones del crecimiento mundial de su demanda superiores al 4,5% anual, tienen que incitar al gobierno a trabajar de forma eficaz en la mejora de los factores de competitividad del conjunto de la industria española, y particularmente en aquellos que son fundamentales para el sector químico, tales como el coste de la energía, el desarrollo de las infraestructuras de transporte, la mejora y simplificación de la legislación técnica que nos afecta, y la mayor defensa comercial de la Unión Europea ante otros competidores internacionales [6].

3.4.2. Estructura empresarial del sector químico en España

Los datos obtenidos del Instituto Nacional de Estadística (INE) sobre la distribución de empresas en el sector químico español (Figura 7A), demuestran que existen 3.034 empresas que operan en el sector. Casi el 54% de ellas (1.634 empresas) cuentan con menos de 10 asalariados en sus plantillas. Por otro lado, en torno al 30 %, que corresponde a unas 902 empresas, cuentan con un rango de asalariados comprendido entre 10 y 49. Estos dos grupos de empresas son los mayoritarios dentro de la distribución general de empresas dentro del sector químico español. Finalmente, las empresas con 500 o más asalariados son minoritarias, representado tan solo el 1,3 % del total (41 empresas).

La industria química española se distribuye geográficamente como se observa en la Figura 7B. Este tipo de industria presenta las mayores concentraciones de empresas químicas en Cataluña y Andalucía. Prácticamente la mitad de la producción del sector se genera en Cataluña (43,0 %). Junto a Madrid (13,5 %), Andalucía (12,7%) y Castilla La Mancha (4,3 %), estas cuatro comunidades agrupan aproximadamente el 74 % de la producción química española. Tarragona es uno de los principales polos químicos del Mediterráneo. Además los principales emplazamientos del sector están situados en

Huelva, Campo de Gibraltar (Algeciras), Puertollano (Castilla La Mancha), Cartagena (Murcia), Santander (Cantabria), Vizcaya (País Vasco), Valencia y Castellón (Comunidad Valenciana).

A

Intervalos de Empleo	Nº de Empresas	% del Total
Menos de 10 asalariados	1.634	53,9 %
De 10 a 49 asalariados	902	29,7 %
De 50 a 99 asalariados	235	7,7 %
De 100 a 199 asalariados	120	4,0 %
De 200 a 499 asalariados	102	3,4 %
500 o más asalariados	41	1,3 %
TOTAL	**3.034**	**100,0 %**

B

Figura 7. (A) Distribución de empresas por número de empleados en España en 2016. **(B)** Implantación territorial del sector químico español (principales zonas de producción).

3.4.3. Demanda y consumo aparente de productos químicos

En la Figura 8 se puede observar un análisis realizado sobre los datos de consumo de productos químicos en España entre los años 2008 y 2016. Se puede ver cómo el consumo de productos químicos decrece aproximadamente un 10 % entre 2008 y 2009. Este factor está asociado a todos los factores derivados de la dura crisis económica que sufrió nuestro país desde 2007. A partir de 2009 el consumo de productos químicos se recuperó, alcanzando en 2011 valores similares a los obtenidos en 2008. En el periodo comprendido entre 2011 y 2013, este consumo descendió un 4 % y a partir de ahí en los siguientes años hasta 2016 aumento extraordinariamente, alcanzando los mejores resultados desde 2008. Concretamente, se observó un aumento en el consumo de productos químicos por habitante del 1,9 % en 2016 respecto al ejercicio anterior en 2015.

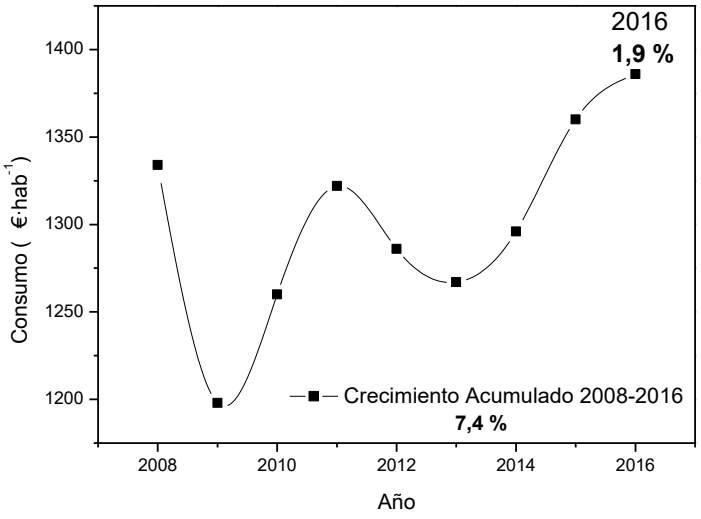

Figura 8. Consumo de productos químicos por habitante.

3.5. Análisis interno de Cathycel

Cathycel es una empresa de nueva creación, en la que los emprendedores involucrados tienen como misión llevar a cabo la implantación de una biorefinería capaz de valorizar residuos de biomasa convirtiéndolos en productos de alto valor añadido mediante el empleo de una tecnología sostenible. Además, ofrece soluciones de I+D+i a las entidades o personas interesadas.

3.5.1. Análisis DAFO

Tras analizar la empresa Cathycel ha sido posible identificar las fortalezas, debilidades, amenazas y oportunidades de dicho proyecto. A continuación, se presenta el análisis DAFO para dicho proyecto:

- **Fortalezas**
  - i) Materia prima del proceso a coste bajo (residuo pulpa remolacha).
  - ii) Tecnología novedosa
  - iii) Equipo humano con elevado conocimiento para desarrollar todas las actividades del proyecto desde el punto de vista tecnológico y de consultoría.
  - iv) Personal especializado en I+D+i con know-how.
  - v) Resultados prometedores validados a nivel de laboratorio.
  - vi) Producción de sorbitol de elevada pureza.
  - vii) Tiempos de producción bajos.
  - viii) Proceso sostenible que usa agua como medio de reacción, evitando el uso de ácidos o disolventes perjudiciales para el medio ambiente.

- **Debilidades**
  - i) Escalabilidad del proceso a nivel industrial.
  - ii) Financiación inicial muy elevada.
  - iii) Falta de personal con experiencia en finanzas y marketing dentro del equipo inicial de Cathycel.
  - iv) Necesidad de ser una marca reconocida.
  - v) Dependencia de la azucarera.

- **Oportunidades**
  - i) Obtención de sorbitol a partir de un residuo como la pulpa de remolacha.
  - ii) Tendencia a buscar soluciones tecnológicas más sostenibles.
  - iii) Actualmente el mercado de los edulcorantes de bajo nivel calórico se encuentra en continuo crecimiento.
  - iv) Economía circular.

- **Amenazas**
  - i) El proceso tecnológico propuesto en el proyecto Cathycel no está patentado aún
  - ii) No tener el dominio de Cathycel.
  - iii) Elevada competencia en cuanto a las labores de consultoría, existen numerosos grupos de investigación y empresas trabajando sobre ello.
  - iv) Regulaciones energéticas.
  - v) Dificultad de entrar en los sectores del mercado en los que compite Cathycel a corto plazo, ya que en muchos casos se componen de empresas multinacionales muy fuertes.

3.5.2. Objetivos de Cathycel

En este apartado se van a presentar los objetivos que se plantea conseguir Cathycel. Estos objetivos se clasifican en cuantitativos y cualitativos.

- **Cualitativos**
  - i) Alcanzar un acuerdo con la azucarera para desarrollar la actividad productiva en sus instalaciones.
  - ii) Diseño y construcción de la biorefinería.
  - iii) Promocionar y potenciar la marca Cathycel.
  - iv) Desarrollar actividades de consultoría para autofinanciación.
  - v) Puesta en marcha de la planta de valorización de biomasa para producción de productos de alto valor añadido.
  - vi) Optimización del proceso productivo.
  - vii) Conseguir un hueco en los sectores de biorefinerías, edulcorantes y productos químicos.
  - viii) Diseño del plan de distribución del producto final.

- **Cuantitativos**
  - i) Conseguir financiación (75.000 € por parte de los “business angels”, 50.000 préstamo bancario a corto plazo y 75.000 € por parte de las ayudas ofrecidas por el CDTI a devolver a partir del año 5).
  - ii) Devolución de la financiación obtenida por CDTI a partir del quinto año.

iii) Obtención de 1.200 Kg de pulpa de remolacha para desarrollar la actividad productiva de cara al primer ejercicio tras el arranque de la planta experimental (año 2).

iv) Fijar la producción anual de sorbitol en 1.000 Kg para el primer año tras la puesta en marcha (año 2).

v) Alcanzar una pureza de sorbitol mayor al 95 %.

vi) Fijar un mínimo de ventas en términos de proyectos de 5 unidades/año.

vii) Incrementar la producción después del segundo año entre el 2 – 4 %.

viii) Obtención de un beneficio sobre las ventas en torno al 20 % en el segundo ejercicio de Cathycel tras la puesta en marcha (tercer año).

3.5.3. Estrategias corporativas y de marketing

A continuación se presentan las principales estrategias corporativas y de marketing que consideramos que nos van a ayudar en la consecución de los objetivos propuestos en el apartado anterior.

- **Estrategias corporativas o globales**

i) Cathycel desarrollará una estrategia genérica de diferenciación. Esto es así ya que Cathycel se caracteriza por la producción de sorbitol a partir de la pulpa de remolacha mediante la utilización de una tecnología novedosa y sostenible. Además, la calidad de nuestro producto es nuestra principal seña de identidad frente a nuestros competidores. El sorbitol que se produce es muy versátil, pudiéndose utilizar como aditivo alimentario o como materia prima en diferentes industrias como alimentaria, farmacéutica y cosmética.

ii) Los mercados a los que se dirige Cathycel no son nuevos, sin embargo aunque el sorbitol es un producto conocido, el hecho de producirlo a partir de un residuo como la pulpa de remolacha y hacerlo con una calidad mayor que los competidores mediante un proceso novedoso, hace que consideremos nuestro producto como un producto nuevo. Por lo tanto haciendo uso de la matriz de Ansoff se

concluye que se llevará a cabo una estrategia de cartera de desarrollo de nuevos producto.

- **Estrategias de marketing**

  i) Cathycel llevará a cabo una estrategia de segmentación ya que el sorbitol como producto estrella de la empresa, abarcará diferentes segmentos del mercado bien diferenciados. Como ya se ha comentado con anterioridad, el sorbitol como edulcorante con bajo poder calórico puede utilizarse directamente por los consumidores como aditivo alimentario. La otra opción es que el sorbitol sea el iniciador o la materia prima de la actividad diaria de industrias como la farmacéutica, cosmética y alimentaria.

  ii) Además Cathycel desarrollará una estrategia de posicionamiento de diferenciación debido al alto grado de innovación, calidad y tecnología incorporado en la producción de sorbitol.

3.5.4. Plan de marketing operativo

Como se identificaba en el análisis DAFO de Cathycel, una de las principales debilidades de la empresa es el hecho de no tener una marca reconocida aún. Por lo tanto los primeros pasos tienen que ser en esa dirección, dándonos a conocer a los potenciales clientes. Para ello se propone la organización de jornadas informativas sobre Cathycel para las empresas y clientes interesados y la asistencia a congresos nacionales e internacionales con nuestra propuesta de negocio. De esta manera Cathycel comenzará a conocerse dentro de los diferentes sectores donde se pretende actuar y al mismo tiempo es una buena opción para conseguir clientes y socios clave. Por otro lado y para dar mayor difusión a Cathycel, consideramos que es importante la publicación de información sobre la empresa en páginas web y revistas especializadas. Desde el punto de vista tanto del sorbitol como de los servicios de consultoría, se llevará a cabo un seguimiento personal que se mantiene en el tiempo como a través de la página web de la empresa, email etc. Cathycel trabajará en torno a una filosfía CRM (Custom Relationship Management) para ganar la lealtad de los clientes por la satisfacción a partir del trato individualizado. La distribución del sorbitol se llevará a cabo mediante

camiones especializados para el transporte de este tipo de productos. Finalmente, en cuanto al proceso productivo, se harán visitas técnicas a la biorefinería tanto para los ciudadanos como para las empresas interesadas en conocer más en profundidad Cathycel.

4. Plan de operaciones

Cathycel se desarrollará en la zona de Castilla y León, ya que tiene una importante presencia de industria azucarera, pudiéndose asociar con una de las empresas azucareras de la región para desarrollar el proceso productivo dentro de sus instalaciones. Concretamente, la biorefinería se situaría en Olmedo, próxima a las instalaciones de la azucarera ACOR. De esta manera, la azucarera dejaría el residuo que se obtiene de su actividad productiva (pulpa de remolacha) para que Cathycel le dé un valor añadido, ya que actualmente lo más común es vender esta pulpa de remolacha a 25 €/tn. A cambio, la azucarera como socio clave se llevará un porcentaje de los beneficios obtenidos de la comercialización del sorbitol a finales de cada ejercicio.

Cathycel es una propuesta ambiciosa, fuertemente basada en una tecnología que inicialmente necesita una fuerte inversión. Por lo tanto, Cathycel recibirá la ayuda de inversores y además se apoyará en las ayudas que ofrece el CDTI para el desarrollo de proyectos de este tipo. Con esta inversión se podría empezar a construir la planta industrial para la obtención de sorbitol a partir de pulpa de remolacha. La construcción se desarrollará bajo nuestra supervisión por una empresa externa especializada. Mientras tanto, Cathycel empezará a realizar labores de consultoría y redacción de proyectos para empresas, universidades y otros clientes interesados, que le permitirán autofinanciarse hasta que la construcción de la planta esté acabada.

Una vez que la planta industrial esté terminada, se pondrá en marcha. El proceso que Cathycel propone para valorizar la pulpa de remolacha y obtener sorbitol, consiste fundamentalmente en dos etapas bien diferenciadas. Una primera etapa de hidrólisis del residuo de pulpa de remolacha y una segunda etapa de hidrogenación del producto obtenido durante la hidrólisis.

La etapa de hidrólisis de pulpa de remolacha consiste en un proceso en el que esta se depolimeriza en un reactor continuo en medio acuoso a una temperatura de 400 ºC y una

presión de 25 MPa. Como resultado de este proceso, se obtiene una corriente rica en hidrolizados de azúcares. Esta tecnología ha sido probada de manera exitosa a nivel de laboratorio tanto con pulpa de remolacha como otros tipos de biomasa como materia prima.

La etapa de hidrogenación consiste en un proceso en el que la corriente de azúcares obtenida en la etapa anterior se introduce en un reactor continuo con un lecho de catalizador de rutenio a una temperatura de 120 ºC y una presión de 5 MPa de hidrógeno. De este proceso se obtiene como resultado una corriente líquida de sorbitol de pureza mayor al 95 %.

Después de las etapas de reacción, para la obtención del sorbitol sólido, se lleva a cabo un proceso de secado en spray. El proceso de secado consiste en bombear la solución acuosa de sorbitol hasta un disco rotativo, donde el fluido es atomizado en millones de microgotas individuales. A través de este proceso el área de la superficie de contacto del producto pulverizado se aumenta enormemente y cuando se encuentra dentro de la cámara con la corriente de aire de secado produce una vaporización rápida del agua, que seca suavemente sin choque térmico, transformándose en polvo y terminando el proceso con la colecta del mismo. Para el proceso de secado, la temperatura de entrada es de 120 ºC, usando un flujo de aire de 1 l/h y una temperatura de salida en torno a 80-90 ºC.

En función de las necesidades de los clientes, Cathycel preparará sorbitol sólido o sirope (líquido). En función de la naturaleza del producto, este se envasará de maneras diferentes. Para el caso del sorbitol líquido se usarán garrafas plásticas de volúmenes variables según las preferencias de nuestros clientes. El producto sólido se envasará en sacos de plástico de 1 Kg como mínimo cuando vaya destinado a la industria. Cuando el cliente final lo quiera utilizar el sorbitol como aditivo alimentario, este será envasado en pequeños sobres de plástico similares a los que actualmente hay para el azúcar o en botes de plástico de 250 g y 500 g. La distribución de los productos finales se llevará a cabo mediante una empresa de transporte externa.

Finalmente, en Cathycel se realizarán auditorías internas tanto para la sección de producción de sorbitol como para la de consultoría por medio de los jefes de cada área. Esto ayudará a una mayor organización de cara a cumplir los objetivos propuestos, además de permitir evaluar y mejorar la eficacia de los procesos de gestión.

5. Plan de recursos humanos

En una primera etapa inicial, Cathycel estará constituida por los tres socios principales (Gloria Esther Alonso Sánchez, Antonio Nieto-Márquez Ballesteros y Alberto Romero Camacho), los cuales han sido los encargados de desarrollar el presente modelo de negocio. Sin embargo, una vez que la planta esté construida, se necesitarán dos personas más, concretamente un director comercial y un director de calidad. A continuación en la Figura 9 se presenta el organigrama para los tres primeros años de Cathycel.

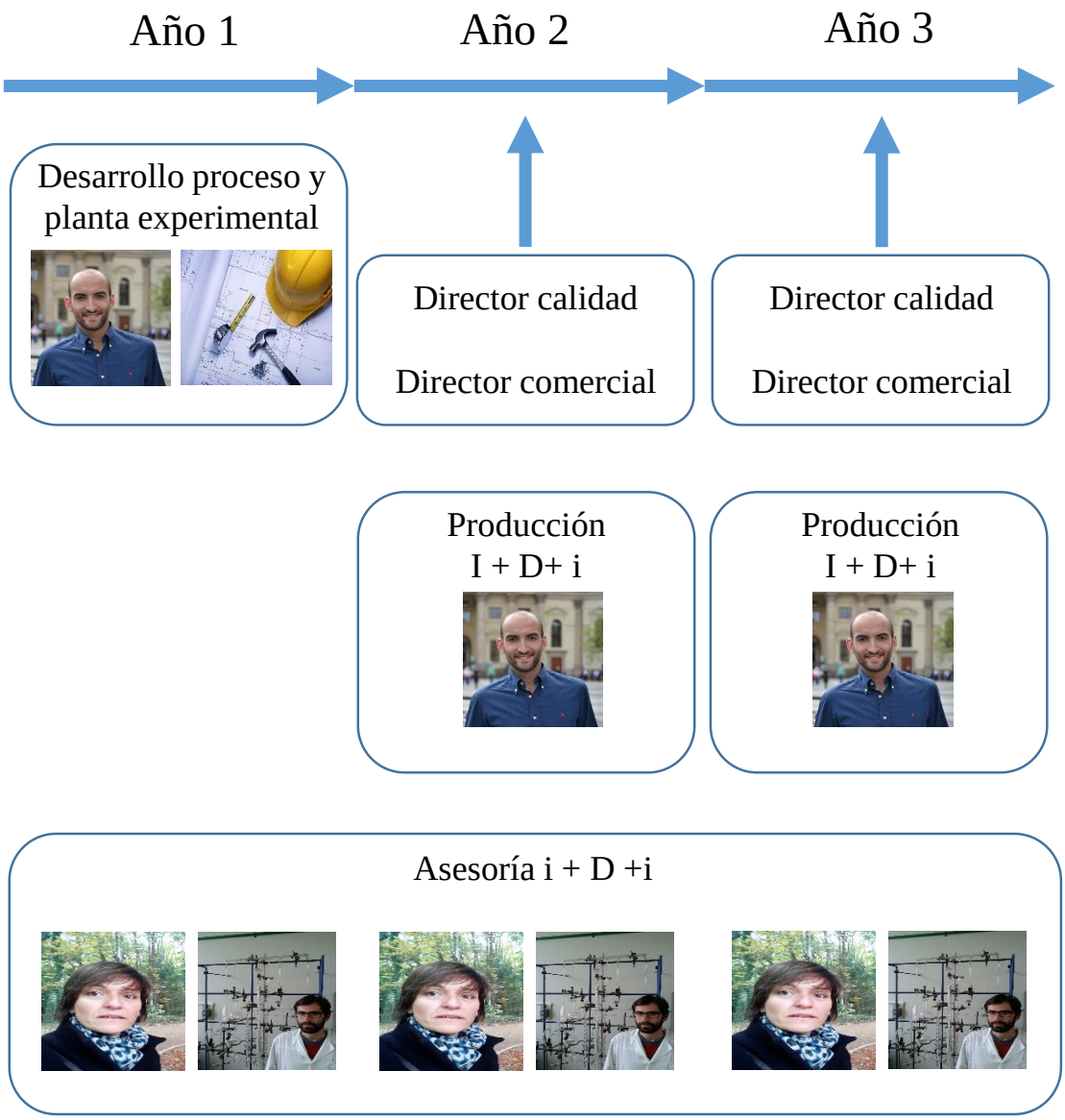

Figura 9. Organigrama funcional de Cathycel para los tres primeros años.

Alberto Romero va a trabajar a tiempo completo en Cathycel, mientras que tanto Gloria Esther Alonso como Antonio Nieto-Márquez compaginarán sus labores docentes

en la Universidad de Valladolid y en la UPM junto con la asesoría de I+D+i a tiempo parcial. Durante el primer año, Cathycel despegará gracias a la construcción de la planta, donde Alberto Romero se encargará de supervisar el desarrollo de la construcción y proceso de la planta productiva. La construcción de la planta será desarrollada por una empresa externa especializada (subcontratación) en este tipo de tareas. Los avances durante este año serán mostrados a los clientes, inversores y empresas interesadas en Cathycel en diferentes reuniones que se organizarán. Alberto Romero irá a diferentes ferias y congresos especializados para mostrar la marca Cathycel y darle una mayor visibilidad. Mientras tanto, Gloria Esther Alonso y Antonio Nieto-Márquez empezarán con todas las tareas de consultoría, donde tendrán los primeros contactos con clientes y conseguirán las primeras solicitudes de redacción de proyectos de investigación o asesoría en diversos temas científico-técnicos.

En el segundo año, donde ya estaría construida la planta experimental a escala industrial, será necesario contratar un director de calidad y comercialización (contratación directa). La calidad es uno de los estandartes de Cathycel y uno de los hechos diferenciadores con respecto a la competencia, por lo tanto consideramos crucial la presencia de la figura de un director de calidad una vez que se empieza a producir sorbitol. El director de comercialización tendrá una elevada responsabilidad para evitar retrasos en los pedidos y mantener contacto directo con los clientes. Ambas figuras ayudarán a crecer a la empresa Cathycel, produciendo sorbitol de una manera muy eficaz, manteniendo el nivel de satisfacción de nuestros potenciales clientes. En esta segunda etapa, ya se pueden entregar los primeros proyectos y las soluciones de I+D+i a los problemas propuestos, obteniendo los beneficios derivados de dicha actividad. El equipo de Cathycel seguirá en cada momento buscando mejoras para optimizar cada vez más el proceso productivo de manera que sea más eficiente.

En el tercer año, la actividad será similar a la de la etapa anterior, se continuará produciendo sorbitol, sin embargo se incrementará la producción entre un 2 – 4 %. Además, seguirán realizándose las labores de asesoría de I+D+i. En esta tercera etapa, vuelve a ser clave la figura del director de calidad, Cathycel no desea que un aumento en la producción, resulte en una reducción de la calidad de su producto.

6. Plan económico financiero

A continuación se presenta el plan económico financiero que se ha estimado para los tres primeros años de Cathycel, sociedad limitada que se creará en el segundo año de actividad.

En la Tabla 1 aparecen detallados los diferentes elementos que forman parte de la inversión inicial que se ha estimado para Cathycel. Se necesita una inversión inicial en concepto de activo no corriente de 170.000 €, desglosada en dos partidas de 20.000 € y 150.000 € asociadas al inmovilizado intangible (alquiler del terreno para actividad productiva a la azucarera) y al material, respectivamente. Los 150.000 € asociados al inmovilizado material, son los que se destinarán a todo lo relacionado con la tecnología y construcción de la planta productiva, que se amortizarán al 12 %. Además como activo corriente se contará con 30.000 €, que será el activo líquido derivado de un determinado porcentaje de las primeras ventas al cierre del primer ejercicio. Por lo tanto el total de la inversión inicial será de 200.000 €.

Tabla 2. Inversión inicial Cathycel.

Concepto	Importe (€)	Amortización (% / €)
Activo no corriente	**170.000**	
- Inmovilizado intangible	20.000	
- Inmovilizado material	150.000	12 / 18.000
Activo Corriente	**30.000**	
- Plazo cobro primera venta	30.000	
TOTAL INVERSIÓN INICIAL	**200.000**	

Una vez presentada la inversión inicial que se necesita, en la Tabla 3 se muestra cual será el plan de financiación de Cathycel. Debido a la gran inversión que hay que hacer para la construcción de la planta y tecnología, será necesaría la financiación por parte de los business angels por una cuantía de 75.000 €. Por otro lado también se cuenta con 75.000 € en forma de préstamo a largo plazo por parte de las ayudas que concede el CDTI. Este préstamo se devolverá a partir del quinto año. Finalmente se cuenta en este apartado de financiación con 50.000 € en concepto de pasivo corriente relacionado con el dinero procedente de las entidades de crédito. Esta cuenta de crédito de 50.000 € va

destinado a financiar los sueldos de los empleados hasta que obtenga los primeros beneficios. Por lo tanto el total de financiación asciende a 200.000 €.

Tabla 3. Plan de financiación.

Concepto	Importe (€)
Patrimonio neto	**75.000**
- Capital y otras aportaciones de socios	75.000
Pasivo no corriente	**75.000**
- Deudas a largo plazo por préstamos recibidos	75.000
Pasivo corriente	**50.000**
- Deudas a corto plazo con entidades de crédito	50.000
TOTAL FINANCIACIÓN	**200.000**

En la Tabla 4, se presentan los resultados de las estimaciones de ventas y consumos para los primeros tres ejercicios de Cathycel. Como ya se ha explicado con anterioridad, Cathycel cuenta con dos tipos de productos, sorbitol del cual se obtendrán beneficios tras la venta a los clientes finales y actividades de consultoría. En el caso del sorbitol, se ha estimado que el precio de producción mediante nuestra metodología sería de unos 25€/Kg y se vendería a 50 €/Kg. Por otro lado, en cuanto a los servicios de consultoría, las ventas se estimas por unidades de I+D+i en forma de proyectos, cada uno con un coste asociado de 10.000 €. Durante el primer año Cathycel se dedicará a redactar cinco proyectos de investigación a cinco clientes diferentes de ámbito nacional, más un proyecto internacional para una universidad extranjera en Letonia. En la Tabla 4 se puede observar que hay un determinado consumo de I+D+i. De las ventas de proyectos de cada año se ha fijado que se consumirán 5 unidades, que van destinadas a los salarios de los trabajadores en cada uno de los ejercicios. En el primer año, aún no estará construida la planta industrial de producción de sorbitol, por lo tanto durante este ejercicio no hay ni ventas ni consumos referentes a esta actividad productiva. En el segundo año, se venden 7 proyectos de I+D+i y además se venderán 500 Kg de sorbitol a 50 €/Kg. En cuanto al consumo en el segundo ejercicio, además de tener en cuenta el consumo fijado para I+D+i, hay que añadir los gastos de producción de 1000 Kg de sorbitol. El gasto de producción de sorbitol es de 25 €/Kg. En este coste de producción están incluidos los gastos de agua, electricidad, catalizador, hidrógeno etc. En el tercer ejercicio, se mantienen las ventas en cuanto a I+D+i, sin embargo se conseguirán más

clientes pudiendo llegar a vender 1000 Kg más 500 Kg que quedan en stock del ejercicio anterior. En este tercer ejercicio, los costes de producción de sorbitol se realizan sobre 1040 unidades ya que a partir del segundo año se había fijado como objetivo incrementar la producción entre un 2 – 4 %.

Tabla 4. Estimación ventas y consumos durante los tres primeros año.

Concepto	**Precio**	**Año 1**		**Año 2**		**Año 3**	
	€/unidad	**Unidad**	**Precio**	**Unidad**	**Precio**	**Unidad**	**Precio**
Ventas			**60.000**		**95.000**		**145.000**
I+D+i	10.000	6	60.000	7	70.000	7	70.000
Sorbitol	50	0	0	500	25.000	1500	75.000
Consumo			**50.000**		**75.000**		**76.000**
I+D+i	10.000	5	50.000	5	50.000	5	50.000
Sorbitol	25	0	0	1000	25.000	1040	26.000

En la Tabla 5, se presenta la cuenta de resultados en cuanto a ganancias y pérdidas provisionales de Cathycel durante los tres primeros años.

Tabal 5. Cuenta de pérdidas y ganancias durante los tres primeros años

Concepto	**Año 1**	**Año2**	**Año 3**
Ventas (€)	60.000	95.000	145.000
Consumos (€)	50.000	75.000	76.000
Amortizaciones (€)	18.000	18.000	18.000
Rdto. Explotación Margen Bruto (€)	-8.000	2.000	51.000
BAII	-8.000	2.000	51.000
Gastos financieros	750	750	750
BAI	-8.750	1.250	50.250
Impuestos	-2.187,50	315,50	12.562,50
Resultado	**-6.562,50**	**937,50**	**37.687,50**
Cash-Flow	**11.437,50**	**18.937,50**	**55.687,50**

Durante el primer año, Cathycel presenta pérdidas en torno a los 6.562,50 €, siendo el cash-flow para este ejercicio de 11.437,50 €. En el segundo año, al aumentar las ventas tanto en términos de proyectos como por la introducción de las ventas de

sorbitol, se obtienen mayores ingresos. Los costes de producción de sorbitol se incluyen en este segundo ejercicio y de ahí el aumento en la partida de consumos. Para el segundo ejercicio se obtienen unas ganancias de 937,50 €, siendo el beneficio estimado sobre las ventas del 1 %. Se observa un dato muy positivo en este segundo ejercicio relacionado con el EBITDA, que será del 21 %. Este valor es muy atractivo de acuerdo con la naturaleza tecnológica y el mercado al que se dirige Cathycel. En el tercer ejercicio de Cathycel, se obtienen ganancias de 37.687,50 €, que corresponden a un beneficio estimado sobre las ventas del 26 %. En este tercer ejercicio, el cash-flow es de 55.687,50 € y el EBITDA es del 48 %. Este resultado indica que Cathycel será un 27 % más rentable en este tercer año. Por lo tanto se puede concluir que Cathycel es rentable. Además en este tercer ejercicio se ha logrado otro de los objetivos propuestos, obtener un beneficio sobre ventas en torno al 20 %.

Finalmente en la Tabla 6, se presenta el balance de situación previsional de Cathycel desde el inicio hasta el tercer año.

Tabla 6. Balance de situación previsional.

	INICIAL	**AÑO1**	**AÑO2**	**AÑO 3**
ACTIVO				
Activo No Corriente:	**170.000,00**	**152.000,00**	**134.000,00**	**116.000,00**
Inmovilizado Intangible	20.000,00	20.000,00	20.000,00	20.000,00
Inmovilizado Material	150.000,00	132.000,00	114.000,00	96.000,00
Inmovilizado Financiero				
Amortización Acumulada				
Activo Corriente:	**30.000,00**	**562,50**	**38.500,00**	**71.687,50**
Existencias			12.500,00	13.500,00
Clientes y otros deudores	30.000,00		9.062,50	34.687,50
Tesorería		562,50	16.937,50	23.500,00
Total activo	**200.000,00**	**152.562,50**	**172.500,00**	**187.687,50**
PATRIMONIO NETO Y PASIVO				
PATRIMONIO NETO:	**75.000,00**	**68.437,50**	**69.375,00**	**107.062,50**
Fondos propios:	**75.000,00**	**68.437,50**	**69.375,00**	**107.062,50**
Capital social	75.000,00	75.000,00	75.000,00	75.000,00
Reservas			-6.562,50	-5.625,00
Resultados del ejercicio		-6.562,50	937,5	37.687,50
Subvenciones, donaciones y legados recibidos				

PASIVO NO CORRIENTE:	75.000,00	75.000,00	75.000,00	75.000,00
Deudas a largo plazo:	**75.000,00**	**75.000,00**	**75.000,00**	**75.000,00**
Deudas a largo plazo por préstamos recibidos	75.000,00	75.000,00	75.000,00	75.000,00
Otra financiación a largo plazo				
PASIVO CORRIENTE:	**50.000,00**	**9.125,00**	**28.125,00**	**5.625,00**
Deudas a corto plazo con entidades de crédito	50.000,00	9.125,00	13.125,00	5.625,00
Acreedores comerciales y otras cuentas a pagar:	**0,00**	**0,00**	**15.000,00**	**0,00**
Proveedores			15.000,00	
Acreedores				
Administraciones Públicas				
Anticipos de clientes				
Total Pasivo	**200.000,00**	**152.562,50**	**172.500,00**	**187.687,50**

7. Estructura legal de la empresa

La estructura legal de la empresa será una sociedad limitada (S.L) formada por 3 socios a partes iguales. La sociedad será creada definitivamente en el segundo año del plan, tras haber conseguido el desarrollo y construcción de la planta productiva. Hasta entonces se continuará trabajando bajo la financiación procedente del CDTI e inversores, adecuando la estructura jurídica y la participación de los socios a las necesidades financieras y el control en la toma de decisiones.

8. Bibliografía

1. BIOENAREA, Biorrefinerías una oportunidad de negocio para las zonas rurales y las industrias: Guía de actuación en las regiones participantes en el Proyecto BIOREF.
2. Smith, D.W.J., State of the art in Biorefinery Development. Tamutech Consultancy for National Non Food Crop Center, 2007.
3. Vélez, I.G., Development of the heterogeneous catalysts for the production of Levulinic acid from furfuryl alcohol. 2015.
4. MERCASA, Alimentación en España 2016 (Producción, Industria, Distribución y consumo). 2016.
5. Solá, A., Los edulcorantes (Parte 1). 2001.
6. FEIQUE,. Radiografía del sector químico español 2017. 2016; Available from: http://www.feique.org/sector-quimico-facturo-17-mas-2016-los-59-000-millones-acumulando-crecimiento-del-187-desde-2007/.

AGRADECIMIENTOS

La tesis doctoral es un largo camino de investigación, lleno de diferentes obstáculos, que los doctorandos debemos superar de la mejor manera posible para obtener el título de doctor. En esta ardua tarea yo no he estado solo, sino que he contado con la ayuda de mucha gente que de una u otra manera han participado en la consecución de la misma.

En primer lugar, agradezco a mi supervisora Esther Alonso por haberme dado la oportunidad de formar parte del Grupo de Procesos a Presión de la Universidad de Valladolid durante estos años y confiar en mí para la realización de esta tesis. Muchas gracias por la ayuda que me has ofrecido durante esta etapa.

Gracias al resto de profesores del Grupo de Procesos de Alta Presión, especialmente a María José Cocero y Soraya Rodríguez que siempre me han ayudado cuando las he necesitado durante estos años.

Quiero agradecer a mi supervisor en la distancia, Antonio Nieto-Márquez, todos los sabios consejos y cariño que he recibido por su parte. Gracias por todo el entusiasmo que has depositado en este proyecto.

Je tiens à remercier Nadine Essayem et Catherine Pinel de m'avoir donné l'occasion de travailler dans l'un des centres de recherche les plus importants d'Europe, IRCELYON. Je me suis senti comme à la maison en dépit du fait d'être si loin de ma famille. Merci beaucoup pour toute la confiance, le soutien et l'amour que vous m'avez apporté, cela a été un vrai plaisir de travailler avec vous et votre équipe tout au long de ces trois mois.

Gracias a todos los compañeros del Departamento de Ingeniería Química de la Universidad de Valladolid, por tantos buenos momentos dentro y fuera del trabajo. Todos habéis contribuido de una manera u otra a que encontrara mi sitio aquí, a que creciera como investigador y a que consiguiera todos los éxitos que he cosechado durante esta tesis doctoral. Muchas gracias a todos.

Gracias a mis compañeros de residencia y a mis compañeros de piso Martijn y Aurelia, con los que he pasado muchos grandes momentos y he entablado una gran amistad.

También quiero dar las gracias a Vito y Lourdes por haber sido como unos padres para mí en Valladolid.

Gracias a mi familia, abuelos, tíos, hermanos y especialmente a mis padres, por su apoyo incondicional en la distancia, por dármelo todo en esta vida y por todo el cariño que me han dado siempre. Gracias a Valladolid porque me ha encantado vivir en esta preciosa ciudad y por permitirme conocer a Marta, la mujer de mi vida, sin ella esta tarea no habría llegado nunca a su fin. Gracias por aguantarme, por quererme tanto, por todo tu apoyo y por darme mucho más de lo que me merezco día a día.

Finalmente, quiero dedicar esta tesis a mi tío Pedro que falleció este año pasado, ya que representa todos los valores que me inculcó desde pequeño. Pedrito, puedes estar tranquilo, esta partida la he jugado hasta el final y la he ganado para ti.

About the author

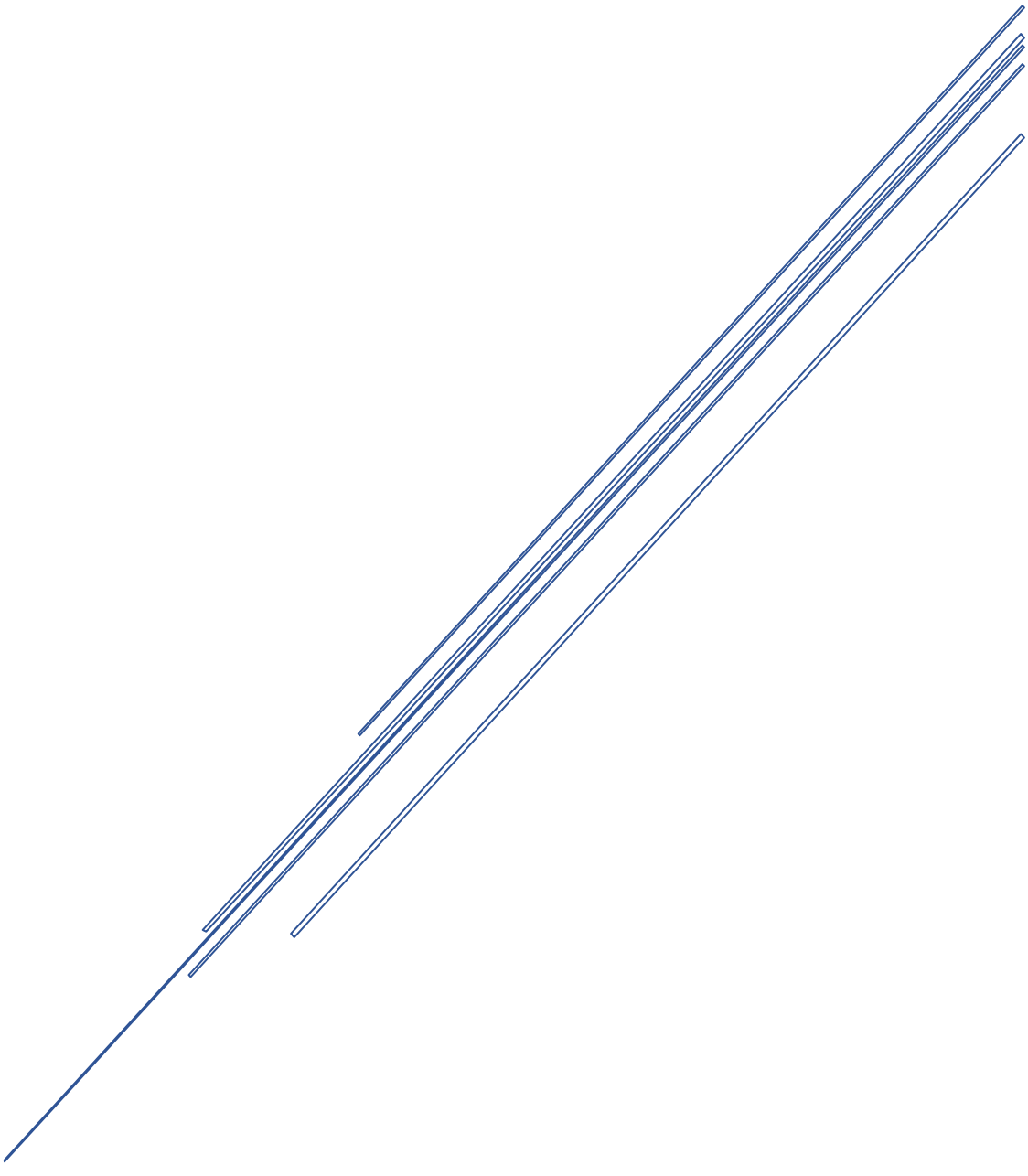

Alberto Romero was born in Madrid in 1988. He grew up in Ciudad Real, where he studied Chemical Engineering in University of Castilla La Mancha (UCLM, Spain) from 2006 to 2011. He obtained I COPIQCLM Award for the best final master thesis on Chemical Engineering in 2011.

He moved to Valladolid in order to start his PhD at the High Pressure Processes Group of University of Valladolid. His PhD is related to cellulosic biomass conversion over mesoporous noble metal catalyst for the production of high valuable chemicals under the supervision of Dr. Esther Alonso (University of Valladolid) and Dr. Antonio Nieto-Márquez (Technical University of Madrid). He also studied a Fluid Thermodynamic Engineering Master in University of Valladolid from 2012 to 2013 and he was awarded as the best student. He developed a stay of research for three months in the "Institut de recherches sur la catalyse et l'environement de Lyon" (Lyon, France) under the supervision of Dr. Catherine Pinel and Dr. Nadine Essayem, where he could continue researching about conversion of cellulosic biomass into alkanes.

PUBLICATIONS

- Romero, A., Nieto-Márquez, A. & Alonso, E. Bimetallic Ru:Ni/MCM-48 catalysts for the effective hydrogenation of d-glucose into sorbitol. *Applied catalysis A: General*, *529*, (2017), 49-59.
- Sanz-Moral, L. M., Romero, A., Holz, F., Rueda, M., Navarrete, A., & Martín, A. Tuned Pd/SiO_2 aerogel catalyst prepared by different synthesis techniques. *Journal of the Taiwan Institute of Chemical Engineers*, *65*, (2016), 515-521.
- Romero, A., Cantero, D. A., Nieto-Márquez, A., Martínez, C., Alonso, E., & Cocero, M. J. Supercritical water hydrolysis of cellulosic biomass as effective pretreatment to catalytic production of hexitols and ethylene glycol over Ru/MCM-48. *Green Chemistry*, *18*, (2016), 4051-4062.
- Romero, A., Alonso, E., Sastre, Á., & Nieto-Márquez, A. Conversion of biomass into sorbitol: Cellulose hydrolysis on MCM-48 and d-Glucose hydrogenation on Ru/MCM-48. *Microporous and Mesoporous Materials*, *224*, (2016), 1-8.

- Sánchez-Bastardo, N., Romero, A., & Alonso, E. Extraction of arabinoxylans from wheat bran using hydrothermal processes assisted by heterogeneous catalysts. *Carbohydrate polymers*, *160,* (2017), 143-152.

SUBMITTED / IN PREPARATION PUBLICATIONS

- Romero, A., Nieto-Márquez, A., Essayem, N., Alonso, E., & Pinel, C. Catalytic conversión of d-glucose into short-chain alkanes over Ru-based catalysts. *Molecular Catalysis.*
- Romero, A., Díaz, J.A., Nieto-Márquez, A., Essayem, N., Alonso, E., & Pinel, C. Catalytic hydrogenolysis of cellobiose into hexitols over Ru/Al-MCM-48. *Bioresource Technology*.
- Andérez, M., Benito-Román, Ó., Romero, A., & Alonso, E. Hydrolytic hydrogenation of cellobiose into hexitols by means of Ru/MCM-48 catalysts. *ACS Research & Engineering Chemistry Research.*
- Sastre, Á., Romero, A., Cabeza, Á. Nieto-Márquez, A., Sobrón, F., García-Serna, J., & Alonso, E. Hydrogen production from cellulose gasification by slow pyrolysis catalyzed by Co/MCM-41: kinetics and modelling. *Journal of Supercritical Fluids.*

CONFERENCE CONTRIBUTIONS

ORAL PRESENTATIONS

- Romero, A., Nieto-Márquez, A. & Alonso, E. Catalytic conversion of cellobiose into hexitols over Ru/Al-MCM48. *Europacat 2017*. Firenze (Italy). August 2017. May 2017.
- Romero, A., Nieto-Márquez, A. & Alonso, E. Bimetallic Ru:Ni/MCM-48 catalysts for the effective hydrogenation of d-glucose into sorbitol. *2nd Green & Sustainable Chemistry Conference.* Berlin (Germany). May 2017.
- Aspromonte, S., Romero, A., Venghi, M., Boix, A., Alonso, E., & Cocero, M.J. Hidrólisis de celulosa empleando catalizadores de Ag soportada en mordenita mesoporosa. *XXV Congreso Iberoamericano de catálisis.* Montevideo (Uruguay), Septemeber 2016.

- Romero, A., Nieto-Márquez, A., Essayem, N., Alonso, E., & Pinel, C. One-pot conversion of D-Glucose into liquid straight-chain alkanes over Ru-based catalysts. *2nd International Conference on Green Chemistry and Sustainable Engineering*. Rome (Italy), July 2016.
- Romero, A., Cantero, D. A., Nieto-Márquez, A., Martínez, C., Alonso, E., & Cocero, M. J. Hidrólisis de pulpa de remolacha en agua supercrítica como pretratamiento a la producción de etilenglicol sobre Ru/MCM-48. *II Encuentro de Jóvenes Investigadores en catálisis de la SECAT.* Ciudad Real (Spain), June 2016.
- Sanz-Moral, L.M., Rueda, M., Navarrete, A., Romero, A., Nieto-Márquez, A., &. Martín, A. Síntesis y funcionalización de aerogeles para su uso en catálisis y almacenamiento de H_2. *II Encuentro de Jóvenes Investigadores en catálisis de la SECAT.* Ciudad Real (Spain), June 2016.
- Aspromonte, S., Romero, A., Venghi, M., Boix, A., Alonso, E., & Cocero, M.J. Mesoporous AgNa-mordenite catalysts for the biomass hydrolysis. *18th International Zeolite Conference: Zeolites for a sustainable world.* Rio de Janeiro (Brazil), June 2016.
- Romero, A., Díaz, J.A., Nieto-Márquez, A., Essayem, N., Alonso, E., & Pinel, C. Catalytic hydrogenolysis of cellobiose into hexitols over Ru/Al-MCM48. *5th Portuguese Young Chemists Meeting (5th PYCheM) and 1st European Young Chemists Meeting (1st EYCheM)*. Guimarães (Portugal), April 2016.
- Benito, Ó., Andérez, M., Romero, A., & Alonso, E. Direct conversion of cellobiose into hexitols by means of ruthenium bifunctional catalysts. *2nd EuChemMS Congress on Green and Sustainable Chemistry*. Lisbon (Portugal), October 2015.
- Romero, A., Cantero, D. A., Nieto-Márquez, A., Martínez, C., Alonso, E., & Cocero, M.J. Ru/MCM-48 catalyst for the hydrogenation of cellulose into sugar alcohols. Use of SCW as pre-treatment. *10th European Congress of Chemical Engineering (ECCE10).* Nice (France), September 2015.
- Romero, A., Nieto-Márquez, A., Sastre, A., & Alonso, E. Catalizadores bimetálicos Ru:Ni/MCM-48 para la hidrogenación selectiva de D-Glucosa. *Congreso de la sociedad española de catálisis SECAT'15.* Barcelona (Spain), July 2015.
- Romero, A., Sastre, Á., Nieto-Márquez, A., & Alonso, E. Preparación de catalizadores mesoporosos de Ni para la hidrogenación selectiva de d-glucosa. *I*

Encuentro de Jovenes Investigadores de la Sociedad Española de Catálisis SECAT'14. Málaga (Spain), June 2014.

- Romero, A., Sastre, Á., Nieto-Márquez, A., & Alonso, E., Design of ruthenium catalysts for the efficient conversion of biomass into sorbitol. *10th International Conference on Renewable Resources and Biorefineries (RRB10).* Valladolid (Spain), June 2014.

POSTER PRESENTATIONS

- Romero, A., Nieto-Márquez, A. & Alonso, E. Bimetallic Ru:Ni/MCM-48 catalysts for the effective hydrogenation of d-glucose into sorbitol. Europacat 2017.Firenze (Italy). August 2017. Poster presentation.
- Martín, A., Navarrete, A., Rueda, M., Sanz-Moral, L.M., & Romero, A. Improvement of the kinetics of hydrogen release from hydrides confined in silica aerogel. *IV Iberoamerican conference on supercritical fluids (PROSCIBA).* Viña del Mar (Chile), March 2016.
- Nieto-Márquez, A., Sastre, Á., Romero, A., Alonso, E., & Cocero, M.J. Preparación supercrítica de catalizadores de cobalto y níquel para la valorización de biomasa. *XVII Congreso peruano de química.* Lima (Peru), October 2014.
- Romero, A., Sastre, Á., Nieto-Márquez, A., & Alonso, E. Preparación de catalizadores mesoporosos de Ni para la hidrogenación selectiva de d-glucosa. *I Encuentro de Jovenes Investigadores de la Sociedad Española de Catálisis SECAT'14.* Málaga (Spain), June 2014.
- Sastre, Á., Romero, A., Nieto-Márquez, A., Cocero, M.J., & Alonso, E. Supercritical Fluid deposition of cobalt nanoparticles over MCM-41: Kinetic models of adsorption. Belgrade (Serbia), September 2013.
- Romero, A., Sastre, Á., Nieto-Márquez, A., & Alonso, E. Supercritical preparation of nickel mesoporous silica catalyst: comparison with wet techniques. *ECCE9 9th European Congress of Chemical Engineering*. The Hague (Netherlands), April 2013.

MAIN SPECIALIZED TRAINING

- Entrepreneurship Santander Yuzz 2017 program. – Valladolid (Spain).

- Be an entrepreneur! – A workshop for curious scientists. Entrepreneur Whorkshop. 3 h – Berlin (Germany).
- Rheological characterization of food carbohydrate systems by Athina Lazaridou. 2 h – Palencia (Spain).
- 2nd Spanish-Italian Summer School on catalysis. Mesostructured catalysts and reactors. 20 h – Seville (Spain).
- 1st Summer School on Green Chemistry. 20 h – La Rochelle (France).
- Life long learning intensive course on process intensivation by high pressure technology – Actual strategies for energy and resources conservation, by International Society for the Advancement of Supercritical Fluids. 90h – Germany (Darmstadt).
- Economy for the leading role of chemical engineer. 20 h – UCLM (Spain).
- Solid State Hydrogen: An overview by Chiara Milanese. 7 h – Valladolid (Spain).
- Writing great papers in international journals – An introduction to researchers by Willey. 3 h - Valladolid (Spain).
- Catálisis ambiental. Preparación y caracterización de catalizadores y adsorbentes para la purificación de corrientes gaseosas by Alicia Boix. 16 h – Valladolid (Spain).
- 2nd Winesense spring school. 37 h – Valladolid (Spain).

PREDOCTORAL STAY

- 3 months stay of research at Institut de recherches sur la catalyse et l'environement de Lyon (IRCELYON, Lyon (France)) under the supervision of Catherine Pinel and Nadine Essayem. September – December 2015.

PhD GRANTS

- Ayuda para la asistencia a congresos internacionales de la Universidad de Valladolid. Julio 2016.

- Ayuda para la asistencia a congresos internacionales de la Universidad de Valladolid. Julio 2016.
- Ayuda para la realización de estancias breves en centros de investigación extranjeros de la Universidad de Valladolid. September 2015 – December 2015.
- ACTION COST FP1306 grant to attend to the 1st Summer School on Green Chemistry in La Rochelle (France). May 2015.
- Ayuda para financiar la contratación predoctoral de personal investigador de la Junta de Castilla y León. May 2015 – May 2018.

PARTICIPATION IN PROJECTS

- CATHYCEL project from the Spanish Government of science and innovation (MINECO, CTQ2011-27347) entitled "Synthesis of catalysts in supercritical carbon dioxide for the selective conversion of cellulose into commodities".

TEACHING EXPERIENCE

- Assistant Professor in the subject called "Iniciación a la investigación", which is involved in the Chemical Engineering Master from University of Valladolid (2017).
- Co-supervision of the master thesis called "Estudio de utilización de catalizadores de rutenio sobre sílices mesoporosas para la hidrogenación de la fracción hemicelulósica de biomasa", which was developed by Juan Castrillo (2017).

AWARDS

- Santander Yuzz 2017 award related to the best business plan entitled Cathycel.
- Greenweekend Valladolid 2017 award associated to the best business plan in Green tecnologies (2017).
- Best Student of Fluid Thermodynamic Engineering Master in University of Valladolid from (2012-2013).
- Best Master Thesis on Chemical Engineering by COPIQCLM (2011).